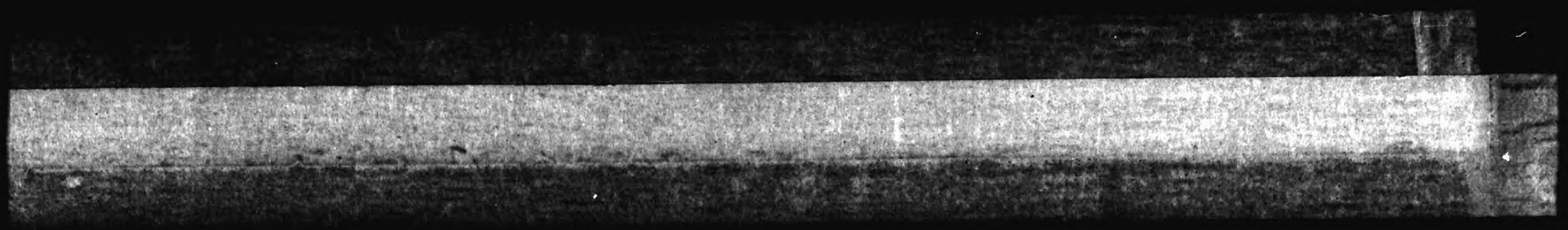

D40838 '82

300

D40838/82.

WOOD D.J

300

COMPLEX BOUNDARY INTEGRAL TECHNIQUES FOR TURBOMACHINERY BLADING

by

DAVID JOHN WOOD

Doctor of Philosophy October 1981

This thesis is submitted in partial fulfilment of the requirements of the Council for National Academic Awards for their degree of Doctor of Philosophy.

Department of Mathematics
The Polytechnic of North London
Holloway Road
London

Rolls-Royce Ltd.
PO Box 3
Filton
Bristol

ABSTRACT

D. J. Wood: Complex boundary integral techniques for turbomachinery blading

Integral equation techniques are used to solve interior and exterior (including cascade) Neumann problems. The equations are in terms of the boundary values of the derivatives of the harmonic function sought. The equations are derived using the complex variables forms of Green's theorem. They are solved numerically using low order complex polynomial approximations. The solution of problems defined on regions with corners is considered.

A complex integral representation which enables a regular function to be generated from its derivatives is derived. Approximations to the representation are given for the case when first order derivatives are known. These approximations are geared to the utilisation of the numerical solutions of the aforementioned integral equations.

Beam element solutions of stress and vibration problems require knowledge of such section properties as torsional stiffness, warping stiffness and shear centre co-ordinates. These section properties are usually expressed as integrals taken over a uniform beam's cross section. It is shown that they can be written as boundary integrals involving the beam's torsion and warping functions. These functions are determined using the previously mentioned integral equations together with the representation of a regular function.

The major practical application of the above techniques is to the analysis of turbomachinery blading at an early stage in the design process.

Finally, the solution of plane elastostatic problems using complex potentials is considered. A 1st Kind integral equation for the first derivative of one of the Goursat functions is introduced. The equation is shown to be derivable from a 2nd Kind equation due to Muskhelishvili. The solution of the equation is discussed in terms of a simple numerical method.

Where appropriate the numerical methods described in this thesis are illustrated by examples.

ACKNOWLEDGEMENTS

I would like to thank both the Polytechnic of North London and Rolls-Royce Ltd. for providing me with the opportunity to undertake the work presented in this thesis.

My especial thanks are due to Dr. Derek Payne whose advice, encouragement and assistance made the presentation of this thesis possible.

Finally, I am very grateful to both Mrs. M. O. Greville and Mrs. A. M. C. Viney who tackled the unenviable task of producing this typescript.

Some Comments On Notation And Terminology

Any notation peculiar to this thesis is introduced as and when it is required. However, the following comments may assist the reader:-

i) $F(\tilde{\zeta})$ denotes a function of the real and imaginary parts of $\zeta = x+iy$, i.e. $F(\tilde{\zeta}) \equiv F(x,y)$. This function is not necessarily regular anywhere in the ζ-plane.

ii) $F(\zeta)$ denotes a function which is regular throughout a specified part of the ζ-plane.

iii) Suffix notation for derivatives is frequently used, e.g. $\varphi_x(\tilde{\zeta}) \equiv \frac{\partial}{\partial x}\varphi(x,y)$.

All references to published material are enclosed in square brackets. Thus [1] refers to the paper numbered 1 in the list of references while [4, pp.245-247] refers to pages 245-247 of the book numbered 4 in the list of references.

Finally, the numerical solution of a specified problem always involves the description of boundary data in a standard form. This description of boundary data is termed "idealisation" throughout this thesis.

CONTENTS

CONTENTS

CONTENTS

CONTENTS

Chapter 1

Introduction

In the last two decades much research has been carried out into the solution of two dimensional elliptic partial differential equations by numerical techniques based on a problem's equivalent boundary integral equation (b.i.e.) formulations. That interest in these techniques has continued throughout this time is, in part, due to the constant attraction of formulating the solution to problems in terms of boundary data alone. Indeed, when one considers the increasingly complex geometries over which solutions to regularly occurring problems are required, it is not surprising that b.i.e. methods are becoming of much more importance as an engineering tool. This fact is illustrated by the effort put into the implementation of these methods by General Electric [1], Pratt & Whitney [2] and Rolls-Royce [3] ; the world's three main Aero-Engine manufacturers.

Recent research into the application of b.i.e. techniques to problems in solid mechanics has mainly been concerned with the solution of problems in two and three dimensional elasticity by techniques based on Somigliana's integral formulae [4, pp.245-247]. In this context the researches of Cruse [5, 6, 7], Lachat and Watson [8] and Chaudonneret [9] are worthy of being mentioned specifically since they have led to such b.i.e. techniques being applied to an increasing number of Stress Engineering problems [2, 3, 10, 11, 12].

Recently some research into the solution of non-linear problems in solid mechanics, notably plasticity and visco-plasticity has also been reported [13, 14] . Again, the techniques used are based on Somigliana's integral formulae.

The references given above relate mainly to work carried out since 1970. An alternative approach to the "classical" problems of linear elastostatics is to represent the required solution of a problem by real or (in two dimensions) complex potentials. Because this approach often enables the equations of elasticity to be written in a much simplified form, e.g. as Laplace's equation or the biharmonic equation, it has been very widely applied (for examples see extensive bibliography given by Jaswon & Symm [15]).

That the equations governing the behaviour of most elastic potentials are so straightforward has meant that considerable effort has been put into the representation of these potentials by boundary integrals. With regard to complex variable methods for two dimensional problems, the representations used by Muskhelishvili [16, pp.405-433] and Mikhlin [17, pp 191-219] are perhaps the most widely known. A large number of real variable representations (covering both two and three dimensional problems) have been considered in detail by Kupradze [18] and Jaswon and Symm [loc. cit.]. More recently, Hamson [19] has given a survey of b.i.e. methods for solving Laplace's equation in two dimensions.

An attractive feature of these potential type b.i.e. methods is that they are applicable to other branches of mathematical physics viz. hydrodynamics, electrostatics, etc. Of these alternative applications, the use of b.i.e. techniques in hydrodynamics has been of particular interest to the author. Indeed, this present work is chiefly concerned with the analysis of incompressible potential flow past one or more aerofoils and its elastic analogy, the torsion of a uniform beam twisted by couples applied over its end sections.

That both of these problems can be reduced to the problem of finding a function φ which satisfies

$$\triangle \varphi = \frac{\partial^2 \varphi}{\partial x^2} + \frac{\partial^2 \varphi}{\partial y^2} = 0$$

within some domain D, and whose normal derivative $\frac{\partial \varphi}{\partial n}$ takes prescribed values on the boundary of D, is well known and will not be demonstrated here. Problems of this type are frequently known as Neumann problems and, as is shown by the previously given references, have usually been solved by the use of some boundary integral representation of the potential function φ. An alternative approach which has been used by the author, and is detailed in the present work, is to solve for the boundary tangential derivative $\frac{\partial \varphi}{\partial s}$ of the potential function. In hydrodynamics, where φ is the velocity potential, this approach has the attraction of yielding the flow velocity both on and off the aerofoil in a straightforward manner. Similarly, the shear stresses in a uniform beam which are due to pure torsion can readily

be evaluated from the knowledge of the appropriate $\frac{\partial \varphi}{\partial s}$ In this latter case φ is the beam's warping function.

The author presents the governing b.i.e. of the above alternative approach to Neumann problems in Chapter 2 and bases his derivation on the uses of the complex variables forms of Green's theorem [20, pp.133-134] previously reported by Payne [21, 22] . The hydrodynamic application of the derived equation appears to have been given initially by Martensen [23] while the elastostatic application appears to have been first given by Rieder [24]. It should be noted that both Martensen and Rieder based their derivations on the superposition of suitable singularities and neither they nor subsequent authors [25, 26, 27] seem to have appreciated that their methods are in fact specialisations of a single technique.

In most of the cases of practical interest one cannot write down the closed form solution of the derived b.i.e. and numerical solutions must be attempted. The numerical techniques for solving the b.i.e. which have been developed by the author are described in Chapters 3 and 4. In these two chapters the author has continued to work in terms of complex variables and, by writing the local derivatives $\frac{\partial \varphi}{\partial s}, \frac{\partial \varphi}{\partial n}$ in terms of the global derivatives $\frac{\partial \varphi}{\partial x}, \frac{\partial \varphi}{\partial y}$, has been able to apply a modification of Atkinson's work on the numerical evaluation of Cauchy integrals [28]. The complex approximations used still result in a system of real linear equations for the unknown approximations to the boundary values of $\frac{\partial \varphi}{\partial s}$.

An attractive feature of the techniques described is that the integrations required in assembling the coefficient matrix of the above system of equations are all path independent. This is in direct contrast to real variable approximations to the same b.i.e. which require geometric approximations when the boundary contour does not comprise of straight lines and/or circular arcs [e.g. 15, pp.143-155].

A number of examples covering problems defined on both simply and multiply connected regions are included in these chapters. These examples illustrate the solution accuracy that has been obtained by the author using the techniques described.

A useful feature of the solution of Neumann type problems by the techniques described in Chapters 2 & 3 of this thesis is that knowledge of the boundary derivatives of a harmonic function φ enables the generation of the function φ together with its harmonic conjugate ψ to be accomplished. The generation of the complex variable function

$$f(\zeta) = \varphi(x,y) + i\psi(x,y) \quad , \quad \zeta = x + iy$$

can be accomplished either by integrating

$$f_\zeta(\zeta) = \frac{\partial \varphi}{\partial x} - i \frac{\partial \varphi}{\partial y}$$ along a path

joining some point ζ_0 to ζ , so that

$$f(\zeta) = f(\zeta_0) + \int_{\zeta_0}^{\zeta} f_t(t)\, dt \quad ,$$

or through the boundary integral representation given in Chapter 5. Although this representation is analogous to one attributed to Vekua by Muskhelishvili [29, pp.192-201] its use in a problem solving context appears to have been neglected.

In the complex form used by the author, the representation offers a straightforward numerical technique for evaluating $f(\zeta)$ from the boundary values of its first (or higher) order derivative. Indeed, utilisation of the complex approximations used in the preceding chapters enables all of the necessary quadratures to be accomplished in a closed and path independent form.

So far in this introduction the solution of the torsion problem for a given section has been considered achieved once the capability of generating the torsional shear stress and warping function at points in the section has been attained. This is not the case in turbomachinery applications where few (if any) of the problems arising in the stressing of turbomachinery components can be reduced to the torsion problem alone. Nevertheless, the solution of stress and vibration problems arising in turbomachinery blading by beam element methods [30, 31] do require the knowledge of a number of blade section properties (the sections of interest being taken at various stations along a blade's longitudinal axis). Of these section properties

the torsional stiffness

$$I_S = I_x + I_y + \iint_R \{x\,\varphi_y(x,y) - y\,\varphi_x(x,y)\}\,dx\,dy$$

warping stiffness

$$I_W = \iint_R \{\varphi(x,y)\}^2\,dx\,dy$$

and shear centre co-ordinates

$$e_x = -\frac{1}{I_x}\iint_R y\,\varphi(x,y)\,dx\,dy$$

$$e_y = \frac{1}{I_y}\iint_R x\,\varphi(x,y)\,dx\,dy \quad ,$$

where $I_x = \iint_R y^2\,dx\,dy$

and $I_y = \iint_R x^2\,dx\,dy$,

are probably the most difficult to evaluate since they depend upon the manner in which a uniform beam, of given cross section R, warps under pure torsion.

Whereas the so-called Dirichlet integral

$$\int_C \varphi(x,y)\,\varphi_n(x,y)\,ds$$

has been used by many authors as a boundary integral representation for the term

$$\iint_R \{y\,\varphi_x(x,y) - x\,\varphi_y(x,y)\}\,dx\,dy$$

in the expression given for I_S [e.g. 4, 15, 16], the determination of I_W and (e_x, e_y) through boundary integral representations has apparently been neglected. However, their determination through finite element and "thin wall" techniques has been reported [e.g. 32, 33] .

That boundary integral representations of all the above section properties can be derived is demonstrated in Chapter 6. Here the author again makes extensive use of the complex forms of Green's Theorems in the derivations given.

With regard to the representations given for I_w and (e_x, e_y), these representations require the knowledge of several regular functions each of which has known first order derivatives. When these functions are not known explicity, as is the case in most practical examples, the representation derived in Chapter 5 yields them implicitly. This use of the representations of Chapter 5 is illustrated in the examples used to validate the contents of Chapter 6.

A further topic which appears to have been neglected by other authors is the coupling of interior Neumann problems with exterior Neumann problems. This coupling of the solution of the two types of Neumann problems does have a design application where the various effects of changes to an aerofoil's geometry are of interest to both aerodynamicists and stress engineers. Accepting that the solutions to the problems of plane, incompressible, potential flow and torsion can (by their very nature) only be used to give an indication of the true situation; it would appear desirable that the designer/engineer should be able to see the effects of design changes as quickly as possible and with the minimum effort on his/her part. In view of this, the author has extended the techniques of Chapters 2, 3 & 4 in such a way that the approximate solution of the two basic problems, i.e. flow and torsion, can be obtained through the numerical solution of a single b.i.e. Details of these extensions are given in Chapter 7 where problems defined on both isolated and cascade aerofoils are considered.

With the exception of a chapter drawing together results and conclusions relating to the complex boundary integral methods developed by the author and their suitability for turbomachinery blading applications, this thesis closes with a chapter detailing further applications of the complex forms of Green's Theorems to problems appertaining to the mathematical theory of elasticity.

A useful feature of the solution of Neumann type problems by the techniques described in Chapters 2 & 3 of this thesis is that knowledge of the boundary derivatives of a harmonic function φ enables the generation of the function φ together with its harmonic conjugate ψ to be accomplished. The generation of the complex variable function

$$f(\zeta) = \varphi(x,y) + i\psi(x,y) \quad , \quad \zeta = x + iy$$

can be accomplished either by integrating

$$f_\zeta(\zeta) = \frac{\partial \varphi}{\partial x} - i \frac{\partial \varphi}{\partial y}$$ along a path

joining some point ζ_0 to ζ , so that

$$f(\zeta) = f(\zeta_0) + \int_{\zeta_0}^{\zeta} f_t(t)\, dt \quad ,$$

or through the boundary integral representation given in Chapter 5. Although this representation is analogous to one attributed to Vekua by Muskhelishvili [29, pp.192-201] its use in a problem solving context appears to have been neglected.

In the complex form used by the author, the representation offers a straightforward numerical technique for evaluating $f(\zeta)$ from the boundary values of its first (or higher) order derivative. Indeed, utilisation of the complex approximations used in the preceding chapters enables all of the necessary quadratures to be accomplished in a closed and path independent form.

So far in this introduction the solution of the torsion problem for a given section has been considered achieved once the capability of generating the torsional shear stress and warping function at points in the section has been attained. This is not the case in turbomachinery applications where few (if any) of the problems arising in the stressing of turbomachinery components can be reduced to the torsion problem alone. Nevertheless, the solution of stress and vibration problems arising in turbomachinery blading by beam element methods [30, 31] do require the knowledge of a number of blade section properties (the sections of interest being taken at various stations along a blade's longitudinal axis). Of these section properties

the torsional stiffness

$$I_S = I_x + I_y + \iint_R \{x\,\varphi_y(x,y) - y\,\varphi_x(x,y)\}\,dx\,dy$$

warping stiffness

$$I_W = \iint_R \{\varphi(x,y)\}^2\,dx\,dy$$

and shear centre co-ordinates

$$e_x = -\frac{1}{I_x}\iint_R y\,\varphi(x,y)\,dx\,dy$$

$$e_y = \frac{1}{I_y}\iint_R x\,\varphi(x,y)\,dx\,dy \quad ,$$

where $$I_x = \iint_R y^2\,dx\,dy$$

and $$I_y = \iint_R x^2\,dx\,dy \quad ,$$

are probably the most difficult to evaluate since they depend upon the manner in which a uniform beam, of given cross section R, warps under pure torsion.

Whereas the so-called Dirichlet integral

$$\int_C \varphi(x,y)\,\varphi_n(x,y)\,ds$$

has been used by many authors as a boundary integral representation for the term

$$\iint_R \{y\,\varphi_x(x,y) - x\,\varphi_y(x,y)\}\,dx\,dy$$

in the expression given for I_S [e.g. 4, 15, 16], the determination of I_W and (e_x, e_y) through boundary integral representations has apparently been neglected. However, their determination through finite element and "thin wall" techniques has been reported [e.g. 32, 33] .

That boundary integral representations of all the above section properties can be derived is demonstrated in Chapter 6. Here the author again makes extensive use of the complex forms of Green's Theorems in the derivations given.

With regard to the representations given for I_w and (e_x, e_y), these representations require the knowledge of several regular functions each of which has known first order derivatives. When these functions are not known explicity, as is the case in most practical examples, the representation derived in Chapter 5 yields them implicitly. This use of the representations of Chapter 5 is illustrated in the examples used to validate the contents of Chapter 6.

A further topic which appears to have been neglected by other authors is the coupling of interior Neumann problems with exterior Neumann problems. This coupling of the solution of the two types of Neumann problems does have a design application where the various effects of changes to an aerofoil's geometry are of interest to both aerodynamicists and stress engineers. Accepting that the solutions to the problems of plane, incompressible, potential flow and torsion can (by their very nature) only be used to give an indication of the true situation; it would appear desirable that the designer/engineer should be able to see the effects of design changes as quickly as possible and with the minimum effort on his/her part. In view of this, the author has extended the techniques of Chapters 2, 3 & 4 in such a way that the approximate solution of the two basic problems, i.e. flow and torsion, can be obtained through the numerical solution of a single b.i.e. Details of these extensions are given in Chapter 7 where problems defined on both isolated and cascade aerofoils are considered.

With the exception of a chapter drawing together results and conclusions relating to the complex boundary integral methods developed by the author and their suitability for turbomachinery blading applications, this thesis closes with a chapter detailing further applications of the complex forms of Green's Theorems to problems appertaining to the mathematical theory of elasticity.

In fact, chapter 8 considers the derivation of a complex boundary integral equation from which the first derivative of one of the Goursat functions [17, pp.179-184] can be determined. The integral equation obtained by the author is a 1st Kind Fredholm type equation and the question as to whether or not it possesses a theoretical solution presents the difficulties normally associated with equations of this type. However, the author does show that a 2nd Kind Fredholm type equation due to Muskhelishvili [loc.cit.] can be obtained from the previously mentioned 1st Kind equation and discusses the question of the existence of solutions to this latter equation making use of the relationship between the two equations.

In common with many of the boundary integral equation formulations for plane problems in elastostatics which involve formulating problems in terms of Airy's stress function [4, pp.204-207] or the Goursat functions, the integral equation derived by the author appears to be suited only to problems without mixed boundary conditions. This has meant that from a turbomachinery applications standpoint the author's integral equation is of limited interest. Because of this only a rudimentary numerical scheme for the solution of the equation is described and the results for an atypical problem are given.

Frequent mention of the use of the complex forms of Green's Theorems has been made in this introduction. These complex forms seem to have been introduced by Milne-Thomson who frequently used them in his work on hydrodynamics [loc.cit.] and elasticity [36]. More recently these forms have been used by Payne [loc.cit.] and Dyer [37].

From Milne-Thomson then, the complex forms of Green's Theorems are:-

$$\int_C F(z,\bar{z})\,dz = 2i \iint_R \frac{\partial}{\partial \bar{z}} \left\{ F(z,\bar{z}) \right\} dx\,dy \qquad (1.1)$$

$$\int_C F(\zeta,\bar{\zeta})\, d\bar{\zeta} = -2i \iint_R \frac{\partial}{\partial \zeta} \left\{ F(\zeta,\bar{\zeta}) \right\} dx\, dy \qquad (1.2)$$

where the function $F(\zeta,\bar{\zeta})$ is a function of the complex variables $\zeta,\bar{\zeta}$ defined over some region R which is bounded by the contour **C.** The conditions of Green's Theorem require that the function $F(\zeta,\bar{\zeta})$ together with its first order derivatives be continuous. A full statement and proof of Green's Theorem is to be found in Apostol [38, pp.283-292].

Chapter 2

INTEGRAL EQUATIONS FOR THE BOUNDARY TANGENTIAL DERIVATIVE OF A HARMONIC FUNCTION

§ 2.1) Introduction

An integral equation approach to interior Neumann problems has recently been given by several authors [25, 26]. In these works an integral equation for the boundary tangential derivative of a harmonic function satisfying Neumann type boundary conditions is derived either by the use of elementary singularities [26] or by Green's third identity [25]. In the case of the superposition approach to Neumann problems occurring in the mathematical theory of elasticity, viz. torsion and flexure, the elementary singularities have been interpreted in terms of the displacements corresponding to a concentrated force acting parallel to the longitudinal axis of a cylinder and a screw dislocation.

Examination of the mathematical expressions for the above displacements shows that they are equivalent to the velocity potentials developed from the point source and the point vortex occurring in plane potential flow. This being the case, the previously cited works may be considered to be extensions of certain superposition techniques which have been developed in aerodynamics [e.g. 24, 27, 39].

In the following sections of this chapter the required b.i.e. for the tangential derivative of a plane harmonic function satisfying Neumann type boundary conditions is derived for both simply and multiply connected regions. Some discussion on the conditions required for the existence of solutions to the b.i.e. is included.

The derivations given in this chapter are based on the complex forms of Green's Theorem (see remarks on pp. 7-8, chapter 1) rather than the previously mentioned superposition techniques or Green's third identity. This approach has been used extensively by Payne [loc.cit.] and also by Dyer [loc.cit.] for problems occurring in turbomachinery aerodynamics but appears to have been neglected as a "tool" for providing solution techniques to problems

occurring in linear elasticity. As will be seen, the complex variables approach is attractive for three reasons, namely

i) It avoids the problem of the manner in which singularities should be interpreted physically.

ii) the free terms of the derived equations include a term allowing for the treatment of problems which are not harmonic in character [21, 22, 37] (see also Chapter 8).

iii) in their complex forms the derived equations can be solved numerically by techniques involving path independent quadratures (see Chapters 3 and 4).

Where they occur, the treatment of Cauchy integrals broadly follows the work of Muskhelishvili [29].

§ 2.2) Integral equation for a simply connected region

Consider the typical region R, shown in Figure 2-1, which is simply connected and bounded by the simple closed curve C_1. In this region the function

$$\tau(\tilde{\zeta}) = \varphi_x(\tilde{\zeta}) - i\,\varphi_y(\tilde{\zeta}) \qquad (2.1)$$

can be constructed from the first partial derivatives of a potential function $\varphi(\tilde{\zeta})$. The function $\tau(\tilde{\zeta})$ can be interpreted as the gradient of $\varphi(\tilde{\zeta})$.

At the point $\omega \epsilon R$, an integral representation for $\tau(\tilde{\omega})$ is obtained in terms of the boundary values of $\tau(\tilde{\zeta})$, and the function $\tau_{\bar{\zeta}}(\tilde{\zeta})$, by considering the function

$$F(\tilde{\zeta},\omega) = \frac{\tau(\tilde{\zeta})}{\zeta - \omega} \qquad (2.2)$$

defined over the region $\tilde{R}$ shown in Figure 2-2. The region $\tilde{R}$ is obtained from R by introducing the circular contour σ which

i) excludes the point ω from $\tilde{R}$

ii) is centred on ω

iii) has radius ε.

Provided that the function $\tau(\tilde{\zeta})$ defined by (2.1) together with its derivatives $\tau_{\xi}(\tilde{\zeta})$, $\tau_{\bar{\zeta}}(\tilde{\zeta})$ are continuous for $\zeta \in R \cup C_1$, the function $F(\tilde{\zeta},\omega)$ and its derivative

$$F_{\bar{\zeta}}(\tilde{\zeta},\omega) = \frac{\tau_{\bar{\zeta}}(\tilde{\zeta})}{\zeta - \omega}$$

are continuous for $\zeta \in \tilde{R} \cup C_1$. Hence, in $\tilde{R}$ the complex form of Green's Theorem

$$\int_{\partial\tilde{R} = C_1 + \sigma} F(\tilde{\zeta},\omega)\, d\zeta = 2i \iint_{\tilde{R}} F_{\bar{\zeta}}(\tilde{\zeta},\omega)\, dx\, dy$$

can be applied to the function defined by (2.2), i.e.

$$\int_{C_1} \frac{\tau(\tilde{\zeta})}{\zeta - \omega} d\zeta + \int_{\sigma} \frac{\tau(\tilde{\zeta})}{\zeta - \omega} d\zeta = 2i \iint_{\tilde{R}} \frac{\tau_{\bar{\zeta}}(\tilde{\zeta})}{\zeta - \omega} dx\, dy \qquad (2.3).$$

The required integral representation is obtained by examining the contribution of

$$\int_{\sigma} \frac{\tau(\tilde{\zeta})}{\zeta - \omega} d\zeta$$

to the left hand side of (2.3) when $\varepsilon \to 0$ and by showing that

$$\lim_{\varepsilon \to 0} \iint_{\tilde{R}} \frac{\tau_{\zeta}(\tilde{\zeta})}{\zeta - \omega} dx\, dy = \iint_{R} \frac{\tau_{\zeta}(\tilde{\zeta})}{\zeta - \omega} dx\, dy \qquad (2.4).$$

The contribution to (2.3) of

$$\int_\sigma \frac{\tau(\tilde{\zeta})}{\zeta-\omega}\,d\zeta$$

when $\varepsilon\to 0$ is readily obtained by expanding $\tau(\tilde{\zeta})$ as a Taylor series about ω so that

$$\lim_{\varepsilon\to 0}\int_\sigma \frac{\tau(\tilde{\zeta})}{\zeta-\omega}\,d\zeta = \tau(\tilde{\omega})\int_\sigma \frac{d\zeta}{\zeta-\omega}$$

$$= -2\pi i\,\tau(\tilde{\omega}).$$

The validity of the expansion comes from the continuity of the derivatives $\tau_{\bar{\zeta}}(\tilde{\zeta}),\ \tau_\zeta(\tilde{\zeta})$ for $\zeta\in R$.

That (2.4) holds can be shown by considering

$$\lim_{\varepsilon\to 0}\iint_{R-\tilde{R}} \frac{\tau_{\bar{\zeta}}(\tilde{\zeta})}{\zeta-\omega}\,dx\,dy$$

where $R-\tilde{R}$ denotes the region bounded externally by σ. In this region write

$$\zeta-\omega = \rho e^{i\theta}$$

and note that, since $\tau_{\bar{\zeta}}(\tilde{\zeta})$ is continuous in R,

$$\left|\tau_{\bar{\zeta}}(\tilde{\zeta})\right| \le M$$

where M is a constant. Hence

$$\lim_{\varepsilon\to 0}\left|\iint_{R-\tilde{R}} \frac{\tau_{\bar{\zeta}}(\tilde{\zeta})}{\zeta-\omega}\,dx\,dy\right| \le \lim_{\varepsilon\to 0} M\left|\int_0^{2\pi}\int_0^{\varepsilon} e^{-i\theta}\,d\rho\,d\theta\right| = 0$$

and (2.4) follows.

Therefore, for $\omega \in R$ but not on C_1, $\tau(\omega)$ may be represented by

$$\tau(\tilde{\omega}) = \frac{1}{2\pi i}\int_{C_1}\frac{\tau(\tilde{\zeta})}{\zeta-\omega}\,d\zeta - \frac{1}{\pi}\iint_R \frac{\tau_{\bar{\zeta}}(\tilde{\zeta})}{\zeta-\omega}\,dx\,dy \qquad (2.5)$$

which clearly reduces to Cauchy's integral formula [35, pp.66-67] when $\tau_{\bar{\zeta}}(\tilde{\zeta}) = 0$ in R.

When ω tends to a point ω_0 on the boundary, the representation (2.5) must be modified to allow for the singularity in the integrand of the contour integral. Note that

$$\lim_{\omega\to\omega_0}\iint_R \frac{\tau_{\bar{\zeta}}(\tilde{\zeta})}{\zeta-\omega}\,dx\,dy = \iint_R \frac{\tau_{\bar{\zeta}}(\tilde{\zeta})}{\zeta-\omega_0}\,dx\,dy .$$

This modification is readily obtained provided that $\tau(\tilde{\zeta})$ is Hölder continuous on C_1 [29, pp.7-21], i.e. for any two points ζ_1, ζ_2 on C_1 the function $\tau(\tilde{\zeta})$ should satisfy

$$\left|\tau(\tilde{\zeta}_2) - \tau(\tilde{\zeta}_1)\right| \le H\left|\zeta_2-\zeta_1\right|^{\mu}$$

where H, μ are constants and $0 < \mu \le 1$. It should be noted that this restriction on $\tau(\tilde{\zeta})$ is more restrictive than the continuity of $\tau(\tilde{\zeta})$, $\zeta \in R \cup C_1$, required by (2.5) [15, p.253].

Consider the integral

$$\Phi(\omega) = \frac{1}{2\pi i}\int_{C_1}\frac{\tau(\tilde{\zeta})}{\zeta-\omega}\,d\zeta$$

which may be written as

$$\Phi(\omega) = \frac{1}{2\pi i}\int_{C_1}\frac{\tau(\tilde{\zeta})-\tau(\tilde{\omega}_0)}{\zeta-\omega}\,d\zeta + \frac{\tau(\tilde{\omega}_0)}{2\pi i}\int_{C_1}\frac{d\zeta}{\zeta-\omega}$$

or, since $\omega \in R$,

$$\Phi(\omega) = \frac{1}{2\pi i} \int_{C_1} \frac{\tau(\tilde{\gamma}) - \tau(\tilde{\omega}_0)}{\gamma - \omega} d\gamma + \tau(\tilde{\omega}_0) .$$

Now let $\omega \to \omega_0$ from inside R so that

$$\lim_{\omega \to \omega_0} \Phi(\omega) = \tau(\tilde{\omega}_0) + \lim_{\omega \to \omega_0} \frac{1}{2\pi i} \int_{C_1} \frac{\tau(\tilde{\gamma}) - \tau(\tilde{\omega}_0)}{\gamma - \omega} d\gamma \quad (2.6).$$

To examine the limiting form of the integral

$$\Psi(\omega, \tilde{\omega}_0) = \frac{1}{2\pi i} \int_{C_1} \frac{\tau(\tilde{\gamma}) - \tau(\tilde{\omega}_0)}{\gamma - \omega} d\gamma$$

consider the difference

$$\Psi(\omega, \tilde{\omega}_0) - \Psi(\omega_0, \tilde{\omega}_0)$$

$$= \frac{1}{2\pi i} \int_{C_1} \frac{\{\tau(\tilde{\gamma}) - \tau(\tilde{\omega}_0)\}(\omega - \omega_0)}{(\gamma - \omega)(\gamma - \omega_0)} d\gamma .$$

A circular arc $\hat{\sigma}$ of radius ρ and centre ω_0 can be described. As shown in Figure 2-3, for sufficiently small ρ this circular arc will only intersect the contour C_1 at the two points ω_1, ω_2 .

Denoting that part of C_1 lying on the segment $\omega_1 \omega_0 \omega_2$ by ℓ and the remainder by $\hat{C} = C_1 - \ell$, the inequality

$$\left| \Psi(\omega, \tilde{\omega}_0) - \Psi(\omega_0, \tilde{\omega}_0) \right| \leq I_1 + I_2$$

may be written. Here

$$I_1 = \frac{1}{2\pi} \int_{\ell} \frac{|\tau(\tilde{\gamma}) - \tau(\tilde{\omega}_0)|\,|\omega - \omega_0|\,|ds|}{|\gamma - \omega|\,|\gamma - \omega_0|} ,$$

$$I_2 = \frac{1}{2\pi} \int_{C_1 - \ell} \frac{|\tau(\tilde{\gamma}) - \tau(\tilde{\omega}_0)|\,|\omega - \omega_0|\,|ds|}{|\gamma - \omega|\,|\gamma - \omega_0|}$$

and

$$|d\gamma| = \left|\frac{d\gamma}{ds}\, ds\right| = |ds| .$$

In order to examine the behaviour of I_1 let $\omega \to \omega_0$ along the vector $\omega_0 - \omega$. Writing

$$\left.\begin{aligned} \alpha &= \arg\left\{\frac{\omega_1 - \omega_0}{\omega - \omega_0}\right\} \\ \beta &= \arg\left\{\frac{\omega - \omega_0}{\omega_2 - \omega_0}\right\} \end{aligned}\right\} \quad 0 < \alpha, \beta < \pi$$

and letting $\delta = |\omega_0 - \omega|$ it can be shown that for γ on the segment $\omega_1 \omega_0$

$$|\gamma - \omega| \geq \delta \sin\alpha$$

while

$$|\gamma - \omega| \geq \delta \sin\beta$$

for γ on the segment $\omega_0 \omega_2$. Hence

$$I_1 \leq \frac{1}{2\pi} \int_{\omega_1}^{\omega_0} \frac{|\tau(\tilde{\gamma}) - \tau(\tilde{\omega}_0)|\,\delta\,|ds|}{\delta \sin\alpha\,|\gamma - \omega_0|} + \frac{1}{2\pi} \int_{\omega_0}^{\omega_2} \frac{|\tau(\tilde{\gamma}) - \tau(\tilde{\omega}_0)|\,\delta\,|ds|}{\delta \sin\beta\,|\gamma - \omega_0|}$$

and, on using the previously specified restriction that $\tau(\tilde{\gamma})$ should be Hölder continuous on C_1, the inequality

$$I_1 \leq \frac{H}{2\pi \sin\alpha} \int_{\omega_1}^{\omega_0} |\gamma - \omega_0|^{\mu - 1}\,|ds| + \frac{H}{2\pi \sin\beta} \int_{\omega_0}^{\omega_2} |\gamma - \omega_0|^{\mu - 1}\,|ds|$$

is obtained. An upper bound for these integrals is given by writing $r = |\zeta - \omega_0|$ and noting that on $\mathcal{L}$ $|ds| \leq K|dr|$ where K is a constant.
Therefore

$$I_1 \leq \frac{HK}{2\pi}\left\{\frac{1}{\sin\alpha}\int_{\omega_1}^{\omega_0} r^{\mu-1}|dr| + \frac{1}{\sin\beta}\int_{\omega_0}^{\omega_2} r^{\mu-1}|dr|\right\}$$

so that

$$I_1 \leq \frac{HK}{2\pi}\left\{\frac{1}{\sin\alpha} + \frac{1}{\sin\beta}\right\}\int_0^{\rho} r^{\mu-1}\,dr$$

whence

$$I_1 \leq \frac{HK\,\rho^{\mu}}{2\pi\,\mu}\left\{\frac{1}{\sin\alpha} + \frac{1}{\sin\beta}\right\}.$$

In order to examine the corresponding behaviour of I_2 choose $\delta \leq \rho/2$ so that, for $\zeta \in C_1 - \mathcal{L}$, $|\zeta - \omega_0| \geq \rho$ and $|\zeta - \omega| \geq \rho/2$.
Therefore

$$I_2 \leq \frac{\delta}{\pi\rho^2}\int_{C_1-\mathcal{L}} |\tau(\tilde{\zeta}) - \tau(\tilde{\omega}_0)|\,|ds| \leq \frac{\delta L}{\pi\rho^2}$$

where L is an upper bound on the integral.

Given some $\varepsilon > 0$ these bounds on I_1, I_2 enable ρ to be chosen such that

$$I_1 < \varepsilon/2$$

while (given ρ) δ can be chosen such that

$$I_2 < \varepsilon/2$$

Hence for these choices of ρ, δ

$$|\Phi(\omega,\tilde{\omega}_0) - \Phi(\omega_0,\tilde{\omega}_0)| < \varepsilon$$

and $\Phi(\omega,\tilde{\omega}_0)$ is continuous onto the boundary as $\omega \to \omega_0$ from inside R.

Using this last result (2.6) may therefore be written as

$$\lim_{\omega \to \omega_0} \Phi(\omega) = \tau(\tilde{\omega}_0) + \Psi(\omega_0, \tilde{\omega}_0)$$

whence the limiting form of (2.5) becomes

$$\Psi(\omega_0, \tilde{\omega}_0) = \frac{1}{\pi} \iint_R \frac{\tau_i(\tilde{\gamma})}{\gamma - \omega_0} \, dx \, dy \qquad (2.7)$$

when $\omega \to \omega_0$ from inside R. That $\Psi(\omega_0, \tilde{\omega}_0)$ exists in the ordinary sense when $\tau(\tilde{\gamma})$ is Hölder continuous on C_1 is seen by considering

$$\Psi(\omega_0, \tilde{\omega}_0) = \frac{1}{2\pi i} \int_{C_1 - l} \frac{\tau(\tilde{\gamma}) - \tau(\tilde{\omega}_0)}{\gamma - \omega_0} \, d\gamma$$

$$+ \frac{1}{2\pi i} \int_{\omega_1}^{\omega_0} \frac{\tau(\tilde{\gamma}) - \tau(\tilde{\omega}_0)}{\gamma - \omega_0} \, d\gamma + \frac{1}{2\pi i} \int_{\omega_0}^{\omega_2} \frac{\tau(\tilde{\gamma}) - \tau(\tilde{\omega}_0)}{\gamma - \omega_0} \, d\gamma$$

with ω_1, ω_2 taken such that $|\omega_0 - \omega_1| \neq |\omega_0 - \omega_2|$.

The form of the integral $\Psi(\omega_0, \tilde{\omega}_0)$ is in fact inconvenient for computational purposes but can be modified by considering the Cauchy principal value of the integral

$$\Phi(\omega_0) = \frac{1}{2\pi i} \int_{C_1} \frac{\tau(\tilde{\gamma})}{\gamma - \omega_0} \, d\gamma \quad , \quad \omega_0 \in C_1 \, .$$

With the segment l again chosen such that

$$\rho = |\omega_0 - \omega_1| = |\omega_0 - \omega_2| \, ,$$

i.e. as in Figure 2-3, the integral $\Phi(\omega_0)$ may be written as

$$\Phi(\omega_0) = \Psi(\omega_0, \tilde{\omega}_0) + \lim_{\rho \to 0} \frac{1}{2\pi i} \int_{C_1 - l} \frac{\tau(\tilde{\omega}_0)}{\gamma - \omega_0} d\gamma \ .$$

The last integral becomes

$$\frac{\tau(\tilde{\omega}_0)}{2\pi i} \int_{C_1 - l} \frac{d\gamma}{\gamma - \omega_0} = \frac{\tau(\tilde{\omega}_0)}{2\pi i} \left[\log(\gamma - \omega_0) \right]_{C_1 - l}$$

$$= \frac{\tau(\tilde{\omega}_0)}{2\pi i} \log \left\{ \frac{\omega_1 - \omega_0}{\omega_2 - \omega_0} \right\} .$$

On writing

$$\alpha_1 = \arg(\omega_1 - \omega_0)$$

$$\alpha_2 = \arg(\omega_2 - \omega_0) \ ,$$

so that

$$\omega_1 - \omega_0 = \rho e^{i\alpha_1}$$

$$\omega_2 - \omega_0 = \rho e^{i\alpha_2} \ ,$$

the integral

$$\frac{\tau(\tilde{\omega}_0)}{2\pi i} \int_{C_1 - l} \frac{d\gamma}{\gamma - \omega_0} = \frac{\tau(\tilde{\omega}_0)}{2\pi} \{\alpha_2 - \alpha_1\}$$

is obtained. Therefore

$$\lim_{\rho \to 0} \frac{\tau(\tilde{\omega}_0)}{2\pi i} \int_{C_1 - l} \frac{d\gamma}{\gamma - \omega_0} = \frac{\tau(\tilde{\omega}_0)}{2\pi} \gamma_0$$

where γ_0 is the local interior angle at ω_0, in which case the Cauchy principal value of $\phi(\omega_0)$ is given by

$$\phi(\omega_0) = \Psi(\omega_0,\tilde{\omega}_0) + \tau(\tilde{\omega}_0)\frac{\gamma_0}{2\pi} \quad .$$

Hence

$$\Psi(\omega_0,\tilde{\omega}_0) = \frac{1}{2\pi i}\int_{C_1}\frac{\tau(\tilde{\tau})}{\tau-\omega_0}d\tau - \tau(\omega_0)\frac{\gamma_0}{2\pi}$$

so that (2.7) may be written in the form

$$\tau(\tilde{\omega}_0) = \frac{1}{\gamma_0 i}\int_{C_1}\frac{\tau(\tilde{\tau})}{\tau-\omega_0}d\tau - \frac{2}{\gamma_0}\iint_R \frac{\tau_{\bar{\tau}}(\tilde{\tau})}{\tau-\omega_0}dx\,dy \qquad (2.8)$$

where the contour integral is taken in its Cauchy principal value sense. Note that for a contour which is smooth at ω_0 $\gamma_0 = \pi$.

For a smooth contour the required integral equation relating the unknown tangential derivative $\varphi_s(\tilde{\tau})$, $\tau \in C_1$, to the known normal derivative $\varphi_n(\tilde{\tau})$, $\tau \in C_1$, is obtained in the following way. On C_1

$$\tau(\tilde{\tau})\,d\tau = \{\varphi_x(\tilde{\tau}) - i\,\varphi_y(\tilde{\tau})\}\{dx + i\,dy\}$$

$$= \{\varphi_x(\tilde{\tau})\,dx + \varphi_y(\tilde{\tau})\,dy\} + i\{\varphi_x(\tilde{\tau})\,dy - \varphi_y(\tilde{\tau})\,dx\}$$

$$= \left[\left\{\varphi_x(\tilde{\tau})\frac{dx}{ds} + \varphi_y(\tilde{\tau})\frac{dy}{ds}\right\} + i\left\{\varphi_x(\tilde{\tau})\frac{dy}{ds} - \varphi_y(\tau)\frac{dx}{ds}\right\}\right]ds$$

where $\underset{\sim}{\xi}$ is the unit tangent vector to C_1 at τ (Figure 2-1). If $\underset{\sim}{\eta}$ is the unit outward drawn normal corresponding to $\underset{\sim}{\xi}$ and $\alpha(\tilde{\tau})$ the angle between the positive real direction and $\underset{\sim}{\eta}$ then

$$\frac{dx}{ds} = -\frac{dy}{dn} = -\sin[\alpha(\tilde{\gamma})]$$

$$\frac{dy}{ds} = \frac{dx}{dn} = \cos[\alpha(\tilde{\gamma})].$$

Hence

$$\tau(\tilde{\gamma})\,d\gamma = \{\varphi_s(\tilde{\gamma}) + i\,\varphi_n(\tilde{\gamma})\}\,ds \qquad (2.9a)$$

and since

$$i\,\tau(\tilde{\gamma})\,e^{i\alpha(\tilde{\gamma})} = i\{\varphi_x(\tilde{\gamma}) - i\,\varphi_y(\tilde{\gamma})\}\{\cos[\alpha(\tilde{\gamma})] + i\sin[\alpha(\tilde{\gamma})]\}$$

the relation

$$i\,\tau(\tilde{\gamma})\,e^{i\alpha(\tilde{\gamma})} = \varphi_s(\tilde{\gamma}) + i\,\varphi_n(\tilde{\gamma}) \qquad (2.9b)$$

can also be noted. The substitution of (2.9) into equations (2.5), (2.8) yields the identities

$$\tau(\tilde{\omega}) = \frac{1}{2\pi i}\int_{C_1} \frac{\varphi_s(\tilde{\gamma}) + i\varphi_n(\tilde{\gamma})}{\gamma - \omega}\,ds - \frac{1}{\pi}\iint_R \frac{\tau_{\bar{\zeta}}(\tilde{\gamma})}{\gamma - \omega}\,dx\,dy \qquad (2.10),$$

$\omega \in R$, and

$$\varphi_s(\tilde{\omega}_0) + i\,\varphi_n(\tilde{\omega}_0) = \frac{e^{i\alpha(\tilde{\omega}_0)}}{\pi}\int_{C_1} \frac{\varphi_s(\tilde{\gamma}) + i\varphi_n(\tilde{\gamma})}{\gamma - \omega_0}\,ds$$

$$-\frac{2i}{\pi}\,e^{i\alpha(\tilde{\omega}_0)}\iint_R \frac{\tau_{\bar{\zeta}}(\gamma)}{\gamma - \omega_0}\,dx\,dy \qquad (2.11),$$

$\omega_0 \in C_1$,

which provide both a means of evaluating $\tau(\omega)$, $\omega \in R$, when $\varphi_s(\tilde{\gamma})$ and $\varphi_n(\tilde{\gamma})$ are known on C_1 and, more importantly, relationships between the boundary values of these derivatives.

The integral equation of major interest in this work is given by the real part of (2.11) above. Letting $\omega_0 = x_0 + iy_0$, $\gamma = x + iy$ this integral equation may be written as

$$\varphi_s(\tilde{\omega}_0) - \frac{1}{\pi} \int_{C_1} \varphi_s(\tilde{\gamma}) K(\tilde{\omega}_0, \tilde{\gamma}) ds$$

$$= \frac{1}{\pi} \int_{C_1} \varphi_n(\tilde{\gamma}) H(\tilde{\omega}_0, \tilde{\gamma}) ds - \frac{1}{\pi} \iint_R f(\tilde{\gamma}) H(\tilde{\omega}_0, \tilde{\gamma}) dx dy \quad (2.12)$$

where

$$K(\tilde{\omega}_0, \tilde{\gamma}) = \frac{(x-x_0)\cos[\alpha(\tilde{\omega}_0)] + (y-y_0)\sin[\alpha(\tilde{\omega}_0)]}{(x-x_0)^2 + (y-y_0)^2} \quad (2.13)$$

$$H(\tilde{\omega}_0, \tilde{\gamma}) = \frac{(y-y_0)\cos[\alpha(\tilde{\omega}_0)] - (x-x_0)\sin[\alpha(\tilde{\omega}_0)]}{(x-x_0)^2 + (y-y_0)^2} \quad (2.14)$$

and

$$f(\tilde{\gamma}) = \Delta\varphi(x,y) = 2\tau_{\Gamma}(\tilde{\gamma}) \quad (2.15)$$

has been taken as a real valued function.

An alternative derivation of (2.12) which is based on Green's third identity has been given by Christiansen for the case when $\varphi(x,y)$ is harmonic in R, i.e. when $f(\tilde{\gamma}) = 0$ for $\gamma \in R$, [25]. This derivation is given entirely in terms of functions of a real variable.

When (2.15) defines a linear problem, equation (2.12) may be considered as a Fredholm integral equation of the second kind for the unknown function $\varphi_s(\tilde{\gamma})$ due to the weakly singular nature of the kernel function $K(\tilde{\omega}_0, \tilde{\gamma})$

[17, pp.59-66] . That $K(\tilde{\omega}_o, \tilde{\zeta})$ is in fact weakly singular, i.e.

$$\lim_{\zeta \to \omega_o} |\zeta - \omega_o| \, K(\tilde{\omega}_o, \tilde{\zeta}) = 0 ,$$

can be demonstrated by writing

$$K(\tilde{\omega}_o, \tilde{\zeta}) = - \frac{1}{r(\tilde{\omega}_o, \tilde{\zeta})} \frac{\partial}{\partial n_o} r(\tilde{\omega}_o, \tilde{\zeta})$$

where $\frac{\partial}{\partial n_o} r(\tilde{\omega}_o, \tilde{\zeta})$ denotes the normal derivative of the distance function $r(\tilde{\omega}_o, \tilde{\zeta}) = |\zeta - \omega_o|$ at ω_o keeping ζ fixed. Hence

$$\lim_{\zeta \to \omega_o} |\zeta - \omega_o| \, K(\tilde{\omega}_o, \tilde{\zeta}) = - \lim_{\zeta \to \omega_o} \frac{\partial}{\partial n_o} r(\tilde{\omega}_o, \tilde{\zeta})$$

writing $\theta = \arg(\zeta - \omega_o)$ so that $(if \quad r \equiv r(\omega_o, \tilde{\zeta}))$

$$\frac{x - x_o}{r} = \cos\theta \quad \text{and} \quad \frac{y - y_o}{r} = \sin\theta$$

one obtains

$$\frac{\partial}{\partial n_o} r(\omega_o, \tilde{\zeta}) = - \{ \cos\theta \cos[\alpha(\tilde{\omega}_o)] + \sin\theta \sin[\alpha(\omega_o)] \}$$

$$= - \cos[\theta - \alpha(\tilde{\omega}_o)]$$

which is Hölder continuous on C_1 and equals zero at $\zeta = \omega_o$ where $\theta = \alpha(\tilde{\omega}_o) + \pi/2$.

That a solution to equation (2.12) exists and is unique can be obtained from the first of the Fredholm alternatives, viz. either the equation of the second kind has a unique solution or the corresponding homogeneous equation and its adjoint have at least one non-trivial solution [5, p.58] . The homogeneous form of (2.12) is

$$\varphi_3(\tilde{\omega}_o) - \frac{1}{\pi} \int_{C_1} \varphi_3(\tilde{\zeta}) \, K(\tilde{\omega}_o, \tilde{\zeta}) \, ds = 0$$

which has as its adjoint the equation

$$\lambda(\tilde{\omega}_0) - \frac{1}{\pi}\int_{C_1} \lambda(\tilde{\tau})\, K(\tilde{\tau}, \tilde{\omega}_0)\, ds = 0 .$$

This last equation is the homogeneous form of the integral obtained from the representation of the solution to Laplace's equation, with Dirichlet type boundary conditions on C_1, by a double-layer potential of unknown density $\lambda(\tilde{\tau})$ [15, pp.32-33]. The equation is known to have only the trivial solution $\lambda(\tilde{\tau}) = 0$ so that, by the previously given Fredholm alternative, the solution $\varphi_3(\tilde{\tau})$ of (2.12) is unique.

It should be noted that an integral equation of the first kind for $\varphi_3(\tilde{\tau})$ is obtained by taking the imaginary part of (2.12). In the notation used previously this equation takes the form

$$\frac{1}{\pi}\int_{C_1} \varphi_3(\tilde{\tau})\, H(\tilde{\omega}_0, \tilde{\tau})\, ds = \frac{1}{\pi}\int_{C_1} \varphi_n(\tilde{\tau})\, K(\omega_0, \tau)\, ds - \varphi_n(\tilde{\omega}_0)$$

$$+ \frac{1}{\pi}\iint_R f(\tilde{\tau})\, K(\tilde{\omega}_0, \tilde{\tau})\, dx\, dy$$

but will not be considered further since a comprehensive theory for equations of this type does not appear to be available.

Note further that for problems in which the function $\varphi(x,y)$ satisfies Laplace's equation in R, i.e.

$$\Delta\, \varphi(x,y) = 0 \quad ; \quad x, y \in R$$

equation (2.12) takes the form

$$\varphi_3(\tilde{\omega}_0) - \frac{1}{\pi}\int_{C_1} \varphi_3(\tilde{\tau})\, K(\tilde{\omega}_0, \tilde{\tau})\, ds = \frac{1}{\pi}\int_{C_1} \varphi_n(\tilde{\tau})\, H(\tilde{\omega}_0, \tilde{\tau})\, ds .$$

§ 2.3) Integral equation for a finite multiply connected region

In the following let the m contours bounding a finite multiply connected region R be identified by C_p, $p=1\ (1)\ m$, with C_1 enclosing all the others. This nomenclature is illustrated by Figure 2-4.

The required integral identity for $\tau(\tilde{\omega})$ when ω lies entirely within the region R is obtained in an analogous way to that used previously. The procedure may be summarised in the following manner:-

i) exclude the point ω from the region R by a small circle centred on ω

ii) apply the complex forms of Green's theorem to the function

$$F(\tilde{\zeta},\omega) = \frac{\tau(\tilde{\zeta})}{\zeta-\omega}$$

defined over the modified region

iii) evaluate the contributions to the various integrals when the radius of the circle excluding ω shrinks to zero.

In this way the representation

$$\tau(\tilde{\omega}) = \frac{1}{2\pi i}\sum_{p=1}^{m}\int_{C_p}\frac{\tau(\tilde{\zeta})}{\zeta-\omega}\,d\zeta - \frac{1}{\pi}\iint_R\frac{\tau_{\bar{\zeta}}(\tilde{\zeta})}{\zeta-\omega}\,dx\,dy$$

is obtained.

Similarly, a repeat of the limiting process of the preceding section on the above identity shows that when ω tends to a boundary point ω_0 from inside R.

$$\tau(\tilde{\omega}_0) = \frac{1}{\gamma_0 i}\sum_{p=1}^{m}\int_{C_p}\frac{\tau(\tilde{\zeta})}{\zeta-\omega_0}\,d\zeta - \frac{2}{\gamma_0}\iint_R\frac{\tau_{\bar{\zeta}}(\tilde{\zeta})}{\zeta-\omega_0}\,dx\,dy.$$

The boundary conditions are again incorporated by use of the relations (2.9),

i.e. $$\tau(\tilde{\zeta})\,d\zeta = \{\varphi_s(\tilde{\zeta}) + i\,\varphi_n(\tilde{\zeta})\}\,ds$$

$$i\,\tau(\tilde{\zeta})\,e^{i\alpha(\tilde{\zeta})} = \varphi_s(\tilde{\zeta}) + i\,\varphi_n(\tilde{\zeta}).$$

Hence, for $\omega \epsilon R$, $\tau(\tilde{\omega})$ may be generated from

$$\tau(\tilde{\omega}) = \frac{1}{2\pi i} \sum_{p=1}^{m} \int_{C_p} \frac{\varphi_s(\tilde{\gamma}) + i\varphi_n(\tilde{\gamma})}{\gamma - \omega} ds - \frac{1}{\pi} \iint_R \frac{\tau_{\bar{\gamma}}(\gamma)}{\gamma - \omega} dx\,dy$$

while the integral equation

$$\varphi_s(\tilde{\omega}_0) - \frac{1}{\pi} \sum_{p=1}^{m} \int_{C_p} \varphi_s(\tilde{\gamma})\ K(\tilde{\omega}_0, \tilde{\gamma})\, ds$$

$$= \frac{1}{\pi} \sum_{p=1}^{m} \int_{C_p} \varphi_n(\tilde{\gamma})\ H(\tilde{\omega}_0, \tilde{\gamma})\, ds - \frac{1}{\pi} \iint_R f(\tilde{\gamma})\, H(\tilde{\omega}_0, \tilde{\gamma})\, dx dy \qquad \ldots\ldots \quad (2.16)$$

may be used to find $\varphi_s(\tilde{\omega}_0)$, the required tangential derivative, for all ω_0 on smooth boundaries. As before,

$$K(\tilde{\omega}_0, \tilde{\gamma}) = \frac{(x - x_0)\cos[\alpha(\tilde{\omega}_0)] + (y - y_0)\sin[\alpha(\tilde{\omega}_0)]}{(x - x_0)^2 + (y - y_0)^2}$$

$$H(\omega_0, \tilde{\gamma}) = \frac{(y - y_0)\cos[\alpha(\tilde{\omega}_0)] - (x - x_0)\sin[\alpha(\tilde{\omega}_0)]}{(x - x_0)^2 + (y - y_0)^2}$$

and

$$f(\tilde{\gamma}) = \Delta\varphi(x, y) = 2\,\tau_{\bar{\gamma}}(\tilde{\gamma}).$$

Equation (2.16) was recently given by Kermanidis [26] for the case when $f(\tilde{\gamma}) = 0$ and $\varphi_n(\tilde{\gamma})$ is the boundary normal derivative of the warping function occurring in pure torsion (see Chapter 6). The derivation given by Kermanidis is based on the superposition technique mentioned at the beginning of this chapter.

Again, when (2.16) defines a linear problem the equation may be considered as a Fredholm integral equation of the second kind for the unknown values of the boundary tangential derivative $\varphi_s(\tilde{\gamma})$. The homogeneous form of this equation is

$$\phi_s(\tilde{\omega}_0) - \frac{1}{\pi} \sum_{p=1}^{m} \int_{C_p} \phi_s(\tilde{z}) K(\tilde{\omega}_0, \tilde{z}) \, ds = 0$$

which has as its adjoint

$$\lambda(\tilde{\omega}_0) - \frac{1}{\pi} \sum_{p=1}^{m} \int_{C_p} \lambda(\tilde{z}) K(\tilde{z}, \tilde{\omega}_0) \, ds = 0 \qquad (2.17).$$

The equation (2.17) may be written as

$$\lambda(\omega_0) + \frac{1}{\pi} \sum_{p=1}^{m} \int_{C_p} \lambda(\tilde{z}) \frac{\partial}{\partial n} \log |z - \omega_0| \, ds = 0$$

where $\frac{\partial}{\partial n} \log |z-\omega_0|$ denotes the normal derivative of the function $\log |z-\omega_0|$ keeping ω_0 fixed and, since

$$\int_{C_p} \frac{\partial}{\partial n} \log |z-\omega_0| \, ds = \begin{cases} \pi & \text{for } \omega_0 \in C_1 \\ -\pi & \text{for } \omega_0 \in C_p, \; p \neq 1 \end{cases}$$

it follows that (2.17) admits the non-trivial solutions

$$\lambda(\tilde{z}) = \lambda_p \qquad (2.18)$$

where

$$\lambda_p = \begin{cases} \text{constant} & \text{for } z \in C_p, \; p \neq 1 \\ 0 & \text{otherwise} \end{cases}.$$

This result could also have been obtained from the observation that the equation

$$\lambda(\tilde{\omega}_0) + \frac{1}{\pi} \int_{C_p} \lambda(\tilde{z}) \frac{\partial}{\partial n} \log |z-\omega_0| \, ds = 0; \quad \omega_0 \in C_p, \; p \neq 1$$

corresponds to the homogeneous form of the double layer potential representation of a function harmonic in an infinite region bounded internally by C_p and which takes prescribed values on C_p. The solution of this problem

is known to be unique to within an arbitrary additive constant [15, pp.32-33] from which the uniqueness of the solutions (2.18) follows.

The relevant Fredholm theorems to be applied here are that:-

i) the homogeneous integral equation and its adjoint have the same finite number of linearly independent solutions

ii) a necessary and sufficient condition for the existence of a solution to the non-homogeneous integral equation is that its free term be orthogonal to any solution of the homogeneous adjoint equation [5, p.58].

From this one may conclude that the homogeneous form of (2.16) has m-1 linearly independent, non-trivial solutions while solutions to (2.16) exist provided that for $p = 2(1)m$

$$\lambda_p \int_{C_p} \left\{ \sum_{q=1}^{m} \int_{C_q} \varphi_n(\tilde{\tau}) H(\tilde{\omega}_p, \tilde{\tau}) \, ds - \iint_R f(\tilde{\tau}) H(\tilde{\omega}_p, \tilde{\tau}) \, dx \, dy \right\} ds_p = 0 \qquad (2.19)$$

where $\omega_p \in C_p$ and ds_p denotes the arc differential at ω_p.

The major application of equation (2.16) has been to the solution of Laplace's equation under Neumann type boundary conditions. For such problems it is readily shown that the orthogonality condition (2.19) is obeyed since

$$\frac{1}{\pi} \int_{C_p} \left\{ \sum_{q=1}^{m} \int_{C_q} \varphi_n(\tilde{\tau}) H(\tilde{\omega}_p, \tilde{\tau}) \, ds \right\} ds_p$$

$$= \int_{C_p} \left\{ \varphi_s(\tilde{\omega}_p) - \frac{1}{\pi} \sum_{q=1}^{m} \int_{C_q} \varphi_s(\tilde{\tau}) K(\tilde{\omega}_p, \tilde{\tau}) \, ds \right\} ds_p$$

$$= \left[\varphi(\omega_p) \right]_{C_p} - \frac{1}{\pi} \sum_{q=1}^{m} \int_{C_q} \varphi_s(\tilde{\tau}) \left\{ \int_{C_p} K(\tilde{\omega}_p, \tilde{\tau}) \, ds_p \right\} ds$$

by Fubini's theorem [38, pp.221-222]. Now for

$$\int_{C_p} K(\tilde{\omega}_p, \tilde{\gamma})\, ds_p = -\int_{C_p} \frac{\partial}{\partial n} \log|\gamma - \omega_p|\, ds_p$$

$$= \begin{cases} \pi & \text{for } \gamma \in C_p \\ 0 & \text{otherwise.} \end{cases}$$

Hence

$$\frac{1}{\pi}\int_{C_p}\left\{\sum_{q=1}^{m}\int_{C_q} \varphi_n(\tilde{\gamma})\, H(\tilde{\omega}_p, \tilde{\gamma})\, ds\right\} ds_p$$

$$= \left[\varphi(\tilde{\omega}_p)\right]_{C_p} - \int_{C_p} \varphi_s(\tilde{\gamma})\, ds$$

$$= 0$$

and the orthogonality condition is satisfied.

It should be noted that a unique solution to the equation

$$\varphi_s(\tilde{\omega}_0) - \frac{1}{\pi}\sum_{p=1}^{m}\int_{C_p} \varphi_s(\tilde{\gamma})\, K(\tilde{\omega}_0, \tilde{\gamma})\, ds$$

$$= \frac{1}{\pi}\sum_{p=1}^{m}\int_{C_p} \varphi_n(\tilde{\gamma})\, H(\tilde{\omega}_0, \tilde{\gamma})\, ds$$

can be obtained by requiring that for $p = 2\,(1)\,m$

$$\int_{C_p} \varphi_s(\gamma)\, ds = \text{constant}.$$

Here the constant is chosen to give a harmonic function that is single or multi-valued as required.

§ 2.4) Integral equation for an infinite region with internal boundaries

The case of an infinite region with internal boundaries can be treated in a manner analogous to that of the preceding section when the functions $\tau(\tilde{\zeta}), \tau_{\bar{\zeta}}(\tilde{\zeta})$ tend to a finite limit as $|\zeta|$ increases. In the case under consideration, the multiply connected region is of the form shown in Figure 2-5 where the contour C_1 is taken to be a circle which encloses the remaining contours.

The required integral equation for the tangential derivative $\varphi_s(\tilde{\zeta})$ on the internal boundaries is obtained by letting the radius of C_1 tend to infinity. Hence, if

$$\lim_{|\zeta|\to\infty} \tau(\tilde{\zeta}) = \sigma$$

where σ is a known complex constant, equation (2.16) is readily shown to take the form

$$\varphi_s(\tilde{\omega}_0) - \frac{1}{\pi}\sum_{p=2}^{m}\int_{C_p} \varphi_s(\tilde{\zeta})\, K(\tilde{\omega}_0,\tilde{\zeta})\, ds + 2\,\mathrm{Im}\left\{\sigma e^{i\alpha(\tilde{\omega}_0)}\right\}$$

$$= \frac{1}{\pi}\sum_{p=2}^{m}\int_{C_p} \varphi_n(\tilde{\zeta})\, H(\tilde{\omega}_0,\tilde{\zeta})\, ds - \frac{1}{\pi}\iint_R f(\tilde{\zeta})\, H(\tilde{\omega}_0,\tilde{\zeta})\, dx\, dy \qquad \ldots\ldots (2.20)$$

where $K(\tilde{\omega}_0,\tilde{\zeta})$, $H(\tilde{\omega}_0,\tilde{\zeta})$, $f(\tilde{\zeta})$ are given by (2.13), (2.14), (2.15) respectively and the contour integrals are taken in the positive sense (i.e. clockwise since this an exterior problem). The integral identity corresponding to (2.20) for a point ω which lies entirely within R can similarly be shown to be

$$\tau(\tilde{\omega}) = \sigma + \frac{1}{2\pi i}\sum_{p=2}^{m}\int_{C_p} \frac{\varphi_s(\tilde{\zeta}) + i\varphi_n(\tilde{\zeta})}{\zeta - \omega}\, ds$$

$$- \frac{1}{\pi}\iint_R \frac{\tau_{\bar{\zeta}}(\zeta)}{\zeta-\omega}\, dx\, dy \qquad (2.21).$$

Because of the manner in which (2.20) was obtained, the remarks concerning the existence and non-uniqueness of solutions to (2.16) are again applicable. Hence it can be concluded that the homogeneous form of (2.20) has $m-1$ non-trivial solutions and that solutions to (2.20) exist whenever

$$\int_{C_p} \left\{ \sum_{q=2}^{m} \int_{C_q} \varphi_n(\tilde{\tau}) H(\tilde{\omega}_p, \tilde{\tau})\, ds - \iint_R f(\tilde{\tau})\, H(\tilde{\omega}_p, \tilde{\tau})\, dx\, dy \right\} ds_p$$

$$= 2 \int_{C_p} Im \left\{ \sigma e^{i\alpha(\tilde{\omega}_p)} \right\} ds_p \quad , \quad p = 2(1)m .$$

Clearly, this last identity is satisfied whenever $\varphi_n(\tilde{\tau})$ is the boundary normal derivative of a function which is harmonic in the infinite region R and satisfies

$$\lim_{|\tilde{\tau}| \to \infty} \quad \tau(\tilde{\tau}) = \text{constant}.$$

An equation similar to (2.20) has previously been given by Payne [21, pp.1-40] for the analysis of the compressible flow through a plane, infinite cascade of aerofoils where a coth kernel function replaces the $(\tau - \omega)^{-1}$ used above. Indeed, Payne shows how the form of (2.20) appropriate to the analysis of the plane incompressible flow past a plane isolated aerofoil, i.e.

$$\varphi_s(\tilde{\omega}) - \frac{1}{\pi} \int_C \varphi_s(\tilde{\tau}) K(\tilde{\omega}, \tilde{\tau})\, ds = -2\, Im \left\{ \sigma e^{i\alpha(\tilde{\omega})} \right\}$$

where C is the contour bounding the aerofoil, can be obtained by considering a cascade with infinite pitch.

§ 2.5) Integral equation for a vertical cascade of aerofoils

In two dimensions a vertical cascade of aerofoils consists of an infinite number of congruent aerofoils equally spaced in the y-direction of the complex ζ-plane. Each of the aerofoils is assumed bounded by a simple closed curve with a continuously turning tangent except, possibly, at the trailing edge where profile may be cusped or pointed. A typical cascade geometry, centred on the profile C_0, is illustrated in Figure 2-6.

Restricting attention to Neumann type problems defined on the region bounded internally by the aerofoils, the required integral equation for the values which $\varphi_s(\tilde{\zeta})$ takes on each of the profiles is readily obtained using a technique analogous to that used in § 2.4).

Consider the region R shown in Figure 2-7 which is bounded on the inside by 2m+1 congruent aerofoils and has for its external boundary the contour ABCDA. The 2m+1 aerofoils are equally spaced in the y-direction (with pitch t) and are centred on the aerofoil C_0. For such a region it was shown in § 2.3) that when ω lies entirely within R, i.e. not on any of the bounding contours, the analytic function $\tau(\zeta)$ may be evaluated at ω by

$$\tau(\omega) = \frac{1}{2\pi i} \sum_{p=-m}^{m} \int_{C_p} \frac{\tau(\zeta)}{\zeta - \omega} d\zeta + \frac{1}{2\pi i} \int_{ABCDA} \frac{\tau(\zeta) d\zeta}{\zeta - \omega} \qquad (2.22)$$

Clearly this is just Cauchy's integral formula applied over the region R.

Imposing the conditions that

i) for $\zeta \in C_0$ $\quad \tau(\zeta) = \tau(\zeta + pit)$; $p = \pm 1, \pm 2, \ldots, \pm m$

ii) for $\zeta \in AB$ $\quad \tau(\zeta) = \tau(\zeta + (2m+1)it)$

iii) for $\zeta = X + iy \in BC$ $\quad \tau(\zeta) =$ constant , τ_D say

iv) for $\gamma = -X + iy \in DA$ $\tau(\gamma) = \text{constant}$, τ_u say the identity (2.22) may be written as

$$\tau(\omega) = \frac{1}{2\pi i}\int_{C_0} \tau(\gamma)\left\{\sum_{p=-m}^{m} \frac{1}{\gamma - \omega + pit}\right\} d\gamma$$

$$+ \frac{1}{2\pi}\,\tau_D \int_{-t/2}^{t/2}\left\{\sum_{p=-m}^{m} \frac{1}{X + i(y+pt) - \omega}\right\} dy$$

$$- \frac{1}{2\pi}\,\tau_u \int_{-t/2}^{t/2}\left\{\sum_{p=-m}^{m} \frac{1}{i(y+pt) - X - \omega}\right\} dy.$$

The terms in the series

$$\sum_{p=-m}^{m} \frac{1}{\gamma - \omega + pit}$$

may be re-arranged to give

$$\sum_{p=-m}^{m} \frac{1}{\gamma - \omega + pit} = \frac{1}{\gamma - \omega} + \sum_{p=1}^{m} \frac{2(\gamma - \omega)}{(\gamma - \omega)^2 + p^2 t^2}$$

When $m \to \infty$ (as it must do for a verical cascade of the type considered here) this series can be summed using complex variable techniques [40, pp.133-135] whence

$$\lim_{m\to\infty} \sum_{p=-m}^{m} \frac{1}{\gamma - \omega + pit} = \frac{\pi}{t} \coth\left\{\frac{\pi}{t}(\gamma - \omega)\right\}$$

and therefore

$$\tau(\omega) = \frac{1}{2\pi i}\int_{C_0} \tau(\xi)\coth\left\{\frac{\pi}{t}(\omega-\xi)\right\}d\xi$$

$$+\frac{1}{2t}\tau_D\int_{-t/2}^{t/2}\coth\left\{\frac{\pi}{t}(X+iy-\omega)\right\}dy$$

$$-\frac{1}{2t}\tau_u\int_{-t/2}^{t/2}\coth\left\{\frac{\pi}{t}(-X+iy-\omega)\right\}dy \qquad (2.23).$$

To obtain an integral identity analagous to (2.21) when an infinite region R is bounded internally by a vertical cascade of aerofoils it remains to consider the behaviour of (2.23) when $X \to \infty$

Consider the function

$$\coth\{z\} = \frac{e^{z}+e^{-z}}{e^{z}-e^{-z}}$$

$$= \frac{1+e^{-2z}}{1-e^{-2z}}$$

For $Re(z)>0$ the denominator of this function may be expanded by the binominal series so that

$$\coth\{z\} = (1+e^{-2z})\sum_{n=0}^{\infty} e^{-2nz}$$

$$= 1 + 2\sum_{n=1}^{\infty} e^{-2nz}$$

Similarly, for $Re(z) > 0$

$$\coth\{-z\} = -1 - 2\sum_{n=1}^{\infty} e^{-2nz}.$$

Using these expressions for $\coth\{\frac{\pi}{t}(x+iy-\omega)\}$ and $\coth\{\frac{\pi}{t}(-x+iy-\omega)\}$ in (2.23) yields, when $X \to \infty$

$$\tau(\omega) = \frac{1}{2ti}\int_{C_0} \coth\{\frac{\pi}{t}(\gamma-\omega)\}\tau(\gamma)\,d\gamma + \frac{1}{2}\{\tau_u + \tau_0\} \qquad (2.24).$$

The above expansions for $\coth\{\pm Z\}$ can also be used to show that

$$\lim_{Re(\omega)\to\pm\infty} \tau(\omega) = \frac{1}{2}\{\tau_u+\tau_0\} \mp \frac{1}{2ti}\int_{C_0}\tau(\gamma)\,d\gamma$$

i.e.

$$\int_{C_0}\tau(\gamma)\,d\gamma = \pm i\{\tau_u - \tau_0\} \qquad (2.25).$$

That $\tau(\omega)$ is periodic with period it (as it must be for the vertical cascade considered here) can be shown by substituting $\omega \pm it$ for ω in (2.24). The result follows on using the relation

$$\coth\{a\pm ib\} = \frac{\cosh a\cos b \pm i\sinh a\sin b}{\sinh a\cos b \pm i\cosh a\sin b}$$

and noting that in this instance $b = \pi$.

The required integral equation for $\phi_s(\tilde{\gamma})$ on C_0 is obtained by considering the limiting form of (2.24) as ω tends to a point $\omega_0 \in C_0$ from inside R (outside the region bounded externally by C_0). Without repeating the analysis of the previous sections (notably § 2.2) it can be shown that

$$\tau(\omega_0) = \tau_u + \tau_D + \frac{1}{ti}\int_{C_0}\tau(\gamma)\coth\{\frac{\pi}{t}(\gamma-\omega)\}\,d\gamma \qquad (2.26)$$

provided that ω_0 is neither a cusp nor a corner.

The relations

$$i\,\tau(\omega_0)\,e^{i\alpha(\tilde{\omega}_0)} = \varphi_s(\tilde{\omega}_0) + i\,\varphi_n(\tilde{\omega}_0)$$

$$\tau(\gamma)\,d\gamma = \{\varphi_s(\tilde{\gamma}) + i\,\varphi_n(\tilde{\gamma})\}\,ds$$

again hold on C_0 so that from (2.26) the identity

$$\varphi_s(\tilde{\omega}_0) + i\,\varphi_n(\tilde{\omega}_0) = i e^{i\alpha(\tilde{\omega}_0)}\{\tau_u + \tau_0\}$$

$$+ \frac{e^{i\alpha(\tilde{\omega}_0)}}{t}\int_{C_0}\{\varphi_s(\tilde{\gamma}) + i\varphi_n(\tilde{\gamma})\}\coth\left\{\frac{\pi}{t}(\gamma-\omega)\right\} \quad (2.27)$$

can be obtained.

As in the preceding sections of this chapter, the identity (2.27) can be split into its real and imaginary parts to give integral equations (for $\varphi_s(\tilde{\omega}_0)$, $\omega_0 \in C_0$) of the second and first kinds respectively. In the case of the second kind equation, use of the expansion

$$\frac{\pi}{t}\coth\left\{\frac{\pi}{t}(\gamma-\omega)\right\} = \frac{1}{\gamma-\omega} + \sum_{p=1}^{\infty}\frac{2(\gamma-\omega)}{(\gamma-\omega)^2 + p^2t^2}$$

shows that the kernel of this integral equation is weakly singular so that the previously mentioned Fredholm theorems can be applied.

In view of the manner in which the identity (2.27) was derived, i.e. extending the derivation used in §2.3), one may conclude that solutions to the real part of (2.27) are not unique. Since the homogeneous form of the equation has one non-trivial solution, the condition

$$\int_{C_0}\varphi_s(\tilde{\gamma})\,d\gamma = \text{constant}$$

can be used to constrain the integral equation so that

$\varphi_s(\tilde{\omega}_0)$, $\omega_0 \in C_0$, is the boundary tangential derivative of a harmonic function which is single or multi valued as required.

That the real part of (2.27) provides the basic equation used in a Martensen type analysis of the flow through a vertical cascade [21, 23, 27] is noted.

§ 2.6) Treatment of Neumann problems in regions bounded by contours with corners

The existence theory used in the preceding sections has been developed specifically for problems defined over regions bounded by smooth contours. In practice, the boundary of a region may contain corners where the direction cosines $\cos(x,n)$ and $\cos(y,n)$ are discontinuous. It follows from this that the kernel function $K(\tilde{\omega}_0,\tilde{\tau})$ given by (2.13) will no longer be weakly singular so that the Fredholm theorems cannot be applied to the derived integral equations.

A further problem arises from the fact (seen below) that the derivatives $\varphi_x(\tilde{\omega})$, $\varphi_y(\tilde{\omega})$ may be singular at a re-entrant corner ω . In this case the required integral equations cannot be derived since the function

$$\tau(\tilde{\tau}) = \varphi_x(\tilde{\tau}) - i\,\varphi_y(\tilde{\tau})$$

is no longer continuous and the complex forms of Green's theorems cannot be applied.

Some progress can be made if one assumes that the function $\varphi(x,y)$ has a known representation $\chi(x,y)$ at each of the corners. Consider the simply connected region shown in Figure 2-8, which has a corner at τ_1 , and assume that in the neighbourhood of τ_1 the functions $\varphi_n(\tilde{\tau})$, $f(\tilde{\tau})$, $\varphi_s(\tilde{\tau})$ can be represented by the functions $\chi_n(\tilde{\tau})$, $\Delta\chi(x,y)$, $\chi_s(\tilde{\tau})$ respectively. With this notation the equation (2.12) may, for $\omega_0 \neq \tau_1$ be written as

$$\hat{\varphi}_s(\tilde{\omega}_0) - \frac{1}{\pi}\int_{C_1} \hat{\varphi}_s(\tilde{\tau})\,K(\omega_0,\tau)\,ds$$

$$= \frac{1}{\pi}\int_{C_1} \hat{\varphi}_n(\tilde{\tau})\,H(\tilde{\omega}_0,\tilde{\tau})\,ds - \frac{1}{\pi}\iint_R \hat{f}(\tilde{\tau})H(\tilde{\omega}_0,\tilde{\tau})\,dx\,dy \qquad (2.28)$$

where $\hat{\phi}_s(\tilde{\tau}) = \phi_s(\tilde{\tau}) - \chi_s(\tilde{\tau})$, $\hat{\phi}_n(\tilde{\tau}) = \phi_n(\tilde{\tau}) - \chi_n(\tilde{\tau})$
and $\hat{f}(\tilde{\tau}) = f(\tilde{\tau}) - \Delta\chi(x,y)$.
The kernel $K(\tilde{\omega}_0, \tilde{\tau})$ of equation (2.28) is once more weakly singular for all $\omega_0 \neq \tau_1$, so that the previously applied Fredholm theory is again applicable (in this instance (2.28) can be written as a system of integral equations). It remains to choose the representation $\chi(x,y)$.

Although the practical details of choosing $\chi(x,y)$ for the case when $\phi_s(\tilde{\tau})$ is the boundary tangential derivative of a harmonic function will be dealt with in some detail in the next chapter, some relevant comment follows.

Consider the function

$$u(\tilde{\tau}) = \sum_{n=0}^{\infty} a_n \rho^{\frac{n\pi}{\gamma}} \cos\left\{\frac{n\pi\theta}{\gamma}\right\} \qquad (2.29)$$

where $\tau - \tau_1 = \rho e^{i\theta}$ and γ is the "interior" angle between tangents on either side of τ_1. This function has zero normal derivative on the arcs $\tau_1\tau_A$, $\tau_1\tau_B$ for all values of γ while its tangential derivative may have a singularity of the type

$$\rho^{\frac{\pi}{\gamma}-1}$$

when $\gamma > \pi$.

Clearly the function $\chi(x,y)$ must be such that the above type of singularity can be modelled when $\gamma > \pi$. Furthermore, consideration of $u(\tilde{\tau})$ shows that the two partial derivatives $\varphi_x(\tilde{\tau})$, $\varphi_y(\tilde{\tau})$ are continuous when $\gamma < \pi$ and, for $\gamma < \pi$, can be obtained explicitly at τ_1 when $\phi_n(\tilde{\tau}_1)$ is specified (see § 3.8).

From the above it can be concluded that the behaviour of $\phi_s(\tilde{\tau})$ at the corner τ_1 can be modelled by the function

$$\chi_s(\tilde{\tau}) = u_s(\tilde{\tau}) + v_s(\tilde{\tau})$$

where $U_s(\tilde{\tau})$ is the boundary tangential derivative of (2.29) and $V_s(\tilde{\tau})$ takes the values of $\varphi_s(\tilde{\tau})$ evaluated under the assumption that $\varphi_x(\tilde{\tau})$, $\varphi_y(\tilde{\tau})$ are continuous at τ_1. The function $\chi_s(\tilde{\tau})$ is also applicable to the case when τ_1 lies on one of the contours bounding a multiply connected region.

When there is more than one corner to be considered, the function $\chi_s(\tilde{\tau})$ must be extended to allow for the possibility that $\varphi_s(\tilde{\tau})$ is singular at each corner where $\gamma > \pi$. Let there be a corner at τ_K where the "interior" angle between tangents on either side of τ_K is given by γ_K. When differentiated the function

$$u^{(K)}(\tilde{\tau}) = \sum_{n=0}^{\infty} a_n^{(K)} \rho_K^{\frac{n\pi}{\gamma_K}} \cos\left\{\frac{n\pi\theta_K}{\gamma_K}\right\} \qquad (2.30),$$

where

$$\tau - \tau_K = \rho_K e^{i\theta_K},$$

will model the possible singularity in $\varphi_s(\tilde{\tau})$ at τ_K. Hence, if the contour bounding R has corners at τ_K, $k = 1(1)S$, the function $\chi_s(\tilde{\tau})$ may be taken to be

$$\chi_s(\tilde{\tau}) = \sum_{K=1}^{S} U_s^{(K)}(\tilde{\tau}) + V_s(\tilde{\tau}) \qquad (2.31)$$

where $U_s^{(K)}(\tilde{\tau})$ is the boundary tangential derivative of (2.30) and $V_s(\tilde{\tau})$ is a function which takes at each of the τ_K the value of $\varphi_s(\tilde{\tau})$ evaluated under the assumption that $\varphi_x(\tilde{\tau})$, $\varphi_y(\tilde{\tau})$ are continuous.

Finally, it should be noted that when $\varphi_x(\tilde{\tau})$ and $\varphi_y(\tilde{\tau})$ are continuous at the τ_K and bounded elsewhere on the boundaries of a finite multiply connected region R, the analysis of § 2.2) and § 2.3) leads to the identity

$$\varphi_s(\tilde{\tau}_K) - \frac{1}{\gamma_K} \sum_{p=1}^{m} \int_{C_p} \varphi_s(\tilde{\tau}) K(\tilde{\tau}_K, \tilde{\tau})\, ds$$

$$= \frac{1}{\gamma_K} \sum_{p=1}^{m} \int_{C_p} \varphi_n(\tau) H(\tilde{\tau}_K, \tilde{\tau})\, ds$$

where $\varphi_s(\tilde{\tau}_K)$ is a double valued.

This identity relates to harmonic problems only and can be extended to the cases when the region is infinite and has internal boundaries. For the reasons previously related, these identities should not be considered as integral equations yielding $\phi_3(\tilde{r})$ at the r_{ik}.

Chapter 3

NUMERICAL SOLUTION OF THE DERIVED INTEGRAL EQUATIONS WHEN THE NUMBER OF BOUNDING CONTOURS IS FINITE

§ 3.1) Introduction

When considering such physical problems as torsion, flexure and plane irrotational flow, the solution of the integral equations derived in Chapter 2 by any means other than numerical could be expected to present considerable difficulties for even the simplest of regions. Indeed, it is unlikely that one would even formulate a problem in terms of these boundary integral equations if the problem was such that a closed form solution was obtainable.

However, numerical techniques for the solution of these boundary integral equations do become important when consideration is given to problems defined on complex geometries such as occur in turbomachinery applications. The numerical techniques developed by the author and presented here make full use of the complex variables formulations given in the preceeding chapter. These techniques are in fact an adaptation of Atkinson's numerical method for evaluating Cauchy integrals [28] and are analogous to those used by Hamson for solving Dirichlet problems by means of a potential of the double layer [19].

For convenience the numerical techniques are described in detail for a finite multiply connected region. The modifications required when dealing with an infinite region bounded by a finite number of contours are given in §3.10).

Consistent with the manner in which the integral equations of the preceeding chapter were obtained, numerical solutions to these integral equations have been found by working with the complex equation

$$\varphi_s(\tilde{\omega}) + i\,\varphi_n(\tilde{\omega}) = \frac{e^{i\alpha(\tilde{\omega})}}{\pi} \int_C \frac{\varphi_s(\tilde{\sigma}) + i\,\varphi_n(\tilde{\sigma})}{\sigma - \omega}\, ds \qquad (3.1)$$

rather than its real variable counterpart. Noting the relations on C

$$i\,\tau(\omega)\, e^{i\alpha(\tilde{\omega})} = \varphi_s(\tilde{\omega}) + i\,\varphi_n(\tilde{\omega}) \qquad (3.2),$$

Chapter 3

NUMERICAL SOLUTION OF THE DERIVED INTEGRAL EQUATIONS WHEN THE NUMBER OF BOUNDING CONTOURS IS FINITE

§ 3.1) Introduction

When considering such physical problems as torsion, flexure and plane irrotational flow, the solution of the integral equations derived in Chapter 2 by any means other than numerical could be expected to present considerable difficulties for even the simplest of regions. Indeed, it is unlikely that one would even formulate a problem in terms of these boundary integral equations if the problem was such that a closed form solution was obtainable.

However, numerical techniques for the solution of these boundary integral equations do become important when consideration is given to problems defined on complex geometries such as occur in turbomachinery applications. The numerical techniques developed by the author and presented here make full use of the complex variables formulations given in the preceeding chapter. These techniques are in fact an adaptation of Atkinson's numerical method for evaluating Cauchy integrals [28] and are analogous to those used by Hamson for solving Dirichlet problems by means of a potential of the double layer [19].

For convenience the numerical techniques are described in detail for a finite multiply connected region. The modifications required when dealing with an infinite region bounded by a finite number of contours are given in §3.10).

Consistent with the manner in which the integral equations of the preceeding chapter were obtained, numerical solutions to these integral equations have been found by working with the complex equation

$$\varphi_s(\tilde{\omega}) + i\,\varphi_n(\tilde{\omega}) = \frac{e^{i\alpha(\tilde{\omega})}}{\pi} \int_C \frac{\varphi_s(\tilde{\gamma}) + i\,\varphi_n(\tilde{\gamma})}{\gamma - \omega}\, ds \qquad (3.1)$$

rather than its real variable counterpart. Noting the relations on C

$$i\,\tau(\omega)\, e^{i\alpha(\tilde{\omega})} = \varphi_s(\tilde{\omega}) + i\,\varphi_n(\tilde{\omega}) \qquad (3.2),$$

where $\tau(\omega) = \varphi_x(\tilde{\omega}) - i\,\varphi_y(\tilde{\omega})$ and

$$\tau(\gamma)\frac{d\gamma}{ds} = \varphi_s(\tilde{\gamma}) + i\,\varphi_n(\tilde{\gamma}) \qquad (3.3),$$

it will be recalled that (3.1) may be written as

$$\tau(\omega) = \frac{1}{\pi i}\int_C \frac{\tau(\gamma)}{\gamma-\omega}\,d\gamma \qquad (3.4).$$

It should also be noted that the boundary condition is that the normal derivative $\varphi_n(\tilde{\gamma})$ be given on the boundary. In many applications the specification of this normal derivative requires that the direction of the (outward drawn) normal be known at a number of boundary points.

§ 3.2) Idealisation of boundary

Let the m contours bounding the region under consideration be identified by C_p, $p=1\ (1)m$, with C_1 enclosing all the others. Each of the C_p contours is considered to be divided into n_p intervals (termed elements) with an element end point (termed a node) as the only point common with adjacent elements. When the boundary is not smooth, the idealisation should be carried out in such a way that all corners lie at nodes. This ensures that all of the elements are smooth arcs.

Using this form of idealisation equation (3.4) can be written as

$$i\pi\tau(\omega) = \sum_{p=1}^{m}\sum_{q=1}^{n_p}\int_{I_{p,q}} \frac{\tau(\gamma)}{\gamma-\omega}\,d\gamma \qquad (3.5)$$

where $\int_{I_{p,q}}$ denotes integration over the q^{th} element of the p^{th} contour and the integral is taken in the positive sense.

A numerical solution of (3.1) is obtained by taking suitable approximations to $\tau(\gamma)$ over each of the elements $I_{p,q}$.

§ 3.3) Piecewise constant approximations

The simplest form of approximation to $\tau(\gamma)$, $\gamma \in C$, is obtained by assuming that $\tau(\gamma)$ takes the complex constant value $\tau_{p,q}$ over the element $I_{p,q}$ and attains this value at the point $\gamma_{p,q}$, $\gamma_{p,q} \in I_{p,q}$. Hence (3.5) may be written as

$$\tau(\omega) \simeq \frac{1}{\pi i}\sum_{p=1}^{m}\sum_{q=1}^{n_p}\tau_{p,q}\int_{I_{p,q}}\frac{d\gamma}{\gamma-\omega}$$

so that, on using (3.2), the relation

$$\varphi_s(\tilde{\omega}) + i\,\varphi_n(\tilde{\omega}) \simeq \frac{1}{\pi i} e^{i\alpha(\tilde{\omega})} \sum_{p=1}^{m} \sum_{q=1}^{n_p} \left\{ \varphi_s(\tilde{\gamma}_{p,q}) + i\,\varphi_n(\tilde{\gamma}_{p,q}) \right\} \Delta_{p,q}(\omega) \qquad \ldots\ldots \quad (3.6),$$

where

$$\Delta_{p,q}(\omega) = e^{-i\alpha(\tilde{\gamma}_{p,q})} \int_{I_{p,q}} \frac{d\gamma}{\gamma - \omega} \quad ,$$

is obtained.

On the element $I_{p,q}$ the point $\gamma_{p,q}$ can be specified arbitrarily provided it is chosen to lie away from the element's end-points. Usually the element's mid-point is chosen.

Once the $\gamma_{p,q}$ have been specified a system of complex linear equations for the unknown $\varphi_s(\tilde{\gamma}_{p,q})$ is obtained by neglecting the error in the approximation leading to (3.6) and identifying ω with each of the points $\gamma_{p,q}$. Since $\varphi_s(\tilde{\gamma})$ is real this complex system of equations can be decoupled into two real linear systems by taking its real and imaginary parts. Consistent with the manner in which the second kind integral equations of the preceding chapter were obtained, only the real part of the complex system of equations is considered here. Hence, if

$$A_{p,q}^{r,s} = Re\left\{ \Delta_{p,q}(\tilde{\gamma}_{r,s}) \right\}$$

$$B_{p,q}^{r,s} = Im\left\{ \Delta_{p,q}(\tilde{\gamma}_{r,s}) \right\}$$

the real system of linear equations

$$\varphi_s(\tilde{\gamma}_{r,s}) - \frac{1}{\pi} \sum_{p=1}^{m} \sum_{q=1}^{n_p} \varphi_s(\tilde{\gamma}_{p,q}) \left\{ \sin\left[\alpha(\tilde{\gamma}_{r,s})\right] A_{p,q}^{r,s} + \cos\left[\alpha(\tilde{\gamma}_{r,s})\right] B_{p,q}^{r,s} \right\}$$

$$= \frac{1}{\pi} \sum_{p=1}^{m} \sum_{q=1}^{n_p} \varphi_n(\tilde{\gamma}_{p,q}) \left\{ \cos\left[\alpha(\tilde{\gamma}_{r,s})\right] A_{p,q}^{r,s} - \sin\left[\alpha(\tilde{\gamma}_{r,s})\right] B_{p,q}^{r,s} \right\} \qquad (3.7)$$

which relate the known $\varphi_n(\tilde{\gamma}_{p,q})$ to the unkown $\varphi_s(\tilde{\gamma}_{p,q})$ is obtained.

so that, on using (3.2), the relation

$$\varphi_s(\tilde{\omega}) + i\,\varphi_n(\tilde{\omega}) \simeq \frac{1}{\pi i} e^{i\alpha(\tilde{\omega})} \sum_{p=1}^{m} \sum_{q=1}^{n_p} \left\{ \varphi_s(\tilde{\gamma}_{p,q}) + i\,\varphi_n(\tilde{\gamma}_{p,q}) \right\} \Delta_{p,q}(\omega) \qquad \ldots\ldots \quad (3.6),$$

where

$$\Delta_{p,q}(\omega) = e^{-i\alpha(\tilde{\gamma}_{p,q})} \int_{I_{p,q}} \frac{d\gamma}{\gamma - \omega} \quad ,$$

is obtained.

On the element $I_{p,q}$ the point $\gamma_{p,q}$ can be specified arbitrarily provided it is chosen to lie away from the element's end-points. Usually the element's mid-point is chosen.

Once the $\gamma_{p,q}$ have been specified a system of complex linear equations for the unknown $\varphi_s(\tilde{\gamma}_{p,q})$ is obtained by neglecting the error in the approximation leading to (3.6) and identifying ω with each of the points $\gamma_{p,q}$. Since $\varphi_s(\tilde{\gamma})$ is real this complex system of equations can be decoupled into two real linear systems by taking its real and imaginary parts. Consistent with the manner in which the second kind integral equations of the preceding chapter were obtained, only the real part of the complex system of equations is considered here. Hence, if

$$A_{p,q}^{r,s} = Re\left\{ \Delta_{p,q}(\tilde{\gamma}_{r,s}) \right\}$$

$$B_{p,q}^{r,s} = Im\left\{ \Delta_{p,q}(\tilde{\gamma}_{r,s}) \right\}$$

the real system of linear equations

$$\varphi_s(\tilde{\gamma}_{r,s}) - \frac{1}{\pi} \sum_{p=1}^{m} \sum_{q=1}^{n_p} \varphi_s(\tilde{\gamma}_{p,q}) \left\{ \sin\left[\alpha(\tilde{\gamma}_{r,s})\right] A_{p,q}^{r,s} + \cos\left[\alpha(\tilde{\gamma}_{r,s})\right] B_{p,q}^{r,s} \right\}$$

$$= \frac{1}{\pi} \sum_{p=1}^{m} \sum_{q=1}^{n_p} \varphi_n(\tilde{\gamma}_{p,q}) \left\{ \cos\left[\alpha(\tilde{\gamma}_{r,s})\right] A_{p,q}^{r,s} - \sin\left[\alpha(\tilde{\gamma}_{r,s})\right] B_{p,q}^{r,s} \right\} \qquad (3.7)$$

which relate the known $\varphi_n(\tilde{\gamma}_{p,q})$ to the unkown $\varphi_s(\tilde{\gamma}_{p,q})$ is obtained.

The coefficients $A^{r,s}_{p,q}$, $B^{r,s}_{p,q}$ are readily evaluated since the integrand $(\tilde{\gamma} - \gamma_{r,s})^{-1}$ is always integrable over the elements $I_{p,q}$ in either the ordinary or Cauchy principal value sense. Therefore, if $\gamma^{(1)}_{p,q}$ and $\gamma^{(2)}_{p,q}$ denote the start and end points of the element $I_{p,q}$,

$$\int_{I_{p,q}} \frac{d\gamma}{\gamma - \gamma_{r,s}} = \begin{cases} \log\left\{\dfrac{\gamma^{(2)}_{p,q} - \gamma_{r,s}}{\gamma^{(1)}_{p,q} - \gamma_{r,s}}\right\} & , \gamma_{r,s} \notin I_{p,q} \\ \log\left\{\dfrac{\gamma^{(2)}_{p,q} - \gamma_{r,s}}{\gamma_{r,s} - \gamma^{(1)}_{p,q}}\right\} & , \gamma_{r,s} \in I_{p,q} \end{cases} .$$

For multiply connected regions the system of equations (3.7) must be singular if it is to represent the behaviour of $\phi_s(\tilde{\gamma})$ correctly. As mentioned in chapter 2, a unique $\phi_s(\tilde{\gamma})$ is obtained by requiring that for $p = 2(1)m$

$$\int_{C_p} \phi_s(\tilde{\gamma})\, ds = \text{constant} .$$

A numerical counterpart of this condition is readily obtained since

$$\begin{aligned} \int_{C_p} \phi_s(\tilde{\gamma})\, ds &= Re\left\{\int_{C_p} \{\phi_s(\tilde{\gamma}) + i\,\phi_n(\tilde{\gamma})\}\, ds\right\} \\ &= Re\left\{\int_{C_p} \tau(\gamma)\, d\gamma\right\} \end{aligned}$$

and, in terms of the previously used approximation to $\tau(\gamma)$, this may be written as

$$\begin{aligned} \int_{C_p} \phi_s(\tilde{\gamma})\, ds &\simeq \sum_{q=1}^{n_p} Re\left\{\tau(\gamma_{p,q}) \int_{I_{p,q}} d\gamma\right\} \\ &\simeq \sum_{q=1}^{n_p} Im\left\{e^{i\alpha(\tilde{\gamma}_{p,q})}\left[\phi_s(\tilde{\gamma}_{p,q}) + i\,\phi_n(\gamma_{p,q})\right]\left[\gamma^{(2)}_{p,q} - \gamma^{(1)}_{p,q}\right]\right\}. \end{aligned}$$

Hence the condition for uniqueness of solution can be approximated by

$$\begin{aligned} &\sum_{q=1}^{n_p} \phi_s(\tilde{\gamma}_{p,q})\left\{\sin[\alpha(\tilde{\gamma}_{p,q})]\,\delta x_{p,q} - \cos[\alpha(\tilde{\gamma}_{p,q})]\,\delta y_{p,q}\right\} \\ &= \text{constant} + \sum_{q=1}^{n_p} \phi_n(\tilde{\gamma}_{p,q})\left\{\sin[\alpha(\tilde{\gamma}_{p,q})]\,\delta y_{p,q} + \cos[\alpha(\tilde{\gamma}_{p,q})]\,\delta x_{p,q}\right\} \end{aligned}$$

. . . . (3.8)

where

$$\delta x_{p,q} = Re\left\{ \tilde{\gamma}^{(2)}_{p,q} - \tilde{\gamma}^{(1)}_{p,q} \right\}$$

$$\delta y_{p,q} = Im\left\{ \tilde{\gamma}^{(2)}_{p,q} - \tilde{\gamma}^{(1)}_{p,q} \right\}$$

and p takes successive integer values from 2 to m.

There are several ways in which the conditions (3.8) can be adjoined to equations (3.7) in order that a unique set of $\varphi_s(\tilde{\gamma}_{p,q})$ be obtained. First, the m-1 equations resulting from (3.8) may be taken as extra equations for the determination of the $N = \sum_{p=1}^{m} n_p$ unknowns. This yields an overdetermined system of N+m-1 equations which may be solved by least squares techniques [15,p.137]. Alternatively, for each of the internal boundaries ω may be identified with only $n_p - 1$ of the $\tilde{\gamma}_{p,q}$, an additional equation coming from the form of (3.8) appropriate to the boundary. Thus a system of N equations is obtained which may be solved by Gaussian elimination. Finally, to each of the equations resulting from identifying ω with the $\tilde{\gamma}_{p,q}$ of a particular internal boundary, the form of (3.8) appropriate to that boundary may be added. This again yields a system of N linear equations which may be solved by Gaussian elimination.

All the results given in this chapter have been obtained using the third of the above alternatives. The first alternative was rejected because the large systems of equations arising in practical problems involving multiply connected regions preclude least squares type solutions by computer. The second alternative was rejected because in practice the equations may be ill-conditioned rather than singular. This leads to the problem of deciding which of the $\tilde{\gamma}_{p,q}$ ω should be identified with.

It should be noted that the piecewise constant approximation described above can be used without modification when the region of interest has corners.

§ 3.4) Piecewise linear approximations I

For regions bounded by the m smooth contours C_p, $p=1(1)m$, a more useful higher order approximation to $\tau(\tilde{\gamma})$, $\tilde{\gamma} \in C_p$ is obtained by assuming that $\tau(\tilde{\gamma})$ varies linearly over the element $I_{p,q}$. For $\tilde{\gamma} \in I_{p,q}$ this assumption leads to the approximation

$$\tau(\gamma) \simeq \left\{ [\gamma^{(2)}_{p,q} - \gamma]\,\tau(\gamma^{(1)}_{p,q}) + [\gamma - \gamma^{(1)}_{p,q}]\,\tau(\gamma^{(2)}_{p,q}) \right\} \cdot \left\{ \gamma^{(2)}_{p,q} - \gamma^{(1)}_{p,q} \right\}^{-1}$$

where $\gamma^{(2)}_{p,q}$ and $\gamma^{(1)}_{p,q}$ again denote the start and end points of the element $I_{p,q}$.

Using this form of approximation allows (3.5) to be written as*

$$\tau(\omega) \simeq \frac{1}{\pi i} \sum_{p=1}^{m} \sum_{q=1}^{n_p} \frac{1}{\gamma^{(2)}_{p,q} - \gamma^{(1)}_{p,q}} \int_{I_{p,q}} \frac{\rho\, d\rho}{\rho - \omega} \left\{ \tau(\gamma^{(2)}_{p,q}) \left[\gamma^{(1)}_{p,q} - \rho \right] + \tau(\gamma^{(1)}_{p,q}) \left[\rho - \gamma^{(2)}_{p,q} \right] \right\}$$

$$\simeq \frac{1}{\pi i} \sum_{p=1}^{m} \sum_{q=1}^{n_p} \frac{\tau(\gamma^{(2)}_{p,q}) - \tau(\gamma^{(1)}_{p,q})}{\gamma^{(2)}_{p,q} - \gamma^{(1)}_{p,q}} \int_{I_{p,q}} \rho\, d\rho$$

$$+ \frac{1}{\pi i} \sum_{p=1}^{m} \sum_{q=1}^{n_p} \frac{[\gamma^{(2)}_{p,q} - \omega]\,\tau(\gamma^{(1)}_{p,q}) + [\omega - \gamma^{(1)}_{p,q}]\,\tau(\gamma^{(2)}_{p,q})}{\gamma^{(2)}_{p,q} - \gamma^{(1)}_{p,q}} \int_{I_{p,q}} \frac{\rho\, d\rho}{\rho - \omega} \qquad (3.9)$$

.....

Writing $\gamma^{(1)}_{p,0} = \gamma^{(2)}_{p-1,n_{p-1}}$ enables (3.9) to be simplified to

$$\tau(\omega) \simeq \frac{1}{\pi i} \sum_{p=1}^{m} \sum_{q=1}^{n_p} \tau(\gamma^{(1)}_{p,q}) \left\{ \frac{\omega - \gamma^{(1)}_{p-1,q}}{\gamma^{(2)}_{p-1,q} - \gamma^{(1)}_{p-1,q}} \int_{I_{p-1,q}} \frac{d\rho}{\rho - \omega} + \frac{\gamma^{(2)}_{p,q} - \omega}{\gamma^{(2)}_{p,q} - \gamma^{(1)}_{p,q}} \int_{I_{p,q}} \frac{d\rho}{\rho - \omega} \right\} \qquad (3.10)$$

This result depending on the continuity of $\tau(\gamma)$ whereby

$$\tau(\gamma^{(1)}_{p,q+1}) = \tau(\gamma^{(2)}_{p,q})$$

and

$$\sum_{p=1}^{m} \sum_{q=1}^{n_p} \left\{ \tau(\gamma^{(2)}_{p,q}) - \tau(\gamma^{(1)}_{p,q}) \right\} = 0 \,.$$

Again, the use of (3.2) enables (3.10) to be written in the form

$$\phi_s(\tilde{\omega}) + i\phi_n(\tilde{\omega}) = \frac{e^{i\alpha(\tilde{\omega})}}{\pi i} \sum_{p=1}^{m} \sum_{q=1}^{n_p} \left\{ \phi_s(\tilde{\gamma}^{(1)}_{p,q}) + i\phi_n(\tilde{\gamma}^{(1)}_{p,q}) \right\} \Delta_{p,q}(\omega) \qquad (3.11)$$

where, in this instance,

$$\Delta_{p,q}(\omega) = e^{-i\alpha(\tilde{\gamma}^{(1)}_{p,q})} \left\{ \frac{\omega - \gamma^{(1)}_{p,q-1}}{\gamma^{(2)}_{p,q-1} - \gamma^{(1)}_{p,q-1}} \int_{I_{p,q-1}} \frac{d\gamma}{\gamma - \omega} + \frac{\gamma^{(2)}_{p,q} - \omega}{\gamma^{(2)}_{p,q} - \gamma^{(1)}_{p,q}} \int_{I_{p,q}} \frac{d\gamma}{\gamma - \omega} \right\} \qquad (3.12)$$

* note that (3.9) represents the product form of the repeated trapezoid rule.

Values for the unknowns $\varphi_s(\tilde{\gamma}^{(1)}_{p,q})$ are obtained by solving the system of linear equations resulting from identifying ω with each of the points $\gamma^{(1)}_{p,q}$. Again, only the real part of the resulting complex system of equations is considered.

For multiply connected regions the condition

$$\int_{C_p} \varphi_s(\tilde{\gamma})\, ds = \text{constant} \quad , \quad p = 2(1)m ,$$

must be adjoined to the system if a unique solution is to be obtained. The piecewise linear approximation used here leads to

$$\int_{C_p} \varphi_s(\tilde{\gamma})ds \simeq Re\left\{\sum_{q=1}^{n_p} \frac{1}{\gamma^{(2)}_{p,q} - \gamma^{(1)}_{p,q}} \int_{I_{p,q}} \left\{[\gamma^{(2)}_{p,q} - \gamma]\,\tau(\gamma^{(1)}_{p,q}) + [\gamma - \gamma^{(1)}_{p,q}]\,\tau(\gamma^{(2)}_{p,q})\right\} d\gamma\right\}$$

or, in terms of the $\gamma^{(1)}_{p,q}$ alone,

$$\int_{C_p} \varphi_s(\tilde{\gamma})ds \simeq \sum_{q=1}^{n_p} Re\left\{\tau(\gamma^{(1)}_{p,q})\left[\int_{I_{p,q-1}} \frac{\gamma - \gamma^{(1)}_{p,q-1}}{\gamma^{(2)}_{p,q-1} - \gamma^{(1)}_{p,q-1}} d\gamma + \int_{I_{p,q}} \frac{\gamma^{(2)}_{p,q} - \gamma}{\gamma^{(2)}_{p,q} - \gamma^{(1)}_{p,q}} d\gamma\right]\right\}.$$

Use of (3.2) in this last expression yields the required numerical counterpart of the uniqueness conditions. Hence the conditions for a unique set of $\varphi_s(\tilde{\gamma}^{(1)}_{p,q})$ can be written as

$$\sum_{q=1}^{n_p} \varphi_s(\tilde{\gamma}^{(1)}_{p,q})\, Im\left\{\tilde{\Delta}_{p,q}\right\} = \text{constant} - \sum_{q=1}^{n_p} \varphi_n(\tilde{\gamma}^{(1)}_{p,q})\, Re\left\{\tilde{\Delta}_{p,q}\right\}$$

where

$$\tilde{\Delta}_{p,q} = e^{-i\alpha(\tilde{\gamma}^{(1)}_{p,q})}\left\{\int_{I_{p,q-1}} \frac{\gamma - \gamma^{(1)}_{p,q-1}}{\gamma^{(2)}_{p,q-1} - \gamma^{(1)}_{p,q-1}} d\gamma + \int_{I_{p,q}} \frac{\gamma^{(2)}_{p,q} - \gamma}{\gamma^{(2)}_{p,q} - \gamma^{(1)}_{p,q}} d\gamma\right\}$$

and p takes successive integer values from 2 to m.

The evaluation of the coefficients $\Delta_{p,q}(\omega)$ is straightforward, examination of (3.12) shows that they are given by

i) for $\omega \notin I_{p,q-1}, I_{p,q}$

$$\Delta_{p,q}(\omega) = e^{i\alpha(\tilde{\gamma}^{(1)}_{p,q})} \left\{ \frac{\omega - \gamma^{(1)}_{p,q-1}}{\gamma^{(2)}_{p,q-1} - \gamma^{(1)}_{p,q-1}} \log\left\{ \frac{\gamma^{(2)}_{p,q-1} - \omega}{\gamma^{(1)}_{p,q-1} - \omega} \right\} + \frac{\gamma^{(2)}_{p,q} - \omega}{\gamma^{(2)}_{p,q} - \gamma^{(1)}_{p,q}} \log\left\{ \frac{\gamma^{(2)}_{p,q} - \omega}{\gamma^{(1)}_{p,q} - \omega} \right\} \right\}$$

ii) for $\omega = \gamma^{(1)}_{p,q-1}$

$$\Delta_{p,q}(\omega) = e^{-i\alpha(\tilde{\gamma}^{(1)}_{p,q})} \frac{\gamma^{(2)}_{p,q} - \omega}{\gamma^{(2)}_{p,q} - \gamma^{(1)}_{p,q}} \log\left\{ \frac{\gamma^{(2)}_{p,q} - \omega}{\gamma^{(1)}_{p,q} - \omega} \right\}$$

iii) for $\omega = \gamma^{(2)}_{p,q-1} = \gamma^{(1)}_{p,q}$

$$\Delta_{p,q}(\omega) = e^{-i\alpha(\tilde{\gamma}^{(1)}_{p,q})} \log\left\{ \frac{\gamma^{(2)}_{p,q} - \omega}{\omega - \gamma^{(1)}_{p,q}} \right\}$$

iv) for $\omega = \gamma^{(2)}_{p,q} = \gamma^{(1)}_{p,q+1}$

$$\Delta_{p,q}(\omega) = e^{-i\alpha(\gamma^{(1)}_{p,q})} \frac{\omega - \gamma^{(1)}_{p,q-1}}{\gamma^{(2)}_{p,q-1} - \gamma^{(1)}_{p,q-1}} \log\left\{ \frac{\gamma^{(2)}_{p,q-1} - \omega}{\gamma^{(1)}_{p,q-1} - \omega} \right\}$$

Note that when the boundaries of the region of interest contain corners, the above approximation technique requires modification. The required modifications are given in §3.8) and §3.9).

§ 3.5) <u>An alternative form for the approximations</u>

When approximations of a higher order than those used in §3.3) and §3.4) are required it becomes convenient to consider a more general formulation of the solution technique. For $\gamma \in I_{p,q}$ write

$$\tau(\gamma) \simeq \sum_{r=1}^{n} M^{(r)}_{p,q}(\gamma)\, \tau(\gamma^{(r)}_{p,q})$$

where $\gamma^{(1)}_{p,q}$, $\gamma^{(n)}_{p,q}$ are the element's end points and the remaining $\gamma^{(r)}_{p,q}$ are distinct nodes lying on the smooth arc which makes up $I_{p,q}$.

Using this notation (3.5) may be written as

$$\tau(\omega) \simeq \frac{1}{\pi i} \sum_{p=1}^{m} \sum_{q=1}^{n_p} \sum_{r=1}^{n} \tau(\gamma_{p,q}^{(r)}) \int_{I_{p,q}} M_{p,q}^{(r)}(\tau) \frac{d\tau}{\tau - \omega}$$

and if $\omega = \gamma_{e,f}^{(s)}$ this last expression may take the form

$$c(\gamma_{e,f}^{(s)})\, \tau(\gamma_{e,f}^{(s)})$$

$$\simeq \frac{1}{\pi i} \sum_{p=1}^{m} \sum_{q=1}^{n_p} \sum_{r=1}^{n} \left\{ 1 - \delta(\gamma_{p,q}^{(r)} - \gamma_{e,f}^{(s)}) \right\} \tau(\gamma_{p,q}^{(r)}) \int_{I_{p,q}} M_{p,q}^{(r)}(\tau) \frac{d\tau}{\tau - \gamma_{e,f}^{(s)}} \quad \ldots\ldots (3.13)$$

where

$$c(\gamma_{e,f}^{(s)}) = 1 - \frac{1}{\pi i} \sum_{p=1}^{m} \sum_{q=1}^{n_p} \sum_{r=1}^{n} \delta(\gamma_{p,q}^{(r)} - \gamma_{e,f}^{(s)}) \int_{I_{p,q}} M_{p,q}^{(r)}(\tau) \frac{d\tau}{\tau - \gamma_{e,f}^{(s)}} \qquad (3.14)$$

and

$$\delta(\gamma_{p,q}^{(r)} - \gamma_{e,f}^{(s)}) = \begin{cases} 1 & \text{if } \gamma_{p,q}^{(r)} = \gamma_{e,f}^{(s)} \\ 0 & \text{otherwise} \end{cases}.$$

The use of relation (3.2) enables (3.13) to be written as

$$c(\gamma_{e,f}^{(s)}) \left\{ \varphi_s(\tilde{\gamma}_{e,f}^{(s)}) + i\, \varphi_n(\tilde{\gamma}_{e,f}^{(s)}) \right\}$$

$$\simeq \sum_{p=1}^{m} \sum_{q=1}^{n_p} \sum_{r=1}^{n} \left\{ 1 - \delta(\gamma_{p,q}^{(r)} - \gamma_{e,f}^{(s)}) \right\} \left\{ \varphi_s(\tilde{\gamma}_{p,q}^{(r)}) + i\, \varphi_n(\tilde{\gamma}_{p,q}^{(r)}) \right\} \Delta_{p,q}^{(r)}(\gamma_{e,f}^{(s)}) \qquad (3.15)$$

where

$$\Delta_{p,q}^{(r)}(\gamma_{e,f}^{(s)}) = \frac{1}{\pi i} \exp\left\{ i\, \alpha(\tilde{\gamma}_{e,f}^{(s)}) - i\, \alpha(\tilde{\gamma}_{p,q}^{(r)}) \right\} \int_{I_{p,q}} M_{p,q}^{(r)} \frac{d\tau}{\tau - \gamma_{e,f}^{(s)}}$$

$\ldots\ldots (3.16)$

The evaluation of the integrals in (3.16) depends on the form of the $M_{p,q}^{(r)}(\tau)$ and is, in general, straightforward since the use of (3.14) in (3.13) avoids the cases when the integrals must be evaluated in their Cauchy principal value sense. The evaluation of $c(\gamma_{e,f}^{(s)})$ is also straightforward,

it may be accomplished by taking $\tau(\gamma)=1$ throughout the region so that

$$C(\gamma_{e,f}^{(g)}) = \sum_{p=1}^{M}\sum_{q=1}^{n_p}\sum_{r=1}^{n}\left\{1-\delta(\gamma_{p,q}^{(r)}-\gamma_{e,f}^{(g)})\right\}\int_{I_{p,q}} M_{p,q}^{(r)}(\gamma)\,\frac{d\gamma}{\gamma-\gamma_{e,f}^{(g)}} \qquad (3.17)$$

This last result coming from (3.13) and where the integrals are, of course, those required in (3.16).

A system of linear equations for the unknown $\phi_s(\tilde{\gamma}_{p,q}^{(r)})$ is obtained by identifying $\gamma_{e,f}^{(g)}$ with each of the (non-corner) $\gamma_{p,q}^{(r)}$ in (3.13), noting the continuity required for $\tau(\gamma)$ and ignoring the error in the approximation. As in the previous sections, only the real part of the resulting system of complex equations is considered.

The numerical counterpart of the uniqueness condition

$$\int_{C_p}\phi_s(\tilde{\gamma})\,ds = \text{constant}\quad,\quad p=2(1)m\,,$$

is readily obtained when the above approximation to $\tau(\gamma)$ is used. Thus, it may be shown that for $p=2(1)m$

$$\sum_{q=1}^{n_p}\sum_{r=1}^{n}\phi_s(\tilde{\gamma}_{p,q}^{(r)})\,Im\left\{\tilde{\Delta}_{p,q}^{(r)}\right\} = \text{constant} - \sum_{q=1}^{n_p}\sum_{r=1}^{n}\phi_n(\tilde{\gamma}_{p,q}^{(r)})\,Re\left\{\tilde{\Delta}_{p,q}^{(r)}\right\}$$

where

$$\tilde{\Delta}_{p,q}^{(r)} = e^{-i\alpha(\tilde{\gamma}_{p,q}^{(r)})}\int_{I_{p,q}} M_{p,q}^{(r)}(\gamma)\,d\gamma\,.$$

This condition is added into the real system of equations obtained above in the manner described in §3.3).

The alternative form described in this section will now be used in the following two sections where the piecewise linear variation of §3.4) will be reconsidered and a piecewise quadratic approximation will be introduced.

§ 3.6) Piecewise linear approximations II

In the notation of the preceeding section, the piecewise linear approximation (3.8) may, for $\gamma\in I_{p,q}$ be written as

$$\tau(\gamma) \simeq M_{p,q}^{(1)}(\gamma)\,\tau(\gamma_{p,q}^{(1)}) + M_{p,q}^{(2)}(\gamma)\,\tau(\gamma_{p,q}^{(2)})$$

where

$$M_{p,q}^{(1)}(\gamma) = \frac{\gamma-\gamma_{p,q}^{(2)}}{\gamma_{p,q}^{(1)}-\gamma_{p,q}^{(2)}}$$

and

$$M_{p,q}^{(2)}(\gamma) = \frac{\gamma-\gamma_{p,q}^{(1)}}{\gamma_{p,q}^{(2)}-\gamma_{p,q}^{(1)}}$$

} i.e. where $M_{p,q}^{(1)}(\gamma)$ and $M_{p,q}^{(2)}(\gamma)$ are Lagrangian interpolation polynomials of degree one

The required system of linear equations is obtained directly from (3.15), (3.16) and (3.17). The values of the integrals appearing in (3.16) (3.17) are readily obtained since

$$\int_{I_{p,q}} M^{(1)}_{p,q}(\xi)\,\frac{d\xi}{\xi-\omega} = \int_{\gamma^{(1)}_{p,q}}^{\gamma^{(2)}_{p,q}} \left\{\frac{\xi-\gamma^{(2)}_{p,q}}{\gamma^{(1)}_{p,q}-\gamma^{(2)}_{p,q}}\right\}\frac{d\xi}{\xi-\omega}$$

$$= \frac{1}{\gamma^{(1)}_{p,q}-\gamma^{(2)}_{p,q}} \int_{\gamma^{(1)}_{p,q}}^{\gamma^{(2)}_{p,q}} \left\{1+\frac{\omega-\gamma^{(2)}_{p,q}}{\xi-\omega}\right\} d\xi \qquad (3.18)$$

and

$$\int_{I_{p,q}} M^{(2)}_{p,q}(\xi)\,\frac{d\xi}{\xi-\omega} = \int_{\gamma^{(1)}_{p,q}}^{\gamma^{(2)}_{p,q}} \left\{\frac{\xi-\gamma^{(1)}_{p,q}}{\gamma^{(2)}_{p,q}-\gamma^{(1)}_{p,q}}\right\}\frac{d\xi}{\xi-\omega}$$

$$= \frac{1}{\gamma^{(2)}_{p,q}-\gamma^{(1)}_{p,q}} \int_{\gamma^{(1)}_{p,q}}^{\gamma^{(2)}_{p,q}} \left\{1+\frac{\omega-\gamma^{(1)}_{p,q}}{\xi-\omega}\right\} d\xi \qquad (3.19)$$

The three cases which need to be considered are

i) $\omega \notin I_{p,q}$, $\omega \neq \gamma^{(1)}_{p,q}$ and $\omega \neq \gamma^{(2)}_{p,q}$ where the integrands of (3.18), (3.19) are well behaved so that

$$\int_{I_{p,q}} M^{(\omega)}_{p,q}(\xi)\,\frac{d\xi}{\xi-\omega} = -1 + \left\{\frac{\omega-\gamma^{(2)}_{p,q}}{\gamma^{(1)}_{p,q}-\gamma^{(2)}_{p,q}}\right\} \log\left[\frac{\gamma^{(2)}_{p,q}-\omega}{\gamma^{(1)}_{p,q}-\omega}\right]$$

and

$$\int_{I_{p,q}} M^{(\omega)}_{p,q}(\xi)\,\frac{d\xi}{\xi-\omega} = 1 + \left\{\frac{\omega-\gamma^{(1)}_{p,q}}{\gamma^{(2)}_{p,q}-\gamma^{(1)}_{p,q}}\right\} \log\left[\frac{\gamma^{(2)}_{p,q}-\omega}{\gamma^{(1)}_{p,q}-\omega}\right]$$

ii) $\omega = \gamma^{(1)}_{p,q}$ when, because of the use of (3.17), only (3.19) need be considered. Hence

$$\int_{I_{p,q}} M^{(2)}_{p,q}(\xi)\,\frac{d\xi}{\xi-\omega} = 1$$

iii) $\omega = \gamma^{(2)}_{p,q}$ when, because of the use of (3.17), only (3.18) need be considered. Hence

$$\int_{I_{p,q}} M^{(\omega)}_{p,q}(\xi)\,\frac{d\xi}{\xi-\omega} = -1 \ .$$

Clearly the formulation of §3.4) can be obtained from that given here.

§ 3.7) Piecewise Quadratic Approximations

The technique described in §3.5) is readily applied to approximations of higher order than the piecewise linear approximation used in §3.6). As an example of this consider the piecewise quadratic approximation obtained by writing, for $\zeta \in I_{p,q}$,

$$\tau(\zeta) \simeq \sum_{r=1}^{3} M_{p,q}^{(r)}(\zeta)\, \tau(\zeta_{p,q}^{(r)})$$

where

$$M_{p,q}^{(1)}(\zeta) = \frac{(\zeta-\zeta_{p,q}^{(2)})(\zeta-\zeta_{p,q}^{(3)})}{(\zeta_{p,q}^{(1)}-\zeta_{p,q}^{(2)})(\zeta_{p,q}^{(1)}-\zeta_{p,q}^{(3)})}$$

$$M_{p,q}^{(2)}(\zeta) = \frac{(\zeta-\zeta_{p,q}^{(1)})(\zeta-\zeta_{p,q}^{(3)})}{(\zeta_{p,q}^{(2)}-\zeta_{p,q}^{(1)})(\zeta_{p,q}^{(2)}-\zeta_{p,q}^{(3)})}$$

$$M_{p,q}^{(3)}(\zeta) = \frac{(\zeta-\zeta_{p,q}^{(1)})(\zeta-\zeta_{p,q}^{(2)})}{(\zeta_{p,q}^{(3)}-\zeta_{p,q}^{(1)})(\zeta_{p,q}^{(3)}-\zeta_{p,q}^{(2)})}$$

It should, perhaps, be noted that $\zeta_{p,q}^{(1)}$ and $\zeta_{p,q}^{(3)}$ are nodes situated at either end of the interval $I_{p,q}$ while $\zeta_{p,q}^{(2)}$ lies on the arc between them.

The required system of linear equations is again obtained directly from (3.15), (3.16) and (3.17). The values of the integrals appearing in (3.16) and (3.17) are readily obtained since

$$\int_{I_{p,q}} M_{p,q}^{(1)}(\zeta)\frac{d\zeta}{\zeta-\omega} = \frac{1}{(\zeta_{p,q}^{(1)}-\zeta_{p,q}^{(2)})(\zeta_{p,q}^{(1)}-\zeta_{p,q}^{(3)})}\int_{\zeta_{p,q}^{(1)}}^{\zeta_{p,q}^{(3)}}\frac{(\zeta-\zeta_{p,q}^{(2)})(\zeta-\zeta_{p,q}^{(3)})}{\zeta-\omega}\,d\zeta$$

$$= \frac{1}{(\zeta_{p,q}^{(1)}-\zeta_{p,q}^{(2)})(\zeta_{p,q}^{(1)}-\zeta_{p,q}^{(3)})}\int_{\zeta_{p,q}^{(1)}}^{\zeta_{p,q}^{(3)}}\left\{\zeta+\left[\omega-\zeta_{p,q}^{(2)}-\zeta_{p,q}^{(3)}\right]+\frac{(\omega-\zeta_{p,q}^{(2)})(\omega-\zeta_{p,q}^{(3)})}{\zeta-\omega}\right\}d\zeta$$

with similar expressions for

$$\int_{I_{p,q}} M_{p,q}^{(2)}(\zeta)\frac{d\zeta}{\zeta-\omega} \quad \text{and} \quad \int_{I_{p,q}} M_{p,q}^{(3)}(\zeta)\frac{d\zeta}{\zeta-\omega}\,.$$

The four cases which need to be considered are:-

i) $\omega \notin I_{p,q}$, $\omega \neq \gamma^{(2)}_{p,q}$ and $\omega \neq \gamma^{(3)}_{p,q}$ where the integrands are well behaved and can be evaluated in closed form.

ii) $\omega = \gamma^{(1)}_{p,q}$ when, because of the use of (3.17), we need only consider

$$\int_{I_{p,q}} M^{(2)}_{p,q}(\xi) \frac{d\xi}{\xi - \omega} = \frac{1}{(\gamma^{(2)}_{p,q} - \gamma^{(1)}_{p,q})(\gamma^{(2)}_{p,q} - \gamma^{(3)}_{p,q})} \int_{\gamma^{(1)}_{p,q}}^{\gamma^{(3)}_{p,q}} (\xi - \gamma^{(3)}_{p,q})\, d\xi$$

and

$$\int_{I_{p,q}} M^{(3)}_{p,q}(\xi) \frac{d\xi}{\xi - \omega} = \frac{1}{(\gamma^{(3)}_{p,q} - \gamma^{(1)}_{p,q})(\gamma^{(3)}_{p,q} - \gamma^{(2)}_{p,q})} \int_{\gamma^{(1)}_{p,q}}^{\gamma^{(3)}_{p,q}} (\xi - \gamma^{(2)}_{p,q})\, d\xi$$

both of which can be evaluated in closed form.

iii) $\omega = \gamma^{(2)}_{p,q}$ when, because of the use of (3.17), we need only consider

$$\int_{I_{p,q}} M^{(1)}_{p,q}(\xi) \frac{d\xi}{\xi - \omega} = \frac{1}{(\gamma^{(1)}_{p,q} - \gamma^{(2)}_{p,q})(\gamma^{(1)}_{p,q} - \gamma^{(3)}_{p,q})} \int_{\gamma^{(1)}_{p,q}}^{\gamma^{(3)}_{p,q}} (\xi - \gamma^{(3)}_{p,q})\, d\xi$$

and

$$\int_{I_{p,q}} M^{(3)}_{p,q}(\xi) \frac{d\xi}{\xi - \omega} = \frac{1}{(\gamma^{(3)}_{p,q} - \gamma^{(1)}_{p,q})(\gamma^{(3)}_{p,q} - \gamma^{(2)}_{p,q})} \int_{\gamma^{(1)}_{p,q}}^{\gamma^{(3)}_{p,q}} (\xi - \gamma^{(1)}_{p,q})\, d\xi$$

both of which can be evaluated in closed form.

iv) $\omega = \gamma^{(3)}_{p,q}$ when, because of the use of (3.17), we need only consider

$$\int_{I_{p,q}} M^{(1)}_{p,q}(\xi) \frac{d\xi}{\xi - \omega} = \frac{1}{(\gamma^{(1)}_{p,q} - \gamma^{(2)}_{p,q})(\gamma^{(1)}_{p,q} - \gamma^{(3)}_{p,q})} \int_{\gamma^{(1)}_{p,q}}^{\gamma^{(3)}_{p,q}} (\xi - \gamma^{(2)}_{p,q})\, d\xi$$

and

$$\int_{I_{p,q}} M^{(2)}_{p,q}(\xi) \frac{d\xi}{\xi - \omega} = \frac{1}{(\gamma^{(2)}_{p,q} - \gamma^{(1)}_{p,q})(\gamma^{(2)}_{p,q} - \gamma^{(3)}_{p,q})} \int_{\gamma^{(1)}_{p,q}}^{\gamma^{(3)}_{p,q}} (\xi - \gamma^{(1)}_{p,q})\, d\xi$$

both of which can be evaluated in closed form.

§3.8) Solution of problems for regions with corners I

When the boundaries of a region include points at which there is no unique outward drawn normal, i.e. corners, the numerical techniques given in section §3.4) to §3.7) require modification.

The necessary modifications are straightforward when the boundary values of the derivatives $\phi_x(\tilde{\gamma})$ and $\phi_y(\tilde{\gamma})$ are continuous functions of arc length. In fact, the specification of Neumann type boundary conditions enables the corner values of these derivatives to be obtained explicitly.

Let there be a corner at the node $\tilde{\gamma}^{(1)}_{p,q}$ ($= \tilde{\gamma}^{(n)}_{p,q-1}$) so that the equations

$$\phi_n(\tilde{\gamma}^{(1)}_{p,q}) = \phi_x(\tilde{\gamma}^{(1)}_{p,q})\cos[\alpha(\tilde{\gamma}^{(1)}_{p,q})] + \phi_y(\tilde{\gamma}^{(1)}_{p,q})\sin[\alpha(\tilde{\gamma}^{(1)}_{p,q})]$$

$$\phi_n(\tilde{\gamma}^{(n)}_{p,q-1}) = \phi_x(\tilde{\gamma}^{(n)}_{p,q-1})\cos[\alpha(\tilde{\gamma}^{(n)}_{p,q-1})] + \phi_y(\tilde{\gamma}^{(n)}_{p,q-1})\sin[\alpha(\tilde{\gamma}^{(n)}_{p,q-1})]$$

can be obtained from the boundary conditions. Therefore

$$\phi_x(\tilde{\gamma}^{(1)}_{p,q}) = \frac{\phi_n(\tilde{\gamma}^{(1)}_{p,q})\sin[\alpha(\tilde{\gamma}^{(n)}_{p,q-1})] - \phi_n(\tilde{\gamma}^{(n)}_{p,q-1})\sin[\alpha(\tilde{\gamma}^{(1)}_{p,q})]}{\sin[\alpha(\tilde{\gamma}^{(n)}_{p,q-1}) - \alpha(\tilde{\gamma}^{(1)}_{p,q})]}$$

$$\phi_y(\tilde{\gamma}^{(1)}_{p,q}) = \frac{\phi_n(\tilde{\gamma}^{(n)}_{p,q-1})\cos[\alpha(\tilde{\gamma}^{(1)}_{p,q})] - \phi_n(\tilde{\gamma}^{(1)}_{p,q})\cos[\alpha(\tilde{\gamma}^{(n)}_{p,q-1})]}{\sin[\alpha(\tilde{\gamma}^{(n)}_{p,q-1}) - \alpha(\tilde{\gamma}^{(1)}_{p,q})]}$$

since $\sin[\alpha(\tilde{\gamma}^{(n)}_{p,q-1}) - \alpha(\tilde{\gamma}^{(1)}_{p,q})] \neq 0$ at a corner.

This solution allows the tangential derivatives at the corner to be written as

$$\phi_s(\tilde{\gamma}^{(1)}_{p,q}) = -\phi_x(\tilde{\gamma}^{(1)}_{p,q})\sin[\alpha(\tilde{\gamma}^{(1)}_{p,q})] + \phi_y(\tilde{\gamma}^{(1)}_{p,q})\cos[\alpha(\tilde{\gamma}^{(1)}_{p,q})]$$

$$\phi_s(\tilde{\gamma}^{(n)}_{p,q-1}) = -\phi_x(\tilde{\gamma}^{(1)}_{p,q})\sin[\alpha(\tilde{\gamma}^{(n)}_{p,q-1})] + \phi_y(\tilde{\gamma}^{(1)}_{p,q})\cos[\alpha(\tilde{\gamma}^{(n)}_{p,q-1})]$$

These values of the discontinuous function $\phi_s(\tilde{\gamma})$ may be substituted into equations (3.15) and the uniqueness condition to give a reduced system of equations for the remaining unknown nodal values of $\phi_s(\tilde{\gamma})$.

An alternative modification has previously been given by Kermanidis [26].

§ 3.9) Solution of problems for regions with corners II

Additional modifications to the previously given numerical methods are required whenever the corners of a region are such that the derivatives $\varphi_x(\tilde{\zeta})$ and $\varphi_s(\tilde{\zeta})$ possess singularities. Consider the simply connected region shown in figure 3-1 which has a re-entrant corner at the point $\zeta_0 = x_0 + i\,y_0$. As mentioned in §2.6), the tangential derivative $\varphi_s(\tilde{\zeta})$ of a harmonic function $\varphi(x,y)$ satisfying Neumann type conditions on the boundary of this region may have a singularity of the type $\rho^{\frac{\pi}{\gamma}-1}$ when $\gamma > \pi$. Here $\rho = |\zeta - \zeta_0|$ and γ is the "interior" angle between tangents on either side of ζ_0.

Using the notation of figure 3-1, it is readily shown that the function

$$\hat{\tau}(\zeta) = \hat{\varphi}_x(\tilde{\zeta}) - i\hat{\varphi}_s(\tilde{\zeta}) = A e^{-i\frac{\pi}{\gamma}\theta_0}(\zeta - \zeta_0)^{\frac{\pi}{\gamma}-1},$$

where A is a real constant, possesses the form of singularity necessary to produce both singular $\hat{\varphi}_s(\tilde{\zeta})$ and zero $\hat{\varphi}_n(\tilde{\zeta})$ at ζ_0. Letting $\alpha(\tilde{\zeta})$ denote the argument of the outward drawn normal to the boundary at ζ, the relation

$$\hat{\varphi}_s(\tilde{\zeta}) + i\hat{\varphi}_n(\tilde{\zeta}) = i e^{i\alpha(\tilde{\zeta})}\hat{\tau}(\zeta)$$

yields

$$\left.\begin{aligned} \hat{\varphi}_n(\tilde{\zeta}) &= 0 \\ \hat{\varphi}_s(\tilde{\zeta}) &= A\rho^{\frac{\pi}{\gamma}-1} \end{aligned}\right\} \text{ for } \zeta \in (\zeta_0, \zeta_A)$$

and

$$\left.\begin{aligned} \hat{\varphi}_n(\tilde{\zeta}) &= 0 \\ \hat{\varphi}_s(\tilde{\zeta}) &= -A\rho^{\frac{\pi}{\gamma}-1} \end{aligned}\right\} \text{ for } \zeta \in (\zeta_B, \zeta_0).$$

The required modifications to the numerical methods are obtained by working with the function

$$g(\zeta) = \psi_x(\tilde{\zeta}) - i\psi_s(\tilde{\zeta}) = \tau(\zeta) - \hat{\tau}(\zeta)$$

rather than $\tau(\zeta)$ itself. Note that the derivatives $\psi_x(\tilde{\zeta})$ and $\psi_s(\tilde{\zeta})$ are continuous on the boundary.

Returning to the rather general approach of §3.5) and writing

$$\psi_s(\tilde{\gamma}) + i\,\psi_n(\tilde{\gamma}) = i e^{i\alpha(\tilde{\gamma})} g(\gamma)$$

equation (3.15) becomes

$$c(\gamma_{1,p}^{(s)})\left\{\psi_s(\tilde{\gamma}_{1,f}^{(s)}) + i\,\psi_n(\tilde{\gamma}_{1,f}^{(s)})\right\}$$

$$\simeq \sum_{q=1}^{n_1}\sum_{r=1}^{n}\left\{1-\delta(\gamma_{1,q}^{(r)}-\gamma_{1,f}^{(s)})\right\}\left\{\psi_s(\tilde{\gamma}_{1,q}^{(r)}) + i\,\psi_n(\tilde{\gamma}_{1,q}^{(r)})\right\}\Delta_{1,q}^{(r)}(\gamma_{1,f}^{(s)}) \quad \ldots\ldots \quad (3.20)$$

A system of linear equations for the unknown $\psi_s(\tilde{\gamma}_{1,q}^{(r)})$ in (3.20) are obtained in the usual way, i.e.

i) in (3.20) $\gamma_{1,f}^{(s)}$ is identified with each of the non-corner $\gamma_{1,q}^{(r)}$

ii) only the real part of (3.20) is considered

iii) the error in the approximation is ignored

iv) the continuity of $\psi_s(\tilde{\gamma}_{1,q}^{(r)})$ at each of the non-corner $\gamma_{1,q}^{(r)}$ is noted.

Denoting by n_c the number of corners in the contour bounding R, application of the above steps (viz. i) to iv)) will result in a system of $(n-1)n_1 - n_c$ distinct linear equations for the $(n-1)n_1 + n_c$ unknown nodal values of $\psi_s(\tilde{\gamma})$ and A. Note that an additional equation allowing for the determination of A is required because the normal derivative $\psi_n(\tilde{\gamma})$ is given by

$$\psi_n(\tilde{\gamma}) = \phi_n(\tilde{\gamma}) - A\,Re\left\{e^{i\left[\alpha(\tilde{\gamma})-\frac{\pi}{\gamma}\theta_0\right]}(\gamma-\gamma_0)^{\frac{\pi}{\gamma}-1}\right\}$$

where Á is a problem dependent constant.

For each corner, two of the additional equations required for a unique solution may be obtained in the manner outlined in §3.8). A further equation is obtained by relaxing the condition that $\gamma_{1,f}^{(s)}$ in (3.20) should only be identified with non-corner $\gamma_{1,q}^{(r)}$ and applying (3.20) at the re-entrant corner γ (in practice this yields two equations only one of which need be considered).

Although only a simply connected region with a single re-entrant corner has been considered here, the extension of the above to simply and multiply connected regions with more than one re-entrant corner is straightforward. Let there be corners at the points $\zeta_k = x_k + iy_k$, $k = o(1)l$. On extending the previously used notation, the function

$$\hat{\tau}(\zeta) = \sum_{k=0}^{l} A_k e^{-i\frac{\pi}{\gamma_k}\theta_k} (\zeta - \zeta_k)^{\frac{\pi}{\gamma_k}-1}$$

possesses the form of singularity required at each corner. The function

$$g(\zeta) = \tau(\zeta) - \hat{\tau}(\zeta)$$

can again be constructed and a system of equations corresponding to (3.20) applied at non-corner $\zeta_{1,2}^{(r)}$ obtained. Similarly, the additional equations which are required for a unique solution (three for each re-entrant corner, two for each of the remaining corners) are obtained by utilising the equations of §3.7) and applying the equation corresponding to (3.20) at each re-entrant corner.

Once the A_k, $k = o(1)l$, and the nodal values of $\psi_s(\tilde{\zeta})$ have been determined, the nodal values of $\phi_s(\tilde{\zeta})$ can be recovered from

$$\phi_s(\tilde{\zeta}) = \psi_s(\tilde{\zeta}) - \sum_{k=0}^{l} A_k \, \mathrm{Im}\left\{ e^{i[\alpha(\tilde{\zeta}) - \frac{\pi}{\gamma_k}\theta_k]} (\zeta - \zeta_k)^{\frac{\pi}{\gamma_k}-1} \right\}.$$

The work of Kermanidis [*loc. cit.*] and Symm [41] on the subject of how to treat corner singularities appearing in the solution of Laplace's equation by boundary integral equation methods is noted.

§ 3.10 Modifications required for infinite regions

When a problem is defined on an infinite region containing a finite number of internal boundaries, the contour c_1 no longer exists and the integral

$$\frac{1}{\pi i}\int_{c_1} \frac{\tau(\zeta)}{\zeta - \omega}\, d\zeta$$

is replaced by the term 2σ where

$$\sigma = \lim_{|\zeta|\to\infty} \tau(\zeta)$$

Hence, (3.13) can be written as

$$c(\tau_{e,f}^{(s)})\,\tau(\tau_{e,f}^{(s)}) \simeq 2\sigma$$

$$+ \frac{1}{\pi i}\sum_{p=2}^{m}\sum_{q=1}^{n_p}\sum_{r=1}^{n}\left\{1-\delta(\tau_{p,q}^{(r)}-\tau_{e,f}^{(s)})\right\}\tau(\tau_{p,q}^{(r)})\int_{I_{p,q}} M_{p,q}^{(r)}(\tau)\frac{d\tau}{\tau-\tau_{e,f}^{(s)}}$$

while (3.15) is replaced by

$$c(\tau_{e,f}^{(s)})\left\{\phi_s(\tilde{\tau}_{e,f}^{(s)}) + i\,\phi_n(\tilde{\tau}_{e,f}^{(s)})\right\} \simeq 2i\sigma\, e^{i\alpha(\tau_{e,f}^{(s)})}$$

$$+\sum_{p=2}^{m}\sum_{q=1}^{n_p}\sum_{r=1}^{n}\left\{1-\delta(\tau_{p,q}^{(r)}-\tau_{e,f}^{(s)})\right\}\left\{\phi_s(\tilde{\tau}_{p,q}^{(r)})+i\,\phi_n(\tilde{\tau}_{p,q}^{(r)})\right\}\Delta_{p,q}^{(r)}(\tau_{e,f}^{(s)}) \quad \ldots\ldots(3.21)$$

The linear equations required for determining the unknown values of $\phi_s(\tilde{\tau}_{p,q}^{(r)})$ are obtained in the manner given previously. It should be noted that the discrete form of the uniqueness condition, i.e. for $p=2(1)m$

$$\sum_{q=1}^{n_p}\sum_{r=1}^{n}\phi_s(\tilde{\tau}_{p,q}^{(r)})\,\mathrm{Im}\left\{\tilde{\Delta}_{p,q}^{(r)}\right\}$$

$$= \text{constant} - \sum_{q=1}^{n_p}\sum_{r=1}^{n}\phi_n(\tilde{\tau}_{p,q}^{(r)})\,\mathrm{Re}\left\{\tilde{\Delta}_{p,q}^{(r)}\right\} \qquad (3.22)$$

remains unchanged.

§ 3.11 Examples

To validate the numerical techniques described in this chapter, the results obtained from three numerical examples are given below. Each of these examples demonstrates at least one of the following problem types:-

i) solution for a simply connected region
ii) solution for a finite multiply connected region
iii) solution for an infinite region with an internal boundary
iv) solution for a region with discontinuities in the argument of the outward drawn normal.

These problem types are typical of practically occurring Neumann problems.

§ 3.11.1) Flexure of a hollow tube

The problem of determining the state of stress in a cantilever beam of uniform cross-section R which is bent by forces applied over its free end in such a way as to be statically equivalent to a load W acting through the section's centroid is described in detail by Love [4,pp.329-348].

Let the axis of z lie along the central-line of the beam, with $z=0$ at the fixed end, and take the axes of x and y as being parallel to the principal axes of the beam's cross-sections at their centroids. For a beam of length l and W acting parallel to the axis of x Love shows that the stress system is given by

$$\sigma_x = \sigma_y = \tau_{xy} = 0$$

$$\sigma_z = -\frac{W(l-z)}{I_y}x$$

$$\tau_{xz} = \mu\tau\,(\varphi_x - y) - \frac{W}{2(1+\sigma)I_y}\left\{\chi_x + \tfrac{1}{2}\sigma x^2 + (1-\tfrac{1}{2}\sigma)y^2\right\}$$

$$\tau_{yz} = \mu\tau\,(\varphi_y + x) - \frac{W}{2(1+\sigma)I_y}\left\{\chi_y + (2+\sigma)xy\right\}$$

where φ and χ are the cross-section's warping and flexure functions respectively,

$$I_y = \iint_R x^2\,dx\,dy$$

σ = Poisson's ratio

μ = modulus of rigidity

and τ is determined such that the couple

$$\iint_R \left\{x\,\tau_{yz} - y\,\tau_{xz}\right\}dx\,dy$$

vanishes. Love also demonstrates that both the warping and flexure functions satisfy Laplace's equation in R,

i.e. $\nabla^2\varphi = \nabla^2\chi = 0$,

together with the boundary conditions

$$\varphi_n = y\cos(x,n) - x\cos(y,n)$$

$$\chi_n = -\left\{\tfrac{1}{2}\sigma x^2 + \left(1-\tfrac{1}{2}\sigma\right)y^2\right\}\cos(x,n) - (2+\sigma)xy\cos(y,n).$$

For a beam whose cross-section is the annular region

$$r_i^2 \le x^2 + y^2 \le r_o^2$$

the boundary condition φ_n reduces to

$$\varphi_n(\tilde{\zeta}) = 0$$

for $\zeta = x+iy$ lying on either inner or outer boundary. Writing $\zeta = re^{i\theta}$, the boundary condition χ_n reduces to

$$\chi_n(\tilde{\zeta}) = -\left(\tfrac{3}{4} + \tfrac{1}{2}\sigma\right)r_o^2\cos\theta + \tfrac{3}{4}r_o^2\cos 3\theta$$

for $\zeta = r_o e^{i\theta}$, i.e. ζ lying on the outer boundary, and

$$\chi_n(\tilde{\zeta}) = \left(\tfrac{3}{4} + \tfrac{1}{2}\sigma\right)r_i^2\cos\theta - \tfrac{3}{4}r_i^2\cos 3\theta$$

for $\zeta = r_i e^{i\theta}$, i.e. ζ lying on the inner boundary.

It is readily shown that, for this region, the harmonic functions

$$\varphi(x,y) = \text{constant}$$

$$\chi(x,y) = -\left(\tfrac{3}{4} + \tfrac{1}{2}\sigma\right)\left\{(r_o^2 + r_i^2)r + \frac{r_o^2 r_i^2}{r}\right\}\cos\theta + \tfrac{1}{4}r^3\cos 3\theta + \text{constant}$$

satisfy the above boundary conditions. The boundary tangential derivatives appropriate to the bending of a hollow, tube-like cantilever beam are therefore

$$\varphi_s(\tilde{\zeta}) = 0$$

$$\chi_s(\tilde{\zeta}) = \left(\tfrac{3}{4} + \tfrac{1}{2}\sigma\right)\left\{r_o^2 + 2r_i^2\right\}\sin\theta - \tfrac{3}{4}r_o^2\sin 3\theta$$

for $\zeta = r_o e^{i\theta}$ and

$$\varphi_s(\tilde{\zeta}) = 0$$

$$\chi_s(\tilde{\zeta}) = -\left(\tfrac{3}{4} + \tfrac{1}{2}\sigma\right)\left\{2r_o^2 + r_i^2\right\}\sin\theta + \tfrac{3}{4}r_i^2\sin 3\theta$$

for $\zeta = r_i e^{i\theta}$.

together with the boundary conditions

$$\varphi_n = y\cos(x,n) - x\cos(y,n)$$

$$\chi_n = -\left\{\tfrac{1}{2}\sigma x^2 + \left(1-\tfrac{1}{2}\sigma\right)y^2\right\}\cos(x,n) - (2+\sigma)xy\cos(y,n).$$

For a beam whose cross-section is the annular region

$$r_i^2 \le x^2 + y^2 \le r_o^2$$

the boundary condition φ_n reduces to

$$\varphi_n(\tilde{\zeta}) = 0$$

for $\zeta = x+iy$ lying on either inner or outer boundary. Writing $\zeta = re^{i\theta}$, the boundary condition χ_n reduces to

$$\chi_n(\tilde{\zeta}) = -\left(\tfrac{3}{4} + \tfrac{1}{2}\sigma\right)r_o^2\cos\theta + \tfrac{3}{4}r_o^2\cos 3\theta$$

for $\zeta = r_o e^{i\theta}$, i.e. ζ lying on the outer boundary, and

$$\chi_n(\tilde{\zeta}) = \left(\tfrac{3}{4} + \tfrac{1}{2}\sigma\right)r_i^2\cos\theta - \tfrac{3}{4}r_i^2\cos 3\theta$$

for $\zeta = r_i e^{i\theta}$, i.e. ζ lying on the inner boundary.

It is readily shown that, for this region, the harmonic functions

$$\varphi(x,y) = \text{constant}$$

$$\chi(x,y) = -\left(\tfrac{3}{4} + \tfrac{1}{2}\sigma\right)\left\{(r_o^2 + r_i^2)r + \frac{r_o^2 r_i^2}{r}\right\}\cos\theta + \tfrac{1}{4}r^3\cos 3\theta + \text{constant}$$

satisfy the above boundary conditions. The boundary tangential derivatives appropriate to the bending of a hollow, tube-like cantilever beam are therefore

$$\varphi_s(\tilde{\zeta}) = 0$$

$$\chi_s(\tilde{\zeta}) = \left(\tfrac{3}{4} + \tfrac{1}{2}\sigma\right)\left\{r_o^2 + 2r_i^2\right\}\sin\theta - \tfrac{3}{4}r_o^2\sin 3\theta$$

for $\zeta = r_o e^{i\theta}$ and

$$\varphi_s(\tilde{\zeta}) = 0$$

$$\chi_s(\tilde{\zeta}) = -\left(\tfrac{3}{4} + \tfrac{1}{2}\sigma\right)\left\{2r_o^2 + r_i^2\right\}\sin\theta + \tfrac{3}{4}r_i^2\sin 3\theta$$

for $\zeta = r_i e^{i\theta}$.

The problem of determining the boundary tangential derivative $\chi_s(\tilde{\gamma})$ for an annular region with $r_o = 1$ and $r_i = \frac{1}{2}$ has been solved by computer programs based on the techniques described in §3.6) and §3.7). The co-ordinates of the boundary nodes were obtained by dividing the total arc length for each contour into N equal intervals. For the piecewise linear approximations of §3.6) each of these intervals corresponded with a boundary element (see §3.2) for a description of how the boundaries of a region may be described in terms of nodes and elements). This contrasted with the piecewise quadratic approximations of §3.7) which required that an element be obtained from a pair of adjacent intervals.

The idealisation for the case N = 20 is shown in figure 3-2 and illustrates the element difference described above. The results obtained using both the piecewise linear and piecewise quadratic approximation techniques for the three cases N = 20, N = 40 and N = 60 are shown in table 3-1. Only the results at nodes common to the three idealisations are given. Further, symmetry has been used to reduce the number of results given to a minimum.

Examination of the previously given expressions for $\chi_n(\tilde{\gamma})$ and $\chi_s(\tilde{\gamma})$ leads to the conclusion that the regular function $\tau(\gamma)$ with boundary values

$$\tau(\gamma) = -i e^{-i\alpha(\tilde{\gamma})} \{ \chi_s(\tilde{\gamma}) + i \chi_n(\tilde{\gamma}) \}$$

is given by

$$\tau(\gamma) = -\left(\tfrac{3}{4} + \tfrac{1}{2}\sigma\right) \left\{ r_o^2 + r_i^2 - \frac{r_o^2 r_i^2}{\gamma^2} \right\} + \tfrac{3}{4}\gamma^2$$

That this function includes a term of the form $1/\gamma^2$ means that this example can never be solved exactly by the techniques of §3.6) and §3.7). However, the results given in table 3-1 demonstrate that an acceptable level of accuracy can be obtained for problems whose analytic solution includes a function with a singularity "close" to a boundary of the region under consideration. As expected, successive refinement of the idealisation improves the accuracy obtained.

In this example it is worth noting that the advantages one might expect to arise from the use of the higher order

approximation of §3.7) are most noticeable in the results obtained for the boundary nearest to the singularity. However, the results for both boundaries illustrate that successive refinements of the idealisation, together with the use of the higher approximation, do yield results which rapidly converge to the (in this case known) true solution.

§ 3.11.2) Test problem for an L-shaped region

As far as the author is aware, the boundary tangential derivatives of the warping and flexure functions for an L-shaped region cannot be obtained from a readily computed mathametical expression. This being the case it was found necessary to apply the solution techniques described in this chapter to an atypical problem defined on an L-shaped region.

The problem chosen was that of determining numerically the boundary tangential derivative $\phi_s(\tilde{\gamma})$ corresponding to the boundary normal derivative

$$\phi_n(\tilde{\gamma}) = Re\left\{\left[\sin\gamma^2 + e^{-i\pi/\gamma\,\theta_0}(\gamma-\gamma_0)^{\frac{\pi}{\gamma}-1}\right]e^{i\alpha(\tilde{\gamma})}\right\}$$

on the L-shaped region shown in figure 3-3. Here γ_0 is the point (1,1) which is marked as **C** in the figure, $\theta_0 = \pi/2$ and $\gamma = \frac{3\pi}{2}$. Clearly, the analytic solution to this problem is

$$\phi_s(\tilde{\gamma}) = -Im\left\{\left[\sin\gamma^2 + e^{-\frac{\pi}{\gamma}\theta_0}(\gamma-\gamma_0)^{\frac{\pi}{\gamma}-1}\right]e^{i\alpha(\tilde{\gamma})}\right\}.$$

The technique used to solve this problem numerically was that described in §3.8) and §3.9). The piecewise quadratic approximations of §3.7) were used where required. An idealisation of the boundary was obtained by dividing each of the region's sides, into N/6 elements of equal length. The idealisation obtained for the case N = 30 is shown figure 3-4.

The results obtained for this problem can be considered in two parts, viz. the approximation to the coefficient (or strength) of the singularity at γ_0 and (in the notation of §3.9)) the approximations to the nodal values of $\phi_s(\tilde{\gamma})$ Results obtained for the three cases N = 30, N = 60 and N = 90 are given in tables 3-2 and 3-4.

The first of these tables, i.e. table 3-2, gives the approximations to the strength of the singularity. In this example the technique described in §3.9) "picked out" the strength of the singularity to an acceptable degree of accuracy even when the crude N = 30 approximation was used. The N = 60 and N = 90 approximations demonstrate the marked improvement that can be obtained by successively refining the mesh (the N = 60 case reduced the relative errors obtained for N = 30 by a factor of ten).

Comparisons of the approximations obtained to the nodal values of $\psi_3(\tilde{r})$ with their true values are given in tables 3-3 and 3-4. Here results are only given at nodes common to the three cases N = 30, N = 60 and N = 90. Further, these comparisons are only given for the sides DA (where $\psi_3(\tilde{r}) = \sin(x^2)$) and AB (where $\psi_3(\tilde{r}) = -\sinh(2xy)\cos(x^2-y^2)$).

These comparisons again demonstrate how successive refinement of the mesh yields considerable improvements in the approximations. This appears to be particularly true when one halves the size of the elements in the initial idealisation (the improvement is approximately the same as that given above).

§ 3.11.3) Flow past on isolated aerofoil

To demonstrate the application of the techniques described in this chapter to problems defined on infinite regions with internal boundaries, the flow of a plane, irrotational, incompressible, inviscid fluid past an isolated aerofoil will be considered. It is well known [e.g. 20, p.153] that the flow of such a fluid gives rise to an analytic complex conjugate velocity

$$\tau(\tilde{z}) = \varphi_x(\tilde{z}) - i\,\varphi_y(\tilde{z})$$

hose real and imaginary parts give the (flow field) velocity components in the global cartesian directions.

The condition that there be no flow across the profile of the aerofoil gives rise to the Neumann type boundary condition

$$\varphi_n(\tilde{\omega}) = 0$$

whence, if $\alpha(\tilde{\omega})$ is the argument of the outward drawn normal at ω,

$$i\,\tau(\omega)\,e^{i\alpha(\tilde{\omega})} = \varphi_s(\tilde{\omega}).$$

From this last expression we conclude that $\varphi_s(\tilde{\omega})$ is just the velocity component directed tangentially to the profile at ω.

For aerofoils whose bounding contour is smooth, i.e. has neither corners nor cusps, two additional conditions on the flow must be specified. These are [21]

i) $\lim_{|z|\to\infty} \tau(z)$, the complex conjugate velocity of the unperturbed flow

ii) $\Gamma = \int_c \varphi_s(\tilde{z})\,ds$ the circulation about the aerofoil

When the bounding contour of a conventional aerofoil is not smooth the first of these conditions remains and the second replaced by the Kutta-Joukowski condition, i.e. the speed of the flow remains finite at the trailing edge [20,p.199]. That there is a unique circulation (and therefore lift) associated with the upstream flow condition and geometric configuration is implicit in this condition.

To handle an aerofoil with a cusp at the trailing edge the numerical method of §3.10) has had to be modified since (3.21) does not hold when $\tilde{z}^{(g)}_{e,\rho}$ lies at a cusp. Because the speed

of the flow remains finite at the cusp, the tangential velocity components will take equal and opposite values at the cusp. Thus, use of the real part of (3.21) for $\bar{\gamma}^{(s)}_{e,f}$ away from the cusp leaves the generated system of equations two equations short.

For the piecewise quadratic approximation of §3.7) this problem of insufficient equations for the determination of a solution has been overcome by requiring that $\tau(\gamma)$ be a linear function of γ over a boundary element which includes the cusp and by including the Kutta-Joukowski condition explicitly. The circulation has been evaluated using an appropriate form of (3.22).

As an example of the numerical method given above, the flow past the Joukowski aerofoil obtained from the circle

$$|Z| = 0.6$$

by the transformation

$$\gamma = Z - 0.1 + 0.25\,(Z - 0.1)^{-1}$$

will be considered. The case when $\lim_{|\gamma|\to\infty} \tau(\gamma) = 1$ has previously been considered by Jaswon and Symm [15, pp.184-187] and will serve as the limiting value of the complex conjugate velocity used in the first part of this example. Using Jaswon and Symm's expression for the complex potential, which can be differentiated to yield $\tau(\gamma)$, or Milne-Thomson's circle theorem (see appendix I) it can be shown that the speed of the flow at the cusped trailing edge (see figure 3-5) is 0.8333. The circulation for this example is zero.

The idealisations used for solving this problem were obtained by placing N equally spaced points around the circle $|Z| = 0.6$. The transformation had the effect of packing nodes in the vicinity of the leading and trailing edges. The idealisation used for the case N = 40 is shown in figure 3-5, the nodes being circled

Approximations to the speed of the flow at the cusp, $q_c^{(N)}$ say, for various values of N are given in table 3-5. Here it is shown that the relative error for even the coarsest idealisation (N=40) is less than 2%, the relative error diminishing to less than ¾% for the finest idealisation (N = 120).

In figure 3-6 the actual values of the signed speed on the aerofoil are compared with the approximations obtained when N = 40. Here it has been assumed that:-

i) $\tilde{\zeta}$ lies on the aerofoil's suction surface when $\varphi_s(\tilde{\zeta}) > 0$

ii) $\tilde{\zeta}$ lies on the aerofoil's pressure surface when $\varphi_s(\tilde{\zeta}) < 0$

iii) the idealisation obtained for the case N = 120 is sufficiently refined to allow the total aerofoil surface length to be calculated by joining the nodes by straight lines and summing the lengths of these lines.

iv) the maximum flow speed occurs at $\zeta = 0.74559 \pm 0.20463i$ and has the value 1.3695.

The aerofoil surface length (alternatively arc length) has been taken to be zero on the pressure surface side of the cusp and incremented as the boundary of the aerofoil is described in the positive sense. Furthermore, all normalisations are with respect to the appropriate maximum.

Figure 3-6 illustrates how well the above numerical method "picks out" the general trend of the speed versus arc length plot for even a coarse idealisation. The accuracy of the approximations to the maximum speed of the flow, $q_{max}^{(N)}$ say, for various values of N is demonstrated in table 3-6 where the maximum relative error obtained (for the case N = 40) is shown to be less than 0.2%.

A feature of the numerical technique described in this section is its ability to solve problems involving a flow with circulation. This is illustrated here by taking the isolated aerofoil considered above together with

$$\lim_{|\zeta|\to\infty} \chi(\zeta) = e^{-i\frac{\pi}{18}},$$

i.e. a unit flow with an incidence of 10°.

Using the previously obtained N = 40 idealisation, the actual values of the signed speed $\varphi_s(\tilde{\zeta})$ are compared with their approximations in figure 3-7. Again, the general trend of the speed versus arc length plot obtained by the numerical method is quite good. However, the plot does indicate that the approximations to the speed of the flow at the cusp and the maximum flow speed are more inaccurate than those obtained in the earlier part of the example. This is confirmed in table 3-7 where the appropriate values are given together with an approximation to the circulation. That the error in the

approximations obtained for this example are higher than those obtained when $\lim_{|\delta|\to\infty} \tau(\delta) = 1$ is not unreasonable when one compares the rapid variation in speed over the suction surface shown in figure 3-7 with that of figure 3-6. Again, the above errors can all be reduced by improvements in the idealisation.

approximations obtained for this example are higher than those obtained when $\lim_{|\delta|\to\infty} \tau(\delta) = 1$ is not unreasonable when one compares the rapid variation in speed over the suction surface shown in figure 3-7 with that of figure 3-6. Again, the above errors can all be reduced by improvements in the idealisation.

Chapter 4

NUMERICAL SOLUTION OF DERIVED INTEGRAL EQUATION FOR A VERTICAL CASCADE

§ 4.1) Introduction

When a problem is defined on a vertical cascade of aerofoils one may either consider an infinite region with some large, but finite, number of internal boundaries, assume that the influence of a boundary remote from a central profile is negligible and use the techniques of the preceding chapter or in some way utilise the cascade equation derived in Chapter 2. Because the former approach can only lead to extremely large systems of equations, the latter approach must be preferable. It is the cascade equation, viz (2.27), which is considered here.

It is probable that the only practical problems which involve cascades arise from the analysis of the flow through a particular cascade. Indeed, in turbomachinery applications interest is directed towards such an analysis rather than the flow past a finite number of aerofoils. This situation for exterior problems contrasts with that for interior problems where each aerofoil can usually be considered in isolation.

In view of the above practical consideration attention will be restricted to the flow of a plane, irrotational, incompressible, inviscid fluid through a vertical cascade. It is well known [20, p.153] that the flow of such a fluid gives rise to an analytic complex conjugate velocity.

$$\tau(\underline{\gamma}) = \varphi_x(\tilde{\underline{\gamma}}) - i\,\varphi_y(\tilde{\underline{\gamma}})$$

whose real and imaginary parts give the velocity components in the global cartesian co-ordinate directions. Denoting the central profile in the cascade by C_1 (rather than the C_0 used in Chapter 2), the condition that there should be no flow across C_1 gives rise to the Neumann type boundary condition

$$\varphi_n(\tilde{\underline{\gamma}}) = 0 \quad , \quad \underline{\gamma} \in C_1 ,$$

whence

$$i\tau(\gamma)\, e^{i\alpha(\tilde{\gamma})} = \phi_s(\tilde{\gamma})$$

where $\alpha(\tilde{\gamma})$ is the argument of the outward drawn vector normal to C_1 at γ . Similarly,

$$\tau(\gamma)\frac{d\gamma}{ds} = \phi_s(\tilde{\gamma}) \quad \text{for} \quad \gamma \in C_1 .$$

That $\tau(\gamma)$ is analytic in the region bounded internally by the cascade's profiles allows $\tau(\omega)$, $\omega \in C_1$, to be generated from

$$\tau(\omega) = \tau_u + \tau_D + \frac{1}{ti}\int_{C_1} \tau(\gamma)\coth\left\{\frac{\pi}{t}(\gamma-\omega)\right\} d\gamma \qquad (4.1),$$

i.e. (2.26), where t is the cascade pitch

$$\tau_u = \lim_{Re\{\gamma\}\to-\infty} \tau(\gamma)$$

$$\tau_D = \lim_{Re\{\gamma\}\to\infty} \tau(\gamma).$$

Further, the Neumann type boundary conditions lead to

$$\phi_s(\tilde{\omega}) = i e^{i\alpha(\tilde{\omega})}\left\{\tau_u + \tau_D\right\}$$

$$+ \frac{e^{i\alpha(\tilde{\omega})}}{t}\int_{C_1} \phi_s(\tilde{\gamma})\coth\left\{\frac{\pi}{t}(\gamma-\omega)\right\} ds \qquad (4.2)$$

and the uniqueness condition

$$\Gamma = \int_{C_1} \gamma(\zeta)\, d\zeta = \int_{C_1} \phi_s(\tilde{\zeta})\, ds \,.$$

The relationships

$$\sigma = \frac{1}{2}\left\{\gamma_u + \gamma_D\right\} \tag{4.3}$$

$$\Gamma = t\, i\left\{\gamma_u - \gamma_D\right\} \tag{4.4}$$

which were obtained in § 2.5) should be noted. Observe that (4.4) demonstrates the ability of a cascade to turn a flow since the upstream and downstream flow conditions only agree when the circulation Γ is zero.

In the remaining sections of this chapter discussion is centred on the solution of a restricted problem. The numerical techniques described for its solution are readily adapted to the solution of more general problems, e.g. the three problems making up the Martensen technique [23].

§ 4.2) <u>A restricted problem</u>

A problem of particular interest in turbomachinery applications occurs when γ_u rather than Γ and σ is given for a cusped blade. In this case the problem becomes one of determining the complex conjugate velocity of the flow through the cascade together with γ_D. Letting

$$\gamma_u = u_u + i\, v_u$$

and

$$\gamma_D = u_D + i\, v_D$$

it follows from (4.4) that

$$0 = u_u - u_D$$

$$\frac{\Gamma}{t} = v_D - v_u \,.$$

Substituting these expressions into (4.3) shows that σ can be expressed as

$$\sigma = u_u + i\left\{\frac{\Gamma}{2t} + v_u\right\}$$

whence (4.1) becomes, for ω away from the cusp,

$$\gamma(\omega) = 2\left\{u_u + i\left[\frac{\Gamma}{2t} + v_u\right]\right\} + \frac{1}{ti}\int_{C_1}\gamma(\xi)\coth\left\{\frac{\pi}{t}(\xi-\omega)\right\}d\xi$$

$$= 2\gamma_u + \frac{i}{t}\int_{C_1}\gamma(\xi)\,d\xi + \frac{1}{ti}\int_{C_1}\gamma(\xi)\coth\left\{\frac{\pi}{t}(\xi-\omega)\right\}d\xi$$

. . . . . (4.5).

Similarly, it follows that (4.2) may be written as

$$\varphi_s(\tilde{\omega}) = 2ie^{i\alpha(\tilde{\omega})}\gamma_u - \frac{e^{i\alpha(\tilde{\omega})}}{t}\int_{C_1}\varphi_s(\tilde{\xi})\left\{1-\coth\left\{\frac{\pi}{t}(\xi-\omega)\right\}\right\}ds$$

. . . . . (4.6).

As in Chapter 2, the solution of the real part of this equation is not unique since no extra condition has yet been built in. This condition is obtained from the Joukowski hypothesis [20, p.199] which requires that the speed of the flow be finite at the cusp. Because (4.6) cannot be applied at the cusp a further condition is (in practice) required. This further condition can be obtained by specifying that, in the vicinity of the cusp, the speed can be approximated by some simple function. In this context the work of Wilkinson [27] is noted. The need for an additional condition is analogous to the requirements of § 3.9).

Note that once a solution to the real part of (4.6) has been obtained, the circulation can be found from

$$\Gamma = \int_{C_1} \varphi_s(\tilde{\gamma})\, ds = \int_{C_1} \tau(\gamma)\, d\gamma$$

and τ_0 obtained from (4.4).

§ 4.3) Numerical solution of the restricted problem

The numerical method for obtaining a solution to this restricted problem is similar to that described in the preceding Chapter, § 3.5) to § 3.10). For this reason only a piecewise quadratic approximation to the boundary values of $\tau(\gamma)$ will be considered in detail.

Let the contour C_1 be divided into n_1 elements each of which is considered to be specified by nodes at the start, "mid" and end points of the element. Further, let the idealisation be carried out in such a way that the cusp lies at a node. Numbering these $2n_1$ nodes in the manner described in § 3.5) and approximating $\tau(\gamma)$ over each element by a piecewise quadratic function in γ enables (4.5) to take the form

$$\tau(\omega) \simeq 2\tau_u + \frac{i}{t} \sum_{q=1}^{n_1} \sum_{r=1}^{3} \tau(\gamma_{1,q}^{(r)}) \int_{I_{1,q}} M_{1,q}^{(r)}(\gamma) \left\{ 1 - \coth\left\{ \frac{\pi}{t}(\gamma - \omega) \right\} \right\} d\gamma \qquad \ldots\ldots (4.7)$$

where

$$M_{1,q}^{(r)}(\gamma) = \frac{(\gamma_{1,q}^{(r)} - \gamma_{1,q}^{(r)})(\gamma - \gamma_{1,q}^{(1)})(\gamma - \gamma_{1,q}^{(2)})(\gamma - \gamma_{1,q}^{(3)})}{(\gamma_{1,q}^{(3)} - \gamma_{1,q}^{(r)})(\gamma_{1,q}^{(r)} - \gamma_{1,q}^{(1)})(\gamma_{1,q}^{(r)} - \gamma_{1,q}^{(2)})(\gamma_{1,q}^{(r)} - \gamma)} .$$

As in Chapter 3, a more convenient form of (4.7) is

$$c(\omega)\,\tau(\omega)$$

$$\simeq 2\tau_u + \frac{i}{t}\sum_{q=1}^{n_1}\sum_{r=1}^{3}\tau(\tau_{1,q}^{(r)})\left\{1-\delta(\tau_{1,q}^{(r)}-\omega)\right\}\int_{I_{1,q}} M_{1,q}^{(r)}(\tau)\left\{1-\coth\left\{\frac{\pi}{t}(\tau-\omega)\right\}\right\}d\tau$$

where

$$c(\omega) = 1 - \frac{i}{t}\sum_{q=1}^{n_1}\sum_{r=1}^{3}\delta(\tau_{1,q}^{(r)}-\omega)\int_{I_{1,q}} M_{1,q}^{(r)}(\tau)\left\{1-\coth\left\{\frac{\pi}{t}(\tau-\omega)\right\}\right\}d\tau$$

and

$$\delta(\tau_{1,q}^{(r)}-\omega) = \begin{cases} 1 & \text{if } \tau_{1,q}^{(r)} = \omega \\ 0 & \text{otherwise} \end{cases}.$$

Similarly, it may be shown that (4.6) can be approximated by

$$c(\omega)\,\varphi_3(\tilde{\omega}) \simeq 2i\tau_u e^{i\alpha(\tilde{\omega})} + \frac{i}{t}\sum_{q=1}^{n_1}\sum_{r=1}^{3}\left\{1-\delta(\tau_{1,q}^{(r)}-\omega)\right\}\varphi_3(\tau_{1,q}^{(r)})\Delta_{1,q}^{(r)}(\omega) \qquad (4.8)$$

where

$$\Delta_{1,q}^{(r)}(\omega) = \exp\left\{i\alpha(\tilde{\omega}) - i\alpha(\tilde{\tau}_{1,q}^{(r)})\right\}\int_{I_{1,q}} M_{1,q}^{(r)}(\tau)\left\{1-\coth\left\{\frac{\pi}{t}(\tau-\omega)\right\}\right\}d\tau.$$

For convenience let the cusp occur at $\gamma^{(1)}_{1,1}$ (and hence at $\gamma^{(3)}_{1,n}$) so that for $q = 2\,(1)\,n$

$$\varphi_s(\tilde{\gamma}^{(1)}_{1,q}) = \varphi_s(\tilde{\gamma}^{(3)}_{1,q-1}) \qquad (4.9).$$

A system of $2n-1$ linear equations for the $2n$ unknowns

$\varphi_s(\tilde{\gamma}^{(1)}_{1,q})$, $\varphi(\tilde{\gamma}^{(2)}_{1,q})$, $q = 1\,(1)\,n$ together with

$\varphi_s(\tilde{\gamma}^{(3)}_{1,n})$ is obtained from the real part of (4.8) by

i) ignoring the error in the approximation

ii) identifying ω with each of the $2n-1$ nodes away from the cusp

iii) applying the continuity condition (4.9).

Two additional equations that can be adjoined to the above system of equations are obtained from the Joukowski hypothesis and by assuming that over the first (or last) element the complex conjugate velocity is linear in γ . Thus, the Joukowski hypothesis leads to

$$\varphi_s(\tilde{\gamma}^{(1)}_{1,1}) = -\varphi_s(\tilde{\gamma}^{(3)}_{1,n})$$

while a linear $\tau(\gamma)$ provides

$$\tau(\gamma^{(2)}_{1,1}) = \frac{\gamma^{(3)}_{1,1} - \gamma^{(2)}_{1,1}}{\gamma^{(3)}_{1,1} - \gamma^{(1)}_{1,1}}\,\tau(\gamma^{(1)}_{1,1}) + \frac{\gamma^{(2)}_{1,1} - \gamma^{(1)}_{1,1}}{\gamma^{(3)}_{1,1} - \gamma^{(1)}_{1,1}}\,\tau(\gamma^{(3)}_{1,1})$$

whence

$$\varphi_s(\tilde{\gamma}_{1,1}^{(2)}) = Re\left\{\frac{\gamma_{1,1}^{(3)} - \gamma_{1,1}^{(2)}}{\gamma_{1,1}^{(3)} - \gamma_{1,1}^{(1)}} \exp\left[\alpha(\tilde{\gamma}_{1,1}^{(2)})i - \alpha(\tilde{\gamma}_{1,1}^{(1)})i\right]\right\}\varphi_s(\tilde{\gamma}_{1,1}^{(1)})$$

$$+ Re\left\{\frac{\gamma_{1,1}^{(2)} - \gamma_{1,1}^{(1)}}{\gamma_{1,1}^{(3)} - \gamma_{1,1}^{(1)}} \exp\left[\alpha(\tilde{\gamma}_{1,1}^{(2)})i - \alpha(\tilde{\gamma}_{1,1}^{(3)})i\right]\right\}\varphi_s(\tilde{\gamma}_{1,1}^{(3)}).$$

The full system of linear equations can be solved by Gaussian elimination so that the problem reduces to one of quadrature.

The use of $\tau(\gamma)$ linear in the vicinity of the cusp can be contrasted with Wilkinson's constant speed assumption [27].

In (4.8) the evaluation of the coefficients of the $\varphi_s(\tilde{\gamma}_{1,q}^{(r)})$ is straightforward when ω corresponds to one of the $\gamma_{1,q}^{(r)}$, $\gamma_{1,p}^{(s)}$ say. It will be recalled that $\gamma_{1,p}^{(s)}$ cannot lie on the cusp.

Consider first the evaluation of $c(\gamma_{1,p}^{(s)})$. The result

$$\frac{\pi}{t}\int_{C_1} \coth\left\{\frac{\pi}{t}(\gamma - \gamma_{1,p}^{(s)})\right\} d\gamma = -\pi i \qquad (4.10)$$

is readily obtained from the identity (2.26), i.e. for $\omega \in C_1$

$$\tau(\omega) = \tau_u + \tau_D + \frac{1}{ti}\int_{C_1} \tau(\gamma)\coth\left\{\frac{\pi}{t}(\gamma - \omega)\right\} d\gamma.$$

Since for $\tau \in I_{1,q}$

$$1 = \sum_{r=1}^{3} M_{1,q}^{(r)}(\tau)$$

the integral (4.10) may be written as

$$\frac{\pi}{t} \sum_{q=1}^{n} \sum_{r=1}^{3} \int_{I_{1,q}} M_{1,q}^{(r)}(\tau) \coth\left\{\frac{\pi}{t}(\tau - \tau_{1,p}^{(s)})\right\} d\tau = -\pi i .$$

On adding $2\pi i$ to both sides, and dividing through by πi this last expression becomes

$$2 - \frac{i}{t} \sum_{q=1}^{n} \sum_{r=1}^{3} \int_{I_{1,q}} M_{1,q}^{(r)}(\tau) \coth\left\{\frac{\pi}{t}(\tau - \tau_{1,p}^{(s)})\right\} d\tau = 1$$

whence

$$2 - \frac{i}{t} \sum_{q=1}^{n} \sum_{r=1}^{3} \left\{1 - \delta(\tau_{1,q}^{(r)} - \tau_{1,p}^{(s)})\right\} \int_{I_{1,q}} M_{1,q}^{(r)}(\tau) \coth\left\{\frac{\pi}{t}(\tau - \tau_{1,p}^{(s)})\right\} d\tau$$

$$= 1 + \frac{i}{t} \sum_{q=1}^{n} \sum_{r=1}^{3} \delta(\tau_{1,q}^{(r)} - \tau_{1,p}^{(s)}) \int_{I_{1,q}} M_{1,q}^{(r)}(\tau) \coth\left\{\frac{\pi}{t}(\tau - \tau_{1,p}^{(s)})\right\} d\tau .$$

Similarly it can be shown that

$$\frac{i}{t}\sum_{q=1}^{n}\sum_{r=1}^{3}\left[1-\delta\left(\gamma_{1,q}^{(r)}-\gamma_{1,p}^{(s)}\right)\right]\int_{I_{1,q}} M_{1,q}^{(r)}(\xi)\,d\xi$$

$$= -\frac{i}{t}\sum_{q=1}^{n}\sum_{r=1}^{3}\delta\left(\gamma_{1,q}^{(r)}-\gamma_{1,p}^{(s)}\right)\int_{I_{1,q}} M_{1,q}^{(r)}(\xi)\,d\xi$$

from which it follows that

$$c\left(\gamma_{1,p}^{(s)}\right)$$

$$= 2 + \frac{i}{t}\sum_{q=1}^{n}\sum_{r=1}^{3}\left\{1-\delta\left(\gamma_{1,q}^{(r)}-\gamma_{1,p}^{(s)}\right)\right\}\int_{I_{1,q}} M_{1,q}^{(r)}(\xi)\left\{1-\coth\left\{\frac{\pi}{t}\left(\xi-\gamma_{1,p}^{(s)}\right)\right\}\right\}d\xi$$

. . . . (4.11)

For computational purposes this form of the coefficient $c\left(\gamma_{1,p}^{(s)}\right)$ is more convenient than the alternative given earlier.

To evaluate

$$\int_{I_{1,q}} M_{1,q}^{(r)}(\xi)\left\{1-\coth\left\{\frac{\pi}{t}\left(\xi-\gamma_{1,p}^{(s)}\right)\right\}\right\}d\xi$$

when $\gamma_{1,p}^{(s)} \neq \gamma_{1,q}^{(r)}$, the only case required due to the use of (4.11), write

$$\int_{I_{1,q}} M_{1,q}^{(r)}(\gamma)\left\{1 - \coth\left\{\frac{\pi}{t}(\gamma - \gamma_{1,p}^{(s)})\right\}\right\} d\gamma$$

$$= \int_{I_{1,q}} M_{1,q}^{(r)}(\gamma)\, d\gamma - \int_{I_{1,q}} M_{1,q}^{(r)}(\gamma) \coth\left\{\frac{\pi}{t}(\gamma - \gamma_{1,p}^{(s)})\right\} d\gamma$$

. . . . (4.12)

and consider separately the two integrals on the right hand side of this expression. If, for convenience, the previously given expression for $M_{1,q}^{(r)}(\gamma)$ is replaced by

$$M_{1,q}^{(r)}(\gamma) = \frac{(\gamma - a)(\gamma - b)}{(c - a)(c - b)}$$

then it is readily shown that the first of the integrals on the right hand side of (4.12) is given by

$$\int_{I_{1,q}} M_{1,q}^{(r)}(\gamma)\, d\gamma = \frac{\gamma_{1,q}^{(3)} - \gamma_{1,q}^{(1)}}{(c-a)(c-b)} \left\{ \frac{(\gamma_{1,q}^{(3)})^2 + \gamma_{1,q}^{(3)}\gamma_{1,q}^{(1)} + (\gamma_{1,q}^{(1)})^2}{3} \right.$$

$$\left. - \frac{\gamma_{1,q}^{(3)} + \gamma_{1,q}^{(1)}}{2}(a+b) + ab \right\}$$

. . . . (4.13)

It would appear that the integrals

$$\int_{I_{1,q}} M_{1,q}^{(r)}(\gamma) \coth\left\{\frac{\pi}{t}(\gamma - \gamma_{1,p}^{(s)})\right\} d\gamma \qquad (4.14)$$

cannot be evaluated in closed form. However, approximations to its value can be obtained by use of the various

expansions available for coth $\left\{\frac{\pi}{t}(z - z^{(s)}_{1,p})\right\}$. One such expansion is obtained below.

§4.4) <u>An expansion of coth z</u>

Consider the expansion

$$\coth z = \frac{1}{z} + 2z \sum_{p=1}^{\infty} \frac{1}{z^2 + p^2\pi^2}$$

which, for some as yet unknown K can be written as

$$\coth z = \frac{1}{z} + 2z \sum_{p=1}^{K-1} \frac{1}{z^2 + p^2\pi^2} + 2z \sum_{q=k}^{\infty} \frac{1}{q^2\pi^2}\left\{1 + \left(\frac{z}{q\pi}\right)^2\right\}^{-1}$$

For z satisfying $|z| < K\pi$, where K is an integer and $K>1$, each term of the form

$$\frac{2z}{q^2\pi^2}\left\{1 + \left(\frac{z}{q\pi}\right)^2\right\}^{-1}$$

can be expressed as

$$\frac{2z}{q^2\pi^2} \sum_{m=0}^{\infty} (-1)^m \left(\frac{z}{q\pi}\right)^{2m}$$

whence, for $|z| < K\pi$,

$$\coth z = \frac{1}{z} + 2z \sum_{p=1}^{K-1} \frac{1}{z^2 + p^2\pi^2} + 2z \sum_{q=K}^{\infty} \sum_{m=0}^{\infty} (-1)^m \frac{z^{2m}}{(q\pi)^{2m+2}}$$

$$= \frac{1}{z} + 2z \sum_{p=1}^{K-1} \frac{1}{z^2 + p^2\pi^2} + 2z \sum_{m=0}^{\infty} (-1)^m z^{2m} \sum_{q=K}^{\infty} \left(\frac{1}{q\pi}\right)^{2m+2}$$

That series of the form

$$\sum_{q=1}^{\infty} \left(\frac{1}{q\pi}\right)^{2n}$$

are related to the Bernoulli numbers B_n by

$$\sum_{q=1}^{\infty} \left(\frac{1}{q\pi}\right)^{2n} = \frac{2^{2n-1}}{(2n)!} B_n$$

[42, p.12] leads to the expression

$$2z \sum_{m=0}^{\infty} (-1)^m z^{2m} \sum_{q=k}^{\infty} \left(\frac{1}{q\pi}\right)^{2m+2}$$

$$= \sum_{m=1}^{\infty} (-1)^{m-1} z^{2m-1} \left\{ \frac{2^{2m} B_m}{(2m)!} - \sum_{n=1}^{k-1} \left(\frac{1}{n\pi}\right)^{2m} \right\}.$$

Hence, for $|z| < k\pi$, coth z can be expanded as

$$\coth z = \frac{1}{z} + 2z \sum_{p=1}^{k-1} \frac{1}{z^2 + p^2\pi^2}$$

$$+ \sum_{m=1}^{\infty} (-1)^{m-1} z^{2m-1} \left\{ \frac{2^{2m} B_m}{(2m)!} - \sum_{n=1}^{k-1} \left(\frac{1}{n\pi}\right)^{2m} \right\}$$

.... (4.15)

When $k = 1$ the expression (4.14) is readily shown to simplify to

$$\coth z = \frac{1}{z} + \sum_{m=1}^{\infty} (-1)^{m-1} z^{2m-1} \left\{ \frac{2^{2m} B_m}{(2m)!} \right\} \qquad (4.16).$$

That the expansions (4.15) and (4.16) can be expected to converge quite quickly is demonstrated in Table 4-1. Here values of the coefficients

$$(-1)^{m-1}\left\{\frac{2^{2m}B_m}{(2m)!} - \sum_{n=1}^{K-1}\left(\frac{1}{n\pi}\right)^{2m}\right\}$$

are given for $k=2(1)5$ and $m=1(1)12$. Values of the coefficients

$$(-1)^{m-1}\left\{\frac{2^{2m}B_m}{(2m)!}\right\},$$

i.e. the coefficients corresponding to the case $k=1$, are also given for $m=1(1)12$.

§ 4.5) Numerical solution of the restricted problem (contd.)

The coefficients (4.14), i.e.

$$\int_{I_{1,2}} M_{1,2}^{(r)}(\gamma)\,\coth\left\{\frac{\pi}{t}\left(\gamma-\gamma_{1,p}^{(s)}\right)\right\}d\gamma,$$

which are required in the numerical solution of (4.8) are readily approximated if use is made of the expansion given above. Because (4.16) is only a special case of (4.15), consider the substitution

$$\frac{\pi}{t}\left(\gamma-\gamma_{1,p}^{(s)}\right) = z$$

in (4.15). This expansion then yields

$$\coth\left\{\frac{\pi}{t}\left(\gamma-\gamma_{1,p}^{(s)}\right)\right\} = \frac{t}{\pi\left(\gamma-\gamma_{1,p}^{(s)}\right)} + \sum_{m=1}^{\infty} A_m\left(\gamma-\gamma_{1,p}^{(s)}\right)^{2m-1}$$

$$+ \frac{2t\left(\gamma-\gamma_{1,p}^{(s)}\right)}{\pi}\sum_{J=1}^{K-1}\frac{1}{\left(\gamma-\gamma_{1,p}^{(s)}\right)^2+(Jt)^2} \qquad (4.17)$$

where

$$A_m = (-1)^{m-1}\left(\frac{\pi}{t}\right)^{2m-1}\left\{\frac{2^{2m}B_m}{(2m)!} - \sum_{n=1}^{K-1}\left(\frac{1}{n\pi}\right)^{2m}\right\} \qquad (4.18),$$

which is valid for

$$\left|\gamma-\gamma_{1,p}^{(s)}\right| < Kt \qquad (4.19).$$

From the condition (4.19) it can be concluded that expansion (4.17) is valid for chord: pitch ratios of less than K . Also, (4.19) should be used to determine K.

Note that for a cascade with infinite pitch, i.e. an isolated aerofoil, (4.17) yields

$$\lim_{t\to\infty} \frac{\pi}{t} \coth\left\{\frac{\pi}{t}\left(\bar{\gamma}-\bar{\gamma}_{1,p}^{(s)}\right)\right\} = \frac{1}{\bar{\gamma}-\bar{\gamma}_{1,p}^{(s)}}$$

as expected.

Returning to the evaluation of (4.14), which shall be denoted by $L_q^{(r)}(\bar{\gamma}_{1,p}^{(s)})$, and making the change of variable $Z = \bar{\gamma} - \bar{\gamma}_{1,p}^{(s)}$ it follows from (4.17) that

$$\frac{\pi}{t} L_q^{(r)}(\bar{\gamma}_{1,p}^{(s)}) = \sum_{J=1-K}^{K-1} \int_{Z_A}^{Z_B} N_q^{(r)}(Z) \frac{dZ}{Z + iJt}$$

$$+ \frac{\pi}{t} \sum_{m=1}^{\infty} A_m \int_{Z_A}^{Z_B} N_q^{(r)}(Z) Z^{2m-1} dZ \qquad \ldots\ldots (4.20)$$

where
$$Z_A = \bar{\gamma}_{1,q}^{(1)} - \bar{\gamma}_{1,p}^{(s)}$$
$$Z_B = \bar{\gamma}_{1,q}^{(3)} - \bar{\gamma}_{1,p}^{(s)}$$
$$N_q^{(r)}(Z) = M_{1,q}^{(r)}(Z + \bar{\gamma}_{1,p}^{(s)}) .$$

The integrations in (4.20) can all be performed in closed form since the case $\bar{\gamma}_{1,q}^{(r)} = \bar{\gamma}_{1,p}^{(s)}$ is not required. Hence, in (4.8) the coefficients of the $\varphi_s(\tilde{\bar{\gamma}}_{1,q}^{(r)})$ can always be evaluated using either (4.11) or (4.20). Clearly, the infinite series in (4.20) requires truncating when some satisfactory level of accuracy in the evaluation of the $L_q^{(r)}(\bar{\gamma}_{1,p}^{(s)})$ has been reached, Table 4-1 is useful for this purpose.

Writing $W = iJt$ and

$$N_q^{(r)}(z) = \frac{(z-D)(z-E)}{(C-D)(C-E)}$$

the relevant coefficients are seen to be

$$\int_{z_A}^{z_B} N_q^{(r)}(z)\, z^{2m-1} dz$$

$$= \frac{1}{(C-D)(C-E)} \left[z^{2m} \left\{ \frac{z^2}{2m+2} - \frac{z(D+E)}{2m+1} + \frac{DE}{2m} \right\} \right]_{z_A}^{z_B}$$

and

$$\int_{z_A}^{z_B} N_q^{(r)}(z) \frac{dz}{z+iJt}$$

$$= \frac{1}{(C-D)(C-E)} \left[z \left\{ \frac{1}{2} z - (W+D+E) \right\} + (W+D)(W+E) \log\{z+W\} \right]_{z_A}^{z_B} .$$

§ 4.6) Example

As an example of the use of the numerical procedures given above, the flow past a cascade of symmetric aerofoils obtained by conformal mapping was considered.

A mapping of the region outside a cascade of flat plates (with zero stagger) which lie in the physical $(\tau = x+iy)$ plane onto the region outside the circle $|t_1| = a$ is given by [43, p.535] .

$$\tau = \frac{t}{2\pi}\left\{\log\left(\frac{1+t_1}{1-t_1}\right) + \log\left(\frac{t_1+a^2}{t_1-a^2}\right)\right\} \qquad (4.21)$$

where t is the cascade pitch. For upstream and downstream flow conditions (in the physical plane) $\tau_u = u_u + i v_u$ and $\tau_D = u_D + i v_D$ respectively, the complex velocity potential in the t_1 - plane is given by [43, p.536]

$$W_1(t_1) = \frac{u_u t}{2\pi}\log\left\{\frac{(t_1+1)(t_1+a^2)}{(t_1-1)(t_1-a^2)}\right\} + i\frac{v_u t}{2\pi}\log\left\{\frac{t_1+1}{t_1+a^2}\right\}$$

$$- i\frac{v_D t}{2\pi}\log\left\{\frac{t_1-1}{t_1-a^2}\right\}$$

The complex conjugate velocity $\tau_1(t_1)$ for the flow in the t_1 -plane is therefore given by

$$\tau_1(t_1) = \frac{dW_1}{dt_1}$$

$$= \frac{u_u t}{2\pi}\left\{\frac{1}{t_1+1} + \frac{1}{t_1+a^2} - \frac{1}{t_1-1} - \frac{1}{t_1-a^2}\right\}$$

$$+ \frac{i v_u t}{2\pi}\left\{\frac{1}{t_1+1} - \frac{1}{t_1+a^2}\right\} - \frac{i v_D t}{2\pi}\left\{\frac{1}{t_1-1} - \frac{1}{t_1-a^2}\right\}$$

A cascade of symmetric aerofoils which have both finite thickness and a cusped trailing edge is obtained by applying (4.21) to the circle

$$|t_2| = |t_1 - t_0| = b > a$$

where t_0 lies on the negative real axis of the t_1-plane, $b + t_0 = a$ and $b - t_0 < 1$. In this case the complex velocity potential in the t_1 plane is given by

$$W_2(t_1) = \frac{U_u t}{2\pi} \log\left\{\frac{(t_2+1+t_0)(a^2+t_2[1+t_0])}{(t_2-1+t_0)(a^2-t_2[1-t_0])}\right\}$$

$$+ i\frac{V_u t}{2\pi} \log\left\{\frac{t_2+1+t_0}{a^2+t_2(1+t_0)}\right\} - i\frac{V_D t}{2\pi} \log\left\{\frac{t_2-1+t_0}{t_2(1-t_0)-a^2}\right\}$$

where $t_2 = t_1 - t_0$.

The complex conjugate velocity $\tau_2(t_1)$ for the flow in the t_1-plane is now given by

$$\tau_2(t_1) = \frac{U_u t}{2\pi}\left\{\frac{1}{t_2+1+t_0} + \frac{1+t_0}{a^2+t_2(1+t_0)} - \frac{1}{t_2-1+t_0} - \frac{1-t_0}{t_2(1-t_0)-a^2}\right\} + i\frac{V_u t}{2\pi}\left\{\frac{1}{t_2+1+t_0} - \frac{1+t_0}{a^2+t_2(1+t_0)}\right\}$$

$$- i\frac{V_D t}{2\pi}\left\{\frac{1}{t_2-1+t_0} - \frac{1-t_0}{t_2(1-t_0)-a^2}\right\} \quad \ldots\ldots (4.22)$$

where $t_2 = t_1 - t_0$.

The above expressions for γ and $\tau_2(t_1)$, viz (4.21) and (4.22), allow the complex conjugate velocity $\tau(\gamma)$ to be evaluated at all points in the physical plane. Hence the tangential velocity component (alternatively signed speed) $\varphi_s(\tilde{\gamma})$ can be obtained for all points lying on the contour bounding each aerofoil in the cascade.

Finally, in problems of the type considered here only the upstream flow condition τ_u is specified. To obtain the downstream flow condition τ_b note that the Joukowski hypothesis requires

$$\tau_z(a) = 0 \qquad (4.23)$$

in which case V_b can be obtained from (4.22). That $u_u = u_b$ has already been stated.

The numerical procedures of § 4.3) to § 4.5) were applied to the cascade of aerofoils obtained by applying (4.21) to the circle

$$|t_1 + 0.1| = 0.6,$$

in which case $a = 0.5$, and taking $t = 4$. The upstream flow condition considered was

$$\tau_u = 1 - i,$$

i.e. a flow having speed $\sqrt{2}$ and an inlet angle of 45°. In this case equation (4.23) yielded a downstream flow condition of

$$\tau_b = 1 - 0.05882i$$

i.e. a flow having speed 1.00173 and exit angle 3.366°.

Figures 4-1 and 4-2 show a typical aerofoil in the cascade and a plot of $\varphi_s(\tilde{s})$ against arc length for the problem under consideration. In Figure 4-2 the $\varphi_s(s)$ and arc length have been normalised to approximations for the maximum speed on aerofoil (=3.6786) and the total arc length (=6.33234)respectively.

Examination of the mapping (4.21) showed that the ratio of chord to pitch was approximately 0.745. This resulted in the use of expansion (4.16) throughout the computations.

The boundary nodes required by the idealisation of § 4.3) were obtained by taking N (N even) equi-spaced points on the circle

$$|t_1 + 0.1| = 0.6$$

Finally, in problems of the type considered here only the upstream flow condition ζ_u is specified. To obtain the downstream flow condition ζ_D note that the Joukowski hypothesis requires

$$\zeta_2(a) = 0 \tag{4.23}$$

in which case V_b can be obtained from (4.22). That $u_u = u_D$ has already been stated.

The numerical procedures of § 4.3) to § 4.5) were applied to the cascade of aerofoils obtained by applying (4.21) to the circle

$$|t_1 + 0.1| = 0.6,$$

in which case $a = 0.5$, and taking $t = 4$. The upstream flow condition considered was

$$\zeta_u = 1 - i,$$

i.e. a flow having speed $\sqrt{2}$ and an inlet angle of 45°. In this case equation (4.23) yielded a downstream flow condition of

$$\zeta_D = 1 - 0.05882i$$

i.e. a flow having speed 1.00173 and exit angle 3.366°.

Figures 4-1 and 4-2 show a typical aerofoil in the cascade and a plot of $\varphi_s(\tilde{\zeta})$ against arc length for the problem under consideration. In Figure 4-2 the $\varphi_s(\zeta)$ and arc length have been normalised to approximations for the maximum speed on aerofoil (=3.6786) and the total arc length (=6.33234)respectively.

Examination of the mapping (4.21) showed that the ratio of chord to pitch was approximately 0.745. This resulted in the use of expansion (4.16) throughout the computations.

The boundary nodes required by the idealisation of § 4.3) were obtained by taking N (N even) equi-spaced points on the circle

$$|t_1 + 0.1| = 0.6$$

Because the point $t_1 = 0.5$ maps into the cusp in the physical plane, the point $t_1 = 0.5$ was taken as the first point on the circle.

The nodes lying on the boundary of the aerofoil (in the physical plane) for the case N = 60 are shown in Figure 4-3. The nodal approximations to $\varphi_s(\tilde{\tau})$ are shown in Figure 4-4 and should be compared with Figure 4-2. That gross errors were occurring, particularly for $Re(\tau) > 0$ is clearly illustrated by these figures.

In an attempt to reduce these errors the problem was solved for the case N = 120. The resulting positions of the boundary nodes used and the approximate $\varphi_s(\tilde{\tau})$ obtained are shown in Figures 4-5 and 4-6 respectively. Comparison of Figure 4-6 with Figure 4-2 shows that although gross errors were still occurring they were confined to the region extending from $Re(\tau) > 0.75$ to the cusp. Indeed, these figures show that good approximations to the location of the leading edge stagnation point and maximum nodal $|\varphi_s(\tilde{\tau})|$ can be obtained despite the gross errors local to the cusp region.

The approximation to the downstream flow condition, $\hat{\tau}_D$ say, for the N = 120 case was

$$\hat{\tau}_D = 1 - 0.15663\, i \quad ,$$

i.e. a flow having speed 1.01219 and exit angle 1.902°.

§ 4.7) Modified Cusp Model

The disappointing results of the preceding section suggest that a more detailed examination of the behaviour of (4.8) when the point ω lies close to the cusp should be undertaken.

Consider the cascade aerofoil shown in Figure 4-7. Here the aerofoil resembles a plate in the vicinity of the cusp, i.e. the aerofoil reduces to zero thickness between the point A and the cusp B. The analysis of Chapter 2 shows that the complex conjugate velocity $\tau(\tau)$, evaluated at a point lying entirely within the flow region R, satisfies the identity

$$2\tau(\omega_0) = \tau_u + \tau_D$$

$$+ \frac{1}{ti}\int_{C_1} \tau(\beta)\coth\left\{\frac{\pi}{t}(\beta-\omega_0)\right\} d\beta \qquad (4.24)$$

where $\omega_0 \in R$ but $\omega_0 \notin C_1$, t is the cascade pitch and

$$\lim_{Re\{\beta\}\to-\infty} \tau(\beta) = \tau_u$$

$$\lim_{Re\{\beta\}\to\infty} \tau(\beta) = \tau_D .$$

It should be noted that the path of integration in (4.24) involves traversing both the suction surface and pressure surface sides of the line AB and that $\tau(\beta)$ may take different values on these surfaces.

Let $\tilde{C}$ be the integration path obtained by omitting the line AB from the contour C_1. Writing $\tau(\beta^+) \equiv \tau(\beta)$ for β on the suction surface side of AB and $\tau(\beta^-) \equiv \tau(\beta)$ for β on the pressure surface side of AB, the identity (4.24) may be given as

$$2\tau(\omega_0) = \tau_u + \tau_D + \frac{1}{ti}\int_{AB} \Delta\tau(\beta)\coth\left\{\frac{\pi}{t}(\beta-\omega_0)\right\} d\beta$$

$$+ \frac{1}{ti}\int_{\tilde{C}} \tau(\beta)\coth\left\{\frac{\pi}{t}(\beta-\omega_0)\right\} d\beta \qquad (4.25)$$

where $\Delta\tau(\beta) = \tau(\beta^+) - \tau(\beta^-)$.

Following the analysis of Chapter 2, the limiting form of (4.25) as ω_0 tends to a point ω_1 on the curve $\tilde{C}$ is clearly

$$\tau(\omega_1) = \tau_u + \tau_D + \frac{1}{ti}\int_{\tilde{C}} \tau(\beta)\coth\left\{\frac{\pi}{t}(\beta-\omega_1)\right\} d\beta$$

$$+ \frac{1}{ti}\int_{AB} \Delta\tau(\beta)\coth\left\{\frac{\pi}{t}(\beta-\omega_1)\right\} d\beta \qquad (4.26)$$

However, when ω_1 tends to a point ω_2 on the line AB the limiting process can be shown to yield

$$\sum \tau(\omega_2) = \tau_u + \tau_D + \frac{1}{\pi i}\int_{\tilde{C}} \tau(\gamma)\coth\left\{\frac{\pi}{t}(\gamma-\omega_2)\right\}d\gamma$$

$$+ \frac{1}{\pi i}\int_{AB} \Delta\tau(\gamma)\coth\left\{\frac{\pi}{t}(\gamma-\omega_2)\right\}d\gamma \qquad (4.27)$$

where $\sum \tau(\omega_2) = \tau(\omega_2^+) + \tau(\omega_2^-)$.

It should be noted that the integrals

$$\int_{\tilde{C}} \tau(\gamma)\coth\left\{\frac{\pi}{t}(\gamma-\omega_1)\right\}d\gamma$$

and

$$\int_{AB} \Delta\tau(\gamma)\coth\left\{\frac{\pi}{t}(\gamma-\omega_2)\right\}d\gamma$$

in (4.23) and (4.24) respectively, need to be interpreted in their Cauchy Principal Value sense.

Although the aerofoil of § 4.6) does not have a portion of its suction surface coinciding with a portion of its pressure surface, examination of Figure 4-1 shows that for $x > 1.3$ the suction and pressure surfaces do lie very close to one another. Indeed, for $x > 1.3$ the distance between points on the boundary which correspond to the same value of x is less than 0.01.

Apparently, as x increases towards the value it takes at the cusp, there is some value of x beyond which equation (4.27) should be used to evaluate the complex conjugate velocity. This use of (4.27) is in preference to the use of either (4.26) or the limiting form of (4.24), i.e. equation (4.1).

The proposed use of (4.27) does present additional problems when one returns to the consideration of the restricted problem described in § 4.2).

Consider again the aerofoil shown in Figure 4-7. For this aerofoil use of (4.26) and (4.27) enables equation (4.5) to be replaced by

$$\tau(\omega_1) = 2\tau_u + \frac{i}{t}\int_{\tilde{C}} \tau(\delta)\left\{1 - \coth\left\{\frac{\pi}{t}(\delta-\omega_1)\right\}\right\}d\delta$$

$$+ \frac{i}{t}\int_{AB} \Delta\tau(\delta)\left\{1 - \coth\left\{\frac{\pi}{t}(\delta-\omega_1)\right\}\right\}d\delta \qquad (4.28)$$

when $\omega = \omega_1 \in \tilde{C}$ and

$$\sum \tau(\omega_2) = 2\tau_u + \frac{i}{t}\int_{\tilde{C}} \tau(\delta)\left\{1 - \coth\left\{\frac{\pi}{t}(\delta-\omega_2)\right\}\right\}d\delta$$

$$+ \frac{i}{t}\int_{AB} \Delta\tau(\delta)\left\{1 - \coth\left\{\frac{\pi}{t}(\delta-\omega_2)\right\}\right\}d\delta \qquad (4.29)$$

when $\omega = \omega_2 \in AB$. Similarly, equation (4.6) is replaced by

$$\varphi_s(\tilde{\omega}_1) = 2ie^{i\alpha(\tilde{\omega}_1)}\tau_u - \frac{e^{i\alpha(\tilde{\omega}_1)}}{t}\int_{\tilde{C}} \varphi_s(\tilde{\delta})\left\{1 - \coth\left\{\frac{\pi}{t}(\delta-\omega_1)\right\}\right\}ds$$

$$- \frac{e^{i\alpha(\omega_1)}}{t}\int_{AB} \Delta\varphi_s(\tilde{\delta})\left\{1 - \coth\left\{\frac{\pi}{t}(\delta-\omega_1)\right\}\right\}ds \qquad (4.30)$$

$$\sum \varphi_s(\tilde{\omega}_2) = 2ie^{i\alpha(\tilde{\omega}_2^+)}\tau_u - \frac{e^{i\alpha(\tilde{\omega}_2^+)}}{t}\int_{\tilde{C}} \varphi_s(\tilde{\delta})\left\{1 - \coth\left\{\frac{\pi}{t}(\delta-\omega_2)\right\}\right\}ds$$

$$- \frac{e^{i\alpha(\tilde{\omega}_2^+)}}{t}\int_{AB} \Delta\varphi_s(\tilde{\delta})\left\{1 - \coth\left\{\frac{\pi}{t}(\delta-\omega_2)\right\}\right\}ds \qquad (4.31)$$

where $\alpha(\tilde{\omega}_2^+)$ denotes the argument of the outward drawn normal to the suction surface side of AB evaluated at the point ω_2 ,

$$\sum \varphi_s(\tilde{\omega}_2) = i e^{i\alpha(\tilde{\omega}_2^+)} \sum \tau(\omega_2)$$

and for $\tau \in AB$

$$\Delta \varphi_s(\tilde{\tau}) = i e^{i\alpha(\tilde{\tau}^+)} \Delta \tau(\tau) = \Delta \tau(\tau) \frac{d\tau}{ds} .$$

It is when one considers just the real parts of equations (4.30) and (4.31) that the additional problems introduced by the proposed use of (4.27) become apparent. Clearly, taking the real parts of equations (4.30) and (4.31) yields just <u>two</u> coupled integral equations for the <u>three</u> unknown functions $\varphi_s(\tilde{\tau})$ $(\tau \in \tilde{C})$, $\Delta\varphi_s(\tilde{\tau})$ $(\tau \in AB)$ and $\sum \varphi_s(\tilde{\tau})$ $(\tau \in AB)$. Thus an underdetermined system of coupled integral equations is obtained.

The coupling of the imaginary part of either equation (4.30) on equation (4.31) to the underdetermined system of integral equations does appear to be one way of providing the additional integral equation required before a solution can be attempted. However, this additional equation would be of the First Kind type and could be expected to complicate the analysis somewhat.

An alternative to the above use of a coupled system of equations is based on the observation that (in practice) the ratio of the length of the line AB to the aerofoil's chord can be expected to be small. When this ratio is small it is not unreasonable to expect $\tau(\tau^+)$ to be approximately equal to $\tau(\tau^-)$ for $\tau \in AB$. Indeed, the shorter the line AB the more likely this is to be true since $\tau(\tau)$ is single valued at the cusp. Setting $\tau(\tau^+) = \tau(\tau^-)$ for $\tau \in AB$ yields $\Delta\tau(\tau) = 0$ whence equations (4.28) and (4.30) become

$$\tau(\omega_1) = 2\tau_u + \frac{i}{t}\int_{\tilde{C}} \tau(\tau)\left\{1 - \coth\left\{\frac{\pi}{t}(\tau-\omega_1)\right\}\right\} d\tau \qquad (4.32)$$

and

$$\varphi_s(\tilde{\omega}_1) = 2ie^{i\alpha(\tilde{\omega}_1)}\chi_u$$

$$-\frac{e^{i\alpha(\tilde{\omega}_1)}}{t}\int_{\tilde{C}}\varphi_s(\tilde{\gamma})\left\{1-\coth\left\{\frac{\pi}{t}(\gamma-\omega_1)\right\}\right\}ds \qquad (4.33)$$

respectively.

Clearly, equations (4.32) and (4.33) are just equations (4.5) and (4.6) with the line AB omitted from the path of integration. A numerical method for the approximate solution of the real part of equation (4.6) had been described in detail in Sections §4.3) to §4.5). This numerical method is based on the approximation of the complex conjugate velocity in equation (4.5) by piecewise quadratic (complex) polynominals. An approximate solution to the real part of equation (4.33) can be obtained in a similar fashion.

There are two major differences between the numerical solution of the real part of equation (4.33) and that used earlier. These differences are:

i) only the contour $\tilde{C}$ is divided into elements, the start node of the first element being taken to lie at the point A.

ii) rather than treating the point A as a cusp and stipulating that $\varphi_s(\tilde{A}^+) = -\varphi_s(\tilde{A}^-)$, the variation in the complex conjugate velocity over the last element of the idealisation may be approximated by a function which is linear in the complex variable γ.

Note that the numerical method of §4.3) to §4.5) already requires that the complex conjugate velocity of the first element be approximated by a function which is linear in γ.

Finally, cusped aerofoils which have suction and pressure surfaces which are nearly co-incident over part of their length, i.e. cusped aerofoils which have negligible thickness in the vicinity of the cusp, can always be approximated by aerofoils of the type shown in Figure 4-7. When such approximations are considered the problem includes that of choosing the point A. In practice a point on the suction surface

corresponding to the point A^+ and a point on the pressure surface corresponding to the point A^- need choosing.

§ 4.8) Example (contd)

To illustrate the improvement in results which can be obtained by making use of the modified cusp model of the preceding section, the example of section § 4.6) was re-considered.

Figure 4-8 shows the positions of the nodes used in the first attempt at finding an improved numerical solution of the specified problem. Excluding the node at the cusp, which now plays no part in the numerical method and is only shown for convenience, there were 55 nodes in the idealisation used. The idealisation was obtained from that shown in Figure 4-3 by omitting from that figure the four nodes nearest to the cusp. This meant that for this example the points A^+ and A^- were not co-incident but were as shown.

Recalling that the upstream flow condition for this example was $\tau_u = 1-i$, the results obtained for the modified cusp model method applied to the idealisation of Figure 4-8 are shown in Figure 4-9. By way of contrast to Figure 4-4, Figure 4-9 allows direct comparison between the nodal values of the normalised $\varphi_s(\tilde{s})$ (drawn with a solid line) and their numerical counterparts (shown dotted). That the normalised arc length is again measured from the cusp and not from A^- to A^+ should be noted.

Examination of Figure 4-9 shows that the relative error of the approximate $\varphi_s(\tilde{s})$ is less than 0.1 for $x < 0.26$. Further examination of this figure shows that the maximum error on the suction surface occurs at the point A^+ and that the error at this point is approximately 22% of $\varphi_s(\tilde{A}^+)$. The maximum error for the pressure surface is approximately 19% of $\varphi_s(\tilde{A}^-)$ and occurs at the point A^-.

True and approximate values of such flow-field parameters as maximum speed on the aerofoil, exit speed and exit angle are compared in Table 4-2. This table shows that even the coarse idealisation of Figure 4-8 yields approximations to the maximum speed on the aerofoil and exit speed which are within 3% of their true values. The approximation to the angle through which the flow is turned is not as good; the

coarse idealisation yielding an angle which is only within 17½% of the true value.

In order to reduce the errors seen in the above approximations (and to test the convergence of the numerical method) the problem was then solved using 113 nodes in the idealisation. Figure 4-10 shows the idealisation which was used. This idealisation was obtained from that illustrated in Figure 4-5 by omitting the six nodes nearest to the cusp (c.f. the manner in which Figure 4-8 was obtained).

Figure 4-11 demonstrates the marked improvement in results which use of the improved idealisation yielded. Indeed, this figure shows that the approximations to $\varphi_s(\tilde{A}^+)$ and $\varphi_s(\tilde{A}^-)$ were obtained to within 10% of their true values. That the points A^+ and A^- illustrated in Figure 4-10 are not the same as those given in Figure 4-8 should be noted.

A comparison between the true and approximate values of the previously mentioned flow-field parameters is given in Table 4-3. This table shows that the improved idealisation reduced the relative error in the approximations to the maximum speed on the aerofoil and exit speed to less than 0.005. The relative error in the angle through which the flow is turned was also much reduced (from 0.17058 to 0.04693).

Additional improvement in results were obtained by refining the idealisation of the aerofoil even further. Figure 4-12 shows an idealisation of the aerofoil which comprises of 229 nodes and has the points A^+ and A^- coinciding with those shown in Figure 4-10. The results obtained using this new idealisation are shown in Figure 4-13 and should be compared with those shown in Figures 4-9 and 4-11.

That the modified cusp model does provide a means of improving the results obtained from the basic numerical method of sections §4.3) to §4.5) can be seen by comparing Figure 4-9 with Figure 4-4 and comparing Figure 4-11 with Figure 4-6. The improvement is most marked in the vicinity of the cusped trailing edge.

Chapter 5

THE GENERATION OF A REGULAR FUNCTION FROM THE BOUNDARY VALUES OF ITS FIRST DERIVATIVE

§ 5.1) Introduction

So far in this thesis, the author has been concerned solely with the determination of the boundary tangential derivative $\varphi_s(\tilde{\tau})$ of a harmonic function $\varphi(x,y)$ from knowledge of the values taken by the boundary normal derivative $\varphi_n(\tilde{\tau})$. In the case of the analysis of the flow past an isolated or cascade aerofoil, a problem can usually be considered to have been solved once $\varphi_s(\tilde{\tau})$ has been determined because of the relationship of $\varphi_s(\tilde{\tau})$ to the speed of the flow.

This is frequently not the case when interior problems such as torsion and flexure are being considered. In these problems knowledge of $\varphi(x,y)$ is often required. Indeed, Chapter 6 demonstrates how both $\varphi(x,y)$ and its harmonic conjugate $\psi(x,y)$ are required when the evaluation of the torsional properties of a plane section is being attempted by boundary integral methods.

In view of the importance of the facility to obtain interior $\varphi(x,y)$ and $\psi(x,y)$ from their boundary normal and boundary tangential derivatives, the author describes in this chapter a number of techniques by which this may be accomplished. The techniques described fall into two categories, viz.

i) the evaluation of the boundary values of $\varphi(x,y)$ and $\psi(x,y)$ by an integration taken around the boundaries of a region followed by the use of Cauchy's integral for evaluating $\varphi(x,y)$ and $\psi(x,y)$ at interior points.

ii) the evaluation of $\varphi(x,y)$ and $\psi(x,y)$ at either boundary or interior points by a boundary integral representation derived in this chapter.

The numerical methods associated with these techniques are discussed but only one example involving ii) is given here. However, ii) is used to obtain the results given in Chapter 6.

The boundary integral representation for evaluating $\varphi(x,y)$ and $\psi(x,y)$ from knowledge of $\varphi_s(\tilde{\tau})$ and $\varphi_n(\tilde{\tau})$ is, in fact, a particular case of a general representation involving derivatives of any specified order. This more general representation is also discussed.

§ 5.1) Use of path independent integrals

Consider the region R which is bounded by the m contours C_p, $p=1(1)m$ and when $m>1$, i.e. the region is multiply connected, let C_1 be the contour enclosing all other contours. When $\varphi(x,y)$ and $\psi(x,y)$ are single valued in R the regular function

$$f(\tau) = \varphi(x,y) + i\psi(x,y) \tag{5.1}$$

may be defined for $\tau = x+iy \in R$.

Denoting the first partial derivatives of $\varphi(x,y)$ by $\varphi_x(\tilde{\tau})$ and $\varphi_y(\tilde{\tau})$, the function

$$\tau(\tau) = \varphi_x(\tilde{\tau}) - i\varphi_y(\tilde{\tau})$$

is also regular and is related to $f(\tau)$ through

$$\tau(\tau) = \frac{d}{d\tau} f(\tau).$$

Hence, given $\varphi_x(\tilde{\tau})$ and $\varphi_y(\tilde{\tau})$ either inside R or on the contours C_p, $f(\tau)$ can be evaluated at the point ω by integration, i.e.

$$f(\omega) = f(\tau_0) + \int_{\tau_0}^{\omega} \tau(\tau)\, d\tau \tag{5.2}$$

where $f(\tau_0)$ is a complex constant giving the value of $f(\tau)$ at some specified point τ_0 and the integral is path independent [35, pp.65-66]. In many applications $f(\tau_0)$ may be assigned an arbitrary value.

When γ_0 and ω lie on the contour C_1, the path of integration may be taken to follow the contour C_1 and the known relation

$$\tau(\gamma) = -i\, e^{-i\alpha(\tilde{\gamma})} \left\{ \phi_s(\tilde{\gamma}) + i\phi_n(\tilde{\gamma}) \right\} \qquad (5.3),$$

$\gamma \in C_p$, used to evaluate $\tau(\gamma)$ on the contour C_1. As in earlier chapters, $\alpha(\tilde{\gamma})$ denotes the argument of the outward normal to the boundary at γ.

For the case when $m \neq 2$, $\gamma_0 \in C_1$ and ω lies on one of the remaining contours, i.e. $\omega \in C_p$ with $p \neq 1$, a path of integration passing through the region must be chosen. The necessary integration can still be performed since Cauchy's integral

$$2\pi i\, \tau(\gamma) = \sum_{p=1}^{m} \int_{C_p} \frac{\tau(z)}{z - \gamma}\, dz \qquad (5.4)$$

can be utilised to evaluate $\tau(\gamma)$ when $\gamma \notin C_p$, $p = 1(1)m$. When any part of the chosen path of integration lies on one of the contours C_p, (5.3) can again be used to provide the necessary values of $\tau(\gamma)$, $\gamma \in C_p$.

When evaluating (5.2) numerically, use can be made of the boundary idealisation of § 3.2) together with boundary approximations to $\tau(\gamma)$ of the form given in § 3.5), i.e. each of the contours C_p is divided into the n_p boundary elements $I_{p,q}$ and for $\gamma \in I_{p,q}$ an approximation of the form

$$\tau(\gamma) \simeq \sum_{r=1}^{n} M_{p,q}^{(r)}(\gamma)\, \tau(\gamma_{p,q}^{(r)}) \qquad (5.5)$$

is assumed. For convenience let $\gamma_0 = \gamma_{1,1}^{(1)}$.

Figures 5-1 to 5-3 show that there are three cases to be considered:-

i) $\omega \in I_{1,g}$ with the path of integration taken to be the union of the arcs $I_{1,1}$ ..... $I_{1,g-1}$ together with that part of the arc $I_{1,g}$ which lies between $\gamma_{1,g}^{(1)}$ and ω.

Since

$$f(\omega) = f(\gamma_{1,g-1}^{(n)}) + \int_{\gamma_{1,g}^{(1)}}^{\omega} P(\zeta)\,d\zeta$$

(5.2) may be approximated by

$$f(\omega) \simeq f(\gamma_{1,1}^{(1)}) + \sum_{g=1}^{g-1} \sum_{r=1}^{n} \tau(\gamma_{1,g}^{(r)}) \int_{I_{1,g}} M_{1,g}^{(r)}(\zeta)\,d\zeta + \sum_{r=1}^{n} \tau(\gamma_{1,g}^{(r)}) \int_{\gamma_{1,g}^{(1)}}^{\omega} M_{1,g}^{(r)}(\zeta)\,d\zeta \qquad (5.6).$$

When the piecewise linear approximation of § 3.6) is used in (5.5) and $\omega = \gamma_{1,g}^{(2)}$, the formula (5.6) gives a complex form of the trapezoidal quadrature formula, i.e.

$$f(\omega) \simeq f(\gamma_{1,1}^{(1)}) + \frac{1}{2} \sum_{g=1}^{g} \{\gamma_{1,g}^{(2)} - \gamma_{1,g}^{(1)}\} \{\tau(\gamma_{1,g}^{(2)}) + \tau(\gamma_{1,g}^{(1)})\}$$

. . . . (5.7)

ii) when ω lies within the region a suitable path of integration is obtained by locating the point on C_1, γ_1 say, nearest to ω and which can be connected to ω by a straight line which does not cross any of the contours. With this integration path (5.2) may be written as

$$f(\omega) = f(\gamma_1) + \int_{\gamma_1}^{\omega} \tau(\zeta)\,d\zeta \qquad (5.8)$$

where, for $\gamma_1 \in I_{1,g}$, (5.6) may be used to approximate $f(\gamma_1)$.
The remaining integral in (5.8) may be approximated by splitting the line joining γ_1 to ω into a number of intervals and applying the composite trapezoidal rule (5.7). Here the $\gamma_{1,g}^{(1)}$ and $\gamma_{1,g}^{(2)}$ are replaced by the start and end points of the intervals, g is

replaced by the number of intervals and $f(\zeta_{1,1}^{(1)})$ is replaced by zero. The use of this quadrature rule requires the knowledge of $\tau(\zeta)$ at points on the line $\zeta_1 \omega$. These values are readily obtained from (5.4) and (5.5) if the previously used boundary idealisation is kept. Hence

$$\tau(\zeta) \simeq \frac{1}{2\pi i} \sum_{p=1}^{m} \sum_{q=1}^{n_p} \sum_{r=1}^{n} \tau(\zeta_{p,q}^{(r)}) \int_{I_{p,q}} M_{p,q}^{(r)}(z) \frac{dz}{z-\zeta} \qquad (5.9)$$

where the integrals can be evaluated in closed form. Note that the integrals required by (5.9) are given in § 3.6) and § 3.7) for the cases when the boundary approximations to $\tau(z)$ are piecewise linear or piecewise quadratic.

iii) when $\omega \in C_p$, $p \neq 1$ the technique is similar to that given in ii) above. Here the straight line which connects C_1 at ζ_1 to C_p at ζ_p and does not cross any of the other contours is chosen as part of the integration path. With this line included in the path of integration, (5.2) may be written as

$$f(\omega) = f(\zeta_0) + \int_{\zeta_0}^{\zeta_1} \tau(\xi) P(\xi)\, d\xi + \int_{\zeta_1}^{\zeta_p} \tau(\xi) P(\xi)\, d\xi + \int_{\zeta_p}^{\omega} \tau(\xi) P(\xi)\, d\xi \qquad (5.10)$$

and the numerical integration along the chosen path to ζ_p may be performed as in ii) above. The final integral on the right hand side of (5.10) may be performed along that part of C_p joining ζ_p to ω and can be evaluated using a suitably modified form of (5.6), i.e. if $\zeta_p = \zeta_{p,g}^{(r)}$ and $\omega \in I_{p,f}$ then

$$f(\omega) \simeq f(\zeta_{(\omega)}^{\delta,\delta}) + \sum_{\delta=\delta}^{\delta-1} \sum_{\nu=1}^{u} \tau(\zeta_{(\nu)}^{\delta,\delta}) \int_{I_{\delta,\delta}} M_{(\nu)}^{\delta,\delta}(\xi) \, d\xi$$

$$+ \sum_{r=1}^{n} \tau(\zeta_{p,f}^{(r)}) \int_{\zeta_{p,f}^{(1)}} M_{p,f}^{(r)}(\xi) \, d\xi .$$

§ 5.3) Use of Cauchy's integral when evaluating at interior points

When the boundary values of the regular function $f(\zeta)$ have been found by the method described in §5.2) - or by some other means - Cauchy's integral

$$f(\omega) = \frac{1}{2\pi i} \sum_{p=1}^{m} \int_{C_p} \frac{f(\zeta)}{\zeta - \omega} \, d\zeta \qquad (5.11)$$

may be used to evaluate $f(\omega)$ provided that ω lies entirely within the region of interest.

If it is assumed that values of $f(\zeta)$ have been obtained at the $\zeta_{p,q}^{(r)}$, $f(\omega)$ may be approximated in a similar fashion to $\tau(\omega)$ i.e. $f(\omega)$ may be written in the form

$$f(\omega) \simeq \frac{1}{2\pi i} \sum_{p=1}^{m} \sum_{q=1}^{n_p} \sum_{r=1}^{n} f(\zeta_{p,q}^{(r)}) \int_{I_{p,q}} M_{p,q}^{(r)}(\zeta) \frac{d\zeta}{\zeta - \omega} \qquad (5.12),$$

and the necessary integrations may usually be performed in a closed form (c.f. Chapter 3). One possible drawback to the use of (5.12) is that the approximation

$$f(\zeta) \simeq \sum_{r=1}^{n} f(\zeta_{p,q}^{(r)}) \, M_{p,q}^{(r)}(\zeta) \qquad , \quad \zeta \in I_{p,q} ,$$

is only of the same order as the previously used approximation to $\tau(\zeta)$. This may be overcome by noting that the

function $\tau(\zeta)$ has already been assumed known at the $\zeta_{p,q}^{(r)}$. In this case $f(\zeta)$ may be approximated in $I_{p,q}$ by

$$f(\zeta) \simeq \sum_{r=1}^{n} \left\{ M_{p,q}^{(r)}(\zeta) f(\zeta_{p,q}^{(r)}) + N_{p,q}^{(r)}(\zeta) \tau(\zeta_{p,q}^{(r)}) \right\} \qquad (5.13)$$

whence the approximation to $f(\omega)$ becomes

$$f(\omega) \simeq \frac{1}{2\pi i} \sum_{p=1}^{m} \sum_{q=1}^{n_p} \sum_{r=1}^{n} \left\{ f(\zeta_{p,q}^{(r)}) \int_{I_{p,q}} M_{p,q}^{(r)}(\zeta) \frac{d\zeta}{\zeta - \omega} + \tau(\zeta_{p,q}^{(r)}) \int_{I_{p,q}} N_{p,q}^{(r)}(\zeta) \frac{d\zeta}{\zeta - \omega} \right\}.$$

The use of a complex Hermite interpolation polynomial in (5.13) would enable $f(\zeta)$ to be approximated in $I_{p,q}$ by a polynomial of degree $2n-1$. In the case $n=2$ (5.13) takes the form

$$f(\zeta) \simeq \frac{(\zeta_{p,q}^{(2)} - \zeta)^2 (\zeta - \zeta_{p,q}^{(1)})}{(\zeta_{p,q}^{(2)} - \zeta_{p,q}^{(1)})^2} \tau(\zeta_{p,q}^{(1)}) + \frac{(\zeta_{p,q}^{(1)} - \zeta)^2 (\zeta - \zeta_{p,q}^{(2)})}{(\zeta_{p,q}^{(2)} - \zeta_{p,q}^{(1)})^2} \tau(\zeta_{p,q}^{(2)})$$
$$+ \frac{(\zeta_{p,q}^{(2)} - \zeta)^2 \{2(\zeta - \zeta_{p,q}^{(1)}) + \zeta_{p,q}^{(2)} - \zeta_{p,q}^{(1)}\}}{(\zeta_{p,q}^{(2)} - \zeta_{p,q}^{(1)})^3} f(\zeta_{p,q}^{(1)})$$
$$+ \frac{(\zeta_{p,q}^{(1)} - \zeta)^2 \{2(\zeta_{p,q}^{(2)} - \zeta) + \zeta_{p,q}^{(2)} - \zeta_{p,q}^{(1)}\}}{(\zeta_{p,q}^{(2)} - \zeta_{p,q}^{(1)})^3} f(\zeta_{p,q}^{(2)}).$$

§ 5.4) A boundary integral representation

A major disadvantage in the use of the path independent integrals of §5.2) comes from the fact that, although $f(\zeta)$ is single valued in some given region, the build up of error which occurs when (5.2) is evaluated numerically may well result in a multivalued approximation to $f(\zeta)$. To some extent, this problem could be overcome by evaluating (5.2) over a number of paths and averaging the result. However, the problem of choosing suitable integration paths remains and is compounded by the need to describe and store these paths when the computations are carried out using a computer.

To overcome these difficulties the author has made use of a boundary integral representation which enables $f(\zeta)$ to be evaluated from knowledge of the boundary values of its derivative $\tau(\zeta)$. This representation of $f(\zeta)$ is analogous to one attributed to Vekua by Muskhelishvili [29, pp.192-201] which is in terms of the boundary values of an unknown real density function $\mu(\tilde{\zeta})$.

Consider the typical region $\tilde{R}$, shown in Figure 5-4, which is simply connected and bounded by the simple closed curve $\partial\tilde{R}$. The curve $\partial\tilde{R}$ comprises of

i) the bounding contour C_1
ii) a small circle σ, with centre ω and radius ϵ, which excludes the point ω from R
iii) cross-cuts AB and DE which connect σ to C_1 and intersect C_1 only at the point $\zeta_0 = A = E$

For convenience in presentation the cross-cuts AB and DE have been drawn with a gap separating them; in practice no gap exists. Note that these cross-cuts are drawn radially from ω.

The function $F(\zeta,\omega)$ defined by

$$F(\zeta,\omega) = \frac{f(\zeta)}{\zeta-\omega}$$

where $f(\zeta) = \varphi(x,y) + i\psi(x,y)$ is the required regular function, is continuous and differentiable in $\tilde{R}$.

Therefore

$$0 = \int_{\partial\tilde{R}} \frac{f(\zeta)\, d\zeta}{\zeta - \omega} \qquad (5.14)$$

by the complex forms of Green's Theorem applied to the function $F(\zeta, \omega)$.

Provided that the function

$$\log(\zeta-\omega) = \ln|\zeta-\omega| + i\arg(\zeta-\omega)$$

remains on a branch appropriate to the cross-cuts AB and DE, i.e. $\log(\zeta-\omega)$ is single valued both inside $\tilde{R}$ and on the contour $\partial\tilde{R}$, the identity (5.14) may be integrated by parts [35, p.72] to give

$$0 = \Big[f(\zeta)\log(\zeta-\omega)\Big]_{\partial\tilde{R}} - \int_{\partial\tilde{R}} \frac{d}{d\zeta} f(\zeta).\log(\zeta-\omega)\, d\zeta \,.$$

Since both $f(\zeta)$ and $\log(\zeta-\omega)$ are single valued on $\partial\tilde{R}$ the first term on the right hand side of this last expression vanishes, i.e.

$$\Big[f(\zeta)\log(\zeta-\omega)\Big]_{\partial\tilde{R}} = 0 \,.$$

It remains to consider the various contributions to

$$\int_{\partial\tilde{R}} \frac{d}{d\zeta} f(\zeta).\log(\zeta-\omega)\, d\zeta \,.$$

As in earlier chapters let

$$\tau(\zeta) = \varphi_x(\tilde{\zeta}) - i\varphi_y(\tilde{\zeta}) = \frac{d}{d\zeta} f(\zeta)$$

and, for convenience, take the imaginary part of $\log(\zeta-\omega)$ to lie in the range

$$0 \le \arg(\zeta-\omega) < 2\pi \,.$$

This requires that the cross-cuts be taken parallel to the real axis of the ζ-plane.

Therefore,

i) the contribution from C_1 is

$$\int_{C_1} \tau(\zeta) \log(\zeta-\omega)\, d\zeta$$

ii) the contribution from σ is obtained by writing $\zeta-\omega = \varepsilon e^{i\theta}$ in which case $d\zeta = i\varepsilon e^{i\theta} d\theta$ and $\log(\zeta-\omega) = \ln\varepsilon + i\theta$.

Hence, the contribution from σ is given by

$$\int_{\sigma} \tau(\zeta)\log(\zeta-\omega)\,d\zeta = -i\varepsilon \int_0^{2\pi} \{\ln\varepsilon + i\theta\}\tau(\theta) e^{i\theta} d\theta$$

iii) the contribution from AB is obtained by writing $\zeta-\omega = \rho e^{i2\pi}$ so that $d\zeta = e^{i2\pi} d\rho$. Hence,

$$\int_A^B \tau(\zeta)\log(\zeta-\omega)\,d\zeta = \int_{\rho(A)}^{\rho(B)} \tau(\rho)\{\ln\rho + 2\pi i\} e^{i2\pi} d\rho.$$

Similarly, the contribution from DE is given by

$$\int_D^E \tau(\zeta)\log(\zeta-\omega)\,d\zeta = \int_{\rho(D)}^{\rho(E)} \tau(\rho)\ln\rho\, d\rho$$

since $\zeta-\omega = \rho$ on DE.

The required integral representation for the function $f(\omega)$, $\omega \in R$, is obtained from (5.14) by adding together the expressions obtained from the above contributions when $\varepsilon \to 0$. Hence,

$$\int_{C_1} \tau(\zeta) \log(\zeta-\omega)\, d\zeta = 2\pi i \int_{\rho(A)}^{\rho(B)} \tau(\rho)\, d\rho$$

$$= 2\pi i \left\{ f(\zeta_0) - f(\omega) \right\}$$

since for $\zeta \in AB$

$$\tau(\rho) = \frac{d}{d\zeta} f(\zeta) = \frac{d}{d\rho} f(\rho) \frac{d\rho}{d\zeta} .$$

The integral representation for $f(\omega)$ is more conveniently written as

$$f(\omega) = f(\zeta_0) - \frac{1}{2\pi i} \int_{C_1} \tau(\zeta) \log(\zeta-\omega)\, d\zeta \qquad (5.15)$$

where $f(\zeta_0)$ can be assigned an arbitrary complex value when it is unknown.

Should the cross-cut AB and DE not lie parallel to the positive real direction, the above analysis can be repeated by considering the required branch of

$$\log(\zeta-\omega) = \ln|\zeta-\omega| + i \arg(\zeta-\omega)$$

to be given by

$$\arg(\zeta_0-\omega) \leq \arg(\zeta-\omega) < \arg(\zeta_0-\omega) + 2\pi.$$

Further, the analysis can be modified to allow for the case when a straight line joining ω to ζ_0 crosses the boundary at points other than ζ_0 . This case requires the use of cross-cuts which are not single straight lines.

Such a cross-cut will be used below for the case when $\omega \in C_1$.

Two features of the derivation of (5.15) that should be noted are that

a) expansions of the functions $f(\zeta)$ and $\gamma(\zeta)$ were not required; only the fact that these functions are continuous in $R \cup C_1$ was used.

b) the term $f(\omega)$, $\omega \in R$, came from an integration taken along the cross-cut AB rather than an integration taken around the circle omitting ω from R.

These features suggest that the lengthy process used to obtain the limiting form of Cauchy's integral (see §2.2) is not required when the form of (5.15) appropriate to the case $\omega \in C_1$ is being sought.

Consider the regions R_1 and R_2 shown in Figure 5-5 which were obtained from the original region R by first using a circular arc σ to omit the boundary point ω from C_1 and then introducing the cross-cuts connecting σ to C_1 . Let the circular arc be centred at ω and of radius, ε say, such that it intersects C_1 at C and F . As in earlier work, the cross-cuts AB and DE have been drawn with a gap separating them which, in practice, does not exist. Note that the cross-cuts are curved because there is no straight line joining ω to ζ_0 which remains in R along the whole of its length.

Denoting the boundaries of the regions R_1 and R_2 by ∂R_1 and ∂R_2 respectively, the complex forms of Green's Theorem yield

$$0 = \int_{\partial R_1} \frac{f(\zeta)}{\zeta - \omega} \, d\zeta \qquad (5.16)$$

$$0 = \int_{\partial R_2} \frac{f(\zeta)}{\zeta - \omega} \, d\zeta \qquad (5.17)$$

when applied to the function

$$F(\zeta, \omega) = \frac{f(\zeta)}{\zeta - \omega} \, .$$

As before, the function

$$f(\zeta) = \varphi(x,y) + i\,\psi(x,y)$$

is the required analytic function.

The function $\log(\zeta-\omega)$ may be defined as a regular function in both R_1 and R_2

$$\left\{ \text{use} \quad \log(\zeta-\omega) = \int_{\zeta_0}^{\zeta} \frac{d\bar{\zeta}}{\bar{\zeta}-\omega} \quad + \text{constant} \right\}$$

because $\omega \notin R_1 \cup \partial R_1$ and $\omega \notin R_2 \cup R_2$. Hence, (5.16) and (5.17) may be integrated by parts to give

$$0 = \left[f(\zeta) \log(\zeta-\omega) \right]_{\partial R_1} - \int_{\partial R_1} \frac{dP}{d\zeta} f(\zeta) \log(\zeta-\omega)\, d\zeta$$

$$= -\int_{\partial R_1} \tau(\zeta) \log(\zeta-\omega)\, d\zeta \qquad (5.18)$$

$$0 = \left[f(\zeta) \log(\zeta-\omega) \right]_{\partial R_2} - \int_{\partial R_2} \frac{dP}{d\zeta} f(\zeta) \log(\zeta-\omega)\, d\zeta$$

$$= -\int_{\partial R_2} \tau(\zeta) \log(\zeta-\omega)\, d\zeta \qquad (5.19)$$

where

$$\tau(\zeta) = \frac{dP}{d\zeta} f(\zeta) = \varphi_x(\tilde{\zeta}) - i\,\varphi_y(\tilde{\zeta}).$$

The required integral representation is obtained by assigning values to $\log(A-\omega)$ and $\log(E-\omega)$, evaluating the various contributions to (5.18) and (5.19), and letting $\varepsilon \to 0$.

Let

$$\log(E-\omega) = \ln|E-\omega| + i\theta$$

$$\log(A-\omega) = \ln|A-\omega| + i(\theta + 2\pi)$$

then, for $\gamma_2 \in DE$ and $\gamma_1 \in AB$,

$$\int_A^B \tau(\gamma_1)\log(\gamma_1-\omega)\,d\gamma_1 = -\int_D^E \tau(\gamma_2)\log(\gamma_2-\omega)\,d\gamma_2 + 2\pi i\int_A^B \tau(\gamma_1)\,d\gamma_1 .$$

The remaining contributions which are obtained when $\varepsilon \to 0$ are

$$\lim_{\varepsilon\to 0}\int_{C_1^{(1)}} \tau(\gamma)\log(\gamma-\omega)\,d\gamma \quad \text{and} \quad \lim_{\varepsilon\to 0}\int_{C_1^{(2)}} \tau(\gamma)\log(\gamma-\omega)\,d\gamma$$

where the values taken by $\log(\gamma-\omega)$ depend on whether $\gamma \in C_1^{(1)}$ or $\gamma \in C_1^{(2)}$. In the former case $\log(\gamma-\omega)$ depends on $\log(A-\omega)$ whereas in the latter case $\log(\gamma-\omega)$ depends on $\log(E-\omega)$.

On adding together these various contributions one obtains

$$0 = \int_{C_1} \tau(\gamma)\log(\gamma-\omega)\,d\gamma + 2\pi i\int_{A=\gamma_0}^{B=\omega} \tau(\gamma)\,d\gamma$$

where

$$\int_{C_1} \tau(\xi) \log(\xi-\omega)\, d\xi = \lim_{\varepsilon\to 0} \int_{C_1''} \tau(\xi) \log(\xi-\omega)\, d\xi + \lim_{\varepsilon\to 0} \int_{C_1^{(\omega)}} \tau(\xi) \log(\xi-\omega)\, d\xi$$

and the $\log(\xi-\omega)$ have the aforementioned interpretation. Therefore, for $\omega \in C_1$, the representation

$$f(\omega) = -\frac{1}{2\pi i} \int_{C_1} \tau(\xi) \log(\xi-\omega)\, d\xi + f(\xi_0) \qquad (5.20)$$

can be written. Clearly, the difference between (5.15) and (5.20) lies in the interpretation of the boundary integral.

Multiply connected regions can be treated in an entirely analogous manner. Figure 5-6 shows a multiply connected region R and indicates the form of the cross-cuts required by the analysis for the case when $\omega \in C_2$. Here $f(\omega)$ may be obtained from the representation

$$f(\omega) = \text{constant} - \frac{1}{2\pi i} \sum_{p=1}^{3} \int_{C_p} \tau(\xi) \log(\xi-\omega)\, d\xi .$$

For the more general case of a finite multiply connected region bounded by the m contours C_p , $p = 1(1)m$, the representation

$$f(\omega) = \text{constant} - \frac{1}{2\pi i} \sum_{p=1}^{m} \int_{C_p} \tau(\xi) \log(\xi-\omega)\, d\xi \qquad (5.21)$$

may be used. The form of the constant depends on the cross-cuts used in the derivation. In most practical applications the constant may be assigned an arbitrary complex value.

§ 5.5) Relationship with Green's Third Identity

The boundary integral representations (5.15) and (5.20) may be used to derive Green's Third identity relating the value of a harmonic function at a point $\omega \in R$ to boundary values of the function and its normal derivative. To illustrate this use, only a simply connected region bounded by the contour C_1 will be considered.

Using the relationship

$$\tau(\gamma)\, d\gamma = \{\varphi_s(\tilde{\gamma}) + i\varphi_n(\tilde{\gamma})\}ds \quad , \quad \gamma \in C_1 ,$$

(5.15) may be written as

$$\varphi(u,v) + i\psi(u,v) = \varphi(x_0,y_0) + i\psi(x_0,y_0) - \frac{1}{2\pi i}\int_{C_1}\{\varphi_s(\tilde{\gamma}) + i\varphi_n(\tilde{\gamma})\}\{\ln|\gamma-\omega| + i\arg(\gamma-\omega)\}ds ;$$

where $\omega = u+iv$, $\gamma_0 = x_0 + iy_0$, $\gamma = x+iy$.

The real part of this identity is

$$\varphi(u,v) = \varphi(x_0,y_0) - \frac{1}{2\pi}\int_{C_1}\{\varphi_s(\tilde{\gamma})\arg(\gamma-\omega) + \varphi_n(\tilde{\gamma})\ln|\gamma-\omega|\}\, ds.$$

The integral

$$\int_{C_1} \varphi_s(\tilde{\gamma})\arg(\gamma-\omega)\, ds$$

may be integrated by parts to give

$$\int_{C_1} \varphi_s(\tilde{\gamma}).\arg(\gamma-\omega)\,ds = \left[\varphi(x,y)\arg(\gamma-\omega)\right]_{C_1}$$

$$-\int_{C_1} \varphi(x,y)\frac{\partial}{\partial s}\left\{\arg(\gamma-\omega)\right\}ds \ .$$

However, (5.15) requires that any integration taken around C_1 should start and finish at γ_0 . Therefore

$$\left[\varphi(x,y)\arg(\gamma-\omega)\right]_{C_1} = 2\pi\,\varphi(x_0,y_0)$$

whence

$$\varphi(u,v) = \frac{1}{2\pi}\int_{C_1}\left\{\varphi(x,y)\frac{\partial}{\partial s}\left\{\arg(\gamma-\omega)\right\} - \varphi_n(\tilde{\gamma})\ln|\gamma-\omega|\right\}ds$$

The above representation of $\varphi(u,v)$, $\omega = u+iv \in R$, is known as Green's third identify [25] from which Green's Boundary Formula [15, pp.57-59, pp.190-212] may be obtained. It is usual to apply the Cauchy-Riemann equations to $\frac{\partial}{\partial s}\left\{\arg(\gamma-\omega)\right\}$ and write

$$\varphi(u,v) = \frac{1}{2\pi}\int_{C_1}\left\{\varphi(x,y)\frac{\partial}{\partial n}\left\{\ln|\gamma-\omega|\right\} - \varphi_n(\tilde{\gamma})\ln|\gamma-\omega|\right\}ds \ .$$

§ 5.6) <u>Numerical evaluation of derived boundary integral representation</u>

The boundary integral representation obtained in § 5.4) is well suited to the methods of approximation used in Chapters 3 and 4. Indeed, the boundary idealisation of § 3.2) and the approximation

$$\tau(\gamma) \simeq \sum_{r=1}^{n} M_{p,q}^{(r)}(\gamma)\, \tau(\gamma_{p,q}^{(r)}) \quad , \quad \gamma \in I_{p,q}$$

enable (5.21) to be approximated by

$$f(\omega) \simeq \text{constant} - \frac{1}{2\pi i} \sum_{p=1}^{m} \sum_{q=1}^{n_p} \sum_{r=1}^{n} \tau(\gamma_{p,q}^{(r)}) \int_{I_{p,q}} M_{p,q}^{(r)}(\gamma) \log(\gamma-\omega)\, d\gamma \qquad \ldots\ldots \quad (5.22)$$

As mentioned previously, care must be taken to ensure that the function $\log(\gamma-\omega)$ is evaluated in accordance with the requirements of the derivation of (5.21).

A technique for keeping track of the values of $\arg(\gamma-\omega)$ which has been used by the author can be obtained from the work of Jaswon and Symm on evaluating conjugate harmonic functions numerically [15, pp.155-157] . Consider the simply connected region shown in Figure 5-7. For $\omega \in R$ choose a fixed direction to be that of the positive x-axis of a cartesian co-ordinate system whose origin is at ω . The angle $\theta(\gamma_0, \omega)$ which the vector $\gamma_0 - \omega$ makes with the fixed direction may be defined such that

$$-\pi < \theta(\gamma_0, \omega) \leq \pi .$$

The function $\arg(\gamma-\omega)$ is now allowed to vary continuously as γ describes the contour C_1 in the positive sense starting from γ_0 . The initial value of $\arg(\gamma_0-\omega)$ is taken to be $\theta(\gamma_0, \omega)$.

In Figure 5-7 those portions of C_1 where the above definition of $\arg(\zeta-\omega)$ results in

$$\arg(\zeta-\omega) = \theta(\zeta,\omega) + 2\pi$$

are shown drawn with a thick line.

From a practical point of view, $\arg(\zeta-\omega)$ can be obtained from

$$\arg(\zeta-\omega) = \theta(\zeta_0,\omega) + \int_{\zeta_0}^{\zeta} d\{\arg(\zeta-\omega)\}$$

$$= \theta(\zeta_0,\omega) + \int_{\zeta_0}^{\zeta} d\{\theta(\zeta,\omega)\}$$

Here the integral is evaluated along C_1 and is understood to be taken in the positive sense.

When $\omega \in C_1$ examination of Figure 5-5 and the derivation of (5.20) shows that $\arg(\zeta-\omega)$ may be defined in a fashion similar to that used above. However, the introduction of the cross-cuts AB and DE requires that $\arg(\zeta-\omega)$ be allowed to jump by the exterior angle between tangents to C_1 at ω as ζ passes through ω. This angle equals π when the boundary is smooth at ω.

The above technique is readily extended to include the case when the region is multiply connected. Let ζ_p be a fixed point defining the start of the p^{th} contour C_p, $p=1(1)M$. For $\zeta \in C_p$ the function $\arg(\zeta-\omega)$, $\omega \notin C_p$ may be obtained from

$$\arg(\zeta-\omega) = \theta(\zeta_p,\omega) + \int_{\zeta_p}^{\zeta} d\{\theta(\zeta,\omega)\} \qquad (5.23)$$

where the integral is evaluated along C_p and is understood to be taken in the positive sense. When $\omega \in C_p$ (5.23) may again be used provided that the previously mentioned jump in $\arg(\zeta-\omega)$ as ζ passes through ω is allowed.

In Figure 5-7 those portions of C_1 where the above definition of $\arg(\zeta-\omega)$ results in

$$\arg(\zeta-\omega) = \theta(\zeta,\omega) + 2\pi$$

are shown drawn with a thick line.

From a practical point of view, $\arg(\zeta-\omega)$ can be obtained from

$$\arg(\zeta-\omega) = \theta(\zeta_0,\omega) + \int_{\zeta_0}^{\zeta} d\{\arg(\zeta-\omega)\}$$

$$= \theta(\zeta_0,\omega) + \int_{\zeta_0}^{\zeta} d\{\theta(\zeta,\omega)\}$$

Here the integral is evaluated along C_1 and is understood to be taken in the positive sense.

When $\omega \in C_1$ examination of Figure 5-5 and the derivation of (5.20) shows that $\arg(\zeta-\omega)$ may be defined in a fashion similar to that used above. However, the introduction of the cross-cuts AB and DE requires that $\arg(\zeta-\omega)$ be allowed to jump by the exterior angle between tangents to C_1 at ω as ζ passes through ω. This angle equals π when the boundary is smooth at ω.

The above technique is readily extended to include the case when the region is multiply connected. Let ζ_p be a fixed point defining the start of the p^{th} contour C_p, $p=1(1)M$. For $\zeta \in C_p$ the function $\arg(\zeta-\omega)$, $\omega \notin C_p$ may be obtained from

$$\arg(\zeta-\omega) = \theta(\zeta_p,\omega) + \int_{\zeta_p}^{\zeta} d\{\theta(\zeta,\omega)\} \qquad (5.23)$$

where the integral is evaluated along C_p and is understood to be taken in the positive sense. When $\omega \in C_p$ (5.23) may again be used provided that the previously mentioned jump in $\arg(\zeta-\omega)$ as ζ passes through ω is allowed.

That the choice of value for $\theta(\zeta_p, \omega)$ is unimportant has been observed. This follows from the fact that if ε is a real constant then

$$\frac{1}{2\pi i}\int_{C_p} \tau(\zeta)\log(\zeta-\omega)\,d\zeta \quad + \frac{\varepsilon}{2\pi}\int_{C_p}\tau(\zeta)\,d\zeta$$

$$= \frac{1}{2\pi i}\int_{C_p}\tau(\zeta)\log(\zeta-\omega)\,d\zeta .$$

Returning to the problem of evaluating (5.22), the integrals

$$\int_{I_{p,q}} M_{p,q}^{(r)}(\zeta)\,\log(\zeta-\omega)\,d\zeta$$

may be evaluated in closed form whenever the $M_{p,q}^{(r)}(\zeta)$ are the coefficients of an n^{th}-order complex interpolation polynomial applied over the interval $I_{p,q}$. As an example of this consider the case when $n = 2$. Here the general form of $M_{p,q}^{(r)}(\zeta)$ is

$$M_{p,q}^{(r)}(\zeta) = \frac{(\zeta-a)(\zeta-b)}{(c-a)(c-b)}$$

where the a, b, c are all complex constants defining the three nodes which specify the element $I_{p,q}$.

An alternative form of $M_{p,q}^{(r)}(\zeta)$, which incorporates ω, is

$$M_{p,q}^{(r)}(\zeta) = \frac{(\zeta-\omega+\omega-a)(\zeta-\omega+\omega-b)}{(c-a)(c-b)}$$

$$= \frac{(\zeta-\omega)^2 + (\zeta-\omega)(2\omega-a-b) + (\omega-a)(\omega-b)}{(c-a)(c-b)} .$$

Therefore, for $\omega \notin I_{p,q}$

$$\int_{I_{p,q}} M_{p,q}^{(r)}(\xi) \log(\xi-\omega)\, d\xi$$

$$= \int_{I_{p,q}} \log(\xi-\omega) \left\{ \frac{(\xi-\omega)^2 + (\xi-\omega)(2\omega-a-b) + (\omega-a)(\omega-b)}{(c-a)(c-b)} \right\} d\xi$$

$$= \frac{1}{(c-a)(c-b)} \left[\frac{1}{3}(\xi-\omega)^3 \left\{ \log(\xi-\omega) - \frac{1}{3} \right\} \right.$$

$$+ \frac{1}{2}(\xi-\omega)^2 \left\{ \log(\xi-\omega) - \frac{1}{2} \right\} (2\omega-a-b)$$

$$\left. + (\omega-a)(\omega-b) \left\{ \log(\xi-\omega) - 1 \right\} \right]_{I_{p,q}}$$

.....(5.24)

When $\omega \in I_{p,q}$ the integrals can all be evaluated by writing

$$\int_{I_{p,q}} M_{p,q}^{(r)}(\xi) \log(\xi-\omega)\, d\xi = \int_{\alpha_{p,q}^{(1)}}^{\omega} M_{p,q}^{(r)}(\xi) \log(\xi-\omega)\, d\xi$$

$$+ \int_{\omega}^{\alpha_{p,q}^{(2)}} M_{p,q}^{(r)}(\xi) \log(\xi-\omega)\, d\xi .$$

These integrals may be evaluated by using expressions similar to (5.24).

§ 5.7) A boundary integral representation involving higher order derivatives

The boundary integral representation (5.21) relating a regular function to its first order derivative may be considered to be a particular case of the more general representation derived below. In contrast to § 5.4), only the simplest case of ω lying entirely within a simply connected region will be considered in detail.

Consider again the simply connected region $\tilde{R}$ shown in Figure 5-4 which is bounded by the simple closed curve $\partial\tilde{R}$. The curve $\partial\tilde{R}$ comprises of

i) the bounding contour C_1

ii) a small circle σ, with centre ω and radius ε, which excludes the point ω from R

iii) cross-cuts AB and DE which connect σ to C_1 and intersect C_1 only at the point $\gamma_0 = A = E$.

As before, the cross-cuts are drawn with a gap separating them although no gap exists.

Denoting by $f(\omega)$ the required regular function evaluated at the point ω , the complex forms of Green's Theorem applied to

$$\frac{f(\gamma)}{\gamma - \omega}$$

yields the result

$$0 = \int_{\partial\tilde{R}} \frac{f(\gamma)\, d\gamma}{\gamma - \omega} \qquad (5.25).$$

Provided that the branch cuts required by the function

$$\log(\gamma-\omega) = \ln|\gamma-\omega| + i\arg(\gamma-\omega)$$

are taken to be the cross-cuts AB and DE, the integral in (5.25) may be integrated by parts n times to give (for $n>1$)

$$= \left[f(\xi) \log(\omega-\xi) \right]_{\partial\tilde{R}}$$

$$+ \left[\sum_{i=1}^{n-1} (-1)^i \frac{d^i}{d\xi^i} f(\xi) . \frac{(\xi-\omega)^i}{i!} \left\{ \log(\xi-\omega) - \sum_{j=0}^{i-1} \frac{1}{i-j} \right\} \right]_{\partial\tilde{R}}$$

. . . . (5.25)

The choice of branch cut given earlier enables the RHS of (5.25) to be set to zero since the relevant functions are all single valued on $\partial\tilde{R}$. Hence (5.25) may be written as

$$(-1)^{n+1} \int_{\partial\tilde{R}} \frac{d^n}{d\xi^n} f(\xi) . \frac{(\xi-\omega)^{n-1}}{(n-1)!} \left\{ \log(\xi-\omega) - \sum_{j=0}^{n-2} \frac{1}{n-j-1} \right\} d\xi = 0$$

or, on dividing through by $(-1)^{n+1}$,

$$\int_{\partial\tilde{R}} \frac{d^n}{d\xi^n} f(\xi) . \frac{(\xi-\omega)^{n-1}}{(n-1)!} \left\{ \log(\xi-\omega) - \sum_{j=0}^{n-2} \frac{1}{n-j-1} \right\} d\xi = 0$$

This last expression may be further simplified to

$$\int_{\partial\tilde{R}} \frac{d^n}{d\xi^n} f(\xi) . \frac{(\xi-\omega)^{n-1}}{(n-1)!} \log(\xi-\omega)\, d\xi = 0 \qquad (5.27)$$

since

$$\int_{\partial\tilde{R}} \frac{d^n}{d\zeta^n} f(\zeta).(\zeta-\omega)^{n-1} = 0 .$$

For convenience take $\arg(\zeta-\omega)$ to lie in the range

$$0 \le \arg(\zeta-\omega) < 2\pi,$$

so that the contributions to the integral in (5.27) are:-

i) $$\int_{C_1} \frac{d^n}{d\zeta^n} f(\zeta).\frac{(\zeta-\omega)^{n-1}}{(n-1)!} \log(\zeta-\omega)\, d\zeta$$

ii) on σ, if $\tau(\zeta) = \frac{d^n}{d\zeta^n} f(\zeta)$ and $\zeta = \varepsilon e^{i\theta} + \omega$,

$$\int_{\sigma} \frac{d^n}{d\zeta^n} f(\zeta).\frac{(\zeta-\omega)^{n-1}}{(n-1)!} \log(\zeta-\omega)\, d\zeta$$

$$= -\frac{i\,\varepsilon^n}{(n-1)!}\int_0^{2\pi} \tau(\theta) e^{i\theta}\{\ln\varepsilon + i\theta\}\, d\theta$$

iii) on AB, if $z-\omega = \rho e^{i2\pi}$ and $\tau(z) = \frac{d^n}{dz^n} f(z)$,

$$\int_A^B \frac{d^n}{dz^n} f(z) . \frac{(\omega - z)^{n-1}}{(n-1)!} \log(\omega - z)\, dz$$

$$= \frac{1}{(n-1)!} \int_{\rho(A)}^{\rho(B)} \tau(\rho)\, \rho^{n-1} \left\{ \ln \rho + 2\pi i \right\} e^{i2\pi}\, d\rho .$$

Similarly, on DE,

$$\int_D^E \frac{d^n}{dz^n} f(z) . \frac{(z-\omega)^{n-1}}{(n-1)!} \log(z-\omega)\, dz$$

$$= \frac{1}{(n-1)!} \int_{\rho(D)}^{\rho(E)} \tau(\rho)\, \rho^{n-1} \ln \rho\, d\rho .$$

The required integral representation for the function $f(\omega)$ is obtained from (5.27) by adding together the expressions obtained from the above contributions when $\varepsilon \to 0$.

Hence

$$\int_{C_1} \frac{d^n}{d\zeta^n} f(\zeta).(\zeta-\omega)^{n-1} \log(\zeta-\omega)\, d\zeta$$

$$= 2\pi i \int_{\rho(B)}^{\rho(A)} \tau(\rho)\rho^{n-1}\, d\rho$$

$$= 2\pi i \int_{\omega}^{\zeta_0} \frac{d^n}{d\zeta^n} f(\zeta).(\zeta-\omega)^{n-1}\, d\zeta \quad .$$

The RHS of this expression may be integrated by parts to give the integral representation

$$(-1)^n 2\pi i f(\omega) = \frac{1}{(n-1)!} \int_{C_1} \frac{d^n}{d\zeta^n} f(\zeta).(\zeta-\omega)^{n-1} \log(\zeta-\omega) d\zeta$$

$$+ g(\omega, \zeta_0) \qquad (5.28)$$

where $g(\omega,\zeta_0)$ is a function involving $f(\zeta_0)$ and the first $n-1$ derivatives of $f(\zeta)$ evaluated at ζ_0 .

Representations analogous to (5.28) can be obtained in a similar fashion when the point ω tends to the boundary and when the region is multiply connected. In the former case, the regions over which the analysis is performed should be of the type shown in Figure 5-5. In the latter case, the function $g(\omega,\zeta_0)$ will depend on all the boundary points which lie on the cross-cuts required to make the region simply connected. In both of these cases care must be taken in the interpretation of $\log(\zeta-\omega)$.

§ 5.8) Example

The numerical technique described in § 5.6) has had extensive use during the provision of the results given in Chapter 6. In that chapter the technique forms an essential part of the method of predicting the torsional properties of plane sections. Because of this usage only one example illustrating the usefulness of the technique will be considered here.

§ 5.8.1) Flexure of A Hollow Tube

In § 3.11.1) the problem of determining the boundary tangential derivative, $\chi_s(\tilde{\tau})$ say, of the flexure function for a hollow tube was considered. For the region under consideration the result

$$\chi(x,y) = -\left(\frac{3}{4} + \frac{1}{2}\sigma\right)\left\{(r_o^2 + r_i^2)r + \frac{r_o^2 r_i^2}{r}\right\}\cos\theta + \frac{1}{4}r^3\cos 3\theta + \text{constant}$$

where $\tau = x+iy = re^{i\theta}$

r_o = outer radius of tube

r_i = inner radius of tube

σ = Poisson's ratio

$\chi(x,y)$ = flexure function for tube,

was given.

The (piecewise quadratic) technique described in § 5.6) has been used to provide approximations to $\chi(x,y)$ for this hollow tube. The results obtained for a number of points on the inner and outer boundaries are shown in Table 5-1. Here the constants of integration in both $\chi(x,y)$ and its approximation have been adjusted to give these functions a value of zero at the point $\tau = r_o e^{i\pi/2}$.

The results were obtained by utilising the true values of the normal derivative of $\chi(x,y)$, i.e.

$$\chi_n(\tilde{\tau}) = \begin{cases} -(3/4 + \frac{1}{2}\sigma)\, r_o^2 \cos\theta + 3/4\, r_o^2 \cos 3\theta & \text{for } \tau \in r_o e^{i\theta} \\ (3/4 + \frac{1}{2}\sigma)\, r_i^2 \cos\theta - 3/4\, r_i^2 \cos 3\theta & \text{for } \tau \in r_i e^{i\theta} \end{cases}$$

together with the appropriate approximations to $\chi_s(\tilde{\tau})$. These approximations correspond to those quoted in Table 3-1.

The results show excellent agreement between true and predicted values of $\chi(x,y)$. As might be expected, the agreement between these values is closer on the outer boundary - away from the singularity of the function $\frac{1}{z}$.

Chapter 6

THE DETERMINATION OF THE TORSIONAL PROPERTIES OF A PLANE SECTION

§ 6.1) Introduction

It is well known in the mathematical theory of elasticity [4, pp.310-328] that the classical torsion problem for a constant section beam twisted about its longitudinal axis can be reduced to the determination of the warping function $\varphi(x,y)$. This function satisfies Laplace's equation

$$\Delta \varphi(x,y) = 0$$

throughout the plane region corresponding to the section of the beam and has the Neumann type boundary condition

$$\varphi_n(x,y) = y\cos(x,n) - x\cos(y,n) \qquad (6.1)$$

Here the normal n is taken to be drawn in the outward sense and cos (x,n), cos (y,n) are the appropriate direction cosines at the point $z = x+iy$. Thus formulated, the solution to the torsion problem can be shown to be unique to within an arbitrary real additive constant [4, p.314].

Denoting by μ and Ω the shear modulus and twist per unit length respectively, the longitudinal displacement $w(x,y)$ is given by

$$w(x,y) = \Omega\,\varphi(x,y) \qquad (6.2)$$

Further, the only non-vanishing stress components are given, in terms of the first partial derivatives of the warping function, by

$$\tau_{xz} = \mu\Omega(\varphi_x - y) \qquad (6.3a)$$

$$\tau_{yz} = \mu\Omega(\varphi_y + x) \qquad (6.3b)$$

If $\psi(x,y)$ denotes the harmonic conjugate of the warping function $\varphi(x,y)$, the stress components may be obtained from

$$\tau_{xz} = \mu\Omega\,(\psi_y - y)$$

$$\tau_{yz} = \mu\Omega\,(x - \psi_x)$$

The function $\psi(x,y)$ is termed the torsion function and may be shown to satisfy the Dirichlet type boundary condition

$$\psi(x,y) = \tfrac{1}{2}(x^2 + y^2) + K_p \qquad (6.4)$$

on each of the contours bounding the region of interest [4, pp.313-314]. Here K_p is a constant particular to the p^{th} contour which must be determined during the solution of a problem.

It should be noted that the physical requirement that the longitudinal displacement $W(x,y)$ be single valued together with (6.4) enable the regular function

$$F(\zeta) = \varphi(x,y) + i\,\psi(x,y) \qquad (6.5)$$

to be defined throughout the region corresponding to the section of the beam.

Because the warping function and its harmonic conjugate are known only for a limited number of regions, numerical techniques for their determination have been developed by a number of authors [e.g. 44, 45]. The technique developed by the present author makes use of the complex variable techniques given in Chapters 2, 3 and 5. This technique may be summarised as follows:-

i) the integral equation for the tangential derivative is solved using the numerical methods of Chapter 3.

ii) the first derivative of the regular function $F(\zeta)$ is obtained on the boundary from the tangential and normal derivatives of the warping function.

iii) the regular function $F(\zeta)$ is obtained on the boundary and throughout the region of interest by the boundary integral representations of Chapter 5.

The numerical methods used are all based on piecewise quadratic approximations to $F_z(\tau)$. These approximations and their associated numerical methods are fully described in § 3.7) and § 5.6). The results obtained by these methods for a number of regions are given in the last section of this chapter.

Beam element solutions to the vibration analysis [e.g. 31] and stress analysis [e.g. 30] of non-uniform beams are important engineering applications of solutions to the torsion problem described above. In these applications the torsional stiffness constant (alternatively torsional rigidity), warping stiffness constant (alternatively warping rigidity) and shear centre co-ordinates are required sectional properties which can only be obtained from knowledge of the warping function particular to a section under consideration. Although boundary integral techniques have been applied to the torsion problem and the evaluation of the torsional stiffness constant by a number of authors [e.g. 26, 44, 45] , the problems of evaluating the warping stiffness constant and determining shear centre co-ordinates by similar techniques appears to have been neglected.

Using the complex forms of Green's Theorem, boundary integral representations of these torsional properties are derived below. Again, the results obtained using these representations for a number of regions are given in the last section of this chapter.

§ 6.2) Boundary Integral Representations Of The Shear Centre Co-ordinates

The shear centre of a uniform cantilever beam subject to an applied shearing force at the free end has been defined as the point at which the force must be applied if there is to be flexure without torsion [46, 47] .

Let z be the longitudinal axis of a uniform beam and x,y the principal directions in the cross section R, the origin being the centroid of the cross-section. Trefftz [46] gives the co-ordinates x_c and y_c of the shear centre as

$$x_c = \frac{-1}{I_x} \iint_R y\, \varphi(x,y)\, dx\, dy \qquad (6.7)$$

$$y_c = \frac{1}{I_y} \iint_R x\, \varphi(x,y)\, dx\, dy \qquad (6.8)$$

where

$$I_x = \iint_R y^2\, dx\, dy\,, \quad I_y = \iint_R x^2\, dx\, dy$$

are the moments of inertia with respect to the principal axes and $\varphi(x,y)$ is the previously defined warping function for the section.

Further, by imposing the constraints that

$$\iint_R \varphi(x,y)\, dx\, dy = 0 \qquad (6.9)$$

and

$$\iint_R \{\varphi(x,y) - x\, y_c + y\, x_c\}^2\, dx\, dy = \text{minimum} \qquad (6.10)$$

it can be shown [47] that the centre of twist - the point at rest in every section when the beam is subjected to a terminal couple - corresponds to the shear centre.

The constraint (6.9) is used in the solution of the Neumann problem governing the warping function to determine the hitherto arbitrary constant. It constrains the average longitudinal displacement $w(x,y)$ to be zero.

The use of (6.9) in the solution of the torsion problem enables a value to be given to the integral in (6.10) i.e.

$$\iint_R \{\varphi(x,y) - x\, y_c + y\, x_c\}^2\, dx\, dy$$

This value is termed the warping stiffness of the section and is denoted by I_w. The use of (6.9) does not affect the location of the shear centre.

The complex forms of Green's Theorem can be used to determine boundary integral representations for x_c and y_c since (6.7), (6.8) may be written as

$$x_c = -\frac{1}{I_x}\ Re\left\{\frac{1}{2i}\iint_R (\zeta-\bar{\zeta})F(\zeta)\,dx\,dy\right\}$$

$$y_c = \frac{1}{I_y}\ Re\left\{\frac{1}{2}\iint_R (\zeta+\bar{\zeta})F(\zeta)\,dx\,dy\right\}$$

where

$$\zeta = x + iy$$

and $F(\zeta)$ is defined by (6.5).
Hence, since $F(\zeta)$ is single valued,

$$x_c = -\frac{1}{I_x}\ Re\left\{\frac{1}{2i}\iint_R \frac{\partial}{\partial\bar{\zeta}}\left[\bar{\zeta}(\zeta-\tfrac{1}{2}\bar{\zeta})\right]F(\zeta)\,dx\,dy\right\}$$

$$= \frac{1}{4I_x}\ Re\left\{\int_C \bar{\zeta}(\zeta-\tfrac{1}{2}\bar{\zeta})F(\zeta)\,d\zeta\right\} \qquad (6.11)$$

and

$$y_c = \frac{1}{I_y}\ Re\left\{\frac{1}{2}\iint_R \frac{\partial}{\partial\bar{\zeta}}\left[\bar{\zeta}(\zeta+\tfrac{1}{2}\bar{\zeta})\right]F(\zeta)\,dx\,dy\right\}$$

$$= \frac{1}{4I_y}\ Im\left\{\int_C \bar{\zeta}(\zeta+\tfrac{1}{2}\bar{\zeta})F(\zeta)\,d\zeta\right\} \qquad (6.12)$$

where C is the boundary of the region R.

§ 6.3) <u>A boundary integral representation of the warping stiffness constant</u>

The warping stiffness constant I_w of a plane section R was defined in the previous section as

$$I_w = \iint_R \{\varphi_c(x,y)\}^2\,dx\,dy$$

where

$$\varphi_c(x,y) = \varphi(x,y) - x\,y_c + y\,x_c \ .$$

It can be shown [34, pp.113-114] that $\varphi_c(x,y)$ is, in fact, the warping function of the section R twisted about a longitudinal axis passing through the shear centre. In this case the additive constant is again determined such that

$$\iint_R \varphi(x,y)\,dx\,dy = \iint_R \varphi_c(x,y)\,dx\,dy = 0 \qquad (6.9).$$

Frequently a given solution, $\hat{\varphi}(x,y)$ say, of the torsion problem does not have this last property and must be adjusted. This adjustment is carried out by noting that (6.9) may be written as

$$\iint_R \varphi_c(x,y)\,dx\,dy = \iint_R \{\hat{\varphi}(x,y) + K\}\,dx\,dy = 0$$

since the required warping function $\varphi_c(x,y)$ is unique only to within an arbitrary constant,
i.e. $\varphi_c(x,y) = \hat{\varphi}(x,y) + K$ where K is the required adjusting constant.
Hence

$$K = -\frac{1}{A}\iint_R \hat{\varphi}(x,y)\,dx\,dy \qquad (6.13)$$

where $A = \iint_R dx\,dy$ is the area of the section R. The identity (6.13) can be put into boundary integral form by writing

$$\hat{F}(z) = \hat{\varphi}(x,y) + i\,\hat{\psi}(x,y)$$

where $\hat{\psi}(x,y)$ is the harmonic conjugate of $\hat{\varphi}(x,y)$ so that

$$K = -\frac{1}{2A}\iint_R \left\{\hat{F}(\zeta) + \overline{\hat{F}}(\bar{\zeta})\right\} dx\,dy$$

$$= -\frac{1}{2A}\iint_R \left\{\frac{\partial}{\partial \bar{\zeta}}\left(\bar{\zeta}\,\hat{F}(\zeta)\right) + \frac{\partial}{\partial \zeta}\left(\zeta\,\overline{\hat{F}}(\bar{\zeta})\right)\right\} dx\,dy$$

$$= \frac{1}{4Ai}\left\{\int_C \zeta\,\overline{\hat{F}}(\bar{\zeta})\,d\bar{\zeta} - \int_C \bar{\zeta}\,\hat{F}(\zeta)\,d\zeta\right\} \qquad (6.14)$$

by the complex forms of Green's Theorem. Alternatively, K may be considered to be the real part of the complex constant

$$J = K + iL$$

with L to be determined such that

$$\iint_R \psi_c(x,y)\,dx\,dy = \iint_R \left\{\hat{\psi}(x,y) + L\right\} dx\,dy$$

Hence

$$J = -\frac{1}{A}\iint_R \hat{F}(\zeta)\,dx\,dy$$

$$= -\frac{1}{2iA}\int_C \bar{\zeta}\,\hat{F}(\zeta)\,d\zeta \qquad (6.15)$$

so that

$$F(\zeta) = \hat{F}(\zeta) + J$$

and

$$\iint_R F(\zeta)\,dx\,dy = 0$$

Clearly, (6.14) is obtainable from (6.15).

In the examples given later the author has used (6.15) to adjust his regular function solving the torsion problem rather than using (6.14) to adjust just the warping function.

To obtain the boundary integral representation of the warping stiffness I_w consider first a simply connected region R bounded by the contour C. This region contains no singularities of the function $F(z)$ so that a regular function $G(\bar{z})$ which satisfies

$$\frac{d}{d\bar{z}} G(\bar{z}) = \bar{F}(\bar{z})$$

may be defined in R.

Utilising $F(z)$, $\hat{I}_w$ may be written as

$$\hat{I}_w = \frac{1}{4} \iint_R \left\{ F(z) + \bar{F}(\bar{z}) \right\}^2 dx\, dy$$

$$= \frac{1}{4} \iint_R \left\{ F(z)^2 + 2F(z)\bar{F}(\bar{z}) + \bar{F}(\bar{z})^2 \right\} dx\, dy$$

or, more conveniently,

$$\hat{I}_w = \frac{1}{4} \iint_R \frac{\partial}{\partial \bar{z}} \left[\bar{z} F(z)^2 + 2F(z)G(\bar{z}) \right] dx\, dy$$

$$+ \frac{1}{4} \iint_R \frac{\partial}{\partial z} \left[z \bar{F}(\bar{z})^2 \right] dx\, dy$$

On applying the complex forms of Green's Theorem to this last expression the required boundary integral representation

$$\hat{I}_w = \frac{1}{8i} \int_C \left\{ \bar{z} F(z)^2 + 2F(z)G(\bar{z}) \right\} dz$$

$$- \frac{1}{8i} \int_C z \bar{F}(\bar{z})^2 d\bar{z} \qquad (6.16)$$

is obtained.

When the region R is multiply connected this representation of the warping rigidity requires modification since the function $G(\bar{\tau})$ may no longer be single valued. To illustrate this, consider the region R bounded by the m contours C_p, $p = 1(1)m$, with C_1 enclosing all the others.

Let the analytic continuation of $F(\tau)$ into the region, R_1 say, bounded on the outside by the contour C_1 be denoted by $F_1(\tau)$. Due to the single valued nature of $F(\tau)$ in R, the only singularities $F_1(\tau)$ may have in R_1 are poles situated in the holes of the region R. The function $F(\tau)$ may therefore be represented in R by

$$F(\tau) = f_R(\tau) + \sum_{k=2}^{m} \sum_{j=1}^{n_k} B_{k,j} \frac{1}{\tau - \tau_{k,j}}$$

where $f_R(\tau)$ is regular in R, $\tau_{k,j}$ is the position of the jth simple pole in the kth hole, and $B_{k,j}$ is the "strength" of the pole at $\tau_{k,j}$. Hence $G(\bar{\tau})$ may be represented by

$$G(\bar{\tau}) = \int \bar{f}_R(\bar{\tau})\, d\bar{\tau} + \sum_{k=2}^{m} \sum_{j=1}^{n_k} \overline{B_{k,j}} \log(\tau - \tau_{k,j}) \qquad (6.17)$$

which is clearly multivalued unless the $B_{k,j}$ are all zero.

Usually the locations of the simple poles $\tau_{k,j}$ are unknown so that an appropriately multivalued $G(\bar{\tau})$ has to be constructed. This is readily accomplished by writing $F(\tau)$ as

$$F(\tau) = f(\tau) + \sum_{k=2}^{m} \frac{A_k}{\tau - \tau_k}$$

where $f(\tau)$ is regular in R, A_k is a complex constant particular to the contour C_k and τ_k is a point in the region bounded on the outside by the contour C_k (i.e. a point in the kth hole). Using this representation of $F(\tau)$, $\bar{F}(\bar{\tau})$ may be integrated to give

$$G(\bar{\zeta}) = g(\bar{\zeta}) + \sum_{k=2}^{m} \bar{A}_k \log(\bar{\zeta} - \bar{\zeta}_k) \qquad (6.18)$$

where

$$\frac{d}{d\bar{\zeta}} g(\bar{\zeta}) = \bar{f}(\bar{\zeta}).$$

Values of the constants A_k are readily obtained by integrating $F(\zeta)$ around each of the contours C_k. Since

$$\int_{C_k} \left\{ f(\zeta) + \sum_{\substack{j=2 \\ j \neq k}}^{m} \frac{A_j}{\zeta - \zeta_j} \right\} d\zeta = 0 ,$$

the required values are, for $k = 2(1)m$

$$A_k = -\frac{1}{2\pi i} \int_{C_k} F(\zeta)\, d\zeta \qquad (6.19).$$

Examination of (6.17) shows that the function $g(\bar{\zeta})$ is also regular in R when the A_k are determined by (6.19).

The procedure used to obtain the required representation of $\hat{I}_w$ when the region is multiply connected is best illustrated by means of the following example.

Consider the doubly connected region R shown in Figure 6-1. For any multiply connected region $\hat{I}_w$ may again be written as

$$\hat{I}_w = \frac{1}{4} \iint_R \left\{ F(\zeta) + \bar{F}(\bar{\zeta}) \right\}^2 dx\, dy$$

or

$$\hat{I}_w = \frac{1}{4} \iint_R \frac{\partial}{\partial \bar{\zeta}} \left[\bar{\zeta} F(\zeta)^2 + 2 F(\zeta) G(\bar{\zeta}) \right] dx\, dy$$

$$+ \frac{1}{4} \iint_R \frac{\partial}{\partial \zeta} \left[\zeta \bar{F}(\bar{\zeta})^2 \right] dx\, dy$$

where $F(\zeta) = \varphi(x,y) + i\psi(x,y)$ and $G(\bar{\zeta})$ is obtained from (6.18), (6.19). The function $\bar{\zeta} F(\zeta)^2$ and its conjugate $\zeta \bar{F}(\bar{\zeta})^2$ are single valued in R so that

$$\iint_R \left\{ \frac{\partial}{\partial \bar{\zeta}} \left[\bar{\zeta} F(\zeta)^2 \right] + \frac{\partial}{\partial \zeta} \left[\zeta \bar{F}(\bar{\zeta})^2 \right] \right\} dx\, dy$$

$$= \sum_{p=1}^{2} \frac{1}{2i} \left\{ \int_{C_p} \bar{\zeta} F(\zeta)^2 \, d\zeta - \int_{C_p} \zeta \bar{F}(\bar{\zeta})^2 \, d\bar{\zeta} \right\}$$

by the complex forms of Green's Theorem. This theorem cannot be applied directly to the term

$$\iint_R \frac{\partial}{\partial \bar{\zeta}} \left[F(\zeta) G(\bar{\zeta}) \right] dx\, dy$$

because of the previously shown multi-valued nature of $G(\bar{\zeta})$. This function is, however, single valued in the simply connected region $\tilde{R}$ shown in Figure 6-2. Clearly the region $\tilde{R}$ is obtained from R by the introduction of the branch cuts LM, DE of the function $\log(\zeta - \zeta_2)$ and if δ represents the distance between the cuts,

i.e. $\delta = |D-M| = |E-L|$

then

$$\lim_{\delta \to 0} \iint_{\tilde{R}} \frac{\partial}{\partial \bar{\zeta}} \left[F(\zeta) G(\bar{\zeta}) \right] dx\, dy = \iint_R F(\zeta) \bar{F}(\bar{\zeta}) \, dx\, dy$$

and

$$\lim_{\delta \to 0} \sum_{p=1}^{2} \int_{\tilde{C}_p} F(\zeta) G(\bar{\zeta}) \, d\zeta = \sum_{p=1}^{2} \int_{C_p} F(\zeta) G(\bar{\zeta}) \, d\zeta .$$

Since $G(\bar{\zeta})$ is single valued in $\tilde{R}$ the term

$$\iint_{\tilde{R}} \frac{\partial}{\partial \bar{\zeta}} \left[F(\zeta) G(\bar{\zeta}) \right] d\zeta$$

may be written as

$$\iint_{\tilde{R}} \frac{\partial}{\partial \bar{\zeta}} \left[F(\zeta) G(\bar{\zeta}) \right] d\zeta = \frac{1}{2i} \int_{\partial \tilde{R}} F(\zeta) G(\bar{\zeta}) d\zeta$$

where $\partial \tilde{R}$ is the simple closed curve bounding $\tilde{R}$. It remains to consider the contributions made to the above contour integral by the various curves which make up $\partial \tilde{R}$. Therefore, i) the contributions from the curves $\tilde{C}_1$ and $\tilde{C}_2$ are

$$\int_{\tilde{C}_1} F(\zeta) \left\{ g(\bar{\zeta}) + \bar{A}_2 \log (\bar{\zeta} - \bar{\zeta}_2) \right\} d\zeta$$

and

$$\int_{\tilde{C}_2} F(\zeta) \left\{ g(\bar{\zeta}) + \bar{A}_2 \log (\bar{\zeta} - \bar{\zeta}_2) \right\} d\zeta$$

respectively.

ii) by writing (for sufficiently small δ)

$$\zeta - \zeta_2 = \rho e^{i\theta} \quad \text{on} \quad DE$$

and

$$\zeta - \zeta_2 = \rho e^{i(\theta + 2\pi)} \quad \text{on} \quad LM,$$

the contributions along the curves LM, DE are seen to be

$$\int_L^M F(\zeta) g(\bar{\zeta}) d\zeta + \bar{A}_2 \int_{\rho(L)}^{\rho(M)} F(\rho) \left\{ \log \rho + i(\theta + 2\pi) \right\} d\rho$$

and

and

$$\int_D^E F(\bar{z})\, g(\bar{z})\, dz \quad + \bar{A}_2 \int_{\rho(D)}^{\rho(E)} F(\rho) \left\{ \log \rho - i\theta \right\} d\rho .$$

The total contribution from the branch cuts to the contour integral is therefore

$$- \bar{A}_2\, 2\pi i \int_{\rho(L)}^{\rho(M)} F(\rho)\, d\rho \;=\; - \bar{A}_2\, 2\pi i \int_L^M F(z)\, dz .$$

Hence, for δ sufficiently small,

$$\int_{\partial \tilde{R}} F(z)\, G(\bar{z})\, dz \;=\; \sum_{p=1}^{2} \int_{\tilde{C}_p} F(z) \left\{ g(\bar{z}) + \bar{A}_2 \log (\bar{z} - \bar{z}_2) \right\} dz$$

$$- 2\pi i\, \bar{A}_2 \int_L^M F(z)\, dz$$

$$= \sum_{p=1}^{2} \int_{\tilde{C}_p} F(z) \left\{ g(\bar{z}) + \bar{A}_2 \log (\bar{z} - \bar{z}_2) \right\} dz$$

$$- 2\pi i\, \bar{A}_2 \left\{ \bar{G}(M) - \bar{G}(L) \right\}$$

where $\bar{G}(M)$ and $\bar{G}(L)$ may be determined from (7.18), (7.19).

The warping rigidity for the doubly connected region under consideration is therefore given by

$$\hat{I}_W \;=\; \frac{1}{4} \sum_{p=1}^{2} \left\{ \mathrm{Im} \left(\int_{C_p} \bar{z}\, F(z)^2\, dz \right) \right.$$

$$\left. + \frac{1}{i} \int_{C_p} F(z) \left(g(\bar{z}) + \bar{A}_2 \log (\bar{z} - \bar{z}_2) \right) dz \right\}$$

$$- \frac{\pi}{2} \left\{ \bar{g}(M) - \bar{g}(L) + A_2 \log (M/L) \right\} \bar{A}_2 \qquad (6.20)$$

The representation (6.20) is readily generalised to the case of the multiply connected region bounded by the m contours C_p, $p = 1(1)m$, with C_1 enclosing the remaining C_p. In this case

$$\hat{I}_w = \frac{1}{4}\sum_{p=1}^{m} I_m\left\{\int_{C_p} \bar{z}\,F(z)^2\,dz\right\}$$

$$+\frac{1}{4i}\sum_{p=1}^{m}\int_{C_p} F(z)\left\{g(\bar{z}) + \sum_{q=2}^{m}\bar{A}_q \log(\bar{z}-\bar{z}_q)\right\}dz$$

$$-\frac{\pi}{2}\sum_{q=2}^{m}\left\{\bar{g}(M_q) - \bar{g}(L_q) + A_q \log\left(M_q/L_q\right)\right\}\bar{A}_q \qquad (6.21)$$

where the M_q, L_q denote the start and end points of the m-1 branch cuts. That the derivation of (6.20) and (6.21) can be performed with branch cuts which are not parallel to the positive x-axis is noted (see § 5.4 for a similar effect).

Although derived as a representation for the warping stiffness constant $\hat{I}_w$, the identity (6.21) may be used to evaluate

$$\iint_R \{\varphi(x,y)\}^2\,dx\,dy$$

whenever $\varphi(x,y)$ is the real part of a function regular in R provided that its harmonic conjugate $\psi(x,y)$ is known. This has proved useful in verifying the representation of the warping stiffness constant since the warping function and its harmonic conjugate are known for only a limited number of regions

As an example illustrating the use of (6.21) consider the annular region shown in Figure 6-3 over which

$$I = \iint_R \left\{x + \frac{x+y}{x^2+y^2}\right\}^2 dx\,dy$$

is to be evaluated. The integrand is the real part of the function

$$F(\zeta) = \zeta + \frac{1+i}{\zeta}$$

which is regular in R. By writing

$$f(\zeta) = \zeta$$
$$\zeta_2 = 0$$
$$A_2 = 1+i$$
$$g(\bar{\zeta}) = \frac{1}{2}\bar{\zeta}^2$$

in (6.21), it is apparent that

$$I = \frac{1}{4}\sum_{p=1}^{2} \mathrm{Im}\left\{ \int_{C_p} \bar{\zeta}\left[\zeta + \frac{1+i}{\zeta}\right]^2 d\zeta \right\}$$
$$+\frac{1}{4i}\sum_{p=1}^{2} \int_{C_p} \left\{\zeta + \frac{1+i}{\zeta}\right\}\left\{\frac{\bar{\zeta}^2}{2} + (1-i)\log\bar{\zeta}\right\} d\zeta$$
$$+\frac{\pi}{2}\left\{\frac{b^2-a^2}{2} + (1+i)\log\left(\tfrac{b}{a}\right)\right\}(1-i) .$$

Since

$$\zeta\bar{\zeta} = \begin{cases} b^2 & \text{on } C_1 \\ a^2 & \text{on } C_2 \end{cases},$$

I may be written as

$$I = \frac{1}{4}\sum_{p=1}^{2} R_p\, \mathrm{Im}\left\{ \int_{C_p} \frac{1}{\zeta}\left[\zeta + \frac{1+i}{\zeta}\right]^2 d\zeta \right\}$$
$$+\frac{1}{4i}\sum_{p=1}^{2} \int_{C_p} \left\{\zeta + \frac{1+i}{\zeta}\right\}\left\{\frac{R_p^4}{2\zeta^2} + 2(1-i)\log R_p - (1-i)\log\zeta\right\} d\zeta$$
$$+\frac{\pi}{2}\left\{\frac{b^2-a^2}{2} + (1+i)\log\left(\tfrac{b}{a}\right)\right\}(1-i)$$

where $R_1 = b$ and $R_2 = a$.

Now for $p = 1, 2$

$$\int_{C_p} \frac{1}{\zeta}\left\{\zeta + \frac{1+i}{\zeta}\right\}^2 d\zeta = \left[\frac{\zeta^2}{2} + 2(1+i)\log\zeta - \frac{(1+i)^2}{2\zeta}\right]_{C_p}$$

$$= (-1)^{p-1} 4\pi i (1+i)$$

and

$$\int_{C_p}\left\{\zeta + \frac{1+i}{\zeta}\right\}\left\{\frac{R_p^4}{2\zeta^2} + 2(1-i)\log R_p - (1-i)\log\zeta\right\} d\zeta$$

$$= \left[\frac{R_p^4}{2}\left\{\log\zeta - \frac{1}{2}\frac{1+i}{\zeta^2}\right\} + (1-i)\zeta^2\log R_p + 4\log R_p\log\zeta\right.$$

$$\left. - (1-i)\frac{\zeta^2}{2}\left\{\log\zeta - \frac{1}{2}\right\} - \left\{\log\zeta\right\}^2\right]_{C_p}$$

$$= (-1)^{p-1}\left\{\pi i R_p^4 + 8\pi i\log R_p - (1-i)\pi i R_p^2 - 4\pi i\log R_p + 4\pi^2\right\}$$

so that

$$I = (b^2-a^2)\pi + \frac{(b^4-a^4)\pi}{4} + \pi\log(b/a) - (1-i)\frac{\pi}{4}(b^2-a^2)$$

$$+ \frac{\pi}{2}\left\{\frac{b^2-a^2}{2} + (1+i)\log(b/a)\right\}(1-i)$$

$$= \pi\left\{(b^2-a^2) + \frac{b^4-a^4}{4} + 2\log(b/a)\right\} \qquad (6.22)$$

In this example, the integral I could have been evaluated by writing the integrand in terms of the polar co-ordinate system shown in Figure 6-3,
i.e.

$$\text{let} \quad x = \rho \cos\theta$$
$$y = \rho \sin\theta$$

so that

$$I = \int_0^{2\pi} \int_a^b \left\{ \rho\cos\theta + \frac{\cos\theta + \sin\theta}{\rho} \right\}^2 \rho \, d\rho \, d\theta$$

$$= \int_0^{2\pi} \left\{ \frac{b^4 - a^4}{8} (1 + \cos 2\theta) + \log(b/a).(1+\sin 2\theta) \right.$$

$$\left. + \frac{b^2 - a^2}{2} (1 - \cos 2\theta) \right\} d\theta$$

$$= \pi \left\{ (b^2 - a^2) + \frac{b^4 - a^4}{4} + 2\log(b/a) \right\}$$

which agrees with (6.22).

Returning to the evaluation of I_w, note that I_w is readily shown to be related to $\hat{I}_w$ through the expression

$$I_w = \hat{I}_w - \left\{ I_x y_c^2 + I_y x_c^2 \right\}$$

Here I_w and $\hat{I}_w$ can be interpreted as the warping stiffness constants for a beam twisted about longitudinal axes passing through the cross-section's shear centre and centroid respectively.

§ 6.4) A Boundary Integral Representation of The Torsional Stiffness Constant

For a constant section beam twisted about its longitudinal axis it is readily shown [4, p.312] that the total force acting on any cross-section is zero,

$$\text{i.e.} \quad \iint_R \tau_{xz}\, dx dy = \iint_R \tau_{yz}\, dx\, dy = 0 \quad ,$$

and that the tractions are statically equivalent to a couple only. If **M** denotes the magnitude of this couple then

$$M = \iint_R \{x\, \tau_{yz} - y\, \tau_{xz}\}\, dx\, dy \qquad (6.23)$$

The substitution of (6.3) into this last expression enables **M** to be written as

$$M = \mu\Omega \iint_R \{ x[\varphi_y(x,y) + x] - y[\varphi_x(x,y) - y] \}\, dx\, dy$$

$$= \mu\Omega \{I_x + I_y\} + \mu\Omega \iint_R \{x\varphi_y(x,y) - y\varphi_x(x,y)\} dx dy$$

where I_x and I_y are the second moments of inertia as before. The quantity

$$\frac{M}{\mu\Omega}$$

is termed the torsional stiffness of the section under consideration and is denoted by I_s. The torsional stiffness is therefore given by

$$I_s = I_x + I_y + \iint_R \{x\varphi_y(x,y) - y\varphi_x(x,y)\} dx dy \qquad (6.24)$$

Although many authors [e.g. 4, 15, 16, 44] write (6.24) in terms of the Dirichlet Integral

$$\int_C \varphi(x,y)\, \varphi_n(x,y)\, ds \quad ,$$

the torsional stiffness can also be obtained in terms of an integral involving the gradient of the warping function. Let $\zeta = x + iy$ be a point in the section twisted about the origin and

$$\tau(\zeta) = \varphi_x(x,y) - i\,\varphi_y(x,y)$$

be the gradient of the warping function arising from this twist. Hence, (6.24) may be written in the form

$$I_s = I_x + I_y - I_m\left\{\iint_R \bar{\zeta}\,\tau(\zeta)\,dx\,dy\right\}$$

or, more conveniently,

$$I_s = I_x + I_y - I_m\left\{\iint_R \frac{\partial}{\partial\bar{\zeta}}\left[\tfrac{1}{2}\bar{\zeta}^2\tau(\zeta)\right]dx\,dy\right\}.$$

Since the function $\tau(\zeta)$ is regular in **R** (so that $\tfrac{1}{2}\bar{\zeta}^2\tau(\zeta)$ is single valued), the complex forms of Green's Theorem can be applied to the integral. Therefore

$$I_s = I_x + I_y - I_m\left\{\frac{1}{2i}\int_C \tfrac{1}{2}\bar{\zeta}^2\tau(\zeta)\,d\zeta\right\}$$

$$= I_x + I_y + R_e\left\{\frac{1}{2}\int_C \tfrac{1}{2}\bar{\zeta}^2\tau(\zeta)\,d\zeta\right\} \qquad (6.25)$$

where **C** is the boundary of the region **R**. Examination of (6.25) shows that this representation does, in fact, contain the Dirichlet Integral

$$\int_C \psi(x,y)\,\psi_n(x,y)\,ds$$

where $\psi(x,y)$ denotes the harmonic conjugate of the warping function $\varphi(x,y)$.

The representation (6.25) has been used by the author when solving the torsion problem by the procedure outlined at the beginning of this chapter. The use of (6.25) rather than equivalent real variable representations involving

explicit Dirichlet Integrals is consistent with the author's previously derived representations of the warping rigidity and shear centre co-ordinates.

That the torsional stiffness $\hat{I}_s$ of a beam twisted about a longitudinal axis passing through the shear centre (x_c, y_c) of its cross-section equals I_s can be shown in the following way. As above, here I_s and $\varphi(x,y)$ are the torsional stiffness and warping function for the section when the longitudinal axis of the beam passes through the centroid of the section with principal axes x, y.

The magnitude of the couple about the shear centre is given by

$$\hat{M} = \mu \Omega \iint_R \left\{(x-x_c)\tau_{yz} - (y-y_c)\tau_{xz}\right\} dx\,dy$$

from which

$$\hat{I}_s = \iint_R \left\{(x-x_c)\left[\varphi_y(x,y) + x\right] - (y-y_c)\left[\varphi_x(x,y) - y\right]\right\} dx\,dy$$

is obtained. This expression for $\hat{I}_s$ can be written as

$$\hat{I}_s = \iint_R \left\{x^2 + x\varphi_y(x,y) + y^2 - y\varphi_x(x,y)\right\} dx\,dy$$

$$+ \iint_R \left\{y_c\varphi_x(x,y) - x_c\varphi_y(x,y)\right\} dx\,dy$$

since x and y are the principal axes of the section with $x = y = 0$ at the centroid. Comparison with (6.24) shows that

$$\hat{I}_s = I_s + \iint_R \left\{y_c\varphi_x(x,y) - x_c\varphi_y(x,y)\right\} dx\,dy$$

$$= I_s$$

This last result is obtained by noting that for the torsion problem under consideration the identities

$$\iint_R \tau_{xz}\, dx\, dy = 0$$

$$\iint_R \tau_{yz}\, dx\, dy = 0$$

have been given. The substitution of (6.3) into these identities yields

$$\iint_R \varphi_x(x,y)\, dx\, dy = \iint_R y\, dx\, dy$$

$$\iint_R \varphi_y(x,y)\, dx\, dy = -\iint_R x\, dx\, dy$$

and the result follows.

§ 6.5) Numerical Evaluation of Boundary Integral Representations

The evaluation of the previously derived boundary integral representations for the torsional stiffness, warping stiffness and shear centre co-ordinates can only be performed for a limited number of sections. In most practical cases the integrations have to be performed by utilising the piecewise polynomial approximations and boundary idealisations of Chapters 3 & 5.

Hence if

$$I_A = \sum_{p=1}^{m} \int_{C_p} H_A(\tilde{\underline{s}})\, d\underline{s}$$

then the approximation

$$I_A \simeq \sum_{p=1}^{m} \sum_{q=1}^{n_p} \sum_{r=1}^{3} H_A(\tilde{\underline{s}}_{p,q}^{(r)}) \int_{I_{p,q}} M_{p,q}^{(r)}(\underline{s})\, d\underline{s} \qquad (6.26)$$

has been used. Similarly, to evaluate

$$I_B = \sum_{p=1}^{m} \int_{C_p} H_B(\tilde{\underline{s}})\, d\underline{s}$$

the approximation

$$I_B \simeq \sum_{p=1}^{m} \sum_{q=1}^{n_p} \sum_{r=1}^{3} H_B(\tilde{\underline{s}}_{p,q}^{(r)}) \int_{I_{p,q}} \bar{M}_{p,q}^{(r)}(\underline{s})\, d\underline{s} \qquad (6.27)$$

has been used.

Note that in (6.26) and (6.27)

$$M_{p,q}^{(r)}(\underline{s}) = \prod_{\substack{j=1 \\ j \neq r}} \frac{(\underline{s}_{p,q}^{(j)} - \underline{s})}{(\underline{s}_{p,q}^{(j)} - \underline{s}_{p,q}^{(r)})} \qquad (6.28)$$

§ 6.6) Examples

Some of the results given in this section have previously appeared in the author's paper:-

"Determination of the torsional properties of a plane section using boundary integral techniques" [48].

§ 6.6.1) Torsional properties of a hollow ellipse

As a first example consider the region lying between the concentric ellipses

$$\left(\frac{x}{a}\right)^2 + \left(\frac{y}{b}\right)^2 = 1$$

$$\left(\frac{x}{a}\right)^2 + \left(\frac{y}{b}\right)^2 = q^2$$

with $q < 1$.

Following Love [4, p.317], the regular function

$$F(\zeta) = \varphi(x,y) + i\,\psi(x,y)$$

with $\zeta = x + iy$

$$\varphi(x,y) = -\frac{a^2 - b^2}{a^2 + b^2}\,xy \qquad (6.29)$$

and

$$\psi(x,y) = \frac{1}{2}\,\frac{a^2-b^2}{a^2+b^2}\,(x^2-y^2) \qquad (6.30)$$

provides the warping and torsion functions for this hollow region. Examination of these functions shows that $F(\zeta)$ may be written as

$$F(\zeta) = \frac{i}{2}\,\frac{a^2-b^2}{a^2+b^2}\,\zeta^2$$

whence

$$\tau(\zeta) = F_\zeta(\zeta)$$

$$= i\,\frac{a^2-b^2}{a^2+b^2}\,\zeta.$$

Because $\tau(\zeta)$ is linear in ζ the numerical techniques of Chapters 3 & 5 can be expected to yield exact values of $\varphi_s(\tilde{\zeta})$ and $F(\zeta)$. This is illustrated in Tables 6-1 to 6-4 where numerical results obtained for the region lying between the ellipses

$$x^2 + 4y^2 = 1$$

$$x^2 + 4y^2 = .81$$

are given. The idealisations used here were obtained by positioning nodes at equal increments of eccentric angle. Thus Table 6-1 and 6-2 were obtained by taking 20 nodes at equal increments of eccentric angle for each boundary. Twice that number was used in obtaining Tables 6-3 and 6-4. Figure 6-4 shows the resulting idealisation for the 20 node case.

Note that the $F(\tau)$ given in the above tables has been adjusted to give

$$\iint_R F(\tau)\, dx\, dy = 0 .$$

This adjustment has been carried out by evaluating (6.15) using a quadrature formula of the type illustrated by (6.26). It will be observed that the imaginary part of the adjusting constant appears to be more sensitive to changes in the idealisation than the real part.

In this example the previously given expressions for $\varphi(x,y)$ and $\psi(x,y)$ can be used to provide formulae for I_s and I_w. Indeed, use of (6.29) and (6.30) in the area integral representations of I_s and I_w lead to the conclusion that

$$I_s = \pi \frac{a^3 b^3}{a^2 + b^2} \left\{1 - q^4\right\}$$

$$I_w = \frac{\pi}{24} \left\{\frac{a^2 - b^2}{a^2 + b^2}\right\}^2 a^3 b^3 \left\{1 - q^6\right\}$$

For the region lying between the ellipses

$$x^2 + 4y^2 = 1$$

$$x^2 + 4y^2 = .81$$

these formulae for I_s and I_w yield

$$I_s = 0.1080$$

$$I_w = 0.002760$$

In Table 6-5 these values are compared with those obtained numerically using the techniques described in this chapter. The idealisations used were again obtained by positioning nodes at equal increments of eccentric angle. Results are given for a 60 node/boundary idealisation as well as the 20 and 40 node/boundary idealisations used earlier.

Approximations to the shear centre co-ordinates x_c, y_c which were obtained for the three idealisations considered are given in Table 6-6. These approximate values compare well with the true values of $x_c = 0$ and $y_c = 0$. These true values are most readily obtained through symmetry considerations.

§ 6.6.2) <u>Torsional properties of a semi-circular region</u>

Consider now the semi-circular region bounded on the outside by the circle

$$x^2 + \left(y - \frac{4}{3\pi}\right)^2 = 1$$

and the line $y = -\frac{4}{3\pi}$. For this region approximate values of the torsional stiffness I_s and shear centre co-ordinate y_c are given by Timoshenko [49, p.373] and Roark [51, p.291] (I_s only). Note that Timoshenko obtains a value for y_c by considering the bending of a uniform cantilever beam [49, ch.11]. This is in direct contrast to the approach used by the present author. The shear centre co-ordinate $x_c = 0$ can be obtained by symmetry considerations.

The numerical techniques described in this chapter have been applied to the above semi-circular region. The resulting approximations to I_s, x_c and y_c are compared with those obtained from Timoshenko and Roark in Table 6-7. The idealisations used by the author were of the type shown in Figure 6-5. Here the nodes on the circular arc CA were positioned at equal increments of the circumferential angle. Nodes on the line ABC were positioned at equal increments of arc length. Figure 6-5 does in fact show the 28 nodes/boundary case, 56 and 84 nodes/boundary cases were also considered.

The approximations to I_w obtained using the 56 and 84 nodes/boundary idealisations were $I_w \simeq 0.5871 \times 10^{-2}$ and $I_w \simeq 0.5902 \times 10^{-2}$ respectively.

§ 6.6.3) Torsional properties of a cambered section

As an example of a cambered region, consider the sector of an annulus shown in Figure 6-6. This region is typical of those open sections which exhibit a high ratio of surface length to area and whose torsional properties can be found using the "thin wall" theory as described by Zbirohowski-Koscia [33]. In this particular example formulae for the torsional stiffness I_s and shear centre co-ordinate y_c can be found in Roark [51, p.302].

The numerical techniques described in this chapter have been applied to the above cambered region. The idealisation used by the author is shown in Figure 6-7. Here there are 51 nodes on both of the circular arcs (this number includes the nodes at A, B, C & D), the nodes being positioned at equal increments of circumferential angle θ. On each of the radial lines AB and CD there are 10 nodes positioned at equal increments of arc length (the number here excludes the nodes at A, B, C & D). Note that the co-ordinates given in Figure 6-7 relate to an origin at the centre of the annulus of which the region is part and not to an origin at the region's centroid.

The approximations to the required torsional properties which were obtained using the above idealisation are compared with their "thin-wall" counterparts in Table 6-8. That there is a 15% difference between values for I_s is noted.

Chapter 7

THE COUPLING OF INTERIOR AND EXTERIOR PROBLEMS FOR SOLID AEROFOIL SECTIONS

§ 7.1) Introduction

In the preceding chapters the author has endeavoured to present a unified approach to two important applications of the two dimensional Neumann problem; viz. the torsion of a constant section beam and the plane, incompressible, inviscid flow past on aerofoil. As appears usual, solutions of these problems have been obtained separately despite their obvious similarities.

In an engineering environment, solutions to both of the above interior and exterior problems are, at times, required for a given aerofoil section. Clearly, it would be desirable to know whether or not techniques are available which allow for the solution of both interior and exterior problems at the same time.

Anticipating the results obtained below and restricting attention to solid, non-cusped aerofoil sections of conventional shape, it can be shown that such a technique is certainly available for both isolated and cascade aerofoils. The technique used is based on the approximate solutions to the integral equations given in previous chapters.

In the following sections of this chapter let

$$\tau(\zeta) = \varphi_x(\tilde{\zeta}) - i\,\varphi_y(\tilde{\zeta})$$

and

$$T(\zeta) = \Phi_x(\tilde{\zeta}) - i\,\Phi_y(\tilde{\zeta})$$

denote the complex potentials obtained from the interior (torsion) and exterior (flow) problems respectively. Further let

$$\oint_C -$$

denote on integration taken anticlockwise around the contour **C**. This notation implies an integration

in the positive sense for interior problems and an integration in the negative sense for exterior problems.

Note that in this chapter the suffix denoting boundary number has been dropped. This is because the problems considered here are solved by integral equations involving a single boundary.

§ 7.2) Coupled Interior/Exterior Problem For Isolated Aerofoils

For an isolated aerofoil the integral identities governing the behaviour of the tangential derivatives of the warping function $\varphi(\tilde{\zeta})$ and velocity potential $\Phi(\tilde{\zeta})$ are obtained from the preceding chapters as

$$\varphi_s(\tilde{\omega}) + i\,\varphi_n(\tilde{\omega}) = \frac{e^{i\alpha(\tilde{\omega})}}{\pi} \oint_C \frac{\varphi_s(\tilde{\zeta}) + i\,\varphi_n(\tilde{\zeta})}{\zeta - \omega}\, ds \qquad (7.1)$$

and

$$\Phi_s(\tilde{\omega}) = 2\sigma i e^{i\alpha(\tilde{\omega})} - \frac{e^{i\alpha(\tilde{\omega})}}{\pi} \oint_C \frac{\Phi_s(\tilde{\zeta})\, ds}{\zeta - \omega} \qquad (7.2)$$

respectively. Here ω is a point lying on a smooth portion of the boundary C, σ is the upstream flow condition on the flow's complex conjugate velocity $T(\zeta)$, $\alpha(\tilde{\omega})$ is the angle between the positive real direction and a normal at ω which is drawn into the infinite region (outward drawn normal for interior problem), and $\varphi_n(\tilde{\zeta})$ is the normal derivative of the aerofoil's warping function.

Note that for the exterior problem the directions of both the normal and tangent to the boundary differ from those used previously. Because of <u>both</u> these differences there is no change of sign on the right hand side of (7.2).

As an alternative to the solution of the interior and exterior problems separately consider the pair of complex

equations

$$\varphi_s(\tilde{\omega}) + \bar{\Phi}_s(\tilde{\omega}) + i\varphi_n(\tilde{\omega})$$

$$= 2\sigma i e^{i\alpha(\tilde{\omega})} + \frac{e^{i\alpha(\tilde{\omega})}}{\pi} \oint_C \frac{\varphi_s(\tilde{\tau}) + i\varphi_n(\tilde{\tau}) - \bar{\Phi}_s(\tilde{\tau})}{\tau - \omega}\, ds \qquad (7.3)$$

$$\varphi_s(\tilde{\omega}) - \bar{\Phi}_s(\tilde{\omega}) + i\varphi_n(\tilde{\omega})$$

$$= -2\sigma i e^{i\alpha(\tilde{\omega})} + \frac{e^{i\alpha(\tilde{\omega})}}{\pi} \oint_C \frac{\varphi_s(\tilde{\tau}) + i\varphi_n(\tilde{\tau}) + \bar{\Phi}_s(\tilde{\tau})}{\tau - \omega}\, ds \qquad (7.4)$$

for the sum and difference of unknown tangential deriatives. Clearly, equations (7.3) and (7.4) are obtained by adding and subtracting (7.1) and (7.2).

A pair of simultaneous Frecholm integral equations of the second kind for the unknowns, $\varphi_s(\tilde{\tau}) - \bar{\Phi}_s(\tilde{\tau})$ and $\varphi_s(\tilde{\tau}) + \bar{\Phi}_s(\tilde{\tau})$, are obtained from the real parts of (7.3) and (7.4). These equations may be written as

$$\varphi_s(\tilde{\omega}) + \bar{\Phi}_s(\tilde{\omega}) - \frac{1}{\pi} \oint_C \left\{\varphi_s(\tilde{\tau}) - \bar{\Phi}_s(\tilde{\tau})\right\} K_1(\tilde{\omega}, \tilde{\tau})\, ds$$

$$= -2\, \mathrm{Im}\left\{\sigma e^{i\alpha(\tilde{\omega})}\right\} + \frac{1}{\pi} \oint_C \varphi_n(\tilde{\tau})\, H_1(\tilde{\omega}, \tilde{\tau})\, ds \qquad (7.5)$$

$$\varphi_s(\tilde{\omega}) - \bar{\Phi}_s(\tilde{\omega}) - \frac{1}{\pi} \oint_C \left\{\varphi_s(\tilde{\tau}) + \bar{\Phi}_s(\tilde{\tau})\right\} K_1(\tilde{\omega}, \tilde{\tau})\, ds$$

$$= 2\, \mathrm{Im}\left\{\sigma e^{i\alpha(\tilde{\omega})}\right\} + \frac{1}{\pi} \oint_C \varphi_n(\tilde{\tau})\, H_1(\tilde{\omega}, \tilde{\tau})\, ds \qquad (7.6)$$

where, if $\omega = x_0 + i y_0$ and $\tilde{\gamma} = x + iy$

$$K_1(\tilde{\omega},\tilde{\gamma}) = \frac{(x-x_0).\cos\{\alpha(\tilde{\omega})\} + (y-y_0).\sin\{\alpha(\tilde{\omega})\}}{(x-x_0)^2 + (y-y_0)^2}$$

$$H_1(\tilde{\omega},\tilde{\gamma}) = \frac{(y-y_0).\cos\{\alpha(\tilde{\omega})\} - (x-x_0).\sin\{\alpha(\tilde{\omega})\}}{(x-x_0)^2 + (y-y_0)^2}$$

That the solution of the system of equations (7.5), (7.6) is not unique follows either from consideration of the homogeneous adjoint system (as in Chapter 2) or from the manner in which the system was obtained. As in Chapter 2, application of the Fredholm theory [17, pp. 30-31] leads to the conclusion that although the solution of the system (7.5), (7.6) is not unique, the corresponding homogeneous system has a non-trivial solution which is unique to within an arbitrary additive constant.

For a smooth profile a unique solution is obtained by requiring that the solution of the exterior problem yield a specified circulation Γ. Since the warping function $\varphi(\tilde{\gamma})$ is single valued on the contour **C**, the specification of Γ yields.

$$\oint_C \{\varphi_s(\tilde{\gamma}) + \mathcal{K}_s(\tilde{\gamma})\} ds = \Gamma \qquad (7.7)$$

$$\oint_C \{\varphi_s(\tilde{\gamma}) - \mathcal{K}_s(\tilde{\gamma})\} ds = -\Gamma \qquad (7.8)$$

These two equations can be adjoined to (7.5), (7.6) when necessary.

If the profile has a point at the trailing edge, $\tilde{\zeta}_0$ say, a unique solution is obtained from the previously shown requirements

$$\Phi_s(\tilde{\zeta}_0) = 0$$

$$\varphi_s(\tilde{\zeta}_0) = -y_0 \sin\{\alpha(\tilde{\zeta}_0)\} - x_0 \cos\{\alpha(\tilde{\zeta}_0)\}$$

Hence four additional equations are given by

$$\varphi_s(\tilde{\zeta}_0) + \Phi_s(\tilde{\zeta}_0) = -y_0 \sin\{\alpha(\tilde{\zeta}_0)\} - x_0 \cos\{\alpha(\tilde{\zeta}_0)\} \qquad (7.9)$$

$$\varphi_s(\tilde{\zeta}_0) - \Phi_s(\tilde{\zeta}_0) = -y_0 \sin\{\alpha(\tilde{\zeta}_0)\} - x_0 \cos\{\alpha(\tilde{\zeta}_0)\} \qquad (7.10)$$

since $\alpha(\tilde{\zeta}_0)$ is double valued at the point.

Equations (7.5), (7.6) can be reduced to a single equation for $\varphi_s(\tilde{\omega}) + \Phi_s(\tilde{\omega})$ by substituting (7.6) for $\varphi_s(\tilde{\zeta}) - \Phi_s(\tilde{\zeta})$ in (7.5). Similarly, an equation for $\varphi_s(\tilde{\omega}) - \Phi_s(\tilde{\omega})$ is obtained by substituting (7.5) for $\varphi_s(\tilde{\zeta}) + \Phi_s(\tilde{\zeta})$ in (7.6). These substitutions lead to the equations

$$\varphi_s(\tilde{\omega}) + \Phi_s(\tilde{\omega}) - \frac{1}{\pi^2}\oint_C K_1(\tilde{\omega},\tilde{\zeta})\left\{\oint_C [\varphi_s(\tilde{t}) + \Phi_s(\tilde{t})] K_1(\tilde{\zeta},\tilde{t})\, ds(\tilde{t})\right\} ds(\tilde{\zeta})$$

$$= -2\,\mathrm{Im}\left\{\sigma e^{i\alpha(\tilde{\omega})}\right\} + \frac{1}{\pi}\oint_C \varphi_n(\tilde{\zeta}) H_1(\tilde{\omega},\tilde{\zeta})\, ds(\tilde{\zeta})$$

$$+ \frac{1}{\pi}\oint_C K_1(\tilde{\omega},\tilde{\zeta})\left\{2\,\mathrm{Im}\left\{\sigma e^{i\alpha(\tilde{\zeta})}\right\} + \frac{1}{\pi}\oint_C \varphi_n(\tilde{t}) H_1(\tilde{\zeta},\tilde{t})\, ds(\tilde{t})\right\} ds(\tilde{\zeta}) \qquad (7.11)$$

and

$$\varphi_s(\tilde{\omega}) - \bar{\varphi}_s(\omega) - \frac{1}{\pi^2}\oint_C K_1(\tilde{\omega},\tilde{\gamma})\left\{\oint\left[\varphi_s(\tilde{t}) - \bar{\varphi}_s(\tilde{t})\right]K_1(\tilde{\gamma},\tilde{t})\,ds(\tilde{t})\right\}ds(\tilde{\gamma})$$

$$= 2\,I_m\left\{\sigma e^{i\alpha(\tilde{\omega})}\right\} + \frac{1}{\pi}\oint_C \varphi_n(\tilde{\gamma})\,H_1(\tilde{\omega},\tilde{\gamma})\,ds(\tilde{\gamma})$$

$$+\frac{1}{\pi}\oint_C K_1(\tilde{\omega},\tilde{\gamma})\left\{\frac{1}{\pi}\oint_C \varphi_n(\tilde{t})\,H_1(\tilde{\gamma},\tilde{t})\,ds(\tilde{t}) - 2\,I_m\left\{\sigma e^{i\alpha(\tilde{\gamma})}\right\}\right\}ds(\tilde{\gamma})$$

. . . . (7.12)

where

$$\oint_C \{-\}\,ds(\tilde{t})$$

denotes an integration taken around the contour with t varying and γ fixed. Similarly,

$$\oint_C \{-\}\,ds(\tilde{\gamma})$$

denotes an integration taken around the contour with γ varying and ω fixed.

A solution to the coupled problem can therefore be obtained by solving (7.11) for $\varphi_s(\tilde{\omega}) + \bar{\varphi}_s(\tilde{\omega})$, $\omega \in C$, and substituting this solution into (7.6) to generate $\varphi_s(\tilde{\omega}) - \bar{\varphi}_s(\tilde{\omega})$. The required $\varphi_s(\tilde{\omega})$ and $\bar{\varphi}_s(\tilde{\omega})$ are readily obtained from these solutions. The solution of (7.11) is, of course, required to satisfy either (7.7) or (7.9).

An alternative approach to the problem which yields similar equations for $\varphi_3(\tilde{\omega}) + \Phi_3(\tilde{\omega})$ and $\varphi_3(\tilde{\omega}) - \Phi_3(\tilde{\omega})$ is obtained by substituting (7.4) into (7.3) and vice versa. Hence, since

$$i \oint_C \frac{e^{i\alpha(\tilde{\tau})}}{\tau - \omega} ds(\tilde{\tau}) = \oint_C \frac{d\tau}{\tau - \omega} = \pi i ,$$

(7.3) can be written as

$$\varphi_3(\tilde{\omega}) + \Phi_3(\tilde{\omega}) + i\varphi_4(\tilde{\omega})$$

$$= \frac{e^{i\alpha(\tilde{\omega})}}{\pi^2} \oint_C \frac{e^{i\alpha(\tilde{\tau})}}{\tau - \omega} \left\{ \oint_C \frac{\varphi_3(\tilde{t}) + \Phi_3(\tilde{t}) + i\varphi_4(\tilde{t})}{t - \tau} ds(\tilde{t}) \right\} ds(\tilde{\tau}) \qquad (7.13)$$

while (7.4) becomes

$$\varphi_3(\tilde{\omega}) - \Phi_3(\tilde{\omega}) + i\varphi_4(\tilde{\omega})$$

$$= \frac{e^{i\alpha(\tilde{\omega})}}{\pi^2} \oint_C \frac{e^{i\alpha(\tilde{\tau})}}{\tau - \omega} \left\{ \oint_C \frac{\varphi_3(\tilde{t}) - \Phi_3(\tilde{t}) + i\varphi_4(\tilde{t})}{t - \tau} ds(t) \right\} ds(\tilde{\tau}) \qquad (7.14)$$

It will be observed that the identities (7.13) and (7.14) correspond to an application of the Poincaré-Bertrand transformation formula [29, pp 56-61] to the functions $\tau(\omega) + T(\omega)$ and $\tau(\omega) - T(\omega)$ respectively.

§ 7.3) Coupled Interior/Exterior Problems For Cascade Aerofoils

When interior Neumann problems have been considered in preceding chapters, their solutions have been considered through an integral equation corresponding to the real part of (7.1). Clearly, if the solution of coupled interior/exterior problems for cascade aerofoils is to be achieved in a similar manner to that given above for isolated aerofoils, it must first be established whether the interior problem can be solved by the use of a representation analagous to

$$\Phi_1(\tilde{\omega}) = 2\sigma i e^{i\alpha(\tilde{\omega})} - \frac{e^{i\alpha(\tilde{\omega})}}{t}\oint_C \Phi_1(\tilde{\zeta}) \coth\left\{\frac{\pi}{t}(\zeta-\omega)\right\} d\zeta \qquad (7.15)$$

This representation having been used in Chapter 4 for the analysis of the flow through a vertical cascade of aerofoils with pitch t and central profile C. The required integral representation for $\Phi_1(\tilde{\omega})$ is readily obtained on recalling the expansion

$$\frac{\pi}{t}\coth\left\{\frac{\pi}{t}(\zeta-\omega)\right\} = \frac{1}{\zeta-\omega} + \sum_{p=1}^{\infty}\frac{2(\zeta-\omega)}{(\zeta-\omega)^2+p^2t^2} \qquad (7.16)$$

For $p>0$ and $\omega, \zeta \in C$ the zeros of $(\zeta-\omega)^2 + p^2t^2$ all lie outside the region bounded by C so that the function

$$F(\zeta,\omega,t) = \sum_{p=1}^{\infty}\frac{2\tau(\zeta).(\zeta-\omega)}{(\zeta-\omega)^2+p^2t^2}$$

is regular inside and on C. Hence for $\omega \in C$

$$\frac{e^{i\alpha(\tilde{\omega})}}{\pi}\oint_C F(\zeta,\omega,t)\,d\zeta = 0 \qquad (7.17)$$

and the addition of (7.17) to (7.1) yields

$$\phi_s(\tilde{\omega}) + i\phi_n(\tilde{\omega})$$

$$= \frac{e^{i\alpha(\tilde{\omega})}}{\pi} \oint_C \left\{ \phi_s(\tilde{s}) + i\phi_n(\tilde{s}) \right\} \left\{ \frac{1}{s-\omega} + \sum_{p=1}^{\infty} \frac{2(s-\omega)}{(s-\omega)^2 + p^2 t^2} \right\} ds.$$

The substitution of (7.16) into this last result leads to

$$\phi_s(\tilde{\omega}) + i\phi_n(\tilde{\omega})$$

$$= \frac{e^{i\alpha(\tilde{\omega})}}{t} \oint_C \left\{ \phi_s(\tilde{s}) + i\phi_n(\tilde{s}) \right\} \cdot \coth\left\{ \frac{\pi}{t}(s-\omega) \right\} ds \qquad (7.18),$$

the required integral representation.

As with the real part of (7.1), the real part of (7.18) is a Fredholm integral equation of the second kind which exhibits a unique solution.

The solution of the coupled interior/exterior problem for a cascade aerofoil can now be obtained in a similar manner to that used for an isolated aerofoil. From (7.15) and (7.18) the system of complex equations

$$\phi_s(\tilde{\omega}) + \bar{\phi}_s(\tilde{\omega}) + i\phi_n(\tilde{\omega}) = 2\sigma i e^{i\alpha(\tilde{\omega})}$$

$$+ \frac{e^{i\alpha(\tilde{\omega})}}{t} \oint_C \left\{ \phi_s(\tilde{s}) - \bar{\phi}_s(\tilde{s}) + i\phi_n(\tilde{s}) \right\} \coth\left\{ \frac{\pi}{t}(s-\omega) \right\} ds \qquad (7.19)$$

$$\phi_s(\tilde{\omega}) - \bar{\phi}_s(\tilde{\omega}) + i\phi_n(\tilde{\omega}) = -2\sigma i e^{i\alpha(\tilde{\omega})}$$

$$+ \frac{e^{i\alpha(\tilde{\omega})}}{t} \oint_C \left\{ \phi_s(\tilde{s}) + \bar{\phi}_s(\tilde{s}) + i\phi_n(\tilde{s}) \right\} \coth\left\{ \frac{\pi}{t}(s-\omega) \right\} ds \qquad (7.20)$$

is obtained. Again, a pair of simultaneous Fredholm integral equations of the second kind for $\phi_s(\tilde{\omega}) + \bar{\phi}_s(\tilde{\omega})$ and $\phi_s(\tilde{\omega}) - \bar{\phi}_s(\tilde{\omega})$ are given by the real parts of (7.19) and (7.20). These equations may be written as

$$\phi_s(\tilde{\omega}) + \bar{\phi}_s(\tilde{\omega}) - \oint_C \left\{ \phi_s(\tilde{s}) - \bar{\phi}_s(\tilde{s}) \right\} K_2(\tilde{\omega}, \tilde{s})\, ds$$

$$= -2\,\mathrm{Im}\left\{ \sigma e^{i\alpha(\tilde{\omega})} \right\} + \oint_C \phi_n(\tilde{s})\, H_2(\tilde{\omega}, \tilde{s})\, ds$$

. . . . . (7.21),

$$\varphi_1(\tilde{\omega}) - \bar{\varphi}_1(\tilde{\omega}) - \oint_C \left\{ \varphi_1(\tilde{\zeta}) + \bar{\varphi}_1(\tilde{\zeta}) \right\} K_2(\tilde{\omega},\tilde{\zeta})\, ds$$

$$= 2\, Im\left\{ \sigma e^{i\alpha(\tilde{\omega})} \right\} + \oint_C \varphi_2(\tilde{\zeta})\, H_2(\tilde{\omega},\tilde{\zeta})\, ds \qquad (7.22)$$

where, if $\omega = x_0 + i y_0$ and $\zeta = x + iy$,

$$K_2(\tilde{\omega},\tilde{\zeta}) = \frac{2}{t} \frac{\cos[\alpha(\tilde{\omega})].\sinh\left[\frac{2\pi}{t}(x-x_0)\right] + \sin[\alpha(\tilde{\omega})].\sin\left[\frac{2\pi}{t}(y-y_0)\right]}{\cosh\left[\frac{2\pi}{t}(x-x_0)\right] - \cos\left[\frac{2\pi}{t}(y-y_0)\right]}$$

and

$$H_2(\tilde{\omega},\tilde{\zeta}) = \frac{2}{t} \frac{\sin[\alpha(\tilde{\omega})].\sinh\left[\frac{2\pi}{t}(x-x_0)\right] - \cos[\alpha(\tilde{\omega})].\sin\left[\frac{2\pi}{t}(y-y_0)\right]}{\cosh\left[\frac{2\pi}{t}(x-x_0)\right] - \cos\left[\frac{2\pi}{t}(y-y_0)\right]}$$

By anology with the exterior problem for a cascade of aerofoils discussed in Chapter 4 and the coupled interior/ exterior problem for isolated aerofoils, the homogeneous form of the system (7.21), (7.23) will have a non-trivial solution which is unique to within an arbitrary ***additive*** constant. A unique solution to the inhomogeneous problem is again obtained by requiring that the solution satisfies either

$$\oint_C \left\{ \varphi_1(\tilde{\zeta}) + \bar{\varphi}_1(\tilde{\zeta}) \right\} ds = \Gamma \qquad (7.7)$$

$$\oint_C \left\{ \varphi_1(\zeta) - \bar{\varphi}_1(\zeta) \right\} ds = -\Gamma \qquad (7.8)$$

for a smooth profile or

$$\varphi_1(\tilde{\zeta}_0) + \bar{\varphi}_1(\tilde{\zeta}_0) = -y_0 \sin[\alpha(\tilde{\zeta}_0)] - x_0 \cos[\alpha(\tilde{\zeta}_0)] \qquad (7.9)$$

$$\varphi_1(\tilde{\zeta}_0) - \bar{\varphi}_1(\tilde{\zeta}_0) = -y_0 \sin[\alpha(\tilde{\zeta}_0)] - x_0 \cos[\alpha(\tilde{\zeta}_0)] \qquad (7.10)$$

at a point $\zeta_0 = x_0 + i y_0$.

A single equation for $\varphi_s(\tilde{\gamma}) + \Phi_s(\tilde{\gamma})$ is obtained by substituting (7.22) for $\varphi_s(\tilde{\gamma}) - \Phi_s(\tilde{\gamma})$ in (7.21). Hence

$$\varphi_s(\tilde{\omega}) + \Phi_s(\tilde{\omega}) - \oint_C K_2(\tilde{\omega},\tilde{\gamma}) \left\{ \oint_C \left\{ \varphi_s(\tilde{t}) + \Phi_s(\tilde{t}) \right\} K_2(\tilde{\gamma},\tilde{t})\, ds(\tilde{t}) \right\} ds(\tilde{\gamma})$$

$$= -2\,\mathrm{Im}\left\{ \sigma e^{i\alpha(\tilde{\omega})} \right\} + \oint_C \varphi_n(\tilde{\gamma})\, H_2(\tilde{\omega},\tilde{\gamma})\, ds(\tilde{\gamma})$$

$$+ \oint_C K_2(\tilde{\omega},\tilde{\gamma}) \left\{ 2\,\mathrm{Im}\left\{ \sigma e^{i\alpha(\tilde{\gamma})} \right\} + \oint_C \varphi_n(\tilde{t})\, H_2(\tilde{\gamma},\tilde{t})\, ds(\tilde{t}) \right\} ds(\tilde{\gamma}) \quad \ldots . \quad (7.23)$$

and the solution of this last equation can be substituted into (7.20) to generate $\varphi_s(\tilde{\omega}) - \Phi_s(\tilde{\omega})$ on **C**. Again, a unique solution to (7.23) is obtained by adjoining either (7.7) or (7.9) to (7.23).

§ 7.4) Numerical Solution of Coupled Interior/Exterior Problems

Because of the complexity of the integral equations obtained above for coupled interior/exterior problems, the solution of these integral equations by analytical procedures is, in general, out of the question. Numerical solutions based on the approximation techniques of Chapters 3 and 4 are, however, readily obtained. As in the discussion on the numerical solution of the exterior problem for a cascade, only piecewise quadratic approximations to the boundary values of

$$\tau(\tilde{\gamma}) + T(\tilde{\gamma})$$

and

$$\tau(\tilde{\gamma}) - T(\tilde{\gamma})$$

will be considered in detail.

Let the contour **C** be divided into **n** elements each of which is considered to be specified by nodes at the start, "mid" and end points of the interval*. Further, if the

* Node specification as in interior problem.

trailing edge is pointed let the idealisation be carried out in such a way that the point lies at a node. As in the preceding chapters, the nodes are numbered such that for the qth element the element's start, "mid" and end points are given by $\beta_q^{(1)}$, $\beta_q^{(2)}$ and $\beta_q^{(3)}$ respectively.*

For $\beta \in I_q$, the qth element, the functions $\tau(\beta)$ and $T(\beta)$ may be approximated by

$$\tau(\beta) = \sum_{r=1}^{3} M_q^{(r)}(\beta)\, \tau(\beta_q^{(r)})$$

and

$$T(\beta) = \sum_{r=1}^{3} M_q^{(r)}(\beta)\, T(\beta_q^{(r)})$$

where

$$M_q^{(r)}(\beta) = \frac{(\beta_q^{(r)} - \beta_q^{(r)})(\beta - \beta_q^{(1)})(\beta - \beta_q^{(2)})(\beta - \beta_q^{(3)})}{(\beta - \beta_q^{(r)})(\beta_q^{(r)} - \beta_q^{(1)})(\beta_q^{(r)} - \beta_q^{(2)})(\beta_q^{(r)} - \beta_q^{(3)})}.$$

On ignoring any error terms, these approximations lead to the expressions

$$\tau(\omega) + T(\omega) = 2\sigma + \frac{1}{\pi i} \sum_{q=1}^{n} \sum_{r=1}^{3} \{\tau(\beta_q^{(r)}) - T(\beta_q^{(r)})\} \int_{I_q} M_q^{(r)}(\beta) \frac{d\beta}{\beta - \omega}$$

$$\tau(\omega) - T(\omega) = -2\sigma + \frac{1}{\pi i} \sum_{q=1}^{n} \sum_{r=1}^{3} \{\tau(\beta_q^{(r)}) + T(\beta_q^{(r)})\} \int_{I_q} M_q^{(r)}(\beta) \frac{d\beta}{\beta - \omega}$$

when ω lies on a smooth portion of the boundary of an isolated aerofoil and

* For convenience let a pointed trailing edge occur at $\beta_1^{(1)} = \beta_n^{(3)}$

$$\tau(\omega) + T(\omega)$$

$$= 2\sigma + \frac{1}{\pi i} \sum_{q=1}^{n} \sum_{r=1}^{3} \left\{ \tau(\gamma_q^{(r)}) - T(\gamma_q^{(r)}) \right\} \int_{I_q} M_q^{(r)}(\gamma) . \coth \left\{ \frac{\pi}{t} (\gamma - \omega) \right\} d\gamma$$

$$\tau(\omega) - T(\omega)$$

$$= -2\sigma + \frac{1}{\pi i} \sum_{q=1}^{n} \sum_{r=1}^{3} \left\{ \tau(\gamma_q^{(r)}) - T(\gamma_q^{(r)}) \right\} \int_{I_q} M_q^{(r)}(\gamma) . \coth \left\{ \frac{\pi}{t} (\gamma - \omega) \right\} d\gamma$$

when ω lies on a smooth portion of the boundary of a cascade aerofoil. In these expressions

$$\int_{I_q} \{ - \} \, d\gamma$$

denotes an integration taken in the positive sense for interior problems, i.e. anti-clockwise.

Use of the relations

$$\tau(\omega) \, i \, e^{i\alpha(\tilde{\omega})} = \varphi_s(\tilde{\omega}) + i \, \varphi_n(\tilde{\omega})$$

$$T(\omega) \, i \, e^{i\alpha(\tilde{\omega})} = \bar{\varphi}_s(\tilde{\omega})$$

leads to the equations

$$\varphi_s(\tilde{\omega}) + i \varphi_n(\tilde{\omega}) + \bar{\varphi}_s(\tilde{\omega}) = 2ie^{i\alpha(\tilde{\omega})} \sigma$$

$$+ \sum_{q=1}^{n} \sum_{r=1}^{3} \left\{ \varphi_s(\gamma_q^{(r)}) + i \varphi_n(\gamma_q^{(r)}) - \bar{\varphi}_s(\gamma_q^{(r)}) \right\} \Delta_q^{(r)}(\tilde{\omega}) \qquad (7.24)$$

$$\varphi_s(\tilde{\omega}) + i \varphi_n(\tilde{\omega}) - \bar{\varphi}_s(\tilde{\omega}) = -2ie^{i\alpha(\tilde{\omega})} \sigma$$

$$+ \sum_{q=1}^{n} \sum_{r=1}^{3} \left\{ \varphi_s(\gamma_q^{(r)}) + i \varphi_n(\gamma_q^{(r)}) + \bar{\varphi}_s(\gamma_q^{(r)}) \right\} \Delta_q^{(r)}(\tilde{\omega}) \qquad (7.25)$$

where

$$\Delta_q^{(r)}(\tilde{\omega}) = \frac{1}{\pi i}\exp\left\{\left[\alpha(\tilde{\omega}) - \alpha(\tilde{\delta}_q^{(r)})\right] i\right\} \int_{I_q} M_q^{(r)}(\delta)\, \frac{d\delta}{\delta - \omega}$$

for an isolated aerofoil and

$$\Delta_q^{(r)}(\tilde{\omega}) = \frac{1}{ti}\exp\left\{\left[\alpha(\tilde{\omega}) - \alpha(\tilde{\delta}_q^{(r)})\right] i\right\} \int_{I_q} M_q^{(r)}(\delta).\coth\left\{\frac{\pi}{t}(\delta-\omega)\right\} d\delta$$

for a cascade.

For the aerofoils of the type considered here the continuity conditions

$$\varphi_s(\tilde{\delta}_q^{(3)}) + \Phi_s(\tilde{\delta}_q^{(3)}) = \varphi_s(\tilde{\delta}_{q+1}^{(1)}) + \Phi_s(\tilde{\delta}_{q+1}^{(1)}) \qquad (7.26)$$

$$\varphi_s(\tilde{\delta}_q^{(1)}) - \Phi_s(\tilde{\delta}_q^{(3)}) = \varphi_s(\tilde{\delta}_{q+1}^{(1)}) - \Phi_s(\tilde{\delta}_{q+1}^{(1)}) \qquad (7.27)$$

apply when $q = 1, 2, \ldots n-1$. On aerofoils without pointed trailing edges $\varphi_s(\tilde{\delta}), \Phi_s(\tilde{\delta})$ also satisfy

$$\varphi_s(\tilde{\delta}_1^{(r)}) + \Phi_s(\tilde{\delta}_1^{(1)}) = \varphi_s(\tilde{\delta}_n^{(3)}) + \Phi_s(\tilde{\delta}_n^{(3)}) \qquad (7.28)$$

$$\varphi_s(\tilde{\delta}_1^{(1)}) - \Phi_s(\tilde{\delta}_1^{(1)}) = \varphi_s(\tilde{\delta}_n^{(3)}) - \Phi_s(\tilde{\delta}_n^{(3)}) \qquad (7.29)$$

Hence, for smooth aerofoils, a system of $4n$ equations for the unknown values of the sum and difference of $\varphi_s(\tilde{\delta})$ and $\Phi_s(\tilde{\delta})$ at each of the $2n$ nodes is obtained by:-

i) identifying ω with each of the nodes

ii) applying the continuity conditions (7.26) to (7.29).

iii) taking only the real parts of (7.24) and (7.25).

The resulting system of equations may be written in block notation as

$$\begin{bmatrix} I & A \\ A & I \end{bmatrix} \begin{bmatrix} \underset{\sim}{x}_1 \\ \underset{\sim}{x}_2 \end{bmatrix} = \begin{bmatrix} \underset{\sim}{b}_1 \\ \underset{\sim}{b}_2 \end{bmatrix} \tag{7.30}$$

where the elements of the vectors $\underset{\sim}{x}_1$, $\underset{\sim}{x}_2$ correspond to the problem unknowns, viz.

$$\underset{\sim}{x}_1 = \begin{bmatrix} \varphi_3(\tilde{\beta}_1^{(0)}) + \varphi_3(\tilde{\beta}_1^{(0)}) \\ \varphi_3(\tilde{\beta}_1^{(1)}) + \varphi_3(\tilde{\beta}_1^{(1)}) \\ \vdots \\ \varphi_3(\tilde{\beta}_n^{(1)}) + \varphi_3(\tilde{\beta}_n^{(1)}) \\ \varphi_3(\tilde{\beta}_n^{(2)}) + \varphi_3(\tilde{\beta}_n^{(2)}) \end{bmatrix} \text{ and } \underset{\sim}{x}_2 = \begin{bmatrix} \varphi_3(\tilde{\beta}_1^{(1)}) - \varphi_3(\tilde{\beta}_1^{(1)}) \\ \varphi_3(\tilde{\beta}_1^{(2)}) - \varphi_3(\tilde{\beta}_1^{(2)}) \\ \vdots \\ \varphi_3(\tilde{\beta}_n^{(1)}) - \varphi_3(\tilde{\beta}_n^{(1)}) \\ \varphi_3(\tilde{\beta}_n^{(2)}) - \varphi_3(\tilde{\beta}_n^{(2)}) \end{bmatrix};$$

$\underset{\sim}{b}_1$, $\underset{\sim}{b}_2$ are the appropriate free terms obtained from i) to iii) above. I and A, which correspond to $2n \times 2n$ identity and coefficient matrices respectively, are also obtained from the above steps i) to iii).

Analagous to the previously given reductions of (7.5), (7.6) to (7.11) and (7.21), (7.22) to (7.23); the system of equations (7.30) may be reduced to

$$(I - A^2)\, \underset{\sim}{x}_1 = \underset{\sim}{b}_1 - A\, \underset{\sim}{b}_2 \tag{7.31}$$

since

$$\underset{\sim}{x}_2 = \underset{\sim}{b}_2 - A\, \underset{\sim}{x}_1 \tag{7.32}$$

It will be observed that the numerical solution of the interior problem for a solid section reduces to the solution of a system of equations with coefficient matrix $I + A$ while the corresponding system of equations for the exterior problem has coefficient matrix $I - A$.

As discussed in Chapter 3, the system of equations corresponding to the exterior problem is either singular or ill conditioned. Writing (7.31) as

$$(I - A)(I + A)\,\underset{\sim}{x}_1 = \underset{\sim}{b}_1 - A\,\underset{\sim}{b}_2$$

it follows that the system (7.31) is also singular or ill conditioned. However, it follows from (7.7) that the solution must also satisfy the auxiliary condition.

$$\Gamma = \sum_{q=1}^{n} \sum_{r=1}^{3} \left\{ \phi_s(\tilde{\delta}_q^{(r)}) + i\phi_n(\tilde{\delta}_q^{(r)}) + \Phi_s(\tilde{\delta}_q^{(r)}) \right\} \delta_q^{(r)} \qquad (7.33)$$

where

$$\delta_q^{(r)} = -i \exp\left\{-i\alpha(\tilde{\delta}_q^{(r)})\right\} \int_{I_q} M_q^{(r)}(\delta)\, d\delta$$

Taking the real part of (7.33) an extra equation which can be adjoined to the system (7.31) is obtained. This yields the overdetermined system.

$$H\,\underset{\sim}{x}_1 = \underset{\sim}{g} \qquad (7.34)$$

Hence, once the elements of the various matrices have been evaluated, the solution of the coupled interior/exterior problem for a smooth aerofoil can be obtained by solving (7.34) for $\underset{\sim}{x}_1$ and generating $\underset{\sim}{x}_2$ from (7.32). Once $\underset{\sim}{x}_1, \underset{\sim}{x}_2$ have been determined the evaluation of the nodal values of $\phi_s(\tilde{\delta})$ and $\Phi_s(\tilde{\delta})$ is a trivial matter.

The evaluation of the elements of H and $\underset{\sim}{g}$ is straightforward and requires the evaluation of the $\Delta_q^{(r)}(\omega)$ and $\delta_q^{(r)}$. The evaluation of these coefficients has been considered in detail in Chapter 3, for isolated aerofoils, and Chapter 4, for cascade aerofoils. The matrix A required by (7.31) and hence (7.34) has been obtained from the coefficient matrix obtained for interior problems by writing this matrix as $I + A$, A^2 has been obtained by matrix multiplication.

In the application of this technique to practical problems where the boundary of an aerofoil is specified by a large number of nodes the system of equations (7.3) is considered to be singular rather than ill-conditioned. This has been found necessary because the amount of (computer) core storage required by the matrices $\mathbf{A}$ and $(\mathbf{I}-\mathbf{A}^2)$ effectively precludes the possibility of solving the overdetermined system (7.34) by numerical techniques such as least squares.

In view of these core storage problems the system (7.31) has been assumed to be singular with the rank of $\mathbf{I}-\mathbf{A}^2$ equal to $2n-1$. This is consistent with the approach used in Chapter 3 for overcoming the same core storage problem. As in that chapter it has also been assumed that the linear dependence of the equations making up (7.31) is such that only one of these equations is redundant. This is consistent with the fact that the homogeneous form of the coupled interior/exterior problem exhibits a non-trivial solution which is unique to an arbitrary *additive* constant. The uniqueness condition is therefore incorporated into equations (7.31) by adding the real part of (7.33) to each of the equations making up (7.31). The resulting system of linear equations is solved by Gaussian elimination.

When the aerofoil has a pointed trailing edge the continuity conditions (7.28), (7.29) no longer apply. The solution at the trailing edge is, however, given by (7.9) and (7.10) whence

$$\phi_s(\tilde{\gamma}_1^{(1)}) + \mathcal{F}_s(\tilde{\gamma}_1^{(0)}) = \phi_s(\tilde{\gamma}_1^{(0)}) - \mathcal{F}_s(\tilde{\gamma}_1^{(0)}) = -\mathrm{Re}\left\{\gamma_1^{(1)} e^{-i\alpha(\tilde{\gamma}_1^{(1)})}\right\} \quad (7.35)$$

$$\phi_s(\tilde{\gamma}_n^{(3)}) + \mathcal{F}_s(\tilde{\gamma}_n^{(3)}) = \phi_s(\tilde{\gamma}_n^{(3)}) - \mathcal{F}_s(\tilde{\gamma}_n^{(3)}) = -\mathrm{Re}\left\{\gamma_n^{(3)} e^{-i\alpha(\tilde{\gamma}_n^{(3)})}\right\} \quad (7.36)$$

In this case a system of $4n-2$ equations for the remaining unknown nodal values of the sum and difference of $\phi_s(\tilde{\gamma})$ and $\mathcal{F}_s(\tilde{\gamma})$ is obtained from (7.24), (7.25) by

iv) identifying ω with each of the nodes where the boundary is smooth.

v) applying the continuity conditions (7.26), (7.27)

vi) taking only the real parts of (7.24) and (7.25)

vii) noting the trailing edge solutions (7.35), (7.36).

The resulting system of equations may again be written in block notation, this time as

$$\begin{bmatrix} I & B \\ B & I \end{bmatrix} \begin{bmatrix} \underset{\sim}{y}_1 \\ \underset{\sim}{y}_2 \end{bmatrix} = \begin{bmatrix} \underset{\sim}{c}_1 \\ \underset{\sim}{c}_2 \end{bmatrix} \qquad (7.38)$$

where the unknowns are given by

$$\underset{\sim}{y}_1 = \begin{bmatrix} \varphi_s(\tilde{\gamma}_1^{(2)}) + \bar{\varphi}_s(\tilde{\gamma}_1^{(2)}) \\ \varphi_s(\tilde{\gamma}_2^{(1)}) + \bar{\varphi}_s(\tilde{\gamma}_2^{(1)}) \\ \varphi_s(\tilde{\gamma}_2^{(2)}) + \bar{\varphi}_s(\tilde{\gamma}_2^{(2)}) \\ \vdots \\ \varphi_s(\tilde{\gamma}_n^{(1)}) + \bar{\varphi}_s(\tilde{\gamma}_n^{(1)}) \\ \varphi_s(\tilde{\gamma}_n^{(2)}) + \bar{\varphi}_s(\tilde{\gamma}_n^{(2)}) \end{bmatrix} \quad \text{and} \quad \underset{\sim}{y}_2 = \begin{bmatrix} \varphi_s(\tilde{\gamma}_1^{(2)}) - \bar{\varphi}_s(\tilde{\gamma}_1^{(2)}) \\ \varphi_s(\tilde{\gamma}_2^{(1)}) - \bar{\varphi}_s(\tilde{\gamma}_2^{(1)}) \\ \varphi_s(\tilde{\gamma}_2^{(2)}) - \bar{\varphi}_s(\tilde{\gamma}_2^{(2)}) \\ \vdots \\ \varphi_s(\tilde{\gamma}_n^{(1)}) - \bar{\varphi}_s(\tilde{\gamma}_n^{(1)}) \\ \varphi_s(\tilde{\gamma}_n^{(2)}) - \bar{\varphi}_s(\tilde{\gamma}_n^{(2)}) \end{bmatrix} ;$$

$\underset{\sim}{c}_1$, $\underset{\sim}{c}_2$ are the appropriate free terms obtained from iv) - vii) above. $\mathbf{I}$ and $\mathbf{B}$ are also obtained from steps iv)-vii) and correspond to (2n-1) x (2n-1) identity and coefficient matrices respectively.*

Analagous to the reduction of (7.30) to (7.31), (7.38) may be reduced to

$$(I - B^2)\,\underset{\sim}{y}_1 = \underset{\sim}{c}_1 - B\,\underset{\sim}{c}_2 \qquad (7.39)$$

* Again, using the results of Chapters 3 & 4 the evaluation of the elements of the various matrices is straightforward.

since

$$\underset{\sim}{y}_2 = \underset{\sim}{c}_2 - B\,\underset{\sim}{y}_1 \qquad (7.40)\,.$$

That the non-uniqueness of the solution to the coupled interior/exterior problem has been eliminated by the use of (7.35), (7.36) leads to the conclusion that the system of equations (7.39) will be non-singular. A solution to (7.39) can therefore be obtained by Gaussian elimination.

Once $\underset{\sim}{y}_1$ and $\underset{\sim}{y}_2$ have been obtained from (7.39) and (7.40) respectively, the evaluation of the nodal values of $\phi_s(\tilde{r})$ and $\frac{\partial \phi_s}{\partial n}(\tilde{r})$ is again a trivial matter.

§ 7.5) Example Of A Coupled Problem For An Isolated Aerofoil

Consider the problem of finding the boundary tangential derivatives of both the warping function and velocity potential of a region which disturbs a uniform stream. In order that comparisons with a known solution can be made, let the region under consideration be bounded by the ellipse

$$x^2 + 4y^2 = 1$$

and take the flow for upstream to have unit velocity and be directed in the positive x-direction, i.e. take $\sigma = 1$. Further, let there be no circulation about the region.

The warping function for an elliptic region has already been used in the examples of Chapter 6 (see § 6.6.1)). The velocity potential for the flow described above can be found by conformal mapping and is given by Milne-Thomson [20, p.167] . These solutions have been used to provide the values of the required tangential derivatives $\varphi_s(\tilde{\tau})$ and $\Phi_s^I(\tilde{\tau})$ given in Table 7-1. The co-ordinates $x = Re(\tau)$ and $y = Im(\tau)$ of the tabulation points were obtained by writing

$$x = \cos\theta$$
$$y = \tfrac{1}{2}\sin\theta$$

and taking twenty nodes at equal increments of the eccentric angle θ.

An implementation of the isolated aerofoil version of the numerical method given in § 7.4) has been applied to the problem under consideration. The nodes required by the method were positioned at the tabulation points used in Table 7-1 and are shown in Figure 7-1. The results obtained using this idealisation are given in Table 7-2 where DPDN, SUM and DIF denote $\varphi_n(\tilde{\tau})$, $\varphi_s(\tilde{\tau}) + \Phi_s(\tilde{\tau})$ and $\varphi_s(\tilde{\tau}) - \Phi_s(\tilde{\tau})$ respectively.

Comparing the two solutions of the interior problem which are given in Tables 7-1 and 7-2 one observes that the only differences between the two solutions occur in the last two places of decimals. As in § 6.5.1), this

level of agreement should be expected since the warping function for the region under consideration is the real part of a function which is quadratic in $\tilde{z}$.

Further examination of Tables 7-1 & 7-2 reveals a much lower level of agreement between the solutions given for the exterior problem. However, considerable improvement in the numerical results for the exterior problem has been obtained by taking twice as many nodes in the idealisation. Figure 7-2 shows the idealisation obtained by using forty nodes at equal increments of eccentric angle θ to generate the x-y co-ordinates of the nodes. The full set of results corresponding to this new idealisation is given in Table 7-3.

A comparison between the known solution for the exterior problem and the corresponding numerical solutions is given in Table 7-4. In this table attention is restricted to that part of the boundary lying in the first quadrant (i.e. $x, y > 0$). The table shows that, excluding the error at the stagnation point, the 40 node idealisation reduces the maximum relative error from more than 14½% to less than 1½%. Note that both idealisations produce a relative error of less than 0.1% at the point where maximum flow speed occurs (i.e. at $x = 0$, $y = 0.5$).

§ 7.6) Example Of A Coupled Problem For A Cascade Aerofoil

Use of the cascade version of the numerical method described in § 7.4) can be demonstrated by considering the interior problem of § 7.5) and taking the exterior problem as one in which both the upstream flow speed and the circulation are set to zero. The solution of this exterior problem is just $\phi_s(\tilde{\tau}) = 0$ while the solution of the interior problem is the boundary tangential derivative of the warping function appropriate to the region bounded by the ellipse

$$x^2 + 4y^2 = 1 \quad .$$

A tabulation of this derivative at a number of points on the ellipse has already been given in Table 7-1.

Numerical solutions making use of the twenty node idealisation shown in Figure 7-1 were obtained for the four values of pitch 3.0, 2.5, 2.0 and 1.5. Full sets of results for these four values of pitch are given in Tables 7-5 to 7-8 respectively. Comparison of these tables with Table 7-1 shows quite clearly that the nodal approximations to $\varphi_s(\tilde{r})$ get considerably worse as the pitch decreases. The tables also show that the accuracy of the nodal approximations to the solution $\bar{\Phi}_s(\tilde{r}) = 0$ also decreases with decreasing pitch.

A further feature of the results is the manner in which the symmetry in the known solution to the interior problem is (to some extent) lost in the approximate solutions. Indeed, examination of Table 7-2 shows that this is also the case for the isolated aerofoil problem considered in § 7.5). It is thought that these features are due to the assumption that the coefficient matrix $I-A^2$ in equation (7.33) is singular rather than ill-conditioned.

Experience (e.g. comparison between Tables 7-2 & 7-3 and Tables 7-8 & 7-9) has shown that the "drift" from symmetric answers is reduced as the idealisation improves. This implies that the assumption of singular $I-A^2$ becomes more reasonable as the problem becomes more detailed. Also, the effect of pitch on the accuracy of solutions diminishes as the problem specification improves. This is clearly demonstrated by the results given in Table 7-9 which were obtained using the forty node idealisation of Figure 7-2 and a pitch of 1.5 - the pitch which gave the worst set of results when the twenty node idealisation was used.

It would appear that the idealisation of a specified contour is inadequate whenever changes in pitch have an effect on the numerical solution of an interior problem defined on the region lying within the contour.

Chapter 8

THE USE OF THE COMPLEX FORMS OF GREEN'S THEOREM IN PLANE ELASTOSTATICS

§ 8.1) Introduction

This chapter describes the work of the author on the solution of plane problems in elastostatics by boundary integral techniques obtainable from the complex forms of Green's theorem. These techniques are applicable to either prescribed boundary traction or prescribed boundary displacement problems but do not appear to be suited to mixed problems in which both types of boundary condition occur.

In an engineering environment frequently occurring plane problems, such as the stressing of turbomachinery blade roots, usually do have mixed boundary conditions. The inability to model this type of problem by the integral equations obtained below has meant that their numerical solution has only been of limited interest. Because of this, only the results obtained from the numerical solution of a simple, atypical problem are given.

It should be noted that one of the integral equations derived below has been given by Muskhelishvili who obtained it in a different way [16, pp. 408-418].

The limited application of the techniques described in this chapter does not imply that boundary integral techniques which are more generally applicable do not exist. On the contrary, a boundary integral technique which has proved successful in turbomachinery applications [e.g. 2, 3, 5] is the technique based on the two dimensional form of Somigliana's identities [15, p.105]. However, this technique falls outside the scope of this thesis since the governing integral equations are not readily cast into a complex variables form.

§ 8.2) Complex Potentials In Plane Elastostatics

It is well known in the mathematical theory of elasticity [e.g. 16, 34] that the stresses and displacements of a homogeneous, isotropic elastic body, in a state of either plane stress or plane strain, can be written in terms of two unrelated complex potentials $\varphi(z)$ and $\psi(z)$. In the standard notation for stresses and displacements which is used by Timoshenko [49, pp.3-12],

the appropriate relations at a point $z = x+iy$ are

$$-2\mu(u+iv) = -\hat{\kappa}\varphi(z) + z\overline{\varphi_z}(\bar{z}) + \overline{\psi}(\bar{z}) \qquad (8.1)$$

$$\sigma_x + \sigma_y = 2\{\varphi_z(z) + \overline{\varphi_z}(\bar{z})\} \qquad (8.2)$$

$$\sigma_y - \sigma_x + 2i\tau_{xy} = 2\{\bar{z}\varphi_{zz}(z) + \psi_z(z)\} \qquad (8.3)$$

where

$$\hat{\kappa} = \begin{cases} 3-4\nu & \text{for plane strain problems} \\ \dfrac{3-\nu}{1+\nu} & \text{for plane stress problems,} \end{cases}$$

ν = Poisson's ratio

and the suffix z denotes differentiation with respect to the complex variable z .

For displacement type boundary conditions equations (8.1) specify sufficient boundary conditions for the determination of $\varphi(z)$ and $\psi(z)$. In the case of traction boundary conditions, viz.

$$T_x = \sigma_x \cos\alpha + \tau_{xy} \sin\alpha$$

$$T_y = \tau_{xy} \cos\alpha + \sigma_y \sin\alpha$$

where the orientation of the axes and α are as shown in Figure 8-1, two relations can be obtained either of which is sufficient for the determination of $\varphi(z)$ and $\psi(z)$.

For each of the contours bounding the elastic body **R**, the required boundary relations at a boundary point are given by Sokolnikoff [34, pp.269-273] as

i) $$T_n - iT_s = \varphi_z(z) + \overline{\varphi_z}(\bar{z}) - e^{2i\alpha}\{\bar{z}\varphi_{zz}(z) + \psi_z(z)\} \qquad (8.4)$$

where T_n and T_s are the tractions in the normal and tangential directions illustrated in Figure 8-1

ii) $$\therefore \int_{z_0}^{z} \{T_x(s) + iT_y(s)\}\,ds + \text{constant}$$

$$= 2\mathcal{K}_{\bar{z}}(\tilde{\bar{z}})$$

$$= \varphi(z) + z\overline{\varphi_z}(\bar{z}) + \overline{\psi}(\bar{z}) \qquad (8.5)$$

where $\chi(\tilde{\tau})$ is the Airy stress function for the problem [4, pp.204-207] and τ_0 is an arbitrary point on the contour under consideration.

The constant appearing in (8.5) above is, in general, complex and must be determined in such a way that the displacements and stresses are both single valued and continuous in R. It may be observed from (8.5) that, in the case when R is simply connected, statical equilibrium allows the constant to be assigned an arbitrary value (usually zero).

When a problem is specified by mixed boundary conditions, the boundary conditions on $\varphi(\tau)$ and $\psi(\tau)$ may be obtained from some combination of (8.1) and (8.4). It should be noted that (8.5) cannot be used for this type of problem because of the integration it requires. This mixed problem will not be considered further, details of its solution by a complex variables super-position technique can be found elsewhere [50].

§ 8.3) The Multi-Valued Nature Of The Complex Potentials

Muskhelishvili has shown [16, pp.120-129] that if R is a finite multiply connected region bounded externally by the contour C_0 and by n interior contours C_k $(k=1,\dots,n)$ and if the stresses and displacements are single valued in R, then $\varphi(\tau)$ and $\psi(\tau)$ can be written as

$$\varphi(\tau) = -\frac{1}{2\pi(1+\hat{k})}\sum_{k=1}^{n}\left\{F_x^{(k)} + iF_y^{(k)}\right\}\log(\tau-\tau_k) + \varphi^*(\tau) \qquad (8.6)$$

$$\psi(\tau) = \frac{\hat{k}}{2\pi(1+\hat{k})}\sum_{k=1}^{n}\left\{F_x^{(k)} - iF_y^{(k)}\right\}\log(\tau-\tau_k) + \psi^*(\tau) \qquad (8.7)$$

Here $(F_x^{(k)}, F_y^{(k)})$ is the resultant vector of external forces applied to the contour C_k, τ_k is an arbitrary point in the region bounded externally by C_k, and the functions $\varphi^*(\tau)$, $\psi^*(\tau)$ are (single valued) regular functions in R.

Muskhelishvili also shows that if R is an infinite region bounded by the contours C_k $(k=1,2,\dots n)$, and if the stress components are bounded in the neighbourhood

of the point at infinity then (8.6), (8.7) can be written as

$$\varphi(\zeta) = -\frac{F_x + iF_y}{2\pi(1+\hat{K})}\log\zeta + (B+Ci)\zeta + \varphi^*(\zeta) \quad (8.8)$$

$$\psi(\zeta) = \frac{\hat{K}F_x - iF_y}{2\pi(1+\hat{K})}\log\zeta + (B'+iC')\zeta + \psi^*(\zeta) \quad (8.9)$$

provided the origin of co-ordinates lies within one of the regions bounded externally by the C_k In (8.8) and (8.9)

$$F_x = \sum_{k=1}^{n} F_x^{(k)}$$

$$F_y = \sum_{k=1}^{n} F_y^{(k)}$$

while the constants B, B', C' are related to the state of stress at infinity by

$$2B - B' = \lim_{|\zeta|\to\infty} \sigma_x$$

$$2B + B' = \lim_{|\zeta|\to\infty} \sigma_y$$

$$C' = \lim_{|\zeta|\to\infty} \tau_{xy}$$

The constant **C** has no effect on the state of stress and is related to the rotation

$$\omega = \lim_{|\zeta|\to\infty} \left\{\frac{\partial v}{\partial x} - \frac{\partial u}{\partial y}\right\}$$

by

$$C = \frac{2\mu}{1+\hat{K}}\,\omega$$

and can be set to zero in the analysis of stress alone (i.e. when displacements are not of interest).

Note that if the displacements are to be bounded at infinity then

i) $F_x = F_y = 0$

ii) $\lim_{|\zeta|\to\infty} \sigma_x = \lim_{|\zeta|\to\infty} \sigma_y = \lim_{|\zeta|\to\infty} \tau_{xy} = 0$

iii) $C = 0$.

Further,

$$\varphi_1^*(\zeta) = \frac{d}{d\zeta}\varphi^*(\zeta)$$

is single valued.

§ 8.4) Integral Equations For $\varphi_z(z)$ and $\varphi(z)$

Consider first the typical region **R** which is shown in Figure 8-1. This region is simply connected and is bounded by the simple closed curve ∂R which comprises of

i) the bounding contour **C**

ii) a small circle σ, with centre **w** and radius ϵ, which excludes the point **w** from **R**.

iii) cross cuts AB and DE which connect σ to **C**.

Let $f(\tilde{z})$ denote the function obtained from

$$f(\tilde{z}) = K\,\varphi(z) + z\,\overline{\varphi}_z(\bar{z}) + \overline{\psi}(\bar{z}) \qquad (8.10)$$

where $K=1$ for problems with traction boundary conditions (8.5) and $K=-\hat{\kappa}$ for problems with displacement boundary conditions (8.1).

With $f(\tilde{z})$ given by (8.10), the function defined by

$$G(\tilde{z}, w) = \frac{f(z)}{\bar{z}-\bar{w}}$$

is continuous and differentiable in $R \cup \partial R$

An application of the complex forms of Green's theorem to the function $G(\tilde{z}, w)$ gives

$$\int_{\partial R} f(\tilde{z})\frac{d\bar{z}}{\bar{z}-\bar{w}} = -2i\iint_R f_z(\tilde{z})\frac{dx\,dy}{\bar{z}-\bar{w}}$$

or, from (8.10),

$$\int_{\partial R} f(\tilde{z})\frac{d\bar{z}}{\bar{z}-\bar{w}} = -2i\iint_R \left\{K\,\varphi_z(z) + \overline{\varphi}_z(\bar{z})\right\}\frac{dx\,dy}{\bar{z}-\bar{w}} \qquad (8.11)$$

Provided that the cross-cuts AB and DE give the branch cuts which are required if the function $\log(\bar{z}-\bar{w})$ is to be single valued in **R**, the complex forms of Green's theorems can be applied to the right hand side of (8.11). Thus (8.11) may be written as

$$\int_{\partial R} f(\tilde{\zeta})\frac{d\bar{\zeta}}{\bar{\zeta}-\bar{w}} = \int_{\partial R} \overline{\varphi}_z(\bar{\zeta})\frac{\zeta-z}{\bar{\zeta}-\bar{w}}\,d\bar{\zeta} - K\int_{\partial R}\varphi_z(\zeta)\log(\bar{\zeta}-\bar{w})\,d\zeta$$

or, if the function $\log(\zeta - w)$ is made single valued in **R** by taking the branch cuts required by $\log_j(\zeta - w)$,

$$\int_{\partial R} f(\tilde{\zeta}) \frac{d\bar{\zeta}}{\bar{\zeta} - \bar{w}} = \int_{\partial R} \bar{\varphi}_\zeta(\bar{\zeta}) \frac{\zeta}{\bar{\zeta} - \bar{w}} d\bar{\zeta}$$

$$- 2K \int_{\partial R} \varphi_\zeta(\zeta) \log|\zeta - w| d\zeta + K \int_{\partial R} \varphi_\zeta(\zeta) \log(\zeta - w) d\zeta \qquad (8.12)$$

When the gap between the cross-cuts is closed and the radius of σ shrinks to zero, i.e. $\varepsilon \to 0$, it is readily shown that

$$2\pi i f(\tilde{w}) + \int_C f(\tilde{\zeta}) \frac{d\bar{\zeta}}{\bar{\zeta} - \bar{w}}$$

$$= 2\pi i w \bar{\varphi}_\zeta(\bar{w}) + \int_C \bar{\varphi}_\zeta(\bar{\zeta}) \frac{\zeta}{\bar{\zeta} - \bar{w}} d\bar{\zeta} + 2\pi i K \varphi(w)$$

$$+ K \int_C \varphi_\zeta(\zeta) \log(\zeta - w) d\zeta - 2K \int_C \varphi_\zeta(\zeta) \log|\zeta - w| d\zeta$$

$$+ \text{constant} \qquad (8.13)$$

Because the analysis required in obtaining this last expression is analogous to that given in Chapters 2 and 5 its details have been omitted. Further, an interpretation of the constant is given in Chapter 5.

Similarly, when **w** tends to a point on the boundary **C** from inside **R**, it may be shown that, for Hölder continuous $f(\tilde{\zeta})$ and $\varphi_\zeta(\zeta)$,

$$f(\tilde{w}) + \frac{1}{\pi i} \int_C f(\tilde{\zeta}) \frac{d\bar{\zeta}}{\bar{\zeta} - \bar{w}} + \text{constant}$$

$$= w \bar{\varphi}_\zeta(\bar{w}) + \frac{1}{\pi i} \int_C \bar{\varphi}_\zeta(\bar{\zeta}) \frac{\zeta}{\bar{\zeta} - \bar{w}} d\bar{\zeta} + 2K \varphi(w)$$

$$+ \frac{K}{\pi i} \int_C \varphi_\zeta(\zeta) \log(\zeta - w) d\zeta - \frac{2K}{\pi i} \int_C \varphi_\zeta(\zeta) \log|\zeta - w| d\zeta \qquad (8.14)$$

where the integrals are interpreted in their Cauchy Principal Value sense.

On recalling that for $w \in C$

$$\varphi_\beta(w) = \frac{1}{\pi i} \int_C \varphi_\beta(\tau) \frac{d\tau}{\tau - w}$$

and

$$\varphi(w) + \text{constant} = -\frac{1}{2\pi i} \int_C \varphi_\beta(\tau) \log(\tau - w)\, d\tau,$$

equation (8.14) may be written as

$$f(\tilde{w}) + \frac{1}{\pi i} \int_C f(\tilde{\tau}) \frac{d\bar{\tau}}{\bar{\tau} - \bar{w}} = \frac{1}{\pi i} \int_C \overline{\varphi_\beta}(\bar{\tau}) \frac{\tau - w}{\bar{\tau} - \bar{w}}\, d\bar{\tau} - \frac{2K}{\pi i} \int_C \varphi_\beta(\tau) \log|\tau - w|\, d\tau \quad \ldots\ldots (8.15)$$

When the appropriate boundary values of $f(\tilde{\tau})$ are substituted into (8.15) a coupled pair of real integral equations of the first kind for the determination of $\varphi_\beta(\tau)$ can be obtained by separating (8.15) into its real and imaginary parts. This coupled pair of integral equations does not appear to have an earlier citation.

Equation (8.15) can also be used in the derivation of a coupled pair of real integral equations for the determination of $\varphi(\tau)$. The required complex equation is obtained by noting that

$$\frac{2}{\pi i} \int_C \varphi_\beta(\tau) \log|\tau - w|\, d\tau = \frac{2}{\pi i} \int_C \log|\tau - w|\, d[\varphi(\tau)]$$

$$= \frac{2}{\pi i} \Big[\varphi(\tau) \log|\tau - w|\Big]_C - \frac{2}{\pi i} \int_C \varphi(\tau)\, d[\log|\tau - w|]$$

and

$$\frac{1}{\pi i}\int_C \overline{\varphi_\zeta(\bar\zeta)}\,\frac{\zeta-w}{\bar\zeta-\bar w}\,d\bar\zeta = \frac{1}{\pi i}\int_C \frac{\zeta-w}{\bar\zeta-\bar w}\,d\left[\bar\varphi(\bar\zeta)\right]$$

$$= \frac{1}{\pi i}\left[\bar\varphi(\bar\zeta)\,\frac{\zeta-w}{\bar\zeta-\bar w}\right]_C - \frac{1}{\pi i}\int_C \bar\varphi(\bar\zeta)\,d\left[\frac{\zeta-w}{\bar\zeta-\bar w}\right]$$

$$= -\frac{1}{\pi i}\int_C \bar\varphi(\bar\zeta)\,d\left[\frac{\zeta-w}{\bar\zeta-\bar w}\right]$$

Hence (8.15) may be written as

$$f(\tilde w) + \frac{1}{\pi i}\int_C f(\zeta)\frac{d\bar\zeta}{\bar\zeta-\bar w} = \frac{2K}{\pi i}\int_C \varphi(\zeta)\,d\left[\log|\zeta-w|\right]$$

$$-\frac{1}{\pi i}\int_C \bar\varphi(\bar\zeta)\,d\left[\frac{\zeta-w}{\bar\zeta-\bar w}\right] \qquad (8.16)$$

The interpretation of this last equation is awkward because of the term involving $d\left[\log|\zeta-w|\right]$. However, (8.16) can be simplified by writing

$$\frac{2}{\pi i}\int_C \varphi(\zeta)\,d\left[\log|\zeta-w|\right] = \frac{1}{\pi i}\int_C \varphi(\zeta)\,d\left[\log\left\{(\bar\zeta-\bar w)(\zeta-w)\right\}\right]$$

$$= \frac{1}{\pi i}\int_C \varphi(\zeta)\,\frac{d\zeta}{\zeta-w} + \frac{1}{\pi i}\int_C \varphi(\zeta)\,\frac{d\bar\zeta}{\bar\zeta-\bar w}$$

whence (8.16) becomes

$$f(\tilde{w}) + \frac{1}{\pi i}\int_C f(\tilde{\zeta})\frac{d\bar{\zeta}}{\bar{\zeta}-\bar{w}}$$

$$= K\varphi(w) + \frac{K}{\pi i}\int_C \varphi(\zeta)\frac{d\bar{\zeta}}{\bar{\zeta}-\bar{w}} - \frac{1}{\pi i}\int_C \varphi(\zeta)\, d\left[\frac{\zeta-w}{\bar{\zeta}-\bar{w}}\right] \qquad (8.17)$$

In contrast with (8.15), (8.17) may be considered as a 2nd kind integral equation.

The complex conjugate of equation (8.17) is given in a slightly different form by Muskhelishvili [16, pp.403-418] who effectively adds

$$K\varphi(w) - \frac{K}{\pi i}\int_C \varphi(\zeta)\frac{d\zeta}{\zeta - w} = 0$$

to the right hand side of (8.17) and obtains the complex conjugate of

$$f(\tilde{w}) + \frac{1}{\pi i}\int_C f(\tilde{\zeta})\frac{d\bar{\zeta}}{\bar{\zeta}-\bar{w}} = 2K\varphi(w) - \frac{K}{\pi i}\int_C \varphi(\zeta)\, d\left[\log\left\{\frac{\zeta-w}{\bar{\zeta}-\bar{w}}\right\}\right]$$

$$- \frac{1}{\pi i}\int_C \bar{\varphi}(\bar{\zeta})\, d\left[\frac{\zeta-w}{\bar{\zeta}-\bar{w}}\right] \qquad (8.18)$$

The coupled pair of real integral equations for the determination of $\varphi(\zeta)$ on **C**, which is obtained by separating (8.18) into its real and imaginary parts, has been studied in detail by several authors [e.g. 17, pp.248-250]. These authors demonstrate that the Fredholm theory can be applied to (8.18) whenever the angle between the normal to **C** and the positive real direction (i.e. the angle $\alpha(\tilde{\zeta})$, $\zeta \in C$) is Hölder continuous.

It may be shown by substitution that the homogeneous form of (8.18), i.e.

$$2K\varphi(w) - \frac{K}{\pi i}\int_C \varphi(\zeta)\, d\left[\log\left\{\frac{\zeta-w}{\bar{\zeta}-\bar{w}}\right\}\right]$$

$$-\frac{1}{\pi i}\int_C \bar{\varphi}(\bar{\zeta})\, d\left[\frac{\zeta-w}{\bar{\zeta}-\bar{w}}\right] = 0$$

has the solution

$$\varphi^{\circ}(\zeta) = \beta + i\gamma + i\delta\zeta \qquad (8.19)$$

where β and γ are arbitrary real constants. The constant δ is also real and arbitrary unless $K \neq 1$ when $\delta = 0$.

That $\varphi^{\circ}(\zeta)$ has the only form that solutions to the homogeneous equation can take follows from the fact that if (8.18) is homogeneous then

$$f(\tilde{w}) + \frac{1}{\pi i}\int_C f(\tilde{\zeta})\frac{d\bar{\zeta}}{\bar{\zeta}-\bar{w}} = 0 \quad , w \in C$$

This identity requires that for all $\zeta \in R$ the condition

$$f_{\zeta}(\tilde{\zeta}) = 0$$

be satisfied. Using (8.10) this condition may be written as

$$K\varphi^{\circ}_{\zeta}(\zeta) + \overline{\varphi^{\circ}_{\zeta}}(\bar{\zeta}) = 0$$

whence (8.19) and the required result follow.

For the case K=1 an integral equation with a unique solution may be obtained by noting that at some point in R, t say, the function $\varphi(\zeta)$ and the imaginary part of $\varphi_{\delta}(\zeta)$ may be assigned arbitrary values without

there being any effect on the stress distribution. The assignment of these arbitrary values will, however, affect the displacements as given by (8.1).

Let

$$\varphi(t) = \mathrm{Im}\left\{\varphi_\gamma(t)\right\} = 0$$

so that

$$\frac{1}{\pi i}\int_C \frac{\varphi(\gamma)}{\gamma - t}\,d\gamma = 0 \tag{8.20}$$

and

$$\frac{1}{\pi i}\int_C \frac{\varphi(\gamma)}{(\gamma - t)^2}\,d\gamma + \frac{1}{\pi i}\int_C \frac{\bar{\varphi}(\bar{\gamma})}{(\bar{\gamma} - \bar{t})^2}\,d\bar{\gamma} = 0 \tag{8.21}$$

These expressions for $\varphi(t)$ and $\mathrm{Im}\left\{\varphi_\gamma(t)\right\}$ may be added to (8.18) whence the integral equation

$$\begin{aligned} f(\tilde{w}) &+ \frac{1}{\pi i}\int_C f(\tilde{\gamma})\frac{d\bar{\gamma}}{\bar{\gamma} - \bar{w}} \\ &= 2\,\varphi(w) - \frac{1}{\pi i}\int_C \varphi(\gamma)\,d\left[\log\left\{\frac{\gamma - w}{\bar{\gamma} - \bar{w}}\right\}\right] \\ &- \frac{1}{\pi i}\int_C \bar{\varphi}(\bar{\gamma})\,d\left[\frac{\gamma - w}{\bar{\gamma} - \bar{w}}\right] + \frac{1}{\pi i}\int_C \frac{\varphi(\gamma)}{(\gamma - t)^2}\,d\gamma \\ &+ \frac{1}{\pi i}\int_C \frac{\bar{\varphi}(\bar{\gamma})}{(\bar{\gamma} - \bar{t})^2}\,d\bar{\gamma} + \frac{1}{\pi i}\int_C \frac{\varphi(\gamma)}{\gamma - t}\,d\gamma \end{aligned} \tag{8.22}$$

is obtained. For suitably smooth **C** this equation may, as in the case of (8.18), be considered as a 2nd kind Fredholm equation for $\varphi(\gamma)$.

That the solution of (8.22) is unique is readily shown by considering the homogeneous form of (8.22). Substitution shows that this equation is also satisfied by (8.19) but in this instance (8.20) and (8.21) show that

$$\varphi_0(\gamma) = 0$$

An application of the Fredholm theory yields the required result.

Clearly, the above comments relating to the solution of (8.18) can be applied to the solution of the equivalent equation (8.17).

In the case of (8.15),

i.e.

$$f(\tilde{w}) + \frac{1}{\pi i}\int_C f(\tilde{\zeta})\frac{d\bar{\zeta}}{\bar{\zeta}-\bar{w}}$$

$$= \frac{1}{\pi i}\int_C \bar{\varphi}_\zeta(\bar{\zeta})\frac{\zeta-w}{\bar{\zeta}-\bar{w}}\,d\bar{\zeta} - \frac{2}{\pi i}\int_C \varphi_\zeta(\zeta)\log|\zeta-w|\,d\zeta \quad ,$$

there is no equivalent to the Fredholm theory. However, one may draw a number of conclusions from the above treatment of (8.18). First, the homogeneous form of (8.15) has a non-trivial solution of the form

$$\varphi^{\bullet}_\zeta(\zeta) = i\delta$$

where δ is an arbitrary real constant. Any solution to (8.15) will therefore be given to within an arbitrary imaginary constant. Secondly, if for some point $t \in R$ we set

$$Im\left\{\varphi_\zeta(t)\right\} = 0$$

then (8.15) may be written as

$$f(\tilde{w}) + \frac{1}{\pi i}\int_C f(\tilde{\zeta})\frac{d\bar{\zeta}}{\bar{\zeta}-\bar{w}}$$

$$= \frac{1}{\pi i}\int_C \bar{\varphi}_\zeta(\bar{\zeta})\frac{\zeta-w}{\bar{\zeta}-\bar{w}}\,d\bar{\zeta} - \frac{2}{\pi i}\int_C \varphi_\zeta(\zeta)\log|w-\zeta|\,d\zeta$$

$$+ \frac{1}{\pi i}\int_C \frac{\varphi_\zeta(\zeta)}{\zeta-t}\,d\zeta + \frac{1}{\pi i}\int_C \frac{\bar{\varphi}_\zeta(\bar{\zeta})}{\bar{\zeta}-\bar{z}}\,d\bar{\zeta} \qquad (8.23)$$

As with the homogeneous form of (8.22), the homogeneous form of (8.23) has only the trivial solution so that any solution of (8.23) will be unique. Thirdly, the previously given

representation for $\varphi(W)$, viz.

$$\varphi(W) + \text{const} = -\frac{1}{2\pi i}\int_C \varphi_\zeta(\zeta)\log(\zeta - W)\,d\zeta \qquad (8.24),$$

generates a solution to (8.22) provided the constant is adjusted to give

$$\varphi(t) = 0 .$$

The above equations for $\varphi(\zeta)$ and $\varphi_\zeta(\zeta)$ were obtained using the assumptions that $\varphi(\zeta)$, $\varphi_\zeta(\zeta)$ and $\psi(\zeta)$ are regular in **R**. For the case **K**=1 these assumptions require the condition

$$\mathrm{Re}\left\{\int_C \bar{f}(\bar{\zeta})\,d\zeta\right\} = 0 \qquad (8.25)$$

to be satisfied. This condition is readily shown on observing that

$$\int_C \bar{f}(\bar{\zeta})\,d\zeta = \int_C \left\{\bar{\varphi}(\bar{\zeta}) + \bar{\zeta}\,\varphi_\zeta(\zeta) + \psi(\zeta)\right\} d\zeta$$

whence

$$\int_C \bar{f}(\bar{\zeta})\,d\zeta = \int_C \left\{\bar{\varphi}(\bar{\zeta}) + \bar{\zeta}\,\varphi_\zeta(\zeta)\right\} d\zeta$$

since $\psi(\zeta)$ is regular in **R**. The right hand side of this last expression may be integrated by parts to give

$$\int_C \bar{f}(\bar{\zeta})\,d\zeta = \int_C \bar{\varphi}(\bar{\zeta})\,d\zeta + \left[\bar{\zeta}\,\varphi(\zeta)\right]_C - \int_C \varphi(\zeta)\,d\bar{\zeta}$$

and, since $\bar{\zeta}\,\varphi(\zeta)$ is single valued on **C**,

$$\int_C \bar{f}(\bar{\zeta})\,d\zeta = \int_C \left\{\bar{\varphi}(\bar{\zeta})\,d\zeta - \varphi(\zeta)\,d\bar{\zeta}\right\} .$$

The right hand side of the above expression is purely imaginary whence (8.25) is obtained.

It can be shown [16, pp.147-148] that (8.25) is obtainable from the condition that the total resultant couple acting upon **C** vanishes, a condition for statical equilibrium.

The analysis for the case $K=-\hat{\kappa}$ follows in an entirely analogous manner and will not be repeated. It suffices to note that any solution of (8.15) will be unique and that (8.18) can be modified to

$$f(\tilde{w}) + \frac{1}{\pi i}\int_C f(\tilde{w})\frac{d\bar{\tau}}{\bar{\tau}-\bar{w}}$$

$$= 2K\varphi(w) - \frac{K}{\pi i}\int_C \varphi(\tau)\, d\left[\log\left\{\frac{\tau-w}{\bar{\tau}-\bar{w}}\right\}\right]$$

$$-\frac{1}{\pi i}\int_C \bar{\varphi}(\bar{\tau})\, d\left[\frac{\tau-w}{\bar{\tau}-\bar{w}}\right] + \frac{1}{\pi i}\int_C \varphi(\tau)\frac{d\tau}{\tau-t} \qquad (8.26)$$

where **t** is some point in **R** at which the value

$$\varphi(t) = 0$$

is assigned. As in the case of (8.22), the solution of (8.26) will be unique.

So far only simply connected regions have been considered. Integral equations similar to (8.15), (8.17) and (8.18) can also be obtained when the region is multiply connected.

Consider a problem where traction type boundary conditions are applied to a multiply connected region **R** which is bounded on the outside by C_0 and has the **m** internal boundaries C_l ; $l=1, \ldots, m$. For this problem the boundary conditions on the contour C_l ($=0,\ldots,m$) may be written as

$$f(\tilde{\tau}) = i\int_{\tau_l^{(0)}}^{\tau}\left\{T_x(s) + i\,T_y(s)\right\} + \gamma_l$$

where γ_l is a constant particular to the contour C_l and $\tau_l^{(0)}$ is an arbitrary point to lie on C_l . Using (8.5)

these boundary conditions may be written as

$$f(\tilde{\tau}) = \varphi(\tau) + \tau\,\overline{\varphi_1}(\overline{\tau}) + \overline{\psi}(\overline{\tau})$$

or, on using the multivalued nature of $\varphi(\tau)$ and $\psi(\tau)$ given in § 8,3),

$$f^*(\tilde{\tau}) = \varphi^*(\tau) + \tau\,\overline{\varphi_1^*}(\overline{\tau}) + \overline{\psi}^*(\overline{\tau}) \qquad (8.27)$$

where

$$f^*(\tilde{\tau}) = f(\tilde{\tau}) + \frac{1}{2\pi(1+\hat{k})}\sum_{j=1}^{m}\left\{F_x^{(j)} + iF_y^{(j)}\right\}\left\{\log(\tau-\tau_j) - \hat{k}\log(\overline{\tau}-\overline{\tau}_j)\right\}$$

$$+ \frac{1}{2\pi(1+\hat{k})}\sum_{j=1}^{m}\frac{F_x^{(j)} - iF_y^{(j)}}{\overline{\tau} - \overline{\tau}_j} \qquad (8.28)$$

The functions $\varphi^*(t)$, $\varphi_1^*(t)$, $\psi^*(t)$ are regular for t in R and defined by (8.6), (8.7).

For an appropriate choice of branch for the function $\log(\tau-\tau_j)$ the function $f^*(\tilde{\tau})$ is single valued on each of the contours C_l. This result is readily obtained by observing that during a circuit in the positive direction of each of the contour C_j $(j=1,\ldots,m)$ the function $f(\tilde{\tau})$ takes on an increment of $i(F_x^{(j)} + iF_y^{(j)})$ while the term.

$$\frac{1}{2\pi(1+\hat{k})}\sum_{j=1}^{m}\left\{F_x^{(j)} + iF_y^{(j)}\right\}\left\{\log(\tau-\tau_j) - \hat{k}\log(\overline{\tau}-\overline{\tau}_j)\right\}$$

decrements by the same amount. That $f^*(\tilde{\tau})$ is single valued on C_0 is obtained from observing that the resultant vector of all external forces acting on $C = \sum_{l=1}^{m} C_l$ is zero if statical equilibrium is to be satisfied.

For the above traction problem the resultant vectors of the external forces applied to each of the internal boundaries are known from the boundary conditions. The function $f^*(\tilde{\tau})$ is therefore given apart from the constants γ_j $(j=1,\ldots,m)$ which must be determined

during the solution of the problem.

The derivations performed in the case of a simply connected region can be repeated for the multiply connected region now being considered provided the regular functions $\varphi^*(z)$, $\varphi_s^*(z)$, $\psi^*(z)$ together with $f^*(\tilde{z})$ are used instead of $\varphi(z)$, $\varphi_s(z)$, $\psi(z)$ and $f(\tilde{z})$. These derivations lead to the integral equations

$$f^*(\tilde{w}) + \frac{1}{\pi i}\sum_{l=0}^{m}\int_{C_l} f^*(\tilde{z})\frac{dz}{z-w} = \frac{1}{\pi i}\sum_{l=0}^{m}\int_{C_l}\bar{\varphi}_s^*(z)\frac{z-w}{z-w}\,dz - \frac{2}{\pi i}\int_{C_l}\varphi_s^*(z)\log|z-w|\,dz \qquad (8.29)$$

for $\varphi_s^*(z)$ and

$$f^*(\tilde{w}) + \frac{1}{\pi i}\sum_{l=0}^{m}\int_{C_l} f^*(\tilde{z})\frac{dz}{z-w} = \varphi^*(w) + \frac{1}{\pi i}\sum_{l=0}^{m}\int_{C_l}\varphi^*(z)\frac{dz}{z-w} - \frac{1}{\pi i}\sum_{l=0}^{m}\int_{C_l}\bar{\varphi}^*(z)\,dz\left[\frac{z-w}{z-w}\right] \qquad (8.30)$$

for $\varphi^*(z)$. For a traction problem equations (8.29) and (8.30) are clearly the multiply connected region counterparts of (8.15) and (8.17), these equations having $K=1$ substituted.

The comments relating to uniqueness of solution and necessary modifications to the equations which were made in respect of (8.15) and (8.17) - with $K=1$ - can be carried over to equations (8.29) and (8.30). These comments will not be repeated here.

Although (8.29) is a first kind equation it would appear to be more useful for multiply connected regions than (8.30). This usefulness is illustrated by the fact that whereas there would appear to be no straightforward manner in which the constants γ_j can be determined when (8.30) is applied, the requirement that $\varphi^*(z)$ be single valued on

each of the contours C_j enables the conditions

$$\int_{C_j} \varphi_\tau^*(\tau)\, d\tau = 0 \quad ; \; j = 1, \ldots, m \tag{8.31}$$

to be specified as auxilliary conditions which the solution must satisfy. With these auxilliary conditions specified the constants γ_j together with the function $\varphi_\tau^*(\tau)$ may be obtained by considering the system (8.30), (8.31), viz.

$$\begin{cases} f^*(\tilde{w}) + \dfrac{1}{\pi i} \displaystyle\sum_{l=0}^{m} \int_{C_l} f^*(\tilde{\tau}) \dfrac{d\bar{\tau}}{\bar{\tau} - \bar{w}} \\ = \dfrac{1}{\pi i} \displaystyle\sum_{l=0}^{m} \int_{C_l} \bar{\varphi}^*(\bar{\tau}) \dfrac{\tau - w}{\bar{\tau} - \bar{w}} d\bar{\tau} - \dfrac{2}{\pi i} \displaystyle\sum_{l=0}^{m} \int_{C_l} \varphi^*(\tau) \log|\tau - w|\, d\tau \\ \\ \displaystyle\int_{C_j} \varphi_\tau^*(\tau)\, d\tau = 0 \quad ; \; j = 1, \ldots, m \, . \end{cases}$$

Note that the constant γ_0 can (and has) been set to zero.

As in the case of the corresponding equation for a simply connected region, any solution $\varphi_\tau^*(\tau)$ of this system may be expected to be unique to within an arbitrary, additive, imaginary constant.

When the multiply connected region R has displacement boundary conditions specified the problem can again be solved by suitably modifying the boundary conditions

$$f(\tilde{\tau}) = -(u + iv)\, 2\mu \, .$$

Using (8.1) these boundary conditions may be written as

$$f(\tilde{\tau}) = -\hat{\kappa}\, \varphi(\tau) + \tau\, \overline{\varphi_\tau}(\bar{\tau}) + \overline{\psi}(\bar{\tau})$$

or, on utilising the representations given in § 8.3),

$$f^*(\tilde{\zeta}) = -\hat{\kappa}\,\varphi^*(\zeta) + \zeta\,\overline{\varphi_\zeta^*}(\bar{\zeta}) + \overline{\psi^*}(\bar{\zeta}) \qquad (8.32)$$

where

$$f^*(\tilde{\zeta}) = -2\mu(u+iv) + \frac{\zeta}{2\pi(1+\hat{\kappa})}\sum_{j=1}^{m}\frac{F_x^{(j)} - iF_y^{(j)}}{\bar{\zeta}-\bar{\zeta}_j}$$

$$-\frac{\hat{\kappa}}{\pi(1+\hat{\kappa})}\sum_{j=1}^{m}\left\{F_x^{(j)} + iF_y^{(j)}\right\}\log|\zeta-\zeta_j| \qquad (8.33)$$

and $\varphi^*(\zeta)$, $\varphi_\zeta^*(\zeta)$, $\psi^*(\zeta)$ are the boundary values of those functions, regular in **R**, which are defined by (8.6), (8.7).

As in the case of a traction problem, where the complex constants γ_j had to be determined, the displacement problem formulated in terms of (8.32), (8.33) requires the determination of the real constants $F_x^{(j)}$, $F_y^{(j)}$. For a displacement problem defined on the multiply connected region **R** the equations analogous to (8.5) and (8.17) are readily shown to be

$$f^*(\tilde{w}) + \frac{1}{\pi i}\sum_{l=0}^{m}\int_{C_l} f^*(\tilde{\zeta})\frac{d\bar{\zeta}}{\bar{\zeta}-\bar{w}}$$

$$= \frac{1}{\pi i}\sum_{l=0}^{m}\int_{C_l}\overline{\varphi_\zeta^*}(\bar{\zeta})\,\frac{\zeta-w}{\bar{\zeta}-\bar{w}}\,d\bar{\zeta} + \frac{2\hat{\kappa}}{\pi i}\sum_{l=0}^{m}\int_{C_l}\varphi_\zeta^*(\zeta)\log|\zeta-w|\,d\zeta \qquad (8.34)$$

and

$$f^*(\tilde{w}) + \frac{1}{\pi i}\sum_{l=0}^{m}\int_{C_l} f^*(\tilde{\zeta})\,\frac{d\bar{\zeta}}{\bar{\zeta}-\bar{w}}$$

$$= -\hat{\kappa}\,\varphi(w) - \frac{\hat{\kappa}}{\pi i}\sum_{l=0}^{m}\int_{C_l}\varphi^*(\zeta)\frac{d\bar{\zeta}}{\bar{\zeta}-\bar{w}} - \frac{1}{\pi i}\sum_{l=0}^{m}\int_{C_l}\varphi^*(\zeta)\,d\left[\frac{\bar{w}-\bar{\zeta}}{w-\zeta}\right]$$

. . . . . (8.35)

respectively. Again, when (8.34) rather than (8.35) is used, the determination of the constants $F_x^{(j)}$, $F_y^{(j)}$ presents no great problem since the condition (8.31) can once more be utilised. Any solution of the system (8.34), (8.31) may be expected to be unique.

Problems defined on infinite regions can be treated in an entirely analogous manner by considering the complex potentials $\varphi^*(\zeta)$, $\psi^*(\zeta)$ defined by (8.8), (8.9). For such problems the required equations may be obtained by taking C_0 to be a circle of radius R_0 and letting R_0 tend to infinity. Note that condition (8.31) holds on all internal boundaries.

§ 8.5) Solution of Problems Via Integral Equations For $\varphi_\zeta(\zeta)$

The solution of both traction and displacement problems in two dimensional elastostatics by the first kind integral equations given in the preceding section is straightforward. For this reason only an outline of the necessary procedures will be given here. As mentioned in § 3.1), these procedures do not appear to be applicable to problems with mixed boundary conditions of the type commonly occurring in turbomachinery applications.

Let the boundary conditions for a problem be given by either (8.28) or (8.32). Boundary conditions in these forms can be used to define problems on simply connected regions by omitting the terms involving $F_x^{(j)}$ and $F_y^{(j)}$.

With these boundary conditions defined, the boundary values of the function $\varphi_\zeta^*(\zeta)$ can be obtained by solving the equation

$$f^*(\tilde{w}) + \frac{1}{\pi i}\int_C f^*(\tilde{\zeta})\frac{d\bar{\zeta}}{\bar{\zeta}-\bar{w}} = \frac{1}{\pi i}\int_C \varphi_\zeta^*(\zeta)\frac{\zeta-w}{\bar{\zeta}-\bar{w}}\,d\bar{\zeta} - \frac{2K}{\pi i}\int_C \varphi_\zeta^*(\zeta)\log|\zeta-w|\,d\zeta \quad \ldots\ldots \quad (8.36)$$

where

$$K = \begin{cases} 1 & \text{for a traction problem} \\ -\hat{\kappa} & \text{for a displacement problem} \end{cases}$$

and $\int_C \text{---}$ denotes $\sum_{l=0}^{m} \int_{C_l} \text{---}$ when the region under consideration is multiply connected. In the case of a traction problem equation (8.36) should be modified in such a way that

$$I_m \left\{ \varphi_\tau(t) \right\} = 0$$

at some interior point t. The manner in which this modification may be carried out is given in § 8,4) for a simply connected region, the modification required for a multiply connected region may be obtained in a similar fashion on noting from (8.6) that

$$\varphi_\tau(t) = -\frac{1}{2\pi(1+\hat{k})} \sum_{j=1}^{m} \left\{ F_x^{(j)} + i F_y^{(j)} \right\} \frac{1}{t-\tau_j} + \varphi_\tau^*(t)$$

Further, for a multiply connected region the m conditions

$$\int_{C_j} \varphi_\tau^*(\tau)\, d\tau = 0 \quad ; \quad j = 1, \ldots, m \tag{8.37}$$

must be adjoined to equation (8.36) so that the unknown constants (τ_j or $F_x^{(j)}$ and $F_y^{(j)}$) may also be determined.

Once a solution to the system of integral equations has been obtained by some means (a numerical solution is given in § 8,6) the boundary values of the regular function $\varphi^*(\tau)$ may be obtained from the representation

$$\varphi^*(W) + \text{const} = -\frac{1}{2\pi i} \int_C \varphi_\tau^*(\tau) \log(\tau - W)\, d\tau \tag{8.38}$$

or, if more convenient, by the integration

$$\varphi^*(W) = \varphi^*(\tau_0) + \int_{\tau_0}^{W} \varphi_\tau^*(\tau)\, d\tau \tag{8.39}$$

The boundary values of the function $\psi^*(\zeta)$ may now be evaluated using

$$\psi^*(\zeta) = \overline{f}^*(\overline{\tilde{\zeta}}) - K\overline{\varphi}^*(\overline{\zeta}) - \overline{\zeta}\,\varphi_\zeta^*(\zeta)$$

where $f^*(\tilde{\zeta})$ is given by (8.28) for a traction problem or by (8.33) for a displacement problem.

At a point t in a multiply connected region R the values of the displacements and stresses are readily found from (8.1) to (8.3) since - by Cauchy's integrals and (8.6), (8.7) -

$$\varphi(t) = -\frac{1}{2\pi(1+\hat{K})}\sum_{j=1}^{m}\left\{F_x^{(j)} + iF_y^{(j)}\right\}\log(t-\zeta_j) + \frac{1}{2\pi i}\int_C \frac{\varphi^*(\zeta)\,d\zeta}{\zeta - t} \qquad (8.40)$$

$$\psi(t) = \frac{\hat{K}}{2\pi(1+\hat{K})}\sum_{j=1}^{m}\left\{F_x^{(j)} - iF_y^{(j)}\right\}\log(t-\zeta_j) + \frac{1}{2\pi i}\int_C \frac{\varphi^*(\zeta)\,d\zeta}{\zeta - t} \qquad (8.41),$$

$$\varphi_\zeta(t) = -\frac{1}{2\pi(1+\hat{K})}\sum_{j=1}^{m}\frac{F_x^{(j)} + iF_y^{(j)}}{t-\zeta_j} + \frac{1}{2\pi i}\int_C \frac{\varphi_\zeta^*(\zeta)\,d\zeta}{\zeta - t} \qquad (8.42),$$

$$\varphi_{\zeta\zeta}(t) = \frac{1}{2\pi i}\int_C \frac{\varphi_\zeta(\zeta)\,d\zeta}{(\zeta - t)^2} \qquad (8.43).$$

The last expression holds since $\varphi_\zeta(\zeta)$ is regular in R, an alternative form for generating $\varphi_{\zeta\zeta}(t)$ is

$$\varphi_{\zeta\zeta}(t) = \frac{1}{2\pi(1+\hat{K})}\sum_{j=1}^{m}\frac{F_x^{(j)} + iF_y^{(j)}}{(t-\zeta_j)^2} + \frac{1}{2\pi i}\int_C \frac{\varphi_\zeta^*(\zeta)\,d\zeta}{(\zeta - t)^2}$$

In the case when the region is simply connected the determination of the displacements and stresses is somewhat simplified since the terms involving $F_x^{(j)}$, $F_y^{(j)}$ in (8.40) to (8.43) do not occur. The regular functions required by (8.1) to (8.3) can therefore be evaluated at t by the use of Cauchy's integrals.

§ 8.6) Numerical Solution of Integral Equation For $\varphi_z(\zeta)$

Because practical applications of the above techniques appear to be somewhat limited, only the simple "piecewise constant" type of solution has been attempted.

As in previous chapters each of the m + 1 contours bounding the region under consideration is divided into N_p ($p=0,\ldots,m$) smooth intervals. The specification of smooth intervals requires that nodes (interval end points) be positioned at any corners. With this boundary idealisation equation (8.36) may be written as

$$f^*(\tilde{\omega}) + \frac{1}{\pi i}\sum_{p=0}^{m}\sum_{q=1}^{N_p}\int_{I_{p,q}} f^*(\tilde{\zeta})\frac{d\bar{\zeta}}{\bar{\zeta}-\bar{\omega}}$$

$$= \frac{1}{\pi i}\sum_{p=0}^{m}\sum_{q=1}^{N_p}\int_{I_{p,q}} \overline{\varphi^*_\zeta}(\bar{\zeta})\frac{\zeta-\omega}{\bar{\zeta}-\bar{\omega}}\,d\bar{\zeta}$$

$$-\frac{2K}{\pi i}\sum_{p=0}^{m}\sum_{q=1}^{N_p}\int_{I_{p,q}} \varphi^*_\zeta(\zeta)\log|\zeta-\omega|\,d\zeta$$

where $\int_{I_{p,q}}$ denotes an integration over $I_{p,q}$, the q^{th} interval of the contour C_p.

The approximation of the boundary condition $f^*(\tilde{\zeta})$ and the unknown function $\varphi^*_\zeta(\zeta)$ by functions which are piecewise constant over each of the intervals $I_{p,q}$ enables the above equation to be approximated by

$$F_{r,s} + \frac{1}{\pi i}\sum_{p=0}^{m}\sum_{q=1}^{N_p} F_{p,q}\int_{I_{p,q}}\frac{d\bar{\zeta}}{\bar{\zeta}-\bar{\omega}}$$

$$= \frac{1}{\pi i}\sum_{p=0}^{m}\sum_{q=1}^{N_p}\overline{\Phi}_{p,q}\int_{I_{p,q}}\frac{\zeta-\omega}{\bar{\zeta}-\bar{\omega}}\,d\bar{\zeta}$$

$$-\frac{2K}{\pi i}\sum_{p=0}^{m}\sum_{q=1}^{N_p}\Phi_{p,q}\int_{I_{p,q}}\log|\omega-\zeta|\,d\zeta \qquad (8.44)$$

where

$$\left.\begin{aligned} F_{p,q} &\simeq f^*(\tilde{\tau}) \\ \Phi_{p,q} &\simeq \varphi_\tau^*(\tau) \end{aligned}\right\} \quad \tau \in I_{p,q}$$

$$F_{r,s} \simeq f^*(\tilde{\omega}) \qquad \omega \in I_{r,s}$$

A numerical solution to the problem can therefore be obtained by choosing a point, $\tau_{p,q}$ say, in each of the intervals $I_{p,q}$ at which $f^*(\tilde{\tau})$ and $\varphi_\tau^*(\tau)$ are to take their constant values $F_{p,q}$ and $\Phi_{p,q}$ respectively. With the $\tau_{p,q}$ chosen a system of linear equations for the unknowns $\Phi_{p,q}$ is obtained by identifying ω with each of the $\tau_{p,q}$.

Of course, the above system of equations is in terms of the complex unknowns $\Phi_{p,q}$ and $\overline{\Phi}_{p,q}$. A coupled system of real equations for the real and imaginary parts of the $\Phi_{p,q}$ is readily obtained by equating the real and imaginary parts of (8.44).

The ancillary conditions (8.37), which are required for the determination of any unknown constants appearing in the previously given expression for $f^*(\omega)$, can be treated in a similar manner. In fact, use of the piecewise constant approximation to $\varphi_\tau^*(\tau)$ enables (8.37) to be written as the m equations

$$\sum_{q=1}^{N_p} \Phi_{p,q} \int_{I_{p,q}} d\tau = 0 \; ; \quad p = 1, \ldots, m \tag{8.45}$$

The system of equations resulting from adjoining (8.45) to (8.44) can be solved by Gaussian Elimination, the uniqueness of solution depending on whether or not a traction problem is under consideration. For the case when the solution is not unique, the equations can be modified to yield a previously specified solution at some interior point. The required modifications are entirely analogous to those given in §8,4).

The above use of piecewise constant approximations effectively reduces the problem to one of quadrature. However, the integrations required by (8.44) (8.45) can all be performed in closed form if each of the intervals $I_{r,7}$ is considered to comprise of two straight line segments joining the nodes at either end of $I_{r,7}$ to the point $z_{r,7}$

§ 8.7) Example

As an example of the technique outlined above a pressurised elliptic cavity which lies in an infinite region will be considered. For convenience it will be assumed that the prescribed pressure P is uniform over the surface of the cavity. A closed form solution to this problem, which is based on the principles of conformal mapping, has been given by Muskhelishvili [16, p.345] .

Following Muskhelishvili, let

$$x + iy = \gamma(Z) = \frac{a+b}{2} Z + \frac{a-b}{2} \frac{1}{Z}$$

be the mapping of the region exterior to the unit circle $|Z| = 1$ onto the region exterior to the ellipse

$$\left(\frac{x}{a}\right)^2 + \left(\frac{y}{b}\right)^2 = 1$$

Denoting $\frac{a+b}{2}$ and $\frac{a-b}{a+b}$ by R and m respectively, the mapping $\gamma(Z)$ can be written as

$$\gamma(Z) = R\left\{Z + \frac{m}{Z}\right\}$$

and the Goursat function $\varphi(Z)$ obtained in the form

$$\varphi(Z) = -\frac{PRm}{Z}$$

That $\varphi(Z)$ is a Goursat function appropriate to the problem defined in the circle plane should be noted.

The required solution of the problem under consideration is, in the physical plane,

$$\varphi_z(z) = \frac{\varphi_\zeta(\zeta)}{\gamma_\zeta(\zeta)}$$

whence

$$\varphi_z(z) = \frac{P R m}{\zeta^2} \cdot \frac{1}{R\left(1 - \frac{m}{\zeta^2}\right)}$$

$$= \frac{P m}{\zeta^2 - m} \qquad (8.46)$$

where

$$\zeta = \frac{z + \sqrt{z^2 - 4R^2 m}}{2R}$$

$$= \frac{z + \sqrt{z^2 - (a^2 - b^2)}}{a + b} .$$

To obtain a numerical solution of this problem for the case when $a = 2$, $b = 1$ and $P = 1$ the co-ordinates of the elliptic boundary were written as

$$x = 2 \cos\theta$$

$$y = \sin\theta$$

with $\theta \in [0, 2\pi]$. The elliptic boundary was then divided into N intervals, the co-ordinates of the interval end points being obtained by letting the start of the first interval lie at $\theta = 2\pi$ and then taking N equal decrements of the eccentric angle θ . Here the decrements $\Delta\theta$ were given by $\Delta\theta = \frac{2\pi}{N}$.

Referring to (8.44), the collocation points $\tau_{p,q}$ were taken to lie at the points corresponding to

$$\theta = 2\pi - (j + \tfrac{1}{2})\Delta\theta \quad ; \quad j = 0, \ldots, N-1$$

The problem under consideration was solved for three values of N, viz. N = 20, 40 & 60. The nodes used in the idealisation for the case N = 60 are shown in Figure 8-2.

Noting from (8.2) that the hydrostatic stress (invariant) $\sigma_H = \sigma_x + \sigma_y$ is given by

$$\sigma_H = 4\,\mathrm{Re}\left\{\phi_0(\tau)\right\}$$

the values of $\mathrm{Re}\left\{\phi_0(\tau)\right\}$ obtained from (8.46) are compared with their numerical counterparts in Figure 8-3. Here the abscissae are given in terms of the eccentric angle θ for $0 \le \theta \le \pi/2$. Use of problem symmetries preclude the need to present results for $\pi/2 < \theta < 2\pi$.

Despite the crudity of the approximations used in this example, Figure 8-3 illustrates the level of agreement between numerical and true values of σ_H which can be obtained from using (8.44) and (8.45). Examination of the Figure shows that for N = 60 the percentage error in the approximation to σ_H at the stress concentration is less than 1%. Clearly, this high level of agreement is partly due to the simple geometry and loading considered.

Chapter 9

CONCLUSION

§ 9.1) Introduction

The main conclusions which can be drawn from the material presented in the first eight chapters of this thesis are summarised in § 9.2) below. Here the opportunity has been taken to highlight some of the examples considered earlier by providing additional results.

§ 9.2) A Summary of Conclusions

A number of methods exist for performing stress and vibration analyses of turbomachinery blading. One method which is frequently used during the design of a blade is the Beam Element Method. This method is essentially a Finite Element Method [52] in which the elements are elastic beams with assignable geometric and torsional properties. In most practical cases the assignment of the torsional properties of a beam involves the numerical determination of the beam's warping function, shear-centre co-ordinates, torsional stiffness constant and warping stiffness constant. For design work, the numerical determination of these four items ideally requires techniques which are simple to use (even when the geometry is complex) and produce acceptably accurate results.

Because of the need to idealise only the boundary of a region rather than the region itself, numerical methods based on a boundary integral approach do satisfy the need for simplicity. The level of accuracy achieved during the solution of a problem must depend on the suitability of the approximations used and how well a given idealisation defines the problem.

As demonstrated by the references given throughout this thesis, most of the published work on the use of boundary integral techniques for the numerical solution of problems in elasticity is given in terms of functions and integrals of real variables. In order that the integrals at the heart of any boundary integral technique can be performed, these techniques usually require the geometry of the region under consideration to be approximated, e.g. in two dimensions geometries are often approximated by a series of straight lines and/or circular arc segments.

Throughout this thesis the author has demonstrated that boundary integral techniques based on the complex variables form of Green's Theorem can be developed for two dimensional problems. A feature of these techniques when applied to problems which are essentially harmonic in character, i.e. involve solutions of Laplace's equation, is that the numerical counterparts of these techniques make use of path independent integrals. This has meant that, with the exception of § 8.6), the author has been able to ignore the need for approximating geometries. Further, the approximation of the behaviour of functions over distinct elements of boundary by low order polynomials (degree ≤ 2) of a single complex variable has enabled the author to evaluate all integrals using closed formulae.

For problems defined on regions bounded by a finite number of contours, the accuracy of solution obtained using the numerical methods developed and presented in Chapters 2, 3, 5, 6 & 7 has depended solely on how well the above polynomial approximations have performed. For the cascade problems described in Chapters 4 & 7 the accuracy of solution also depends on the truncation of a series expansion of the kernel function $\coth\left\{\frac{\pi}{t}(\tau-\omega)\right\}$. Although no rigorous analysis of the theoretical error bounds associated with the approximations used has been performed, the results given throughout this thesis do demonstrate the high level of practical accuracy which can be achieved using methods based on second order polynomial approximations.

Despite the lack of rigorous error analysis some general comment on accuracy can be made about the solution of torsion problems and the determination of torsional properties. At the beginning of Chapter 6 the procedure to be followed during the determination of a beam's warping function was outlined as:-

i) solve the integral equation for the boundary tangential derivative of the warping function $\varphi(\tilde{\tau})$

ii) construct the boundary values of the first order derivatives $\varphi_x(\tilde{\tau})$ and $\varphi_y(\tilde{\tau})$

iii) generate the regular function $\varphi(\tilde{\tau}) + i\,\psi(\tilde{\tau})$ using the boundary integral representation derived in Chapter 5.

The function $\psi(\tilde{\underline{s}})$ is the harmonic conjugate of the warping function and is determined to within an additive constant using the technique outlined above. As mentioned in Chapter 6, the function $\psi(\tilde{\underline{s}})$ is termed the torsion function and satisfies the Dirichlet type boundary conditions

$$\psi(\tilde{\underline{s}}) = \frac{1}{2}|\underline{s}|^2 + K_p$$

where K_p is a constant particular to the p^{th} bounding contour C_p and $\underline{s} \in C_p$. Therefore, an indication of the error in the solution of the torsion problem can be obtained by subtracting $\frac{1}{2}|\underline{s}|^2$ from the numerical approximation to the boundary values of $\psi(\tilde{\underline{s}})$. The approximation to $\psi(\tilde{\underline{s}})$ is exact when the resulting difference is constant on each of the boundary contours.

With regard to the determination of the torsional properties of thin-walled beams using the methods described in this thesis, the author has observed that the distance between adjacent nodes on the contours bounding the region of interest should be less than one half the local wall thickness (c.f. the idealisation shown in Figure 6-7). Experience has shown that results which are somewhat inaccurate may be obtained when this basic rule is not followed. One consequence of the above observation is that a beam whose cross-section exhibits a high ratio of arc length to area may require the use of several hundred nodes before the problem is adequately defined.

Some care should also be taken in the positioning of the additional nodes required by the representation of the warping stiffness constant for a multiply connected region. Again, experience has shown that an additional node should be positioned at (approximately) the centre of the largest circle which can be inscribed in each of the cross-section's holes. With the additional nodes positioned in this manner, the logarithmic terms in equation (6.21) vary much less rapidly over the internal boundaries than they do when the additional nodes are positioned elsewhere.

In practical situations corners are usually replaced by blend radii. However, in order to strike a balance between theory and practice, some discussion on the topic of the

solution of Neumann problems defined on regions whose boundary contours contain corners was included in Chapters 2 & 3. The method of solution proposed by the author for regions with re-entrant corners was illustrated by the example of § 3.11.2) where a simple problem with a known solution was defined on an L-shaped region. In view of the high level of accuracy achieved in this example it is a worthwhile exercise to consider the same region with the more typical torsion type boundary conditions.

The dimensions of the L-shaped region considered were shown in Figure 3-3 and are repeated in Figure 9-1. The idealisations used were obtained by splitting each straight line segment bounding the region into N/6 equal intervals and positioning nodes at the ends of each interval. The resulting idealisation for the N=60 case is shown in Figure 9-2, N=120 and N=180 cases were also considered. For a point $\tilde{\tau} = x + iy$ on the bounding contour, the boundary condition on the normal derivative of the warping function was

$$\varphi_n(\tilde{\tau}) = y.\cos\alpha - x.\sin\alpha$$

where α is the argument of the outward drawn normal at $\tilde{\tau}$.

As discussed in § 2.6) and § 3.9), a singularity in the boundary tangential derivative $\varphi_s(\tilde{\tau})$ may exist at the point marked C in Figure 9-1. Taking r to be distance measured from C then the singularity will have the form $A_c r^{-1/3}$ where A_c is a constant indicating the "strength" of the singularity at C. Approximations to the constant A_c which were obtained using the three cases of N mentioned above are given in Table 9-1. At the time of writing the author is unaware of any published results with which these values of A_c can be compared. However, Kermanidis [loc.cit.] does give approximations to the normalised maximum shear stress

$$\tau = \frac{\max(\tau_{xz}, \tau_{yz})}{\mu\Omega}$$

on the segments AB and EA shown in Figure 9-1. Comparable values of τ using the methods described in this thesis are

given in Table 9-2. That only maximum nodal values are given in this table should be noted. Comparison of these values with those given by Kermanidis shows differences of at most 2½% of Kermanidis' values. From a Stress Engineering point of view, the 2½% difference is negligible.

The basic numerical method developed in Chapter 3 for determining nodal approximations to the boundary tangential derivative of a harmonic function was extended to cascade problems in Chapter 4. In this chapter attention was focused on the flow about a vertical cascade of aerofoils with cusped trailing edges. The results of the example (§ 4.6) which were obtained without taking into account the effect of the cusp on the governing integral equation produced significant errors. This was shown quite clearly by Figures 4-4 & 4-6.

A more detailed examination of the flow model in the vicinity of the cusp led to the introduction of a pair of coupled integral equations, viz. equations (4.30) & (4.31). This pair of coupled equations took into account the proximity of an aerofoil's suction surface to its pressure surface in the neighbourhood of the cusp. The need for equation (4.31) was then eliminated by assuming that the speed of the flow between a point A^+ on the suction surface and the cusp equalled the speed of the flow between a point A^- on the pressure surface and the cusp.

One problem associated with the use of the modified cusp model which was not considered in Chapter 4 is the effect which the choice of A^+ and A^- may have on the numerical solutions obtained. Referring specifically to the example of (§4.6) and (§4.8), Table 9-3 allows comparison between true and approximate values of flow speed obtained for six choices of A^+ and A^-. The idealisation used to obtain these results was of the type shown in Figure 4-12, i.e. the nodes lying between the cusp and the points A^+ & A^- were omitted from an N=240 idealisation. Further results for the six choices of A^+ & A^- considered are given in Table 9-4 where approximations to exit speed, exit angle and the angle

through which the flow is turned by the cascade are displayed. Examination of these results demonstrates that the points A^+ and A^- do have optimum positions. For the example considered, the x-ordinates of these optimum positions lie in the range $1.35 < x < 1.38$. This is further illustrated by Figure 9-3 where a plot of exit angle versus x-ordinate of point A^+ is given. Clearly, the choice of A^+ and A^- too close to the cusp can have a significant effect on results.

The use of boundary integral techniques to couple together interior and exterior Neumann problems defined on solid aerofoil sections of conventional shape was considered in Chapter 7. Here it was shown that solutions to both interior and exterior problems defined on either isolated or cascade aerofoils could be obtained through consideration of a single integral equation. A numerical solution of this equation which made use of the approximations and integral formulae developed in Chapters 3 & 4 was presented and illustrated by two simple examples. In view of the attention which the solution of harmonic problems by boundary integral techniques has received (see extensive bibliography in [15]), it is in many ways remarkable that the simple coupling described by the author does not appear to have received more attention elsewhere.

Some consideration to the problems of plane elastostatics, i.e. plane stress and plane strain, was given in Chapter 8. These problems are of considerable importance when the design and lifing of turbomachinery components are being undertaken. Using the complex variables forms of Greens's Theorem a boundary integral equation for the first derivative of one of the Goursat functions was derived. In common with other potential methods for the solution of plane stress and plane strain problems, the derived equation had a much simpler form than the integral equations based on Somigliana's integral formulae.

The design and lifing of turbomachinery components frequently involves the stressing of components with boundaries which are subjected to a mixture of known tractions and displacements. Unfortunately, the manner in which a problem's boundary conditions are incorporated into the free

term of the integral equation derived in Chapter 8 precludes the equation's use for problems involving mixed boundary conditions. For this reason the integral equation is of limited practical interest.

At an early stage of these conclusions it was mentioned that the level of accuracy achieved during the numerical solution of a problem must depend on the suitability of the approximations used. The suitability of low order polynomials of a single complex variable to the numerical solution of the range of problems considered by the author has been demonstrated by the results presented throughout this thesis. By way of contrast to the numerical methods developed in the main text of this thesis, the author has also carried out a preliminary investigation into the solution of flow problems using a novel numerical method based on Milne-Thomson's Circle Theorem. The approximations required by this method are developed in Appendix 1 where some numerical results obtained for a simple problem are also given. To date the author has had insufficient experience with the method for much general comment to be made. However, examination of the results given in Appendix 1 does indicate that this novel method will perform at least as well as the first order polynomial approximations developed in § 3.4) and § 3.6). It seems likely that the method could provide a method of analysing the flow past circular arc aerofoils which involves the solution of small systems of linear equations.

REFERENCES

1. Rizzo, F.J. and Shippy, D.J. (1977)."An advanced boundary integral equation method for three-dimensional thermoelasticity", Int. J. Num. Meth. Engng 11, 1753-1768.

2. Cruse, T.A. and Wilson, R.B. (1978). "Advanced applications of boundary-integral equation methods", Nucl. Eng. Des. 46, 223-234

3. Wood D.J. (1980). "Stressing by Boundary Elements - current status and future developments", BSR 4260, Private Data Rolls-Royce Ltd.

4. Love, A.E.H. (1927). "A treatise on the Mathematical Theory of Elasticity", 4th edition, Cambridge University Press

5. Cruse, T.A. (1977). "Mathematical Foundations of the Boundary-Integral Equation Method in Solid Mechanics", AFOSR-TR-77-1002

6. Cruse, T.A. (1978). "Two Dimensional BIE Fracture Mechanics Analysis". In "Recent Advances in Boundary Element Methods" (C.A. Brebbia, Ed.) Pentech Press, London.

7. Cruse, T.A. (1975). "Boundary Integral Equation Method for Three Dimensional Elastic Fracture Mechanics Analysis", AFOSR-TR-75-0813.

8. Lachat, J.C. and Watson, J.O. (1976). "Effective numerical treatment of boundary integral equations: a formulation for three dimensional elastostatics", Int. J. Num. Meth. Engng 10,991-1005

9. Chaudonneret, M. (1978). "On the discontinuity of the stress vector in the boundary integral equation method for elastic analysis". In "Recent Advances in Boundary Element Methods" (C. A. Brebbia, Ed.), Pentech Press, London.

10. Wilson, R.B., Potter, R.G. and Wong, J.K. (1978). "Boundary - integral equation analysis of an advanced turbine disk rim slot". In AGARD/PEP Symposium on "Stresses, Vibration, Structural Integration and Engine Integrity", Cleveland, Ohio (USA) 23-27 Oct. 1978

11. Abdul-Mihsein, M.J., Fenner, R.T. and Tan, C.L. (1979). "Boundary integral equation analysis of elastic stresses around on oblique hole in a flat plate", J. Strain Analysis 14, 179-185.

12. Tan, C.L. and Fenner, R.T. (1980), "Stress intensity factors for semi-elliptical surface cracks in pressurised cylinders using the boundary integral equation method", Int. J. Fracture 16, 233-245.

13. Banerjee, P.K. and Mustoe, G.G. (1978). "The boundary element method for two-dimensional problems of elasto-plasticity". In "Recent Advances in Boundary Element Methods" (C.A. Brebbia, Ed.), Pentech Press, London

14. Chaudonneret, M. (1978). "The calculation of stress concentrations in disk slots". In AGARD/PEP Symposium on "Stresses, Vibration, Structural Integration and Engine Integrity", Cleveland, Ohio (USA) 23-17 Oct. 1978

15. Jaswon, M.A. and Symm, G.T. (1977). "Integral equation methods in potential theory and elastostatics", Academic Press, London.

16. Muskhelishvili, N.I. (1953). "Some Basic Problems of the Mathematical Theory of Elasticity", Noordhoff, Groningen.

17. Mikhlin, S.G. (1963). "Integral Equations" Pergamon, London.

18. Kupradze, V.D. (1965). "Potential Methods in the Theory of Elasticity", Israel Program for Scientific Translations, Jerusalem.

19. Hamson, M.J. (1978). "Integral equation methods in the numerical solution of boundary-value problems for Laplace's equation for two dimensional regions bounded by polygons". M.Phil. Thesis, University of London.

20. Milne-Thomson, L.M. (1968). "Theoretical Hydrodynamics ", 5th edition, Macmillan, London.

21. Payne, D. (1964). "Isolated and Cascade Aerofoils", M.Sc. Thesis, University of London.

22. Payne, D. (1969). "Contributions to the Theoretical Aerodynamics of Turbomachinery Blade Rows", Ph.D. Thesis, Univeristy of London.

23. Martensen, E. (1959). "Berechnung der Druckverteilung an Gitterprofilen in ebener Potentialstromung mit einer Fredholmschen Integralgleichung", Arch. Rat. Mech. Anal.3, 235-270.

24. Reider, G. (1969). "Eine Variante zur Integralgleichung von Windisch für das Torsionsproblem", Zeit, Angew, Math. Mech. 49, 351-358.

25. Christiansen, S. (1978). "A review of some integral equations for solving the Saint-Venant torsion problem", J. Elasticity 8, 1-19.

26. Kermanidis, T. (1976). "Kupradze's functional equation for the torsion problem of prismatic bars", Computer Methods Appl. Mech. Engng. 7, 39-46 and 249-259.

27. Wilkinson, D.H. (1967). "A numerical solution of the analysis and design problems for the flow past one or more aerofoils or cascades", R & M No.3545

28. Atkinson, K. (1972). "The numerical evaluation of the Cauchy transform on a simple closed curve", SIAM J. Numer. Anal. 9, 284-299

29. Muskhelishvili, N.I. (1953). "Singular Integral Equations", Noordhoff, Groningen.

30. Pittaluga, A. (1978). "Recent developments in the theory of thin-walled beams", Computers & Structures 9, 69-79.

31. Beglinger, V. and Schlachter, W (1978). "Influence of Support Elasticity, Shear Deformation, Rotary Inertia and Cross-Sectional Warping on the Natural Frequencies of Turbomachine Blades", Sulzer Research Number 1978, 19-26

32. Ohtsuka, M. (1974)"Untwist of Rotating Blades," J. Engng for Power, TRANS ASME 74-GT-2

33. Zkirohowski-Koscia, K. (1967). "Thin Walled Beams", Crosby Lockwood, London.

34. Sokolnikoff, I.S. (1956). "Mathematical Theory of Elasticity", 2nd Edition, Mc-Graw Hill, New York.

35. Copson, E.T. (1935). "An introduction to the Theory of Functions of a Complex Variable", Oxford University Press.

36. Milne-Thompson, L.M.(1960). "Plane Elastic Systems", Springer-Verlag, Berlin.

37. Dyer, G.F. (1979). "Mathematical Methods for the Aerodynamic Design of Turbomachinery Blade Cascades for High Subsonic and Transonic Flow", Ph.D. Thesis, CNAA.

38. Apostol, T.M. (1957). "Mathematical Analysis", Addison-Wesley, New York.

39. Hess, J.L. & Smith, A.M.O. (1967). "Calculation of potential flow about arbitrary bodies". In "Progress in Aeronautical Sciences 8", Pergamon, London.

40. Phillips, E.G. (1957). "Functions of a Complex Variable," 8th Ed., Oliver and Boyd, Edinburgh.

41. Symm, G.T. (1973). "Treatment of singularities in the solution of Laplace's equation by an integral equation method", NPL Report NAC 31

42. Dwight, H.B. (1961). "Tables of integrals and other mathematical data", 4th Ed., Macmillan, New York.

43. Thwaites, B. (1960). "Incompressible Aerodynamics", Oxford University Press.

44. Jaswon, M.A. and Ponter, A.R.S. (1963). "An integral equation solution of the torsion problem", Proc. Roy. Soc. (A) 273, 237-246.

45. Souchet, R. and Robinaud, D. (1980). "Boundary Integral Formulations of the Torsion Problem". In "New Developments in Boundary Element Methods" (C. A. Brebbia, Ed.), CML Publications, Southampton.

46. Trefftz, E. (1935). "Uber den Schubmittelpunkt in einem durch eine Einzellast gebogenen Balken", Z. angew. Math. Mech. 15, 220-225.

47. Weinstein, A. (1947). "The centre of shear and the centre of twist", Quart. Applied Math. 5, 97-99.

48. Wood, D.J. (1980). "Determination of the torsional properties of plane sections using boundary integral techniques", App. Math. Modelling 4, 410-416.

49. Timoshenko, S. and Goodier, J.N. (1951). "Theory of Elasticity", 2nd Ed., McGraw-Hill, New York.

50. Oliveira, E.R.A. (1968). "Plane stress analysis by a general integral method", Journal of Eng. Mech. Div. ASCE EMI, 79-101.

51. Roarck, R.J. and Young, W.C. (1975). "Formulas for stress and strain", McGraw-Hill Kogakusha, Tokyo.

52. Zienkiewicz, O.C. (1977). "The Finite Element Method", McGraw-Hill, London.

APPENDIX 1

A NUMERICAL METHOD BASED ON MILNE-THOMSON's CIRCLE THEOREM

§A1.1) Introduction

In chapters 3 and 4 the author was concerned with the use of low order complexpolynomials in the solution of problems with Neumann type boundary conditions. The approximations used were such that values of the potential function's normal derivative $\varphi_n(\tilde{T})$ had to be given explicitly. Numerical techniques whereby the boundary values of the normal derivative are incorporated into the solution technique implicitly appear to have been ignored.

In order that this situation be (in some way) rectified, the author has carried out a preliminary study on a technique applicable to the analysis of the plane, potential flow of an incompressible, inviscid fluid past on isolated aerofoil. This approach to flow problems makes use of the known solution to the problem of an infinitely long circular cylinder disturbing a uniform stream.

An outline description of the aforementioned "implicit" numerical technique is given below. Some results obtained by applying the technique to a simple example, viz. the flow past on ellipse, are also given.

It would appear that the technique to be described is applicable to aerofoils whose bounding contours consist of (or can be approximated by) a series of circular arcs. It does not appear to be directly applicable to more general Neumann problems where the boundary values of the potential function's normal derivative may be non-zero.

§A1.2) A numerical method based on Milne-Thomson's circle theorem

Let **C** denote the contour bounding some isolated aerofoil which disturbs a uniform stream whose complex conjugate velocity is given by σ. Following the analysis of chapter 2, the complex conjugate velocity [20,p153] of the perturbed flow, $\tau(\zeta)$ say, can be represented on **C** by

$$\tau(\omega) = 2\sigma + \frac{1}{\pi i}\int_C \tau(\zeta)\frac{d\zeta}{\zeta-\omega} \qquad \text{(A1.1)}$$

where $\omega \in C$, provided that ω does not lie at a "corner" or a cusp. Further, on the contour C, the tangential component of the velocity vector, $q(\tilde{\zeta})$ say, can be represented by

$$q(\tilde{\omega}) = 2\sigma i e^{i\alpha(\tilde{\omega})} + \frac{e^{i\alpha(\tilde{\omega})}}{\pi}\int_C q(\zeta)\frac{ds}{\zeta-\omega} \qquad \text{(A1.2)}$$

where $\alpha(\tilde{\omega})$ denotes the argument of the outward drawn normal to C at ω.

If the contour C is assumed to comprise of a sequence of circular arcs $I_1,\ldots,I_n$ (A1.1) may be written as

$$\tau(\omega) = 2\sigma + \frac{1}{\pi i}\sum_{j=1}^{n}\int_{I_j}\tau(\zeta)\frac{d\zeta}{\zeta-\omega}$$

where $\int_{I_j}$ denotes an integration (in the positive sense) taken along the jth circular arc.

The circular arc I_j is an arc of the contour bounding a circular cylinder and if this cylinder is placed in the uniform stream $X_j(\zeta-Z_j)$, with a circulation $2\pi\gamma_j$ about the cylinder, then the complex potential $W_j(\zeta)$ of the disturbed flow is given by

$$W_j(\zeta) = X_j(\zeta-Z_j) + \overline{X}_j\frac{a_j^2}{\zeta-Z_j} + i\gamma_j \log\left\{\frac{\zeta-Z_j}{a_j}\right\} \qquad \text{(A1.3)}$$

where Z_j is the centre and a_j the radius of the circle. The complex conjugate velocity $\tau_j(\zeta)$ of this flow is obtained from the relation

$$\tau_j(\zeta) = \frac{d}{d\zeta}W_j(\zeta)$$

and therefore

$$\tau_j(\zeta) = X_j - \overline{X}_j\frac{a_j^2}{(\zeta-Z_j)^2} + i\frac{\gamma_j}{\zeta-Z_j} \qquad \text{(A1.4)}$$

The approximate solution to (A1.2) is obtained by assuming that the complex conjugate velocities $\overline{v}(z)$ and $\overline{v}_j(z)$ behave identically over the j^{th} circular arc. The assumption that the uniform stream $X_j\,(z-z_j)$ is parallel to the x-axis, i.e. X_j is real, is also made.

For $z \in I_j$ one may write

$$z - z_j = a_j e^{i\theta_j(\tilde{z})}$$

and if z_j , z_{j+1} denotes the start and end points of I_j so that

$$s_j = \frac{\theta_j(\tilde{z}_{j+1}) - \theta_j(\tilde{z}_j)}{\left|\theta_j(\tilde{z}_{j+1}) - \theta_j(\tilde{z}_j)\right|} \qquad \left[\text{with } z_1 \equiv z_{n+1}\right]$$

then, on noting that for I_j

$$i\, s_j\, \overline{v}_j(z)\, e^{i\theta_j(\tilde{z})} = q_j(\tilde{z}) \qquad \text{(A1.5)}$$

where $q_j(\tilde{z})$ denotes the (signed) speed of the flow at z, for X_j real it follows from (A1.4) that

$$q_j(\tilde{z}) = -i\, s_j e^{i\theta_j(\tilde{z})}\left\{ X_j\left(e^{-2i\theta_j(\tilde{z})} - 1\right) - i\,\frac{\gamma_j}{a_j} e^{-i\theta_j(\tilde{z})}\right\} .$$

Therefore

$$q_j(\tilde{z}) = -s_j\left\{ i\, X_j\left(e^{-i\theta_j(\tilde{z})} - e^{i\theta_j(\tilde{z})}\right) + \frac{\gamma_j}{a_j}\right\}$$

$$= -s_j\left\{ 2\, X_j \sin\theta_j(\tilde{z}) + \frac{\gamma_j}{a_j}\right\} \qquad \text{(A1.6)}$$

Hence, on the circular arc I_j

$$q_j(\tilde{z}_j) = -s_j\left\{ 2\, X_j \sin\theta_j(\tilde{z}_j) + \frac{\gamma_j}{a_j}\right\}$$

$$q_j(\tilde{z}_{j+1}) = -s_j\left\{ 2\, X_j \sin\theta_j(\tilde{z}_{j+1}) + \frac{\gamma_j}{a_j}\right\}$$

and solving for X_j, γ_j yields

$$X_j = -\frac{1}{2s_j}\left\{\frac{q_j(\tilde{\tau}_j) - q_j(\tilde{\tau}_{j+1})}{\sin\theta_j(\tilde{\tau}_j) - \sin\theta_j(\tilde{\tau}_{j+1})}\right\} \qquad \text{(A1.7)}$$

$$\gamma_j = \frac{a_j}{s_j}\left\{\frac{q_j(\tilde{\tau}_j).\sin\theta_j(\tilde{\tau}_{j+1}) - q_j(\tilde{\tau}_{j+1}).\sin\theta_j(\tilde{\tau}_j)}{\sin\theta_j(\tilde{\tau}_j) - \sin\theta_j(\tilde{\tau}_{j+1})}\right\} \qquad \text{(A1.8)}$$

provided that $\sin\theta_j(\tilde{\tau}_j) \neq \sin\theta_j(\tilde{\tau}_{j+1})$.

If $\hat{\tau}(\omega)$ is the required approximation to $\tau(\omega)$ then from (A1.1) and (A1.4) $\hat{\tau}(\omega)$ may be written as

$$\hat{\tau}(\omega) = 2\sigma + \frac{1}{\pi i}\sum_{j=1}^{n}\int_{I_j}\left\{X_j\left[1 - \frac{a_j^2}{(\tau - z_j)^2}\right] + i\frac{\gamma_j}{\tau - z_j}\right\}\frac{d\tau}{\tau - \omega}$$

or

$$\hat{\tau}(\omega) = 2\sigma + \sum_{j=1}^{n}\left\{\Delta_{1j}(\omega).X_j + \Delta_{2j}(\omega).\gamma_j\right\} \qquad \text{(A1.9)}$$

where

$$\Delta_{1j}(\omega) = \frac{1}{\pi i}\int_{I_j}\left\{1 - \frac{a_j^2}{(\tau - z_j)^2}\right\}\frac{d\tau}{\tau - \omega}$$

$$\Delta_{2j}(\omega) = \frac{1}{\pi}\int_{I_j}\frac{d\tau}{(\tau - z_j)(\tau - \omega)}.$$

Use of partial fractions allows $\Delta_{1j}(\omega)$ and $\Delta_{2j}(\omega)$ to be written as

$$\Delta_{1j}(\omega) = \frac{1}{\pi i}\int_{I_j}\left\{\left[1 - \frac{a_j^2}{(z_j - \omega)^2}\right]\frac{1}{\tau - \omega} - \frac{a_j^2}{(z_j - \omega)(\tau - z_j)^2} + \frac{a_j^2}{(z_j - \omega)^2(\tau - z_j)}\right\}d\tau \qquad \text{(A1.10)}$$

and

$$\Delta_{2j}(\omega) = \frac{1}{\pi}\int_{I_j}\left\{\frac{1}{(z_j - \omega)(\tau - z_j)} - \frac{1}{(z_j - \omega)(\tau - \omega)}\right\}d\tau \qquad \text{(A1.11)}$$

respectively.

The $q_j(\tilde{\gamma}_j)$ are introduced into equation (A1.9) by substituting the expressions obtained earlier for X_j and γ_j, viz. (A1.7) and (A1.8).
Hence

$$\hat{\zeta}(\omega) = 2\sigma + \sum_{j=1}^{n} \left\{ \delta_{1,j}(\omega) q_j(\tilde{\gamma}_j) + \delta_{2,j}(\omega) q_j(\tilde{\gamma}_{j+1}) \right\} \qquad \text{(A1.12)}$$

where

$$\delta_{1,j}(\omega) = -\frac{1}{S_j\{\sin\theta_j(\tilde{\gamma}_j) - \sin\theta_j(\tilde{\gamma}_{j+1})\}} \left\{ \frac{\Delta_{1j}(\omega)}{2} - a_j \sin\theta_j(\tilde{\gamma}_{j+1})\, \Delta_{2j}(\omega) \right\} \qquad \text{(A1.13)}$$

$$\delta_{2,j}(\omega) = -\frac{1}{S_j\{\sin\theta_j(\tilde{\gamma}_j) - \sin\theta_j(\tilde{\gamma}_{j+1})\}} \left\{ a_j \sin\theta_j(\tilde{\gamma}_j)\, \Delta_{2j}(\omega) - \frac{\Delta_{1j}(\omega)}{2} \right\} \qquad \text{(A1.14)}$$

For a smooth profile the condition that the complex conjugate velocity be continuous at all points on the contour **C** requires that

$$q_j(\tilde{\gamma}_{j+1}) = q_{j+1}(\tilde{\gamma}_{j+1})$$

whence (A1.12) may be written in the form

$$\hat{\zeta}(\omega) = 2\sigma + \sum_{j=1}^{n} \left\{ q_j(\tilde{\gamma}_j)\, \delta_{1,j}(\tilde{\omega}) + q_{j+1}(\tilde{\gamma}_{j+1})\, \delta_{2,j}(\omega) \right\}$$

or, more conveniently,

$$\hat{\zeta}(\omega) = 2\sigma + \sum_{j=1}^{n} q_j(\tilde{\gamma}_j) \left\{ \delta_{1,j}(\omega) + \delta_{2,j-1}(\omega) \right\} \qquad \text{(A1.15)}$$

The equation relating the approximate (signed) speed at the point ω on **C**, $q(\tilde{\omega})$ say, to the $q_j(\tilde{\gamma}_j)$ is obtained by applying the relation

$$q(\tilde{\omega}) = i e^{i\alpha(\tilde{\omega})} \hat{\zeta}(\omega)$$

to equation (A1.15). As in earlier chapters, $\alpha(\tilde{\omega})$ denotes the argument of the outward drawn normal at ω. Equation (A1.15) can therefore be written as

$$q(\tilde{\omega}) = 2i e^{i\alpha(\tilde{\omega})} \sigma + i e^{i\alpha(\tilde{\omega})} \sum_{j=1}^{n} q_j(\gamma_j) \left\{ \delta_{1,j}(\omega) + \delta_{2,j-1}(\omega) \right\} \qquad \text{(A1.16)}$$

Applying (A1.16) at each of the n arc points ζ_k and setting

$$q_k(\tilde{\zeta}_k) = q(\tilde{\zeta}_k) \quad , \quad k = 1(1)n$$

the set of complex linear equations

$$2i\sigma e^{i\alpha(\tilde{\zeta}_k)} = q_k(\tilde{\zeta}_k) - ie^{i\alpha(\tilde{\zeta}_k)} \sum_{j=1}^{n} q_j(\tilde{\zeta}_j)\left\{\delta_{1,j}(\zeta_k) + \delta_{2,j-1}(\zeta_k)\right\} \qquad \text{(A1.17)}$$

is obtained for the real unknowns $q_j(\tilde{\zeta}_j)$. Consistent with chapters 2, 3 and 4, values for these unknowns are obtained by solving the real part of (A1.17).

Note that since

$$e^{i\alpha(\tilde{\zeta}_k)} = s_k e^{i\theta_k(\tilde{\zeta}_k)}$$

equations (A1.17) may be written as

$$2i\sigma s_k e^{i\theta_k(\tilde{\zeta}_k)} = q_k(\tilde{\zeta}_k) - is_k e^{i\theta_k(\tilde{\zeta}_k)} \sum_{j=1}^{n} q_j(\tilde{\zeta}_j)\left\{\delta_{1,j}(\zeta_k) + \delta_{2,j-1}(\zeta_k)\right\} \qquad \text{(A1.18)}$$

The comments made in chapter 3 about the singular (or possibly ill-conditioned) nature of (A1.17) again apply. As in that chapter, a unique solution of (A1.17) is obtained by adjoining to these equations a suitable approximation to the circulation Γ.

An approximation to the circulation, $\hat{\Gamma}$ say, can be obtained from the boundary approximation to $\hat{\tau}(\zeta)$ since $\hat{\Gamma}$ may be written as

$$\hat{\Gamma} = \sum_{j=1}^{n} \int_{I_j} \tau_j(\zeta)\, d\zeta \qquad \text{(A1.19)}$$

Using the relation

$$\tau_j(\zeta) = \frac{d}{d\zeta} W_j(\zeta)$$

and (A1.3), expression (A1.19) may be written in the form

$$\hat{\Gamma} = \sum_{j=1}^{n} \left\{ W_j(\tilde{\gamma}_{j+1}) - W_j(\tilde{\gamma}_j) \right\}$$

$$= \sum_{j=1}^{n} \left\{ (\gamma_{j+1} - \gamma_j) X_j \left[1 - \frac{a_j^2}{(\gamma_{j+1} - Z_j)(\gamma_j - Z_j)} \right] + i\,\sigma_j \log\left(\frac{\gamma_{j+1} - Z_j}{\gamma_j - Z_j} \right) \right\}$$

On substituting (A1.7), (A1.8) for X_j and σ_j respectively, this last expression can be written in terms of the $q_j(\tilde{\gamma}_j)$. Hence,

$$\hat{\Gamma} = \sum_{j=1}^{n} \left[\frac{(\gamma_{j+1} - \gamma_j)}{2 s_j} \left\{ \frac{a_j^2}{(\gamma_{j+1} - Z_j)(\gamma_j - Z_j)} - 1 \right\} \left\{ \frac{q_j(\tilde{\gamma}_j) - q_j(\tilde{\gamma}_{j+1})}{\sin\theta_j(\tilde{\gamma}_j) - \sin\theta_j(\tilde{\gamma}_{j+1})} \right\} + i \frac{a_j}{s_j} \left\{ \frac{q_j(\tilde{\gamma}_j)\sin\theta_j(\tilde{\gamma}_{j+1}) - q_j(\tilde{\gamma}_{j+1})\sin\theta_j(\tilde{\gamma}_j)}{\sin\theta_j(\tilde{\gamma}_j) - \sin\theta_j(\tilde{\gamma}_{j+1})} \right\} \log\left(\frac{\gamma_{j+1} - Z_j}{\gamma_j - Z_j} \right) \right]$$

and making use of the continuity of $\hat{\Gamma}(\tilde{\gamma})$ at $\gamma = \gamma_{j+1}$ yields

$$\hat{\Gamma} = \sum_{j=1}^{n} \left\{ q_j(\tilde{\gamma}_j) A_j + q_{j+1}(\tilde{\gamma}_{j+1}) B_j \right\}$$

where

$$A_j = \frac{1}{s_j \{ \sin\theta_j(\tilde{\gamma}_j) - \sin\theta_j(\tilde{\gamma}_{j+1}) \}} \left\{ \frac{(\gamma_{j+1} - \gamma_j)}{2} \left[\frac{a_j^2}{(\gamma_{j+1} - Z_j)(\gamma_j - Z_j)} - 1 \right] + i\, a_j \sin\theta_j(\tilde{\gamma}_{j+1}) \log\left(\frac{\gamma_{j+1} - Z_j}{\gamma_j - Z_j} \right) \right\} \qquad \text{(A1.20)}$$

$$B_j = \frac{-1}{s_j \{ \sin\theta_j(\tilde{\gamma}_j) - \sin\theta_j(\tilde{\gamma}_{j+1}) \}} \left\{ \frac{\gamma_{j+1} - \gamma_j}{2} \left[\frac{a_j^2}{(\gamma_{j+1} - Z_j)(\gamma_j - Z_j)} - 1 \right] - i\, a_j \sin\theta_j(\tilde{\gamma}_j) \log\left(\frac{\gamma_{j+1} - Z_j}{\gamma_j - Z_j} \right) \right\} \qquad \text{(A1.21)}$$

Again, for a smooth profile it is convenient to write (A1.19) as

$$\hat{\Gamma} = \sum_{j=1}^{n} q_j(\tilde{\delta}_j)\{A_j + B_{j-1}\}$$

Using this expression for $\hat{\Gamma}$, equations (A1.17) may be replaced by

$$2i\sigma e^{i\alpha(\tilde{\delta}_k)} + \Gamma$$

$$= q_k(\tilde{\delta}_k) + \sum_{j=1}^{n} q_j(\tilde{\delta}_j)\left\{A_j + B_{j-1} - ie^{i\alpha(\tilde{\delta}_k)}\left(\delta_{1,j}(\delta_k) + \delta_{2,j-1}(\delta_k)\right)\right\}$$

and values for the $q_j(\tilde{\delta}_j)$ obtained by applying Gaussian elimination to the real part of these equations.

When the trailing edge of the aerofoil is pointed or cusped, the equations (A1.17) are readily modified (c.f. chapter 4). Let the nodes defining the profile be numbered such that the point or cusp lies at δ_1, the start of the first circular arc. In this case the point or cusp also lies at δ_{n+1}, the end of the last circular arc.

With the nodes numbered in this way and making use of the continuity condition

$$q_j(\tilde{\delta}_{j+1}) = q_{j+1}(\tilde{\delta}_{j+1})$$

for $j = 1(1)n-1$, equation (A1.16) becomes

$$q(\tilde{\omega}) = 2ie^{i\alpha(\tilde{\omega})}\sigma + ie^{i\alpha(\tilde{\omega})}\sum_{j=2}^{n} q_j(\tilde{\delta}_j)\left\{\delta_{1,j}(\omega) + \delta_{2,j-1}(\omega)\right\}$$

$$+ ie^{i\alpha(\tilde{\omega})}\left\{q_1(\tilde{\delta}_1).\delta_{1,1}(\omega) + q_n(\tilde{\delta}_{n+1}).\delta_{2,n}(\omega)\right\}$$

where the coefficients $\delta_{1,j}(\omega)$, $\delta_{2,j}(\omega)$ etc. are again given by (A1.13) and (A1.14). Identifying ω with each of the $n-1$ arc points δ_k, $k = 2(1)n$ yields the equations

$$2ie^{i\alpha(\tilde{\delta}_k)}\sigma = q_k(\tilde{\delta}_k) - ie^{i\alpha(\tilde{\delta}_k)}\sum_{j=2}^{n} q_j(\tilde{\delta}_j)\left\{\delta_{1,j}(\delta_k) + \delta_{2,j-1}(\delta_k)\right\}$$

$$- ie^{i\alpha(\tilde{\delta}_k)}\left\{q_1(\tilde{\delta}_1).\delta_{1,1}(\delta_k) + q_n(\tilde{\delta}_{n+1}).\delta_{2,n}(\delta_k)\right\}$$

(A1.22)

As in the case of equations (A1.17), only the real parts of equations (A1.22) are considered when obtaining a solution to a given problem.

If the trailing edge is pointed, the continuity of the velocity components $\varphi_x(\tilde{\gamma})$, $\varphi_y(\tilde{\gamma})$ (required if the speed of the flow is to remain finite) leads to the conclusion that the trailing edge is a stagnation point i.e.

$$q_1(\tilde{\gamma}_1) = q_n(\tilde{\gamma}_{n+1}) = 0$$

The remaining $q_j(\tilde{\gamma}_j)$, $j = 2(1)n$, can be obtained by writing (A1.22) as

$$2ie^{i\alpha(\tilde{\gamma}_k)}\sigma = q_k(\tilde{\gamma}_k) - ie^{i\alpha(\tilde{\gamma}_k)}\sum_{j=2}^{n} q_j(\tilde{\gamma}_j)\{\delta_{1,j}(\gamma_k) + \delta_{2,j-1}(\gamma_k)\},$$

$k = 2(1)n$, and solving in the usual manner.

When the trailing edge is cusped an additional equation may again be obtained from the assumption that the speed of the flow remains finite (and is single valued) at the cusp. As in the case of the vertical cascade considered in chapter 4, one further equation is required if there is to be a unique solution to the specified problem.

When the trailing edge is cusped or pointed, the approximation to the circulation may be written as

$$\hat{\Gamma} = \sum_{j=2}^{n}\{A_j + B_{j-1}\}q_j(\tilde{\gamma}_j) + A_1 q_1(\tilde{\gamma}_1) + B_n q_n(\tilde{\gamma}_{n+1})$$

where the A_j, B_j etc. are given by (A1.20) and (A1.21). Clearly, $\hat{\Gamma}$ may be evaluated using the above expression once the $q_j(\tilde{\gamma}_j), q_1(\tilde{\gamma}_1)$ and $q_n(\tilde{\gamma}_{n+1})$ have been determined.

With reference to the coefficients (A1.10) and (A1.11), it should be noted that these coefficients can be evaluated separately provided that $\omega \neq \gamma_j$ and $\omega \neq \gamma_{j+1}$. These integrations are similar to those required in chapter 3 and are not repeated here.

When the integrations required by (A1.10) and (A1.11) cannot be performed separately the coefficients of the types $\{\delta_{1,j}(\omega) + \delta_{2,j-1}(\omega)\}, \delta_{1,1}(\omega)$ and $\delta_{2,n}(\omega)$, which

occur in (A1.17) and (A1.22), must be simplified. There are three cases to be considered:-

i) $\underline{\omega = \gamma_{j-1}}$

since $\int_{I_j} \frac{d\zeta}{\zeta - \gamma_{j-1}}$ exists in the Riemann sense attention can be restricted to terms involving

$\int_{I_{j-1}} \frac{d\zeta}{\zeta - \gamma_{j-1}}$, i.e. $\delta_{2,j-1}(\gamma_{j-1})$.

Now

$$\Delta_{1,j-1}(\gamma_{j-1}) = \frac{1}{\pi i}\int_{I_{j-1}} \left\{ \left[1 - \frac{a_{j-1}^2}{(z_{j-1} - \gamma_{j-1})^2} \right] \frac{1}{\zeta - \gamma_{j-1}} - \frac{a_{j-1}^2}{(z_{j-1} - \gamma_{j-1})(\zeta - z_{j-1})^2} + \frac{a_{j-1}^2}{(z_{j-1} - \gamma_{j-1})^2 (\zeta - z_{j-1})} \right\} d\zeta$$

and

$$\Delta_{2,j-1}(\gamma_{j-1}) = \frac{1}{\pi}\int_{I_{j-1}} \left\{ \frac{1}{(z_{j-1} - \gamma_{j-1})(\zeta - z_{j-1})} - \frac{1}{(z_{j-1} - \gamma_{j-1})(\zeta - \gamma_{j-1})} \right\} d\zeta$$

which may be written as

$$\Delta_{1,j-1}(\gamma_{j-1}) = \frac{1}{\pi i}\int_{I_{j-1}} \left\{ \left[1 - e^{-2i\theta_{j-1}(\tilde{\gamma}_{j-1})} \right] \frac{1}{\zeta - \gamma_{j-1}} - \frac{a_{j-1}^2}{(z_{j-1} - \gamma_{j-1})(\zeta - z_{j-1})^2} + \frac{a_{j-1}^2}{(z_{j-1} - \gamma_{j-1})^2 (\zeta - z_{j-1})} \right\} d\zeta$$

and

$$\Delta_{2,j-1}(\gamma_{j-1}) = \frac{1}{\pi}\int_{I_{j-1}} \left\{ \frac{1}{(z_{j-1} - \gamma_{j-1})(\zeta - z_{j-1})} + \frac{e^{-i\theta_{j-1}(\tilde{\gamma}_{j-1})}}{a_{j-1}(\zeta - \gamma_{j-1})} \right\} d\zeta$$

since

$$\gamma_{j-1} - z_{j-1} = a_{j-1} e^{i\theta_{j-1}(\tilde{\gamma}_{j-1})}.$$

Letting

$$D_{j-1} = \sin\theta_{j-1}(\gamma_{j-1}) - \sin\theta_{j-1}(\tilde{\gamma}_j)$$

the coefficient $\delta_{2,j-1}(\tilde{\gamma}_{j-1})$ simplifies to

$$\delta_{2,j-1}(\gamma_{j-1}) = -\frac{1}{2\pi i\, s_{j-1} D_{j-1}(z_{j-1} - \gamma_{j-1})}\int_{I_{j-1}} \left\{ \frac{a_{j-1}^2}{(\zeta - z_{j-1})^2} - \frac{a_{j-1}}{(\zeta - z_{j-1})} \left[\frac{a_{j-1}}{(z_{j-1} - \gamma_{j-1})} - 2i\sin\theta_{j-1}(\gamma_{j-1}) \right] \right\} d\zeta \qquad \text{(A1.23)}$$

ii) $\underline{\omega = \gamma_j}$

here

$$\Delta_{1,j}(\gamma_j) = \frac{1}{\pi i}\int_{I_j}\left\{\left[1 - e^{-2i\theta_j(\tilde{\gamma}_j)}\right]\frac{1}{\gamma-\gamma_j} - \frac{a_j^2}{(z_j-\gamma_j)(\gamma-z_j)^2} + \frac{a_j^2}{(z_j-\gamma_j)^2(\gamma-z_j)}\right\}d\gamma$$

and

$$\Delta_{2,j}(\gamma_j) = \frac{1}{\pi}\int_{I_j}\left\{\frac{1}{(z_j-\gamma_j)(\gamma-z_j)} + \frac{e^{-i\theta_j(\tilde{\gamma}_j)}}{a_j(\gamma-\gamma_j)}\right\}d\gamma.$$

Therefore

$$\delta_{1,j}(\gamma_j) = \frac{1}{2\pi i s_j D_j (z_j-\gamma_j)}\int_{I_j}\left\{\frac{a_j^2}{(\gamma-z_j)^2} - \frac{a_j}{\gamma-z_j}\left[\frac{a_j}{z_j-\gamma_j} - 2i\sin\theta_j(\tilde{\gamma}_{j+1})\right]\right\}d\gamma$$
$$- \frac{e^{-i\theta_j(\tilde{\gamma}_j)}}{\pi s_j}\int_{I_j}\frac{d\gamma}{\gamma-\gamma_j}$$

where $D_j = \sin\theta_j(\tilde{\gamma}_j) - \sin\theta_j(\tilde{\gamma}_{j+1})$.

Similarly it can be shown that

$$\delta_{2,j-1}(\gamma_j) = \frac{-1}{2\pi i s_{j-1} D_{j-1}(z_{j-1}-\gamma_j)}\int_{I_{j-1}}\left\{\frac{a_{j-1}^2}{(\gamma-z_{j-1})^2}\right.$$
$$\left. - \frac{a_{j-1}}{(\gamma-z_{j-1})}\left[\frac{a_{j-1}}{z_{j-1}-\gamma_j} - 2i\sin\theta_{j-1}(\tilde{\gamma}_{j-1})\right]\right\}d\gamma - \frac{e^{-i\theta_{j-1}(\gamma_j)}}{\pi s_{j-1}}\int_{I_{j-1}}\frac{d\gamma}{\gamma-\gamma_j}$$

whence

$$\delta_{1,j}(\gamma_j) + \delta_{2,j-1}(\gamma) = \frac{1}{2\pi i s_j D_j(z_j-\gamma_j)}\int_{I_j}\left\{\frac{a_j^2}{(\gamma-z_j)^2} - \frac{a_j}{\gamma-z_j}\left[\frac{a_j}{z_j-\gamma_j} - 2i\sin\theta_j(\tilde{\gamma}_{j+1})\right]\right\}d\gamma$$
$$- \frac{1}{2\pi i s_{j-1} D_{j-1}(z_{j-1}-\gamma_j)}\int_{I_{j-1}}\left\{\frac{a_{j-1}^2}{(\gamma-z_{j-1})^2} - \frac{a_{j-1}}{\gamma-z_{j-1}}\left[\frac{a_{j-1}}{z_{j-1}-\gamma_j} - 2i\sin\theta_{j-1}(\tilde{\gamma}_{j-1})\right]\right\}d\gamma$$
$$- \frac{e^{-i\theta_j(\tilde{\gamma}_j)}}{\pi s_j}\int_{\gamma_{j-1}}^{\gamma_{j+1}}\frac{d\gamma}{\gamma-\gamma_j} \qquad \text{(A1.24)}$$

since

$$\frac{e^{-i\theta_{j-1}(\tilde{\gamma}_j)}}{s_{j-1}} = \frac{e^{-i\theta_j(\tilde{\gamma}_j)}}{s_j}.$$

iii) $\underline{\omega = \gamma_{j+1}}$

since $\int_{I_{j-1}} \frac{d\gamma}{\gamma - \gamma_{j+1}}$ exists in the Riemann sense attention can be restricted to terms involving $\int_{I_j} \frac{d\gamma}{\gamma - \gamma_{j+1}}$, i.e. $\delta_{1,j}(\gamma_{j+1})$.

Now

$$\Delta_{1,j}(\gamma_{j+1}) = \frac{1}{\pi i}\int_{I_j}\left\{\left[1 - e^{-2i\theta_j(\tilde{\gamma}_{j+1})}\right]\frac{1}{\gamma - \gamma_{j+1}} - \frac{a_j^2}{(z_j - \gamma_{j+1})(\gamma - z_j)^2} + \frac{a_j^2}{(z_j - \gamma_{j+1})^2(\gamma - z_j)}\right\}d\gamma$$

and

$$\Delta_{2,j}(\gamma_{j+1}) = \frac{1}{\pi}\int_{I_j}\frac{d\gamma}{(z_j - \gamma_{j+1})(\gamma - z_j)} + \frac{1}{\pi}\int_{I_j}\frac{e^{-i\theta_j(\tilde{\gamma}_{j+1})}}{a_j(\gamma - \gamma_{j+1})}\,d\gamma$$

so that $\delta_{1,j}(\gamma_{j+1})$ can be written as

$$\delta_{1,j}(\gamma_{j+1}) = \frac{1}{2\pi i\, s_j D_j(z_j - \gamma_{j+1})}\int_{I_j}\left\{\frac{a_j^2}{(\gamma - z_j)^2} - \frac{a_j}{\gamma - z_j}\left[\frac{a_j}{(z_j - \gamma_{j+1})} - 2i\sin\theta_j(\tilde{\gamma}_{j+1})\right]\right\}d\gamma \qquad \text{(A1.25)}$$

Each of the three expressions (A1.23) to (A1.25) can be evaluated in closed form.

§ A1.3) Example

Some verification of the numerical method described in §A1.2) above has been achieved by considering the flow past an elliptic body disturbing a uniform stream. In order that a straightforward comparison could be made with both known and numerical solutions to this problem, the elliptic body was taken to be bounded by the ellipse

$$x^2 + 4y^2 = 1$$

while the flow far upstream was considered to have unit velocity and to be directed in the positive x-direction, i.e. $\sigma = 1$ was taken. Further, it was assumed that there was no circulation about the elliptic body. That this problem is just the exterior problem considered in §7.5) should be noted.

The idealisation used to achieve a numerical solution was that used in §7.5) and shown in Figure 7-1. More precisely, the start and end points (nodes) of the arcs Γ_1, ...Γ_N were obtained by writing the boundary in the form.

$$x = \cos\theta$$
$$y = \tfrac{1}{2}\sin\theta$$

and taking 20 nodes at equal increments of the eccentric angle θ. The centre of each of the arcs in the approximation was obtained by finding the point of intersection of the bisector of the line joining the nodes at either end of the arc with the (ellipses) outward drawn normal to the node at the start of the arc. All other parameters were based on these calculated centres and the assumption that each circular arc was the shortest route (along the appropriate circle) between the start and end points of the arc.

Approximations to the required speed of the flow found using the numerical method of §A1.2) together with the idealisation described above are given in Table A1-1. Here the solutions obtained are compared with their true values (c.f. §7.5.1) and corresponding tables) and a solution obtained using the piecewise linear approximation of §3.4). Results are given for nodes in the first quadrant ($x, y \geq 0$) only.

Examination of Table A1-1 does show that, for this example, the error obtained using the numerical method described in this appendix has much less variation over the boundary than does the solution obtained using the technique given in § 3.4). At present there is insufficient experience in the use of the method described in § A1.2) for more general comment to be made.

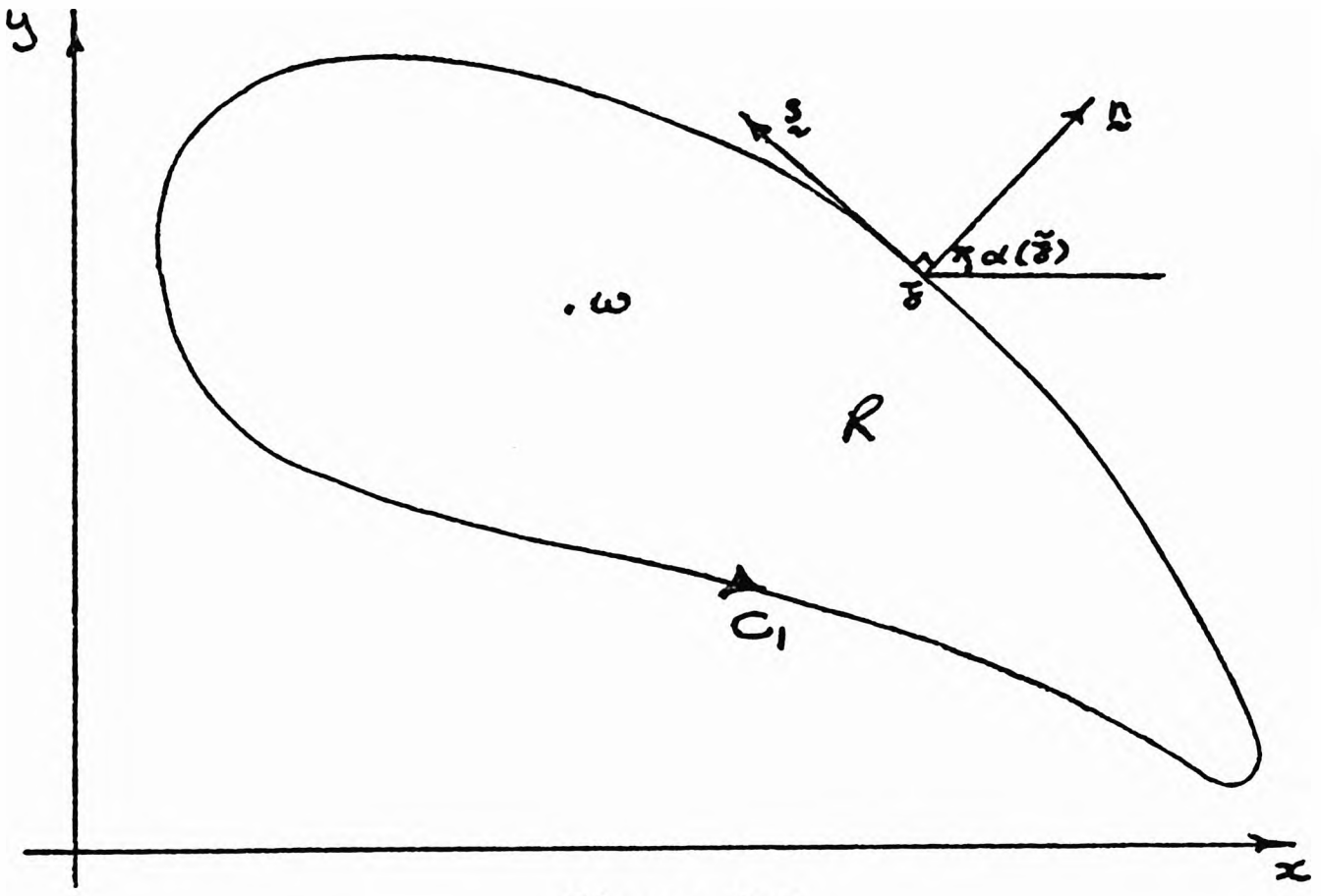

Figure 2-1

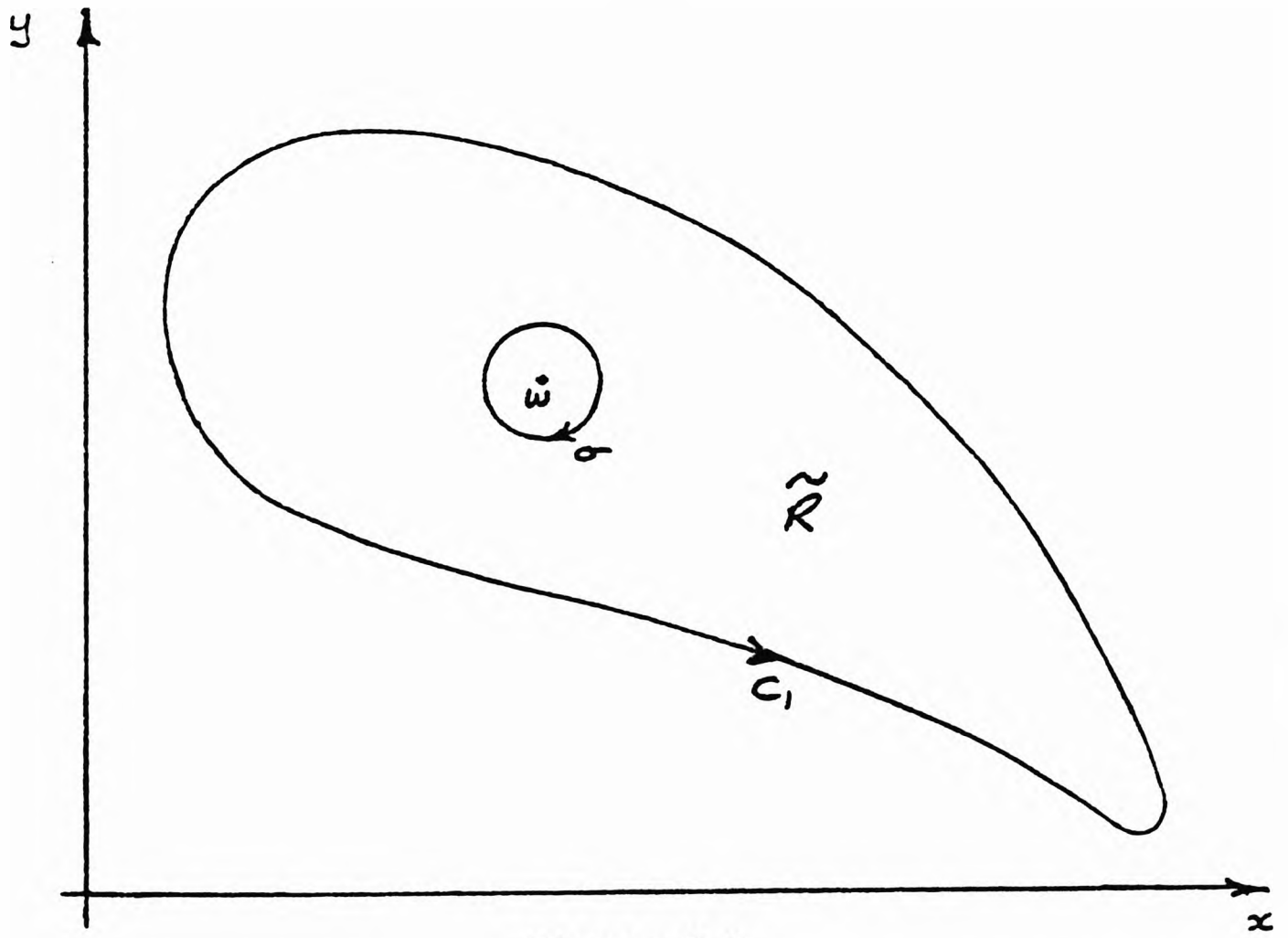

Figure 2-2

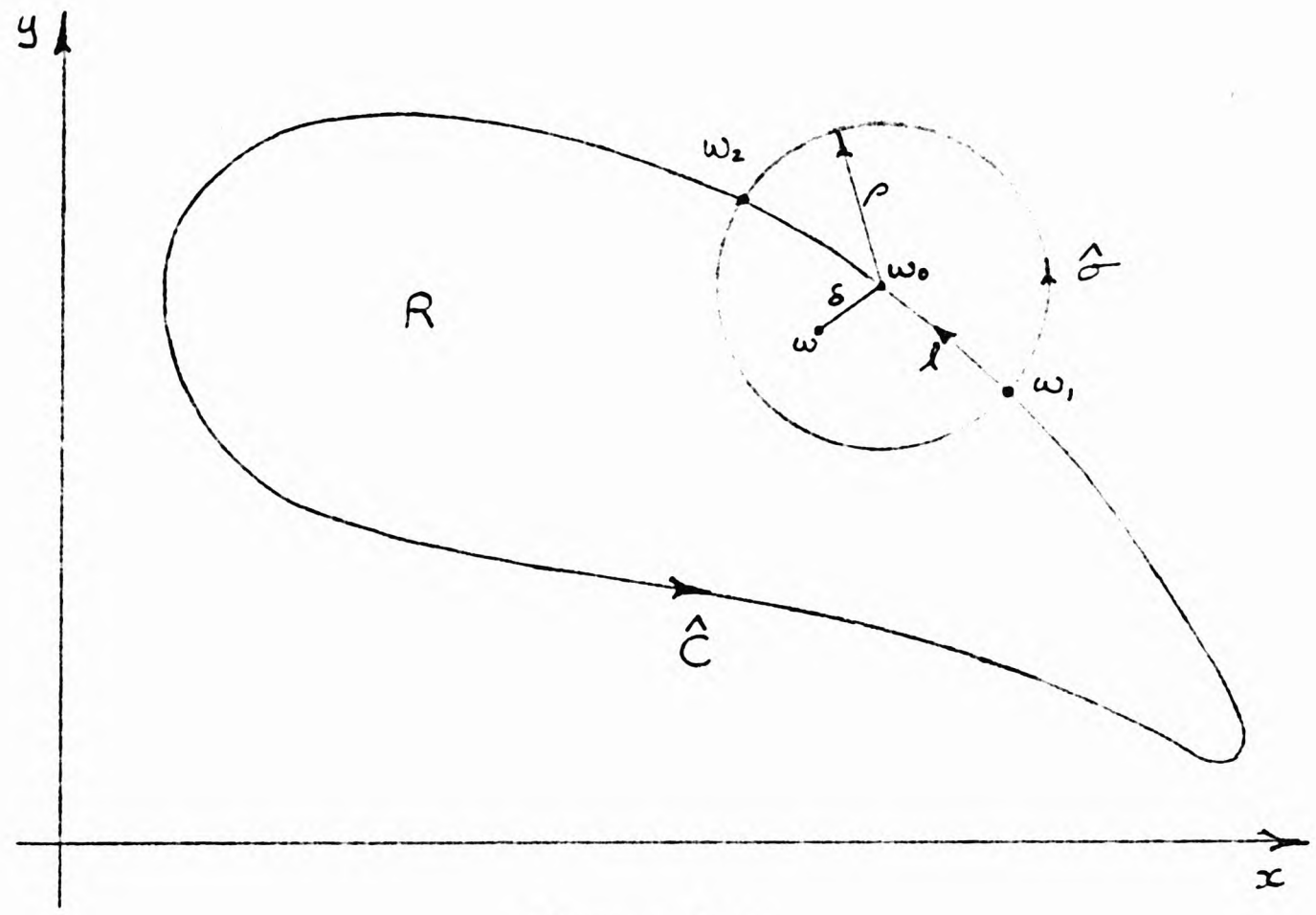

Figure 2-3

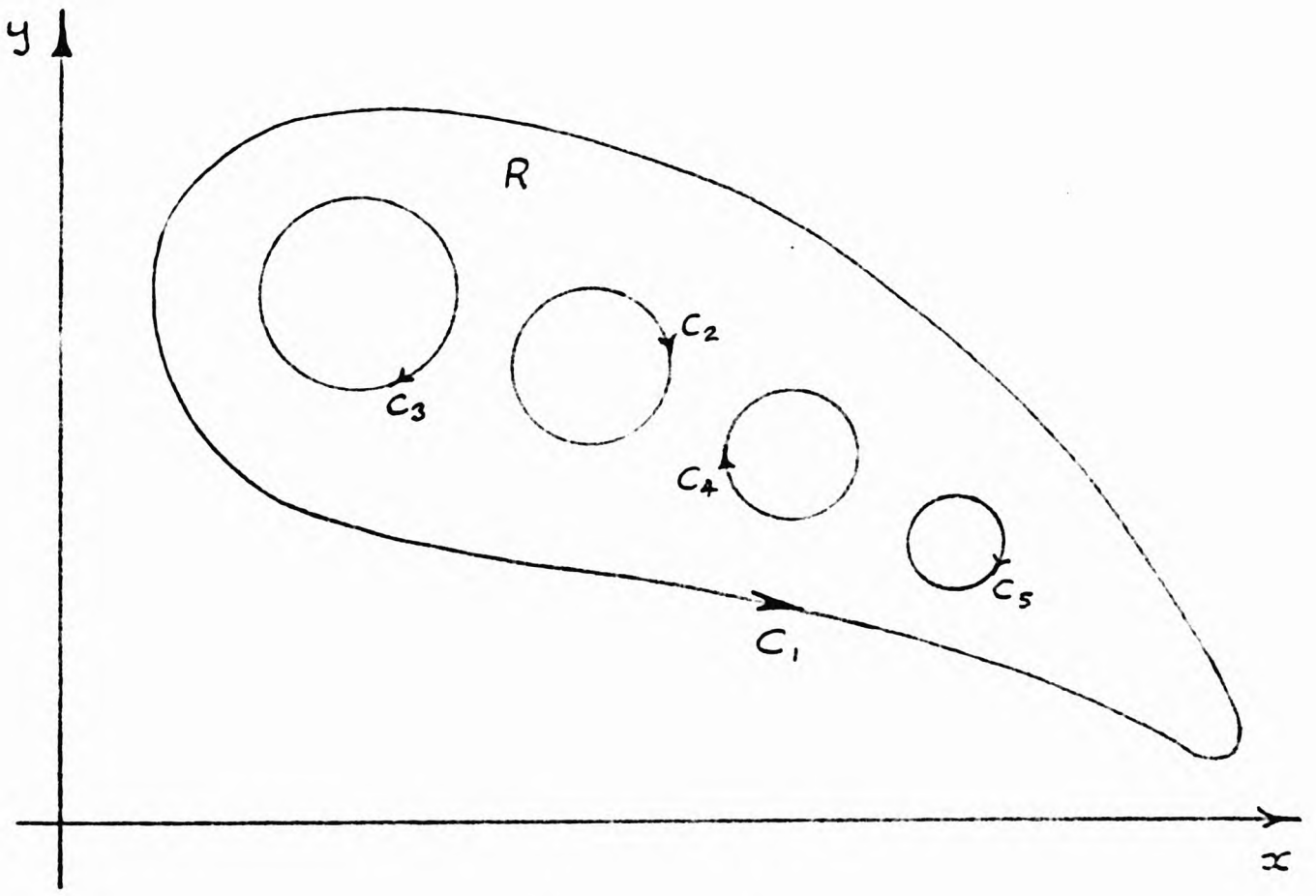

Figure 2-4

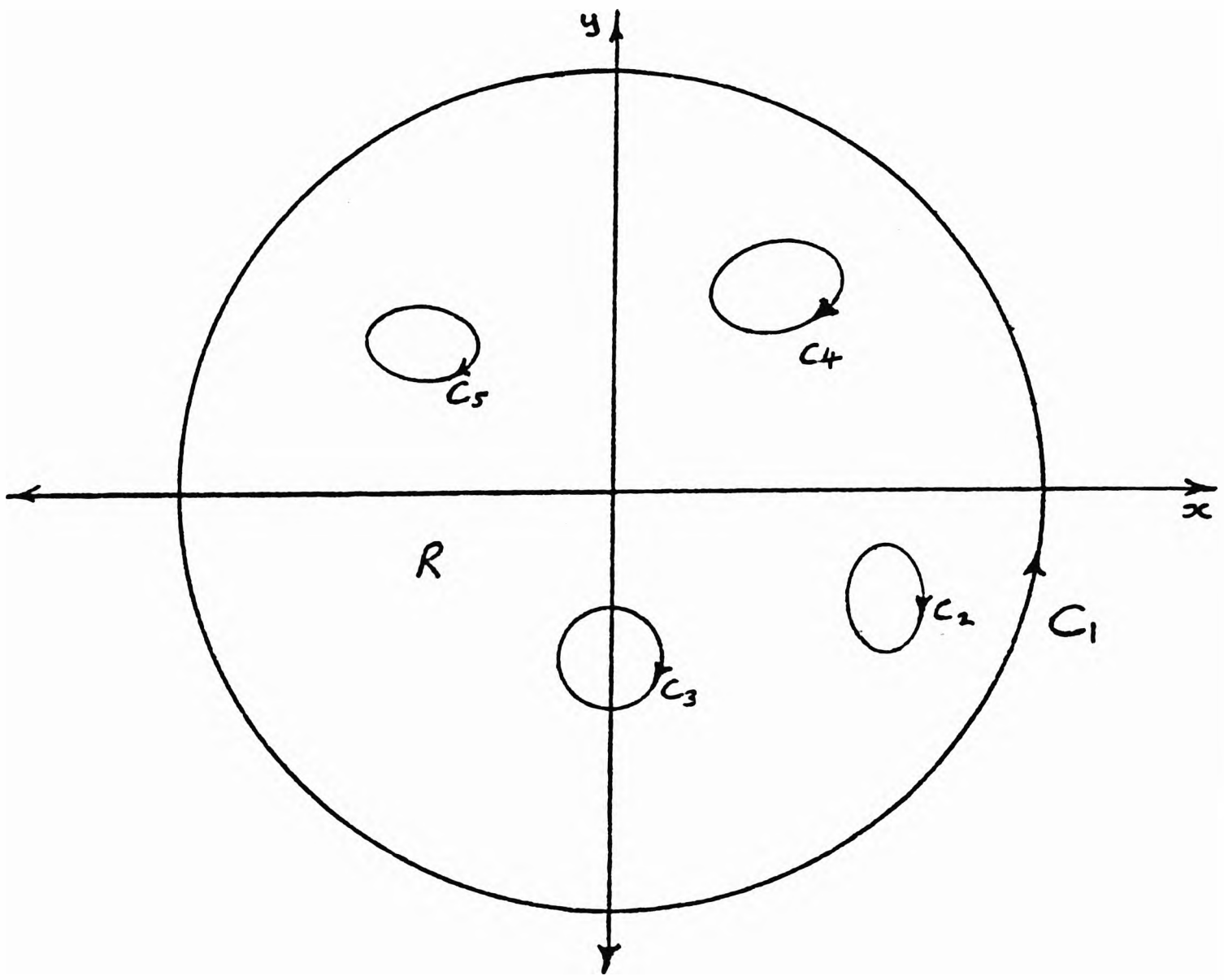

Figure 2-5

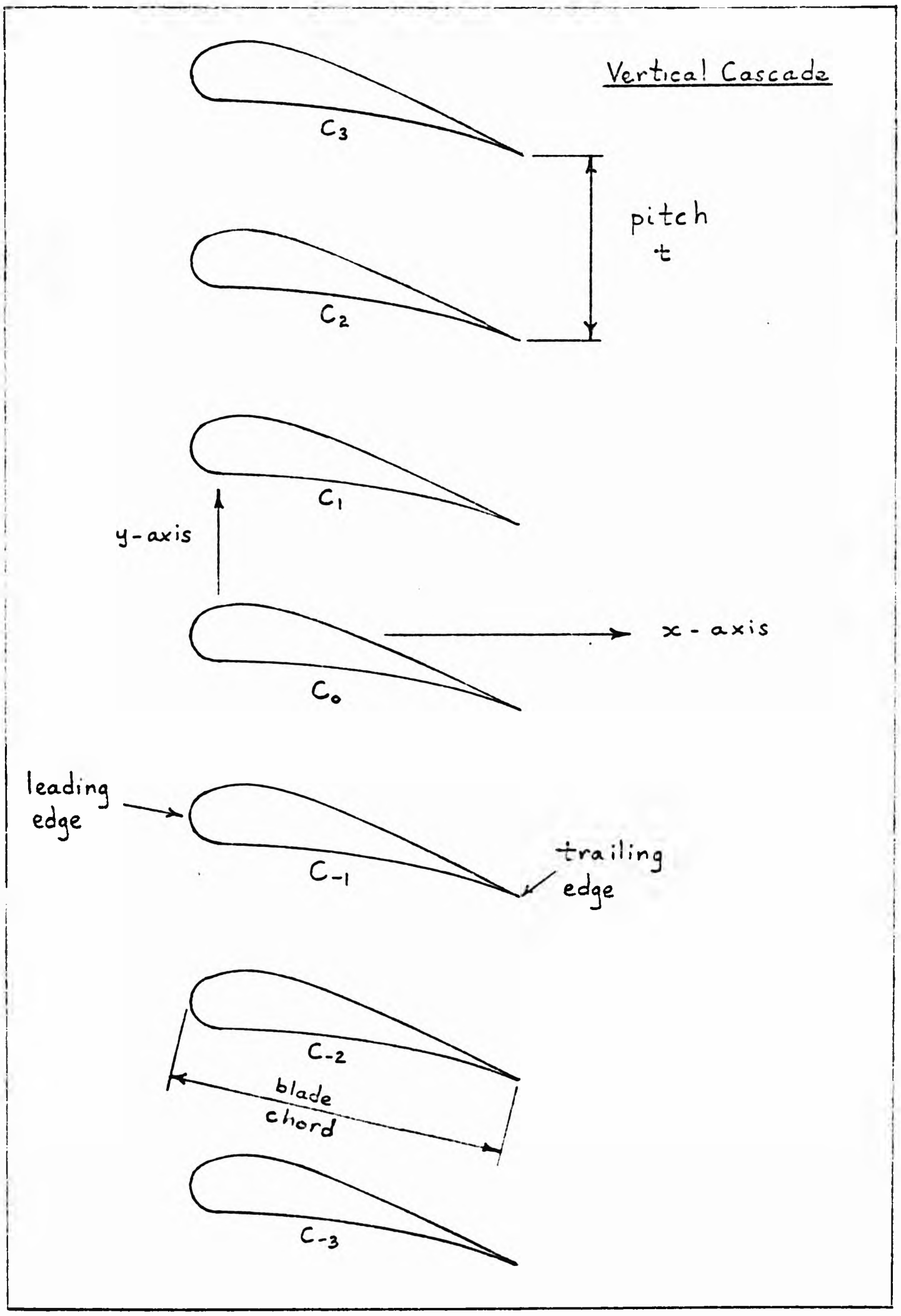
Vertical Cascade
C3
pitch
t
C2
C1
y-axis
x-axis
C0
leading
edge
C-1
trailing
edge
C-2
blade
chord
C-3

Figure 2-6

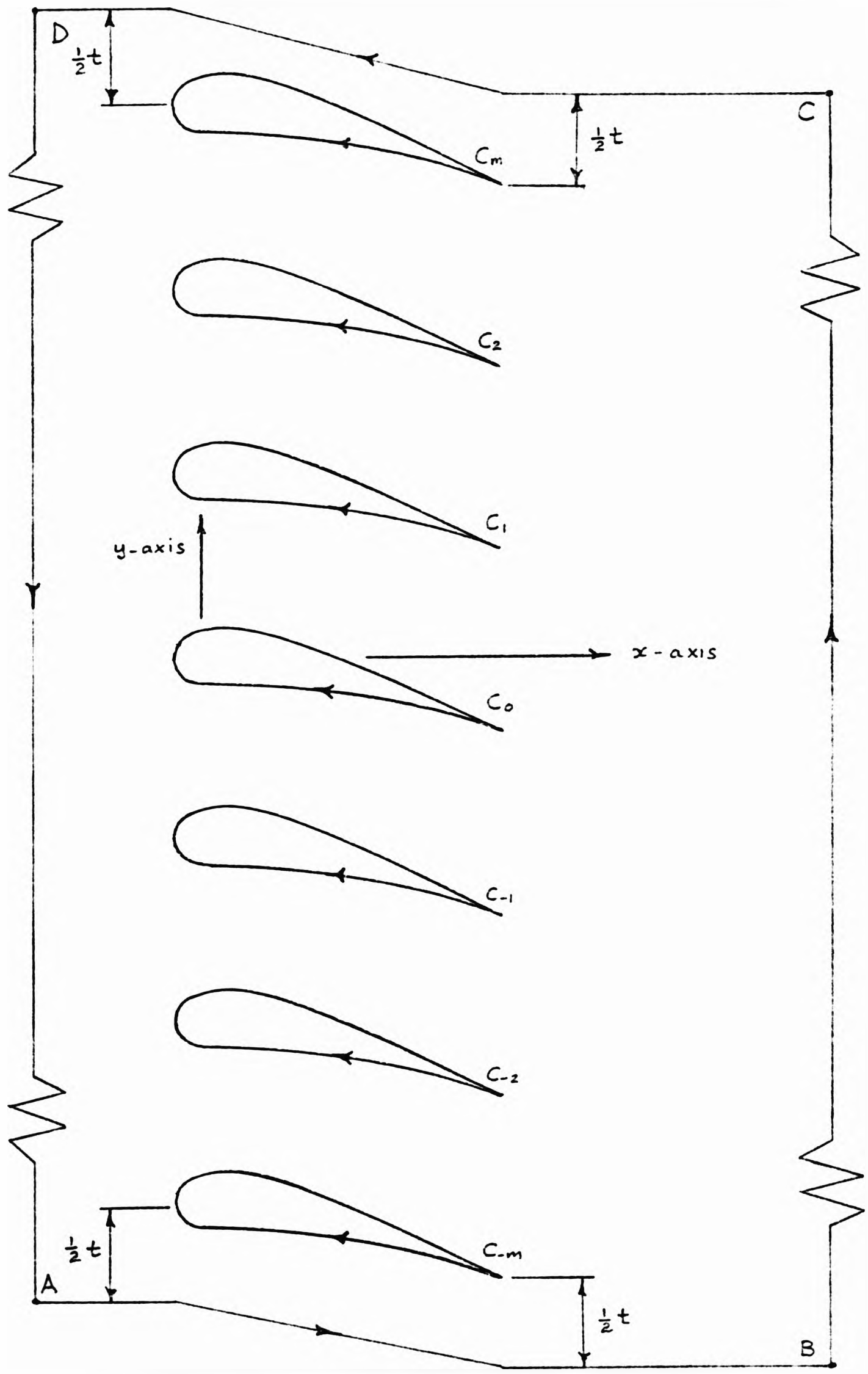

Figure 2-7

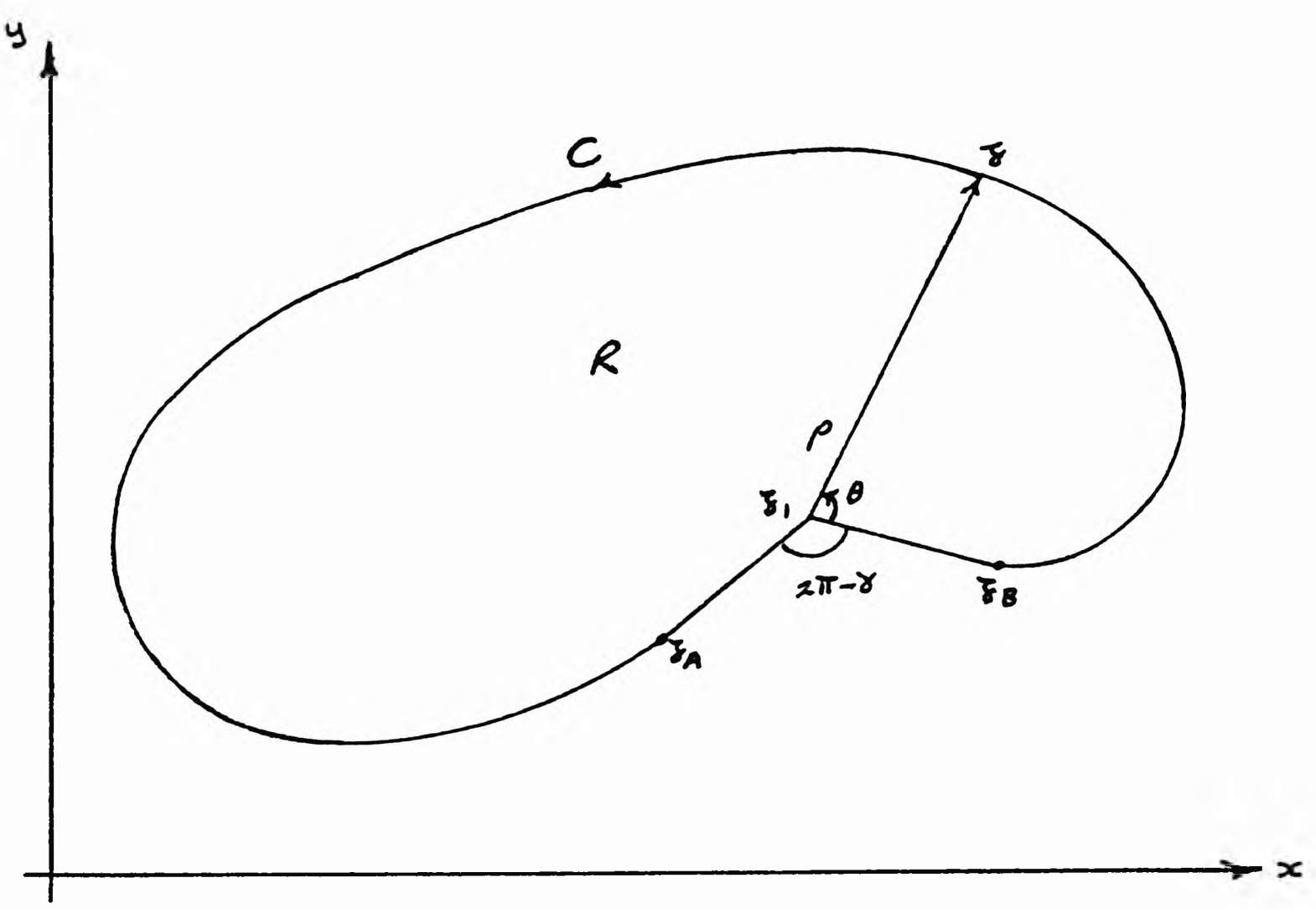

Figure 2-8

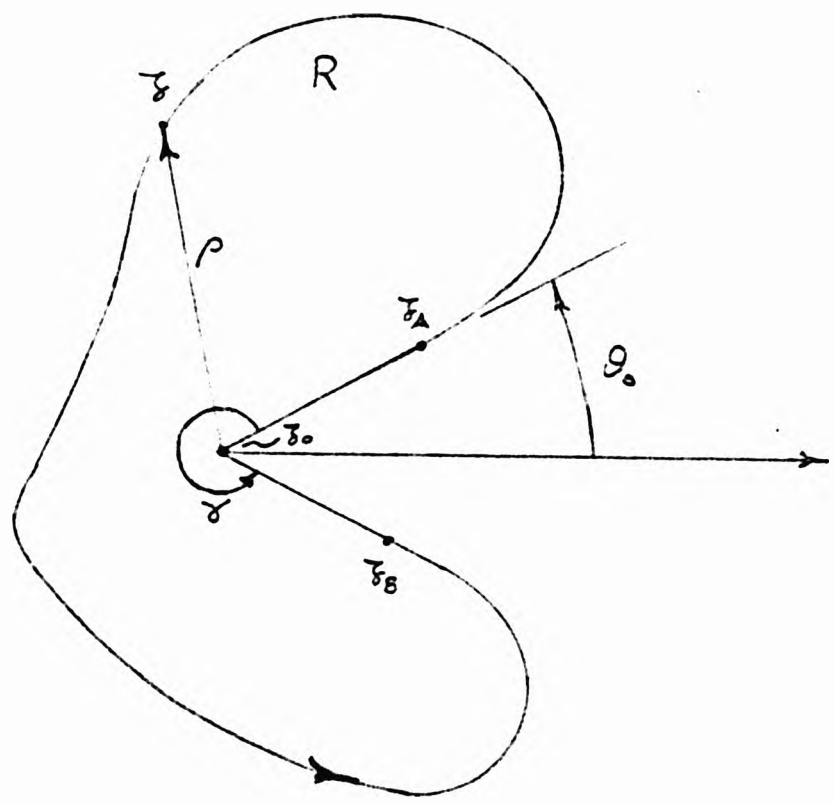

Figure 3-1

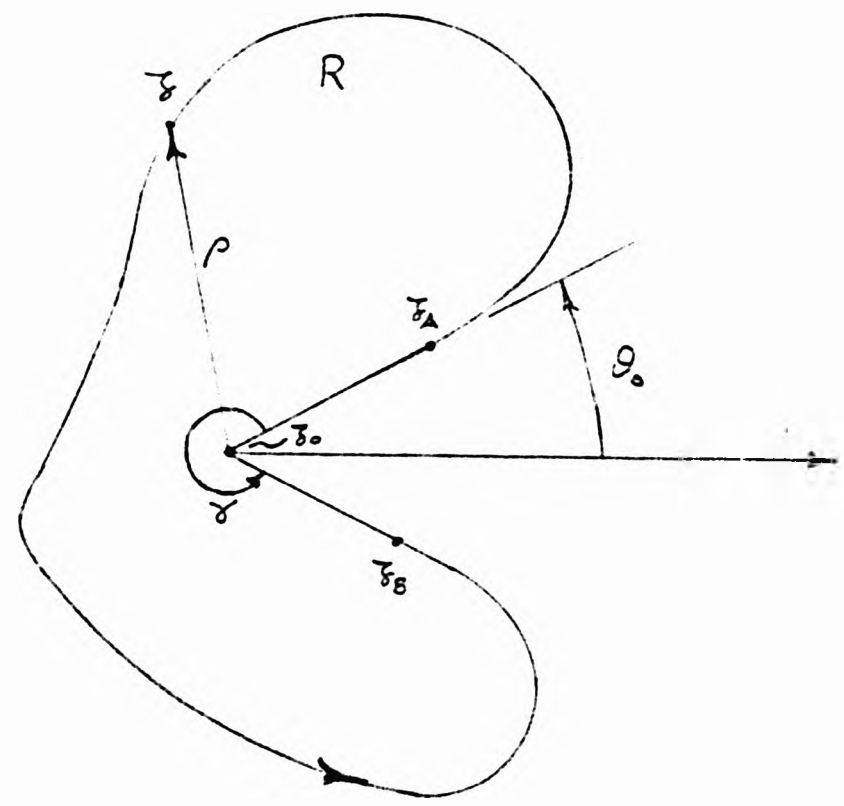

Figure 3-1

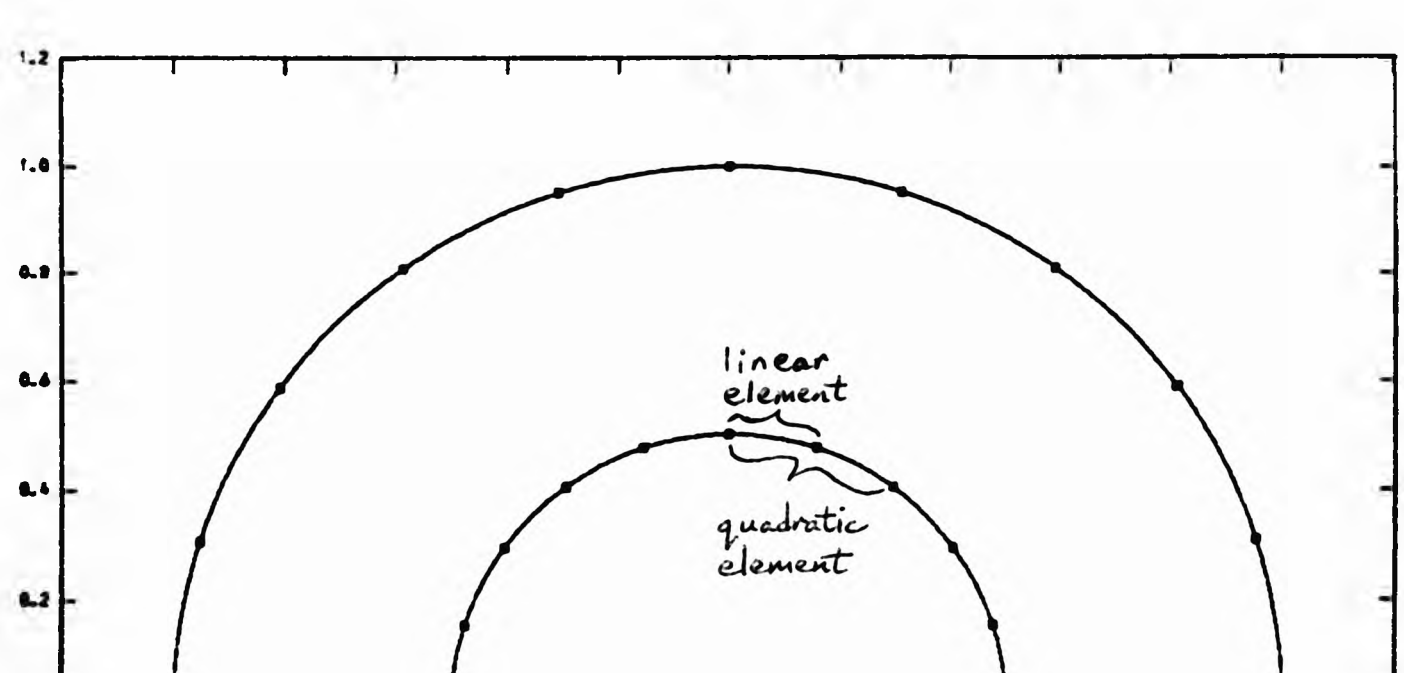

Figure 3-2

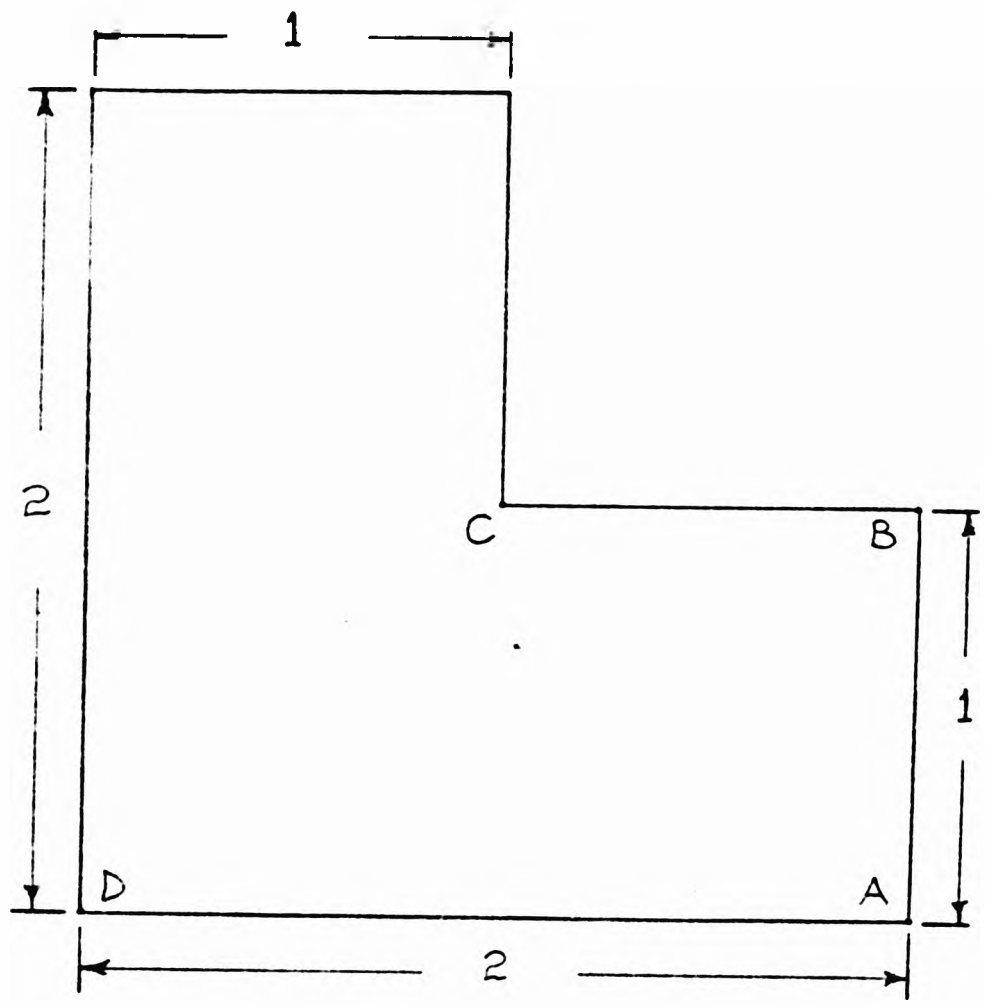

Figure 3-3

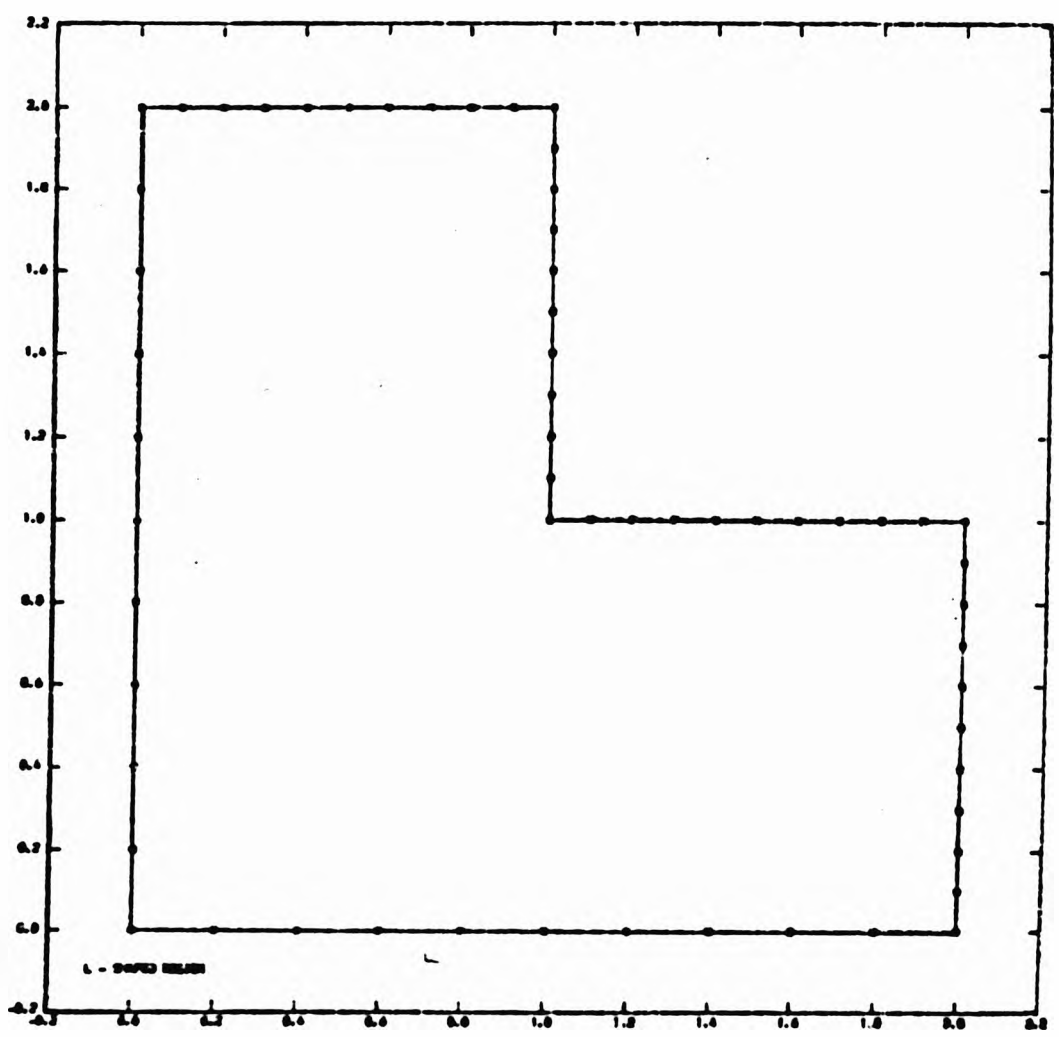

Figure 3-4

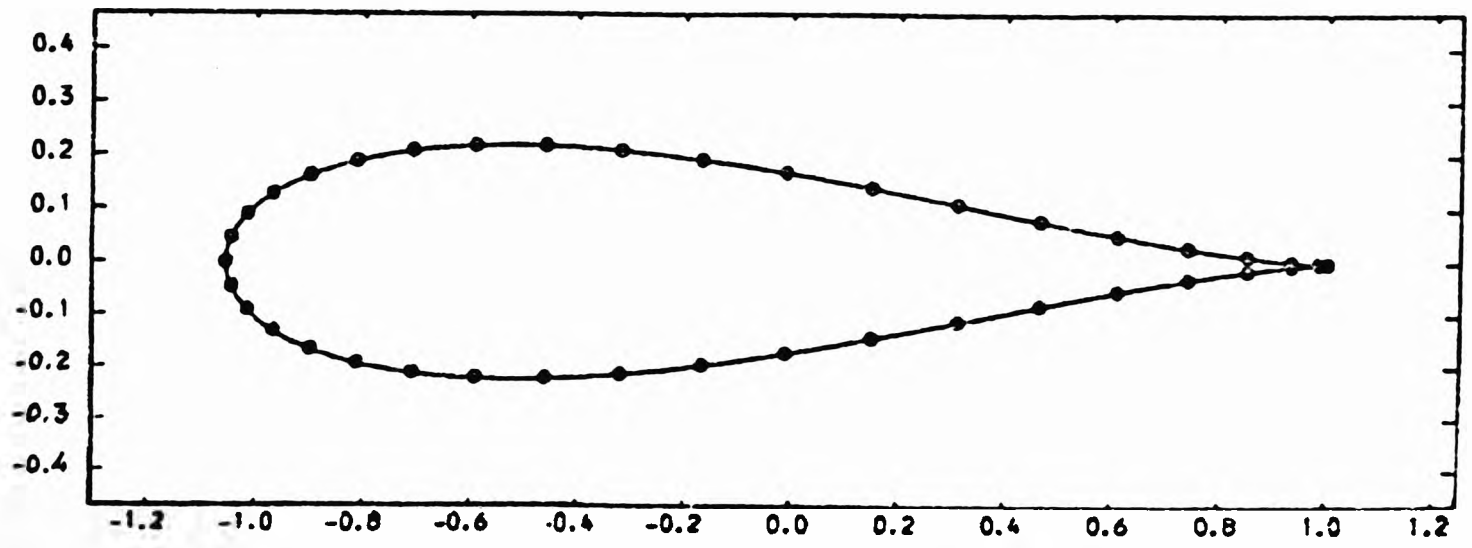

Figure 3-5

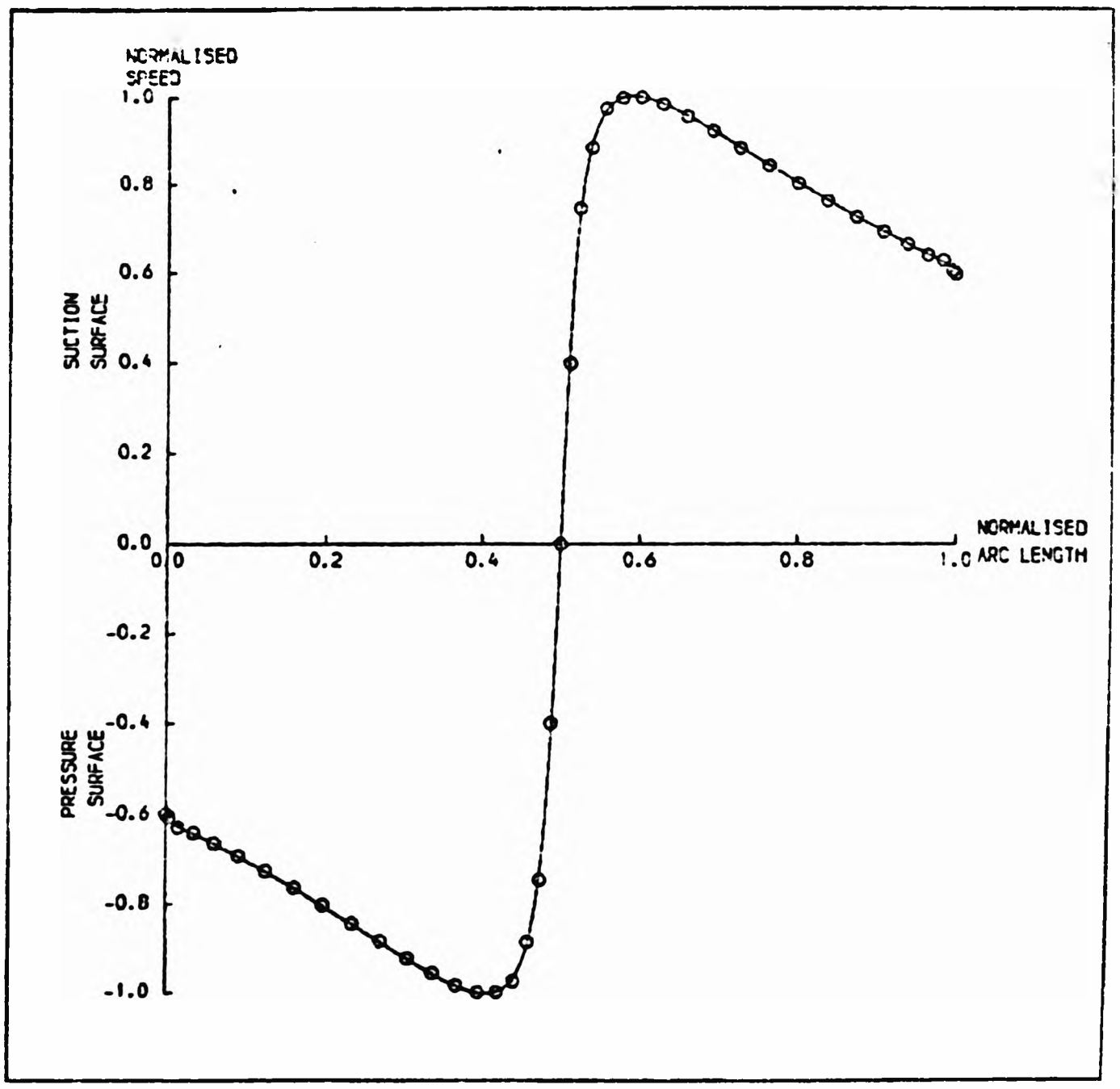

Figure 3-6

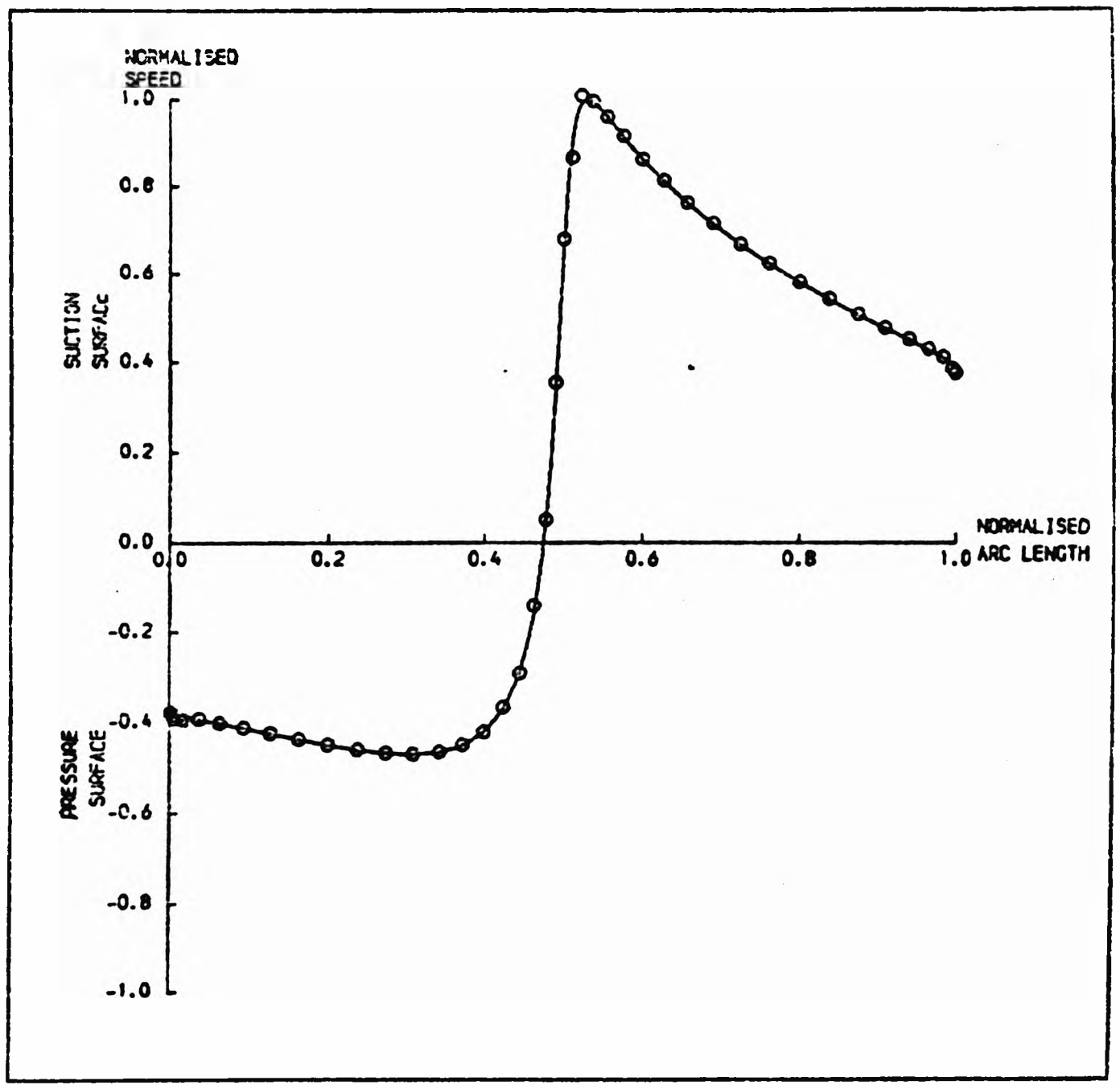
NORMALISED
SPEED
1.0
0.8
0.6
0.4
0.2
0.0
-0.2
-0.4
-0.6
-0.8
-1.0
SUCTION
SURFACE
PRESSURE
SURFACE
0.0
0.2
0.4
0.6
0.8
1.0
NORMALISED
ARC LENGTH

Figure 3-7

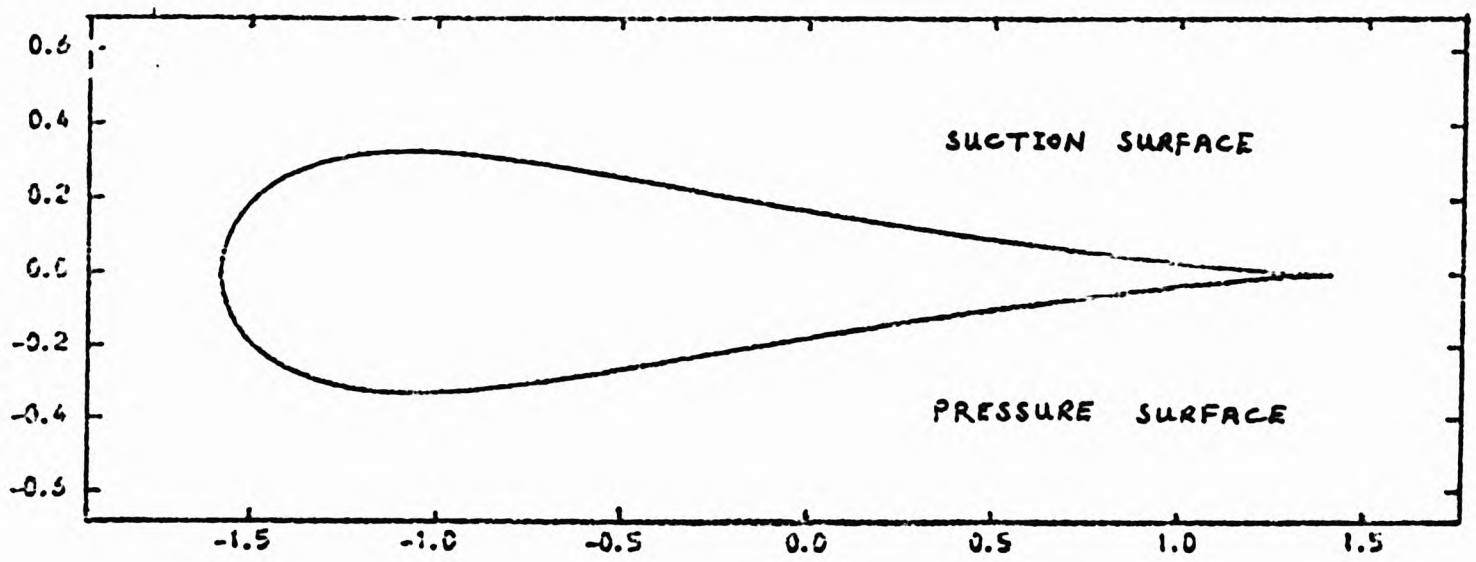

Figure 4-1

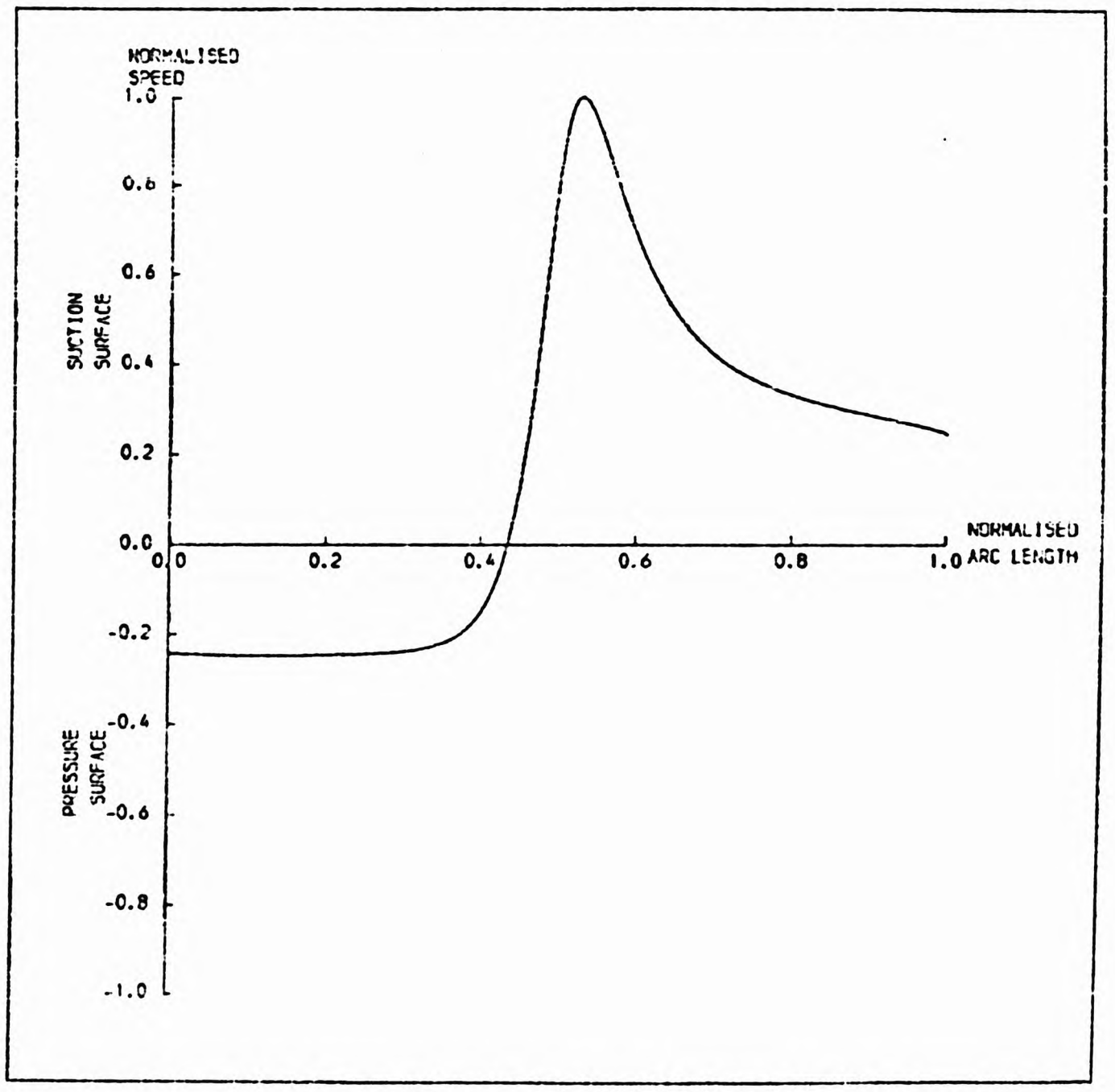

Figure 4-2

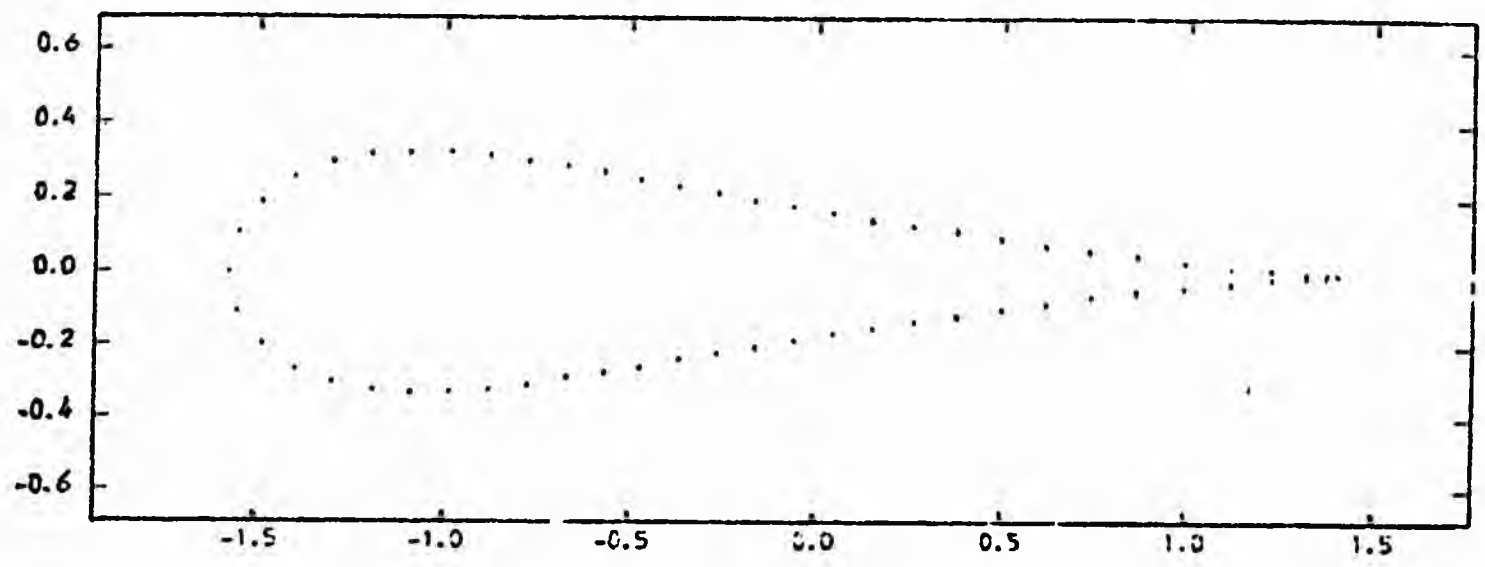

Figure 4-3

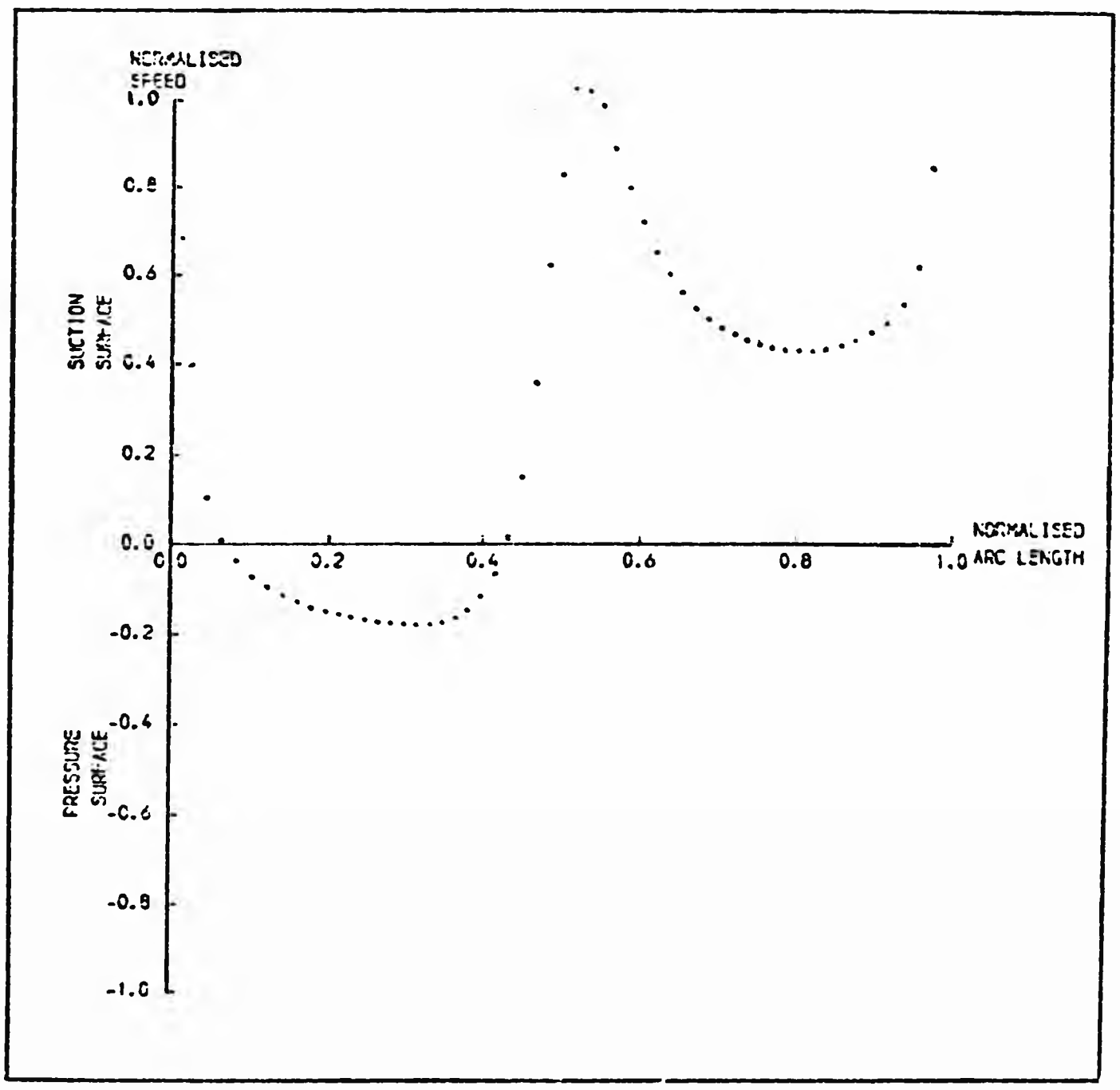

Figure 4-4

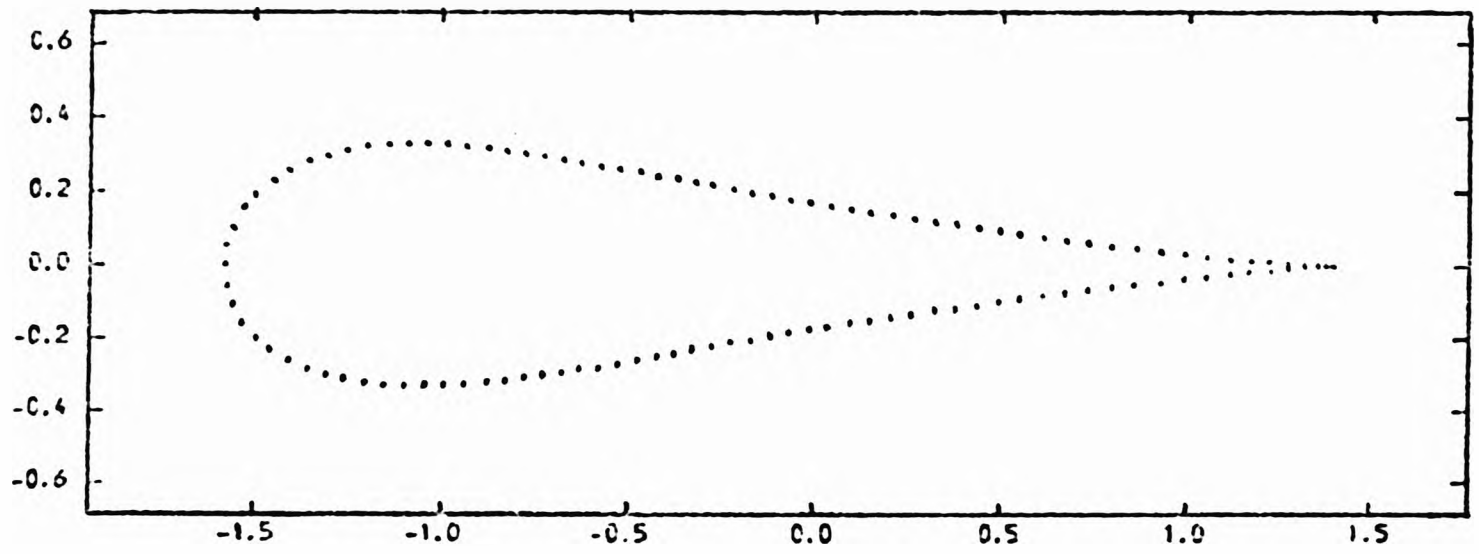

Figure 4-5

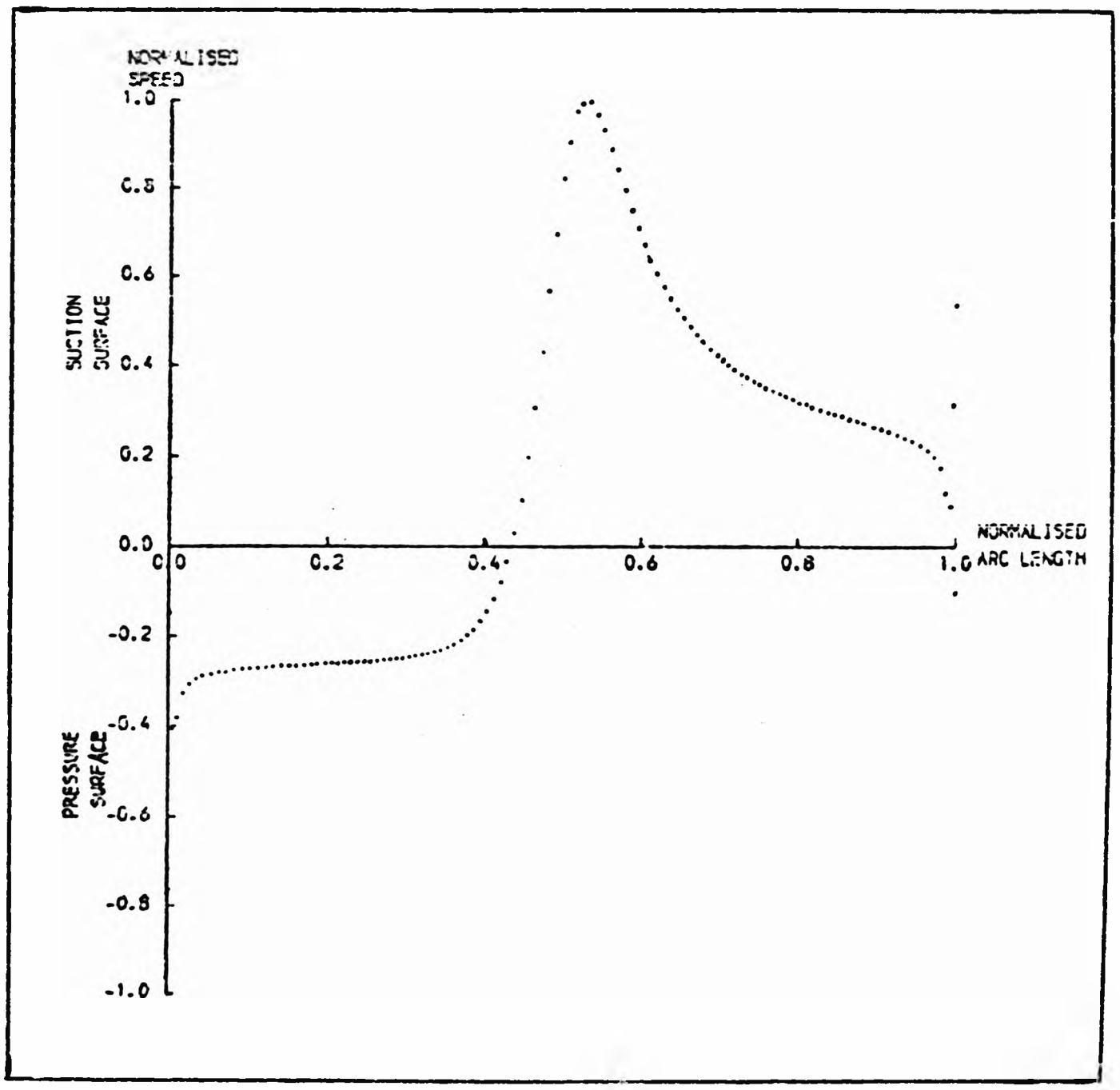

Figure 4-6

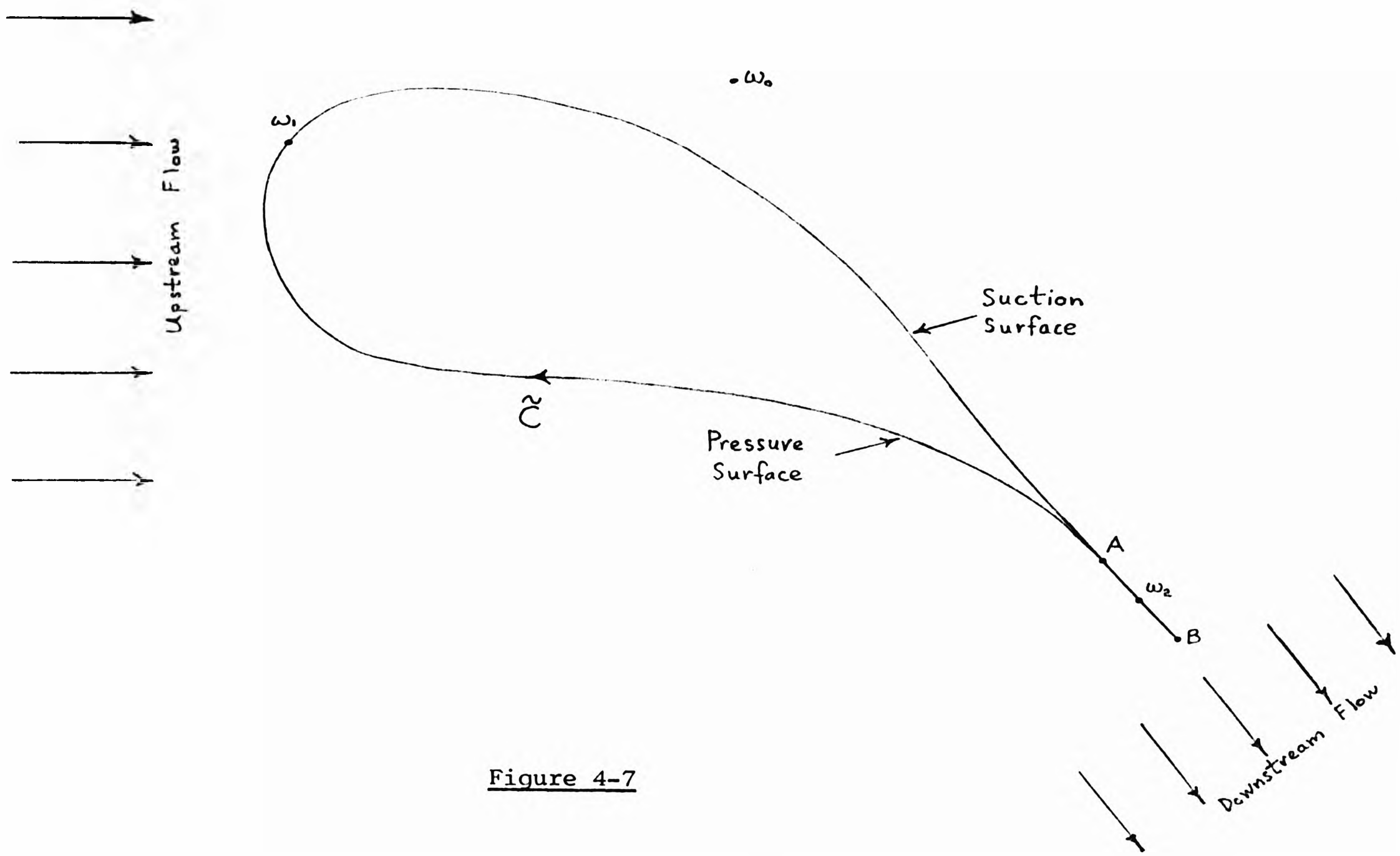
Upstream Flow
ω_1
$-\omega_0$
Suction Surface
$\tilde{C}$
Pressure Surface
A
ω_2
B
Downstream Flow

Figure 4-7

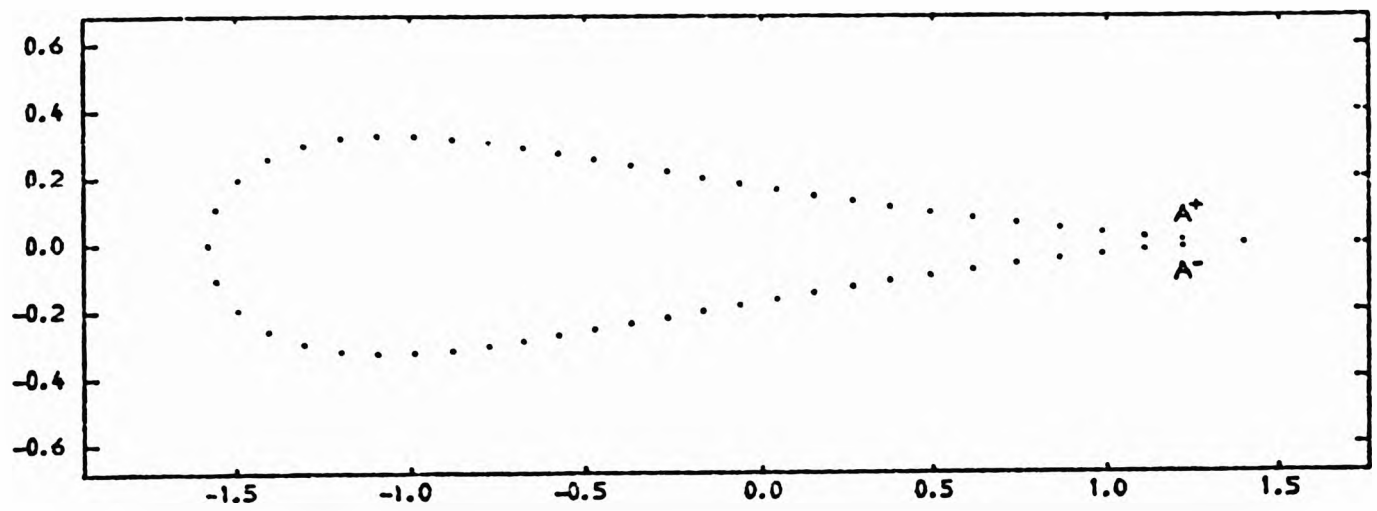

Figure 4-8

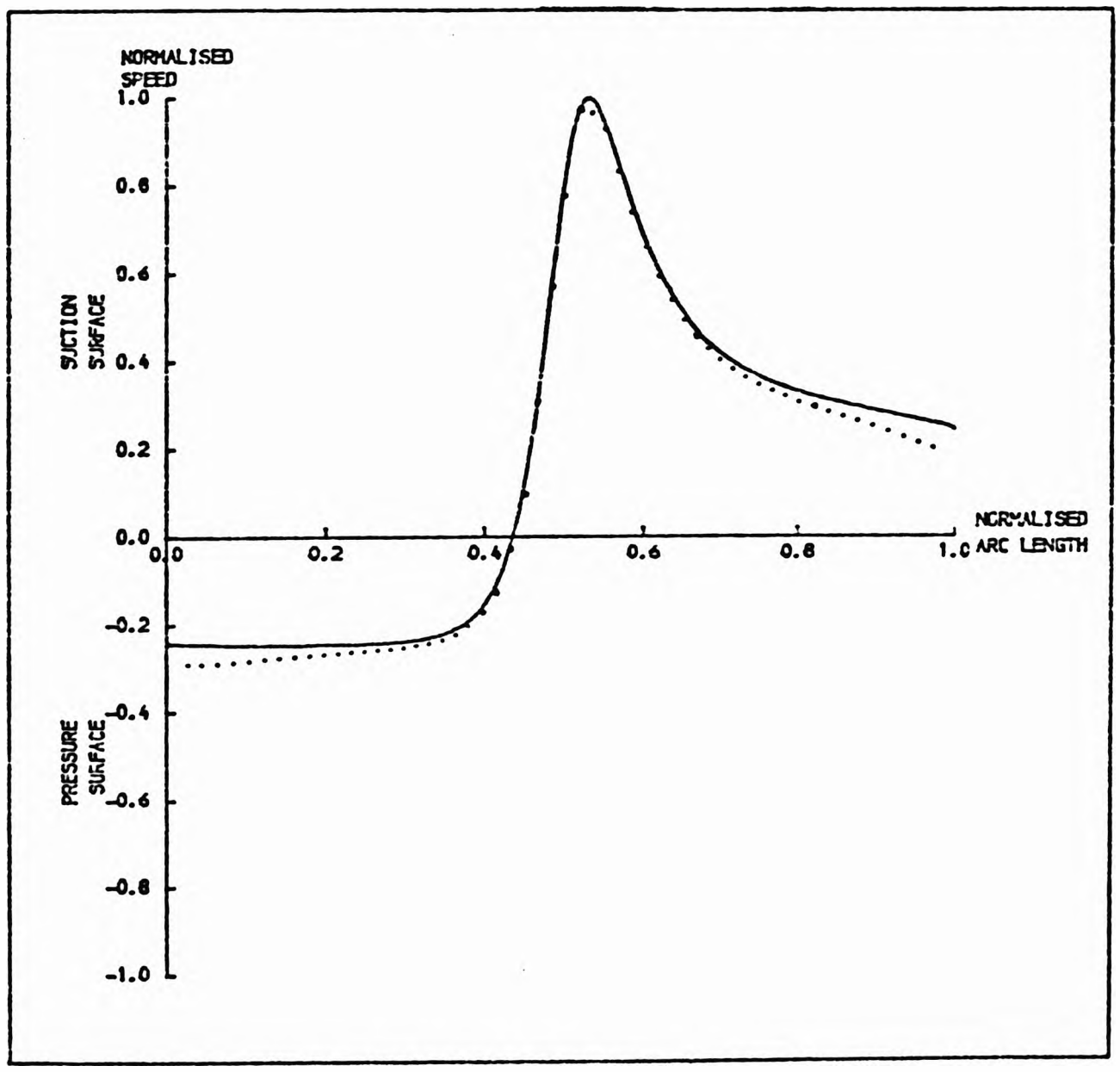

Figure 4-9

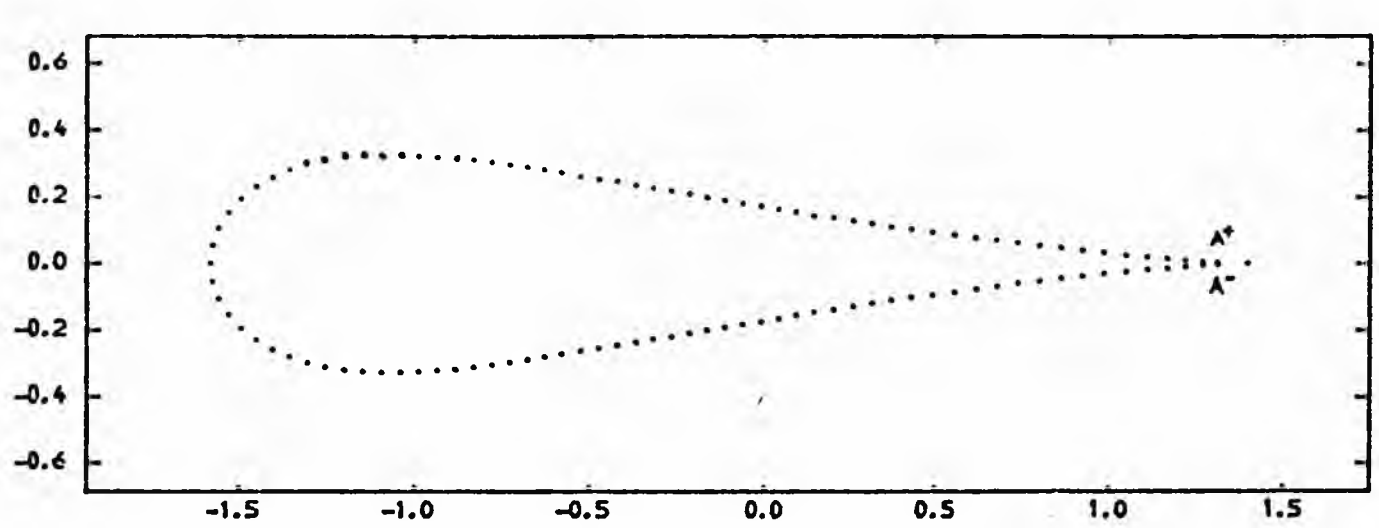

Figure 4-10

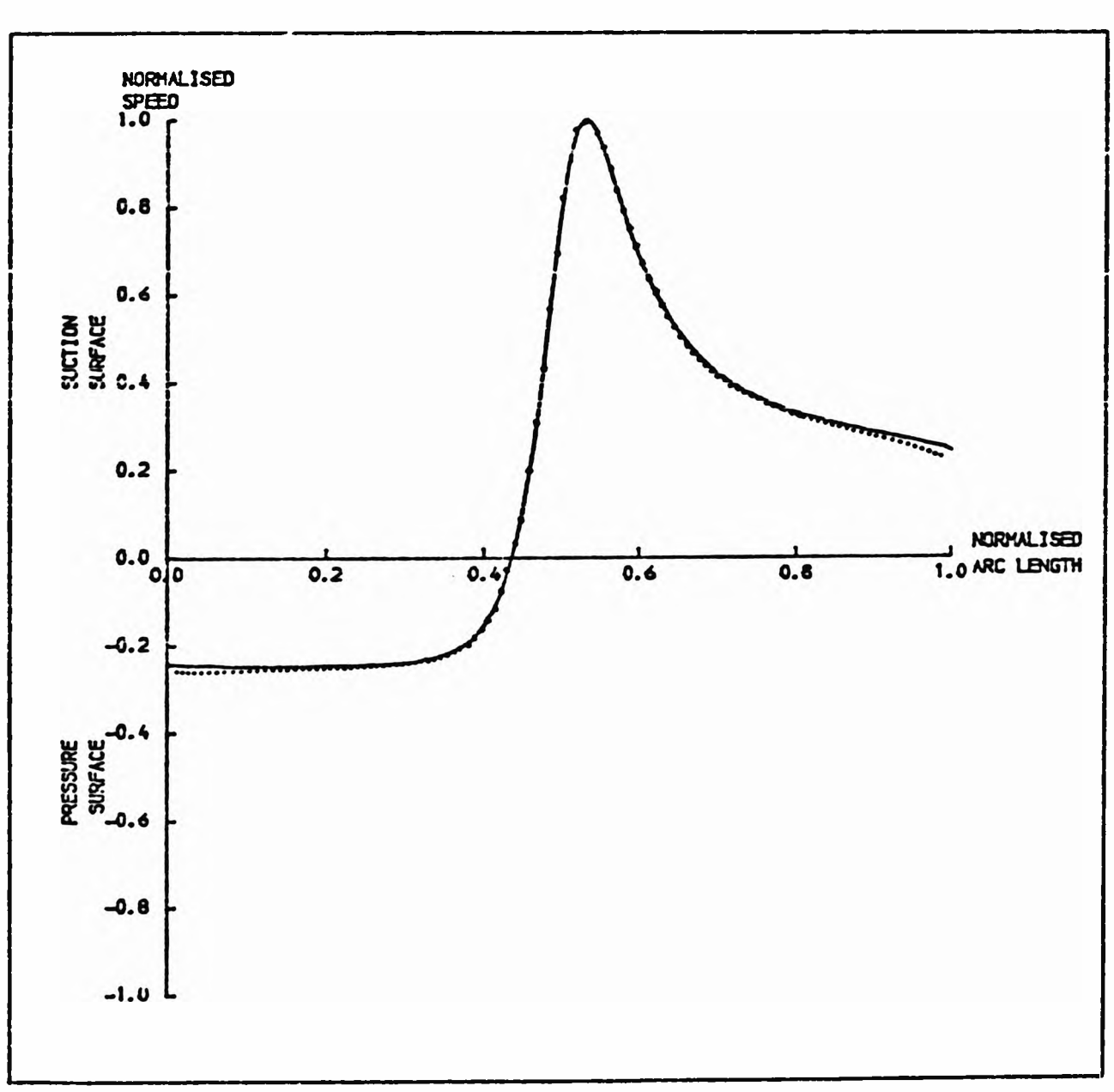

Figure 4-11

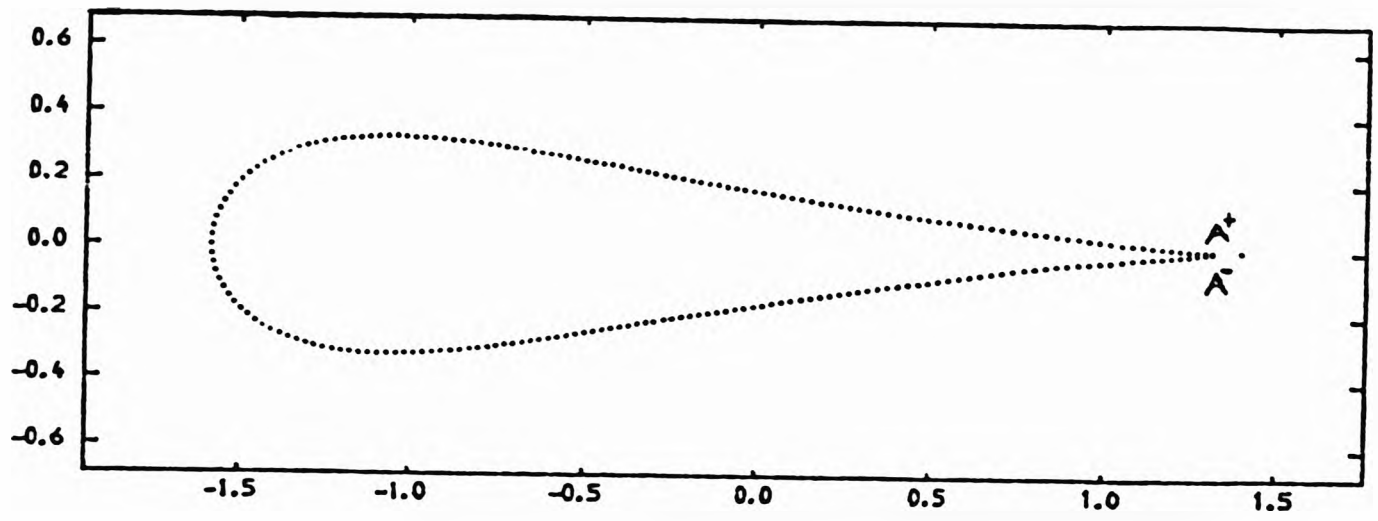

Figure 4-12

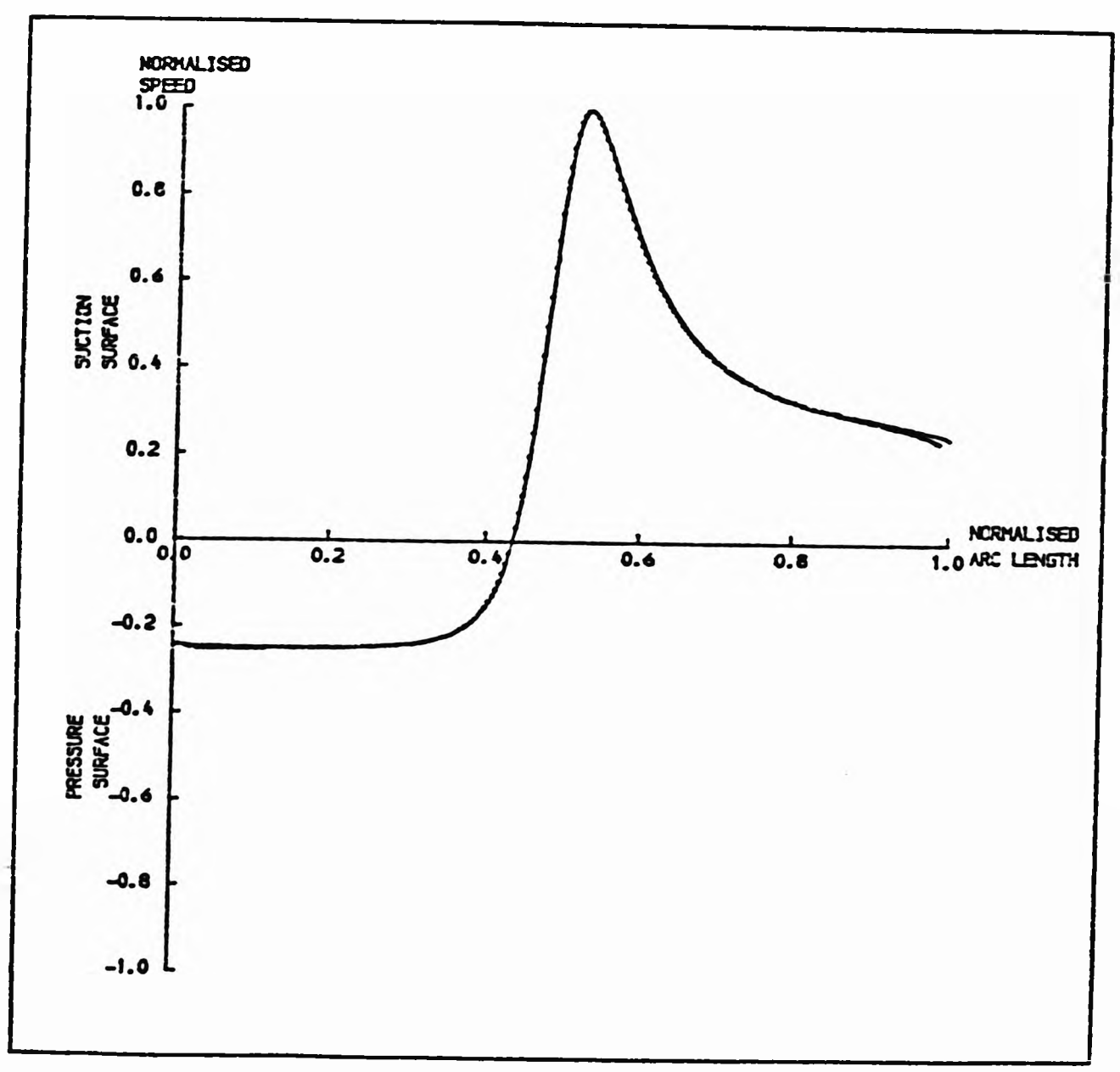

Figure 4-13

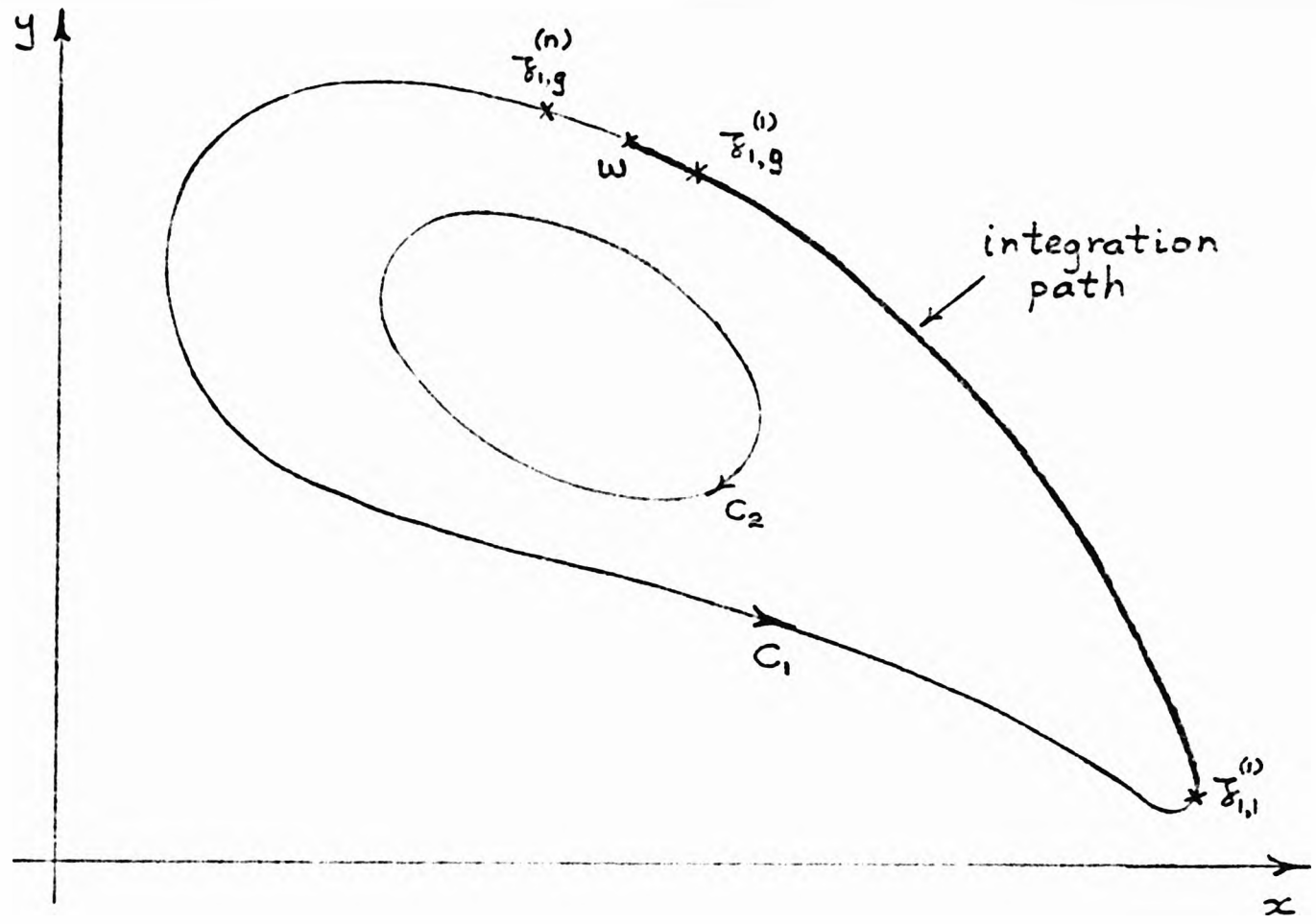

Figure 5-1

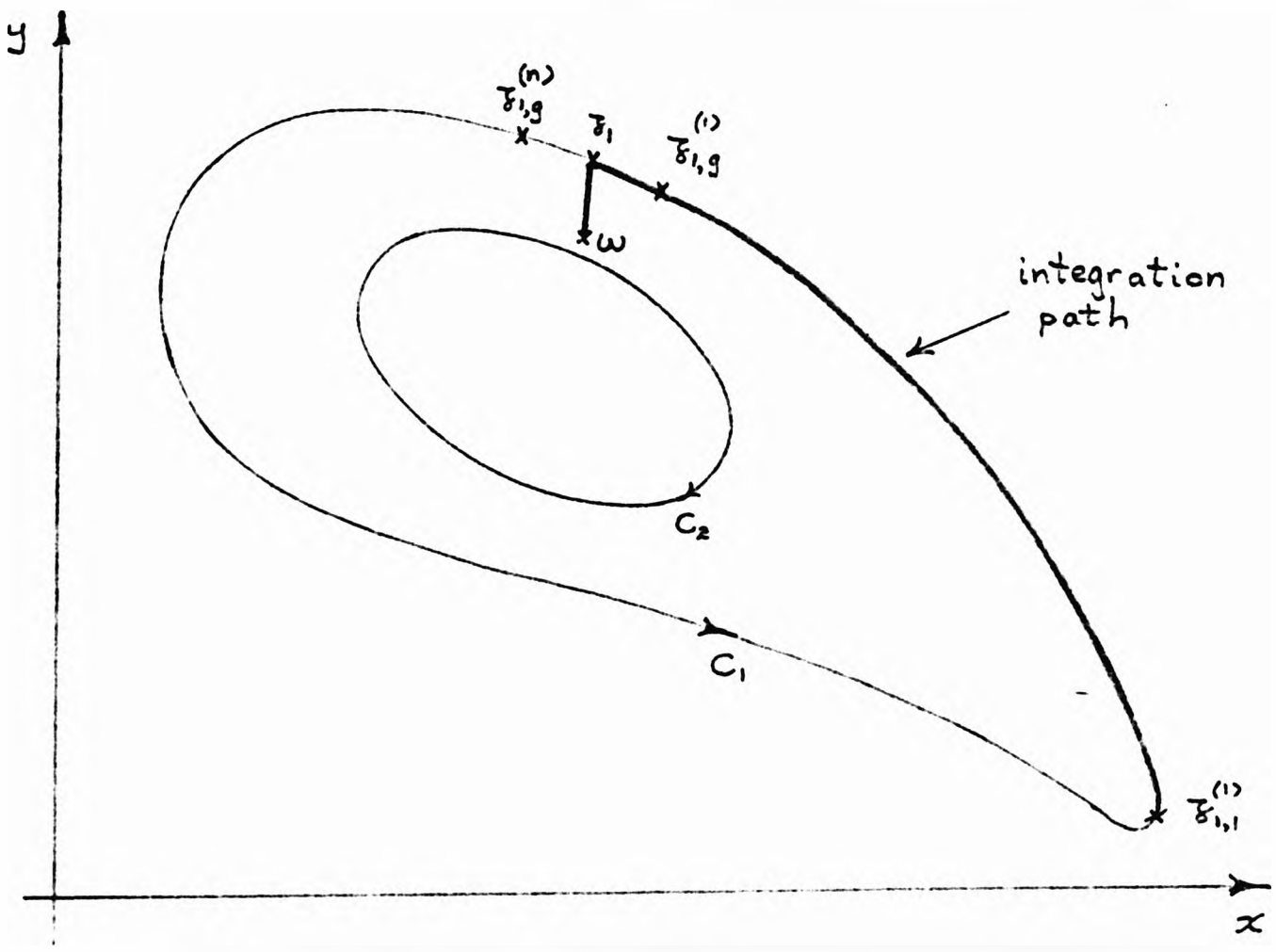

Figure 5-2

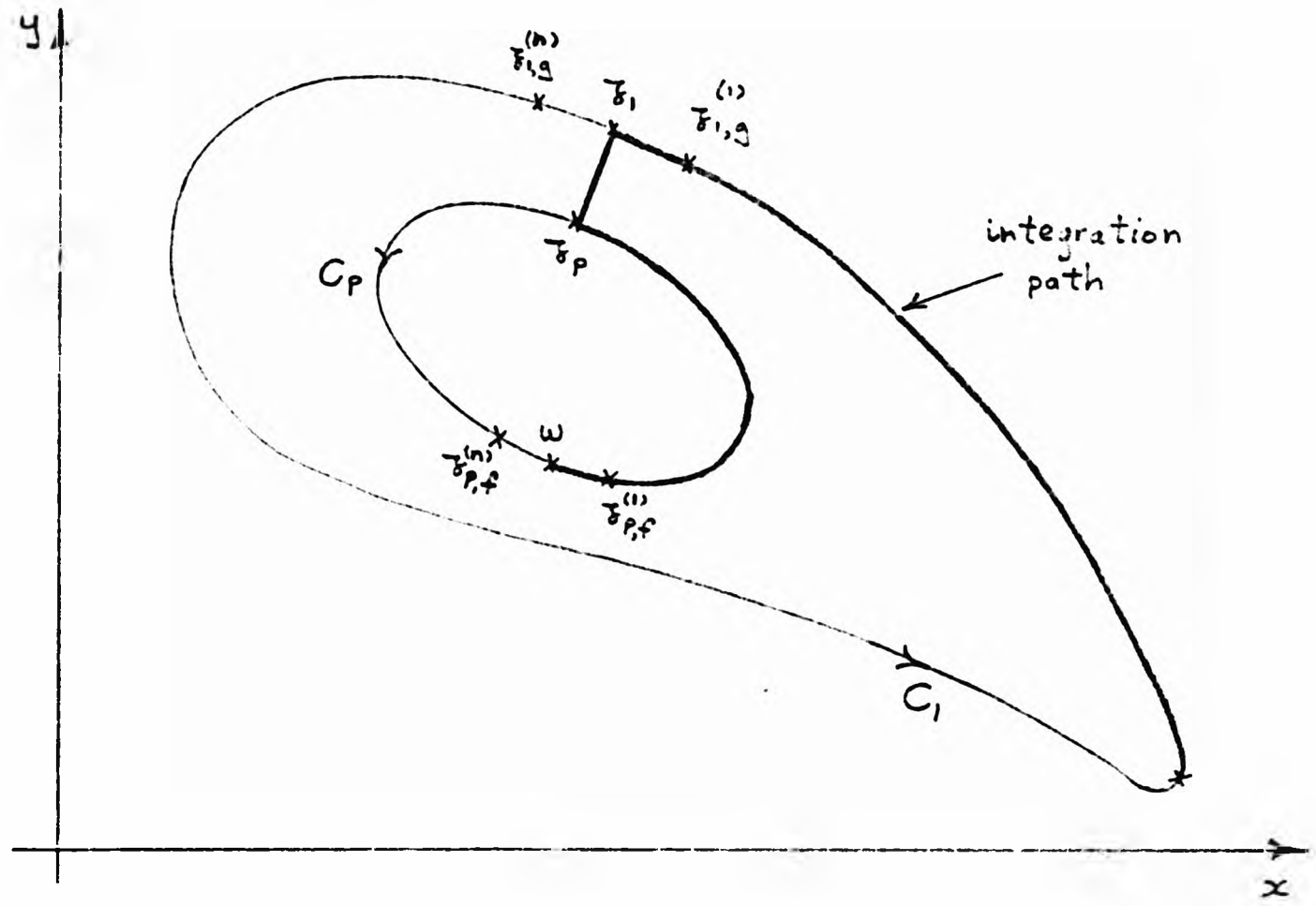

Figure 5-3

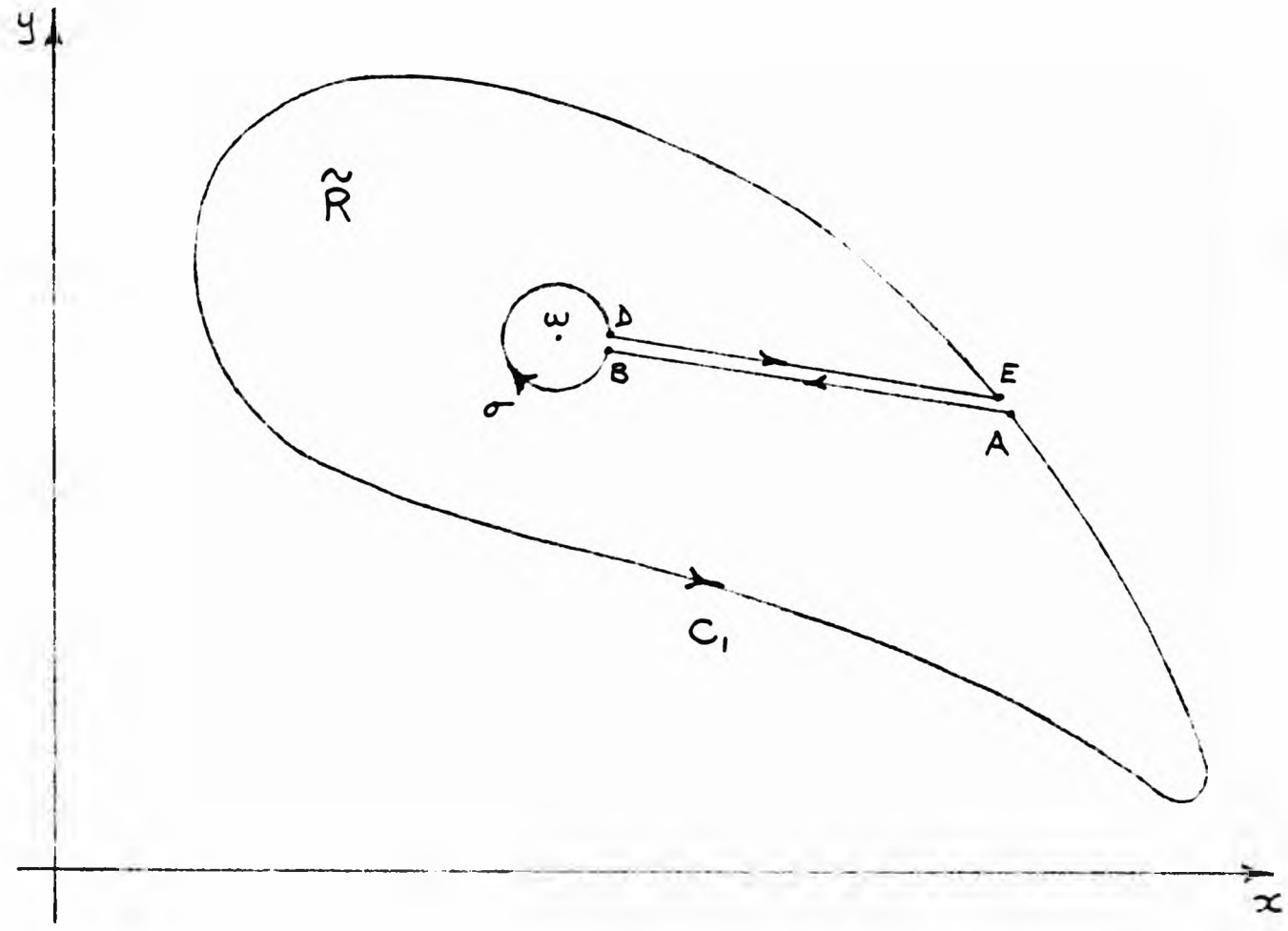

Figure 5-4

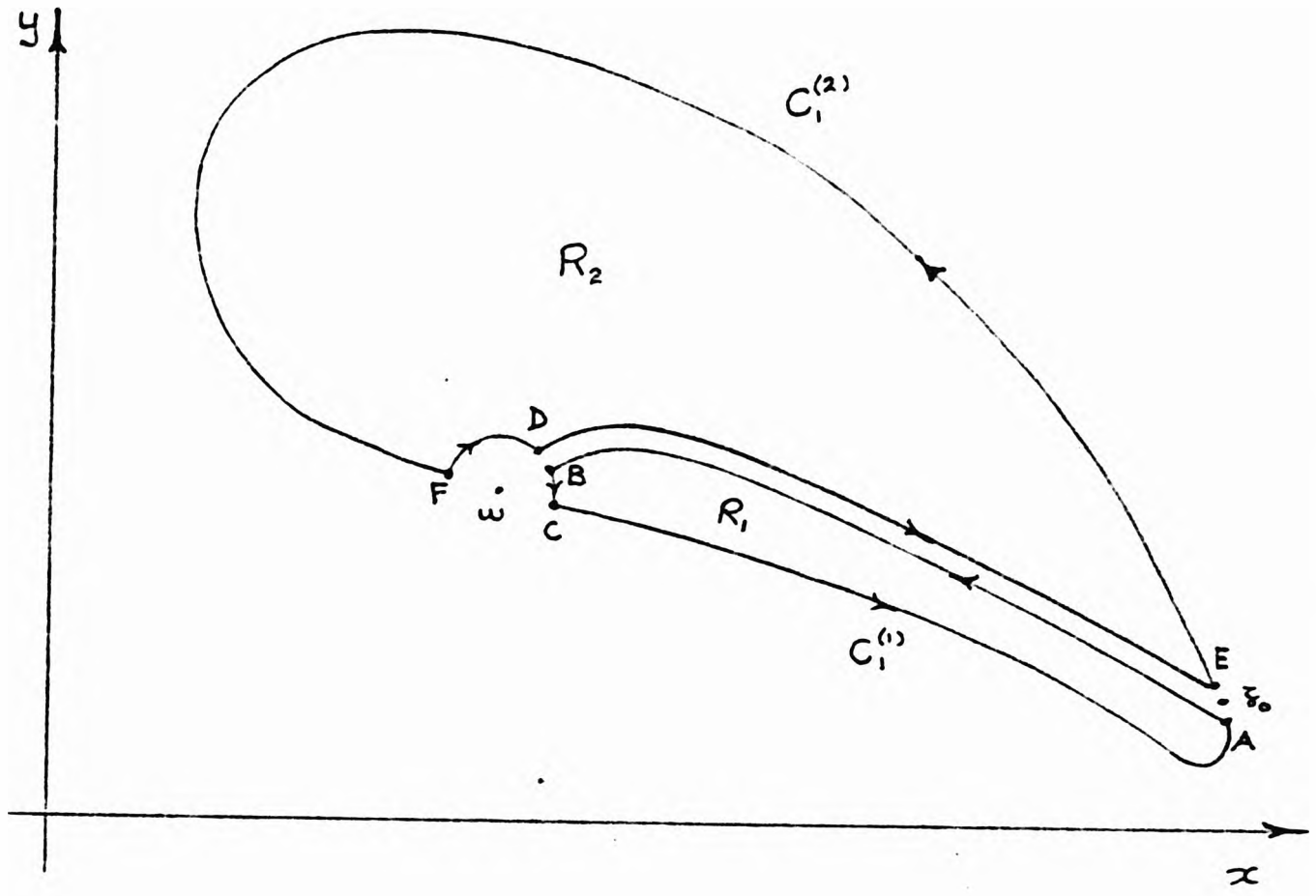

Figure 5-5

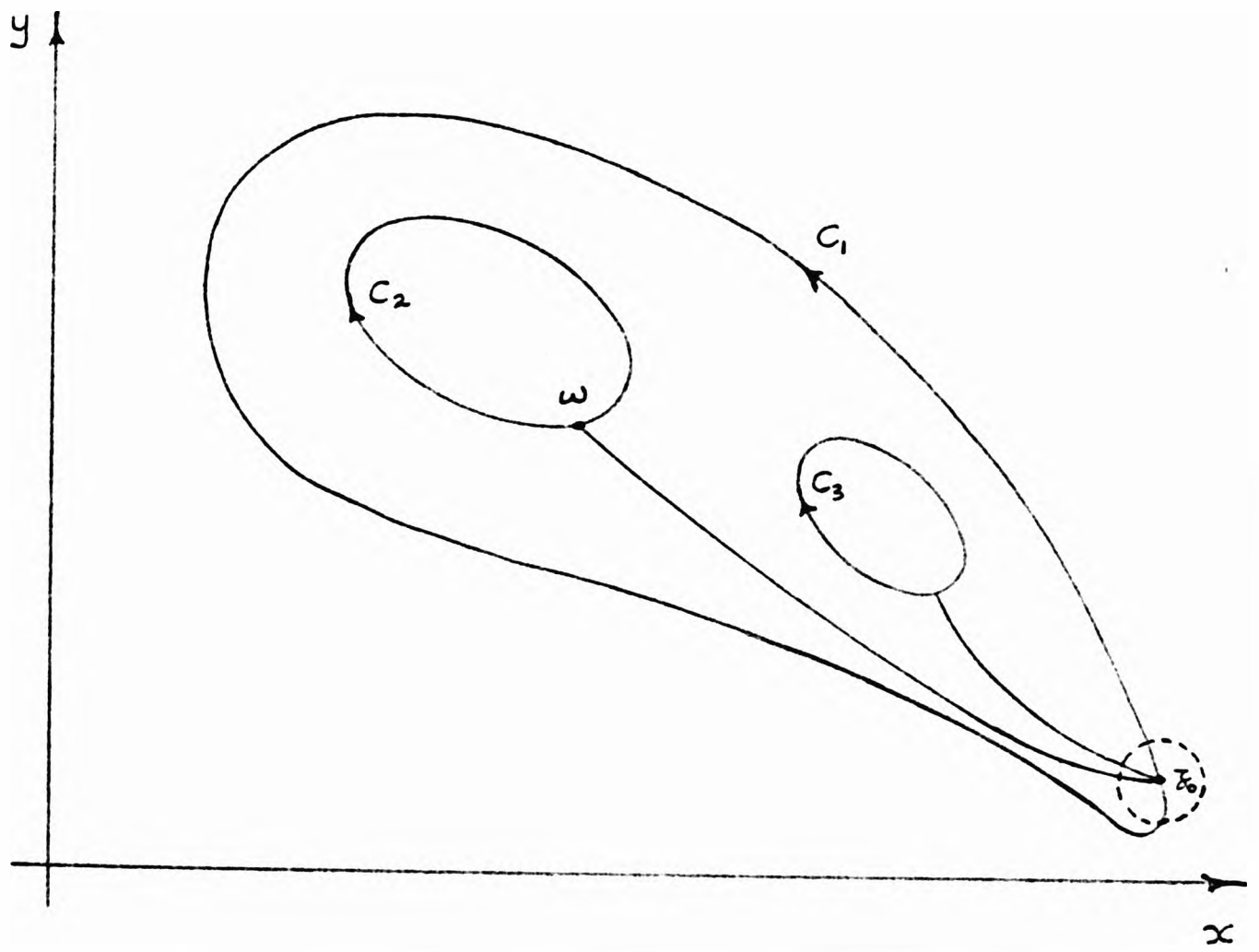

Figure 5-6

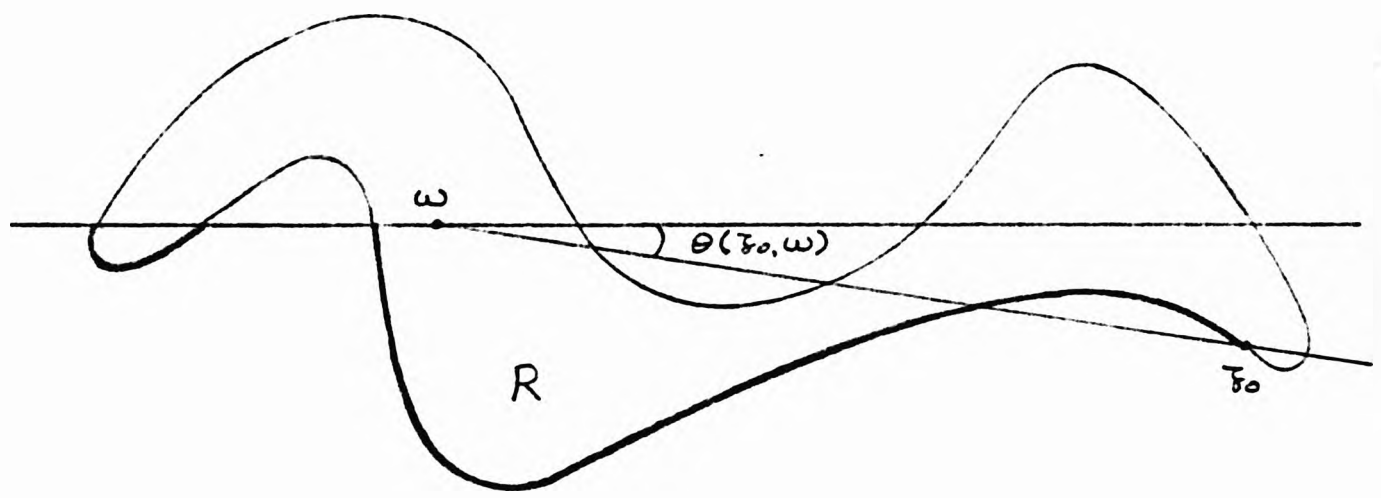

Figure 5-7

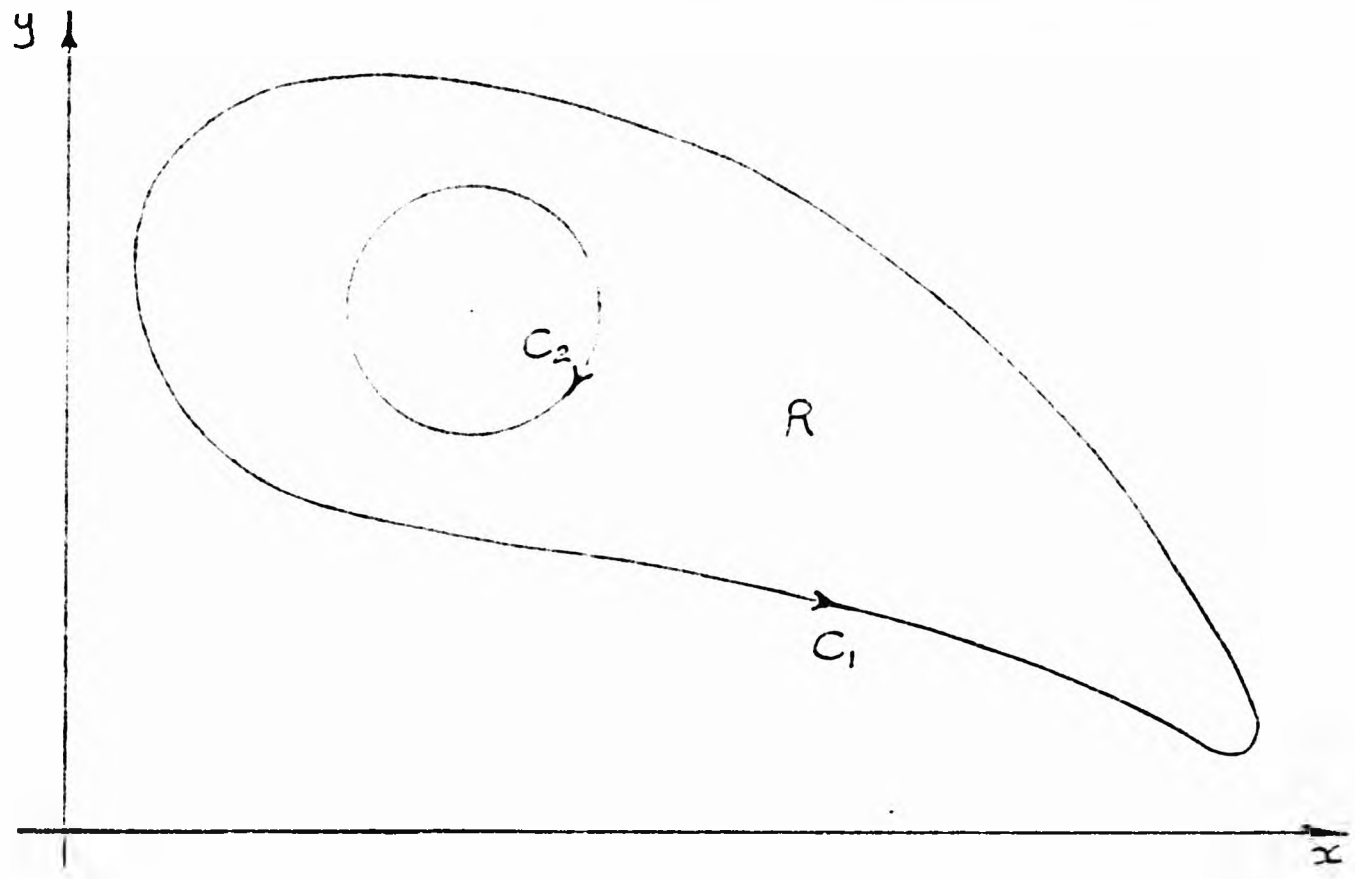

Figure 6-1

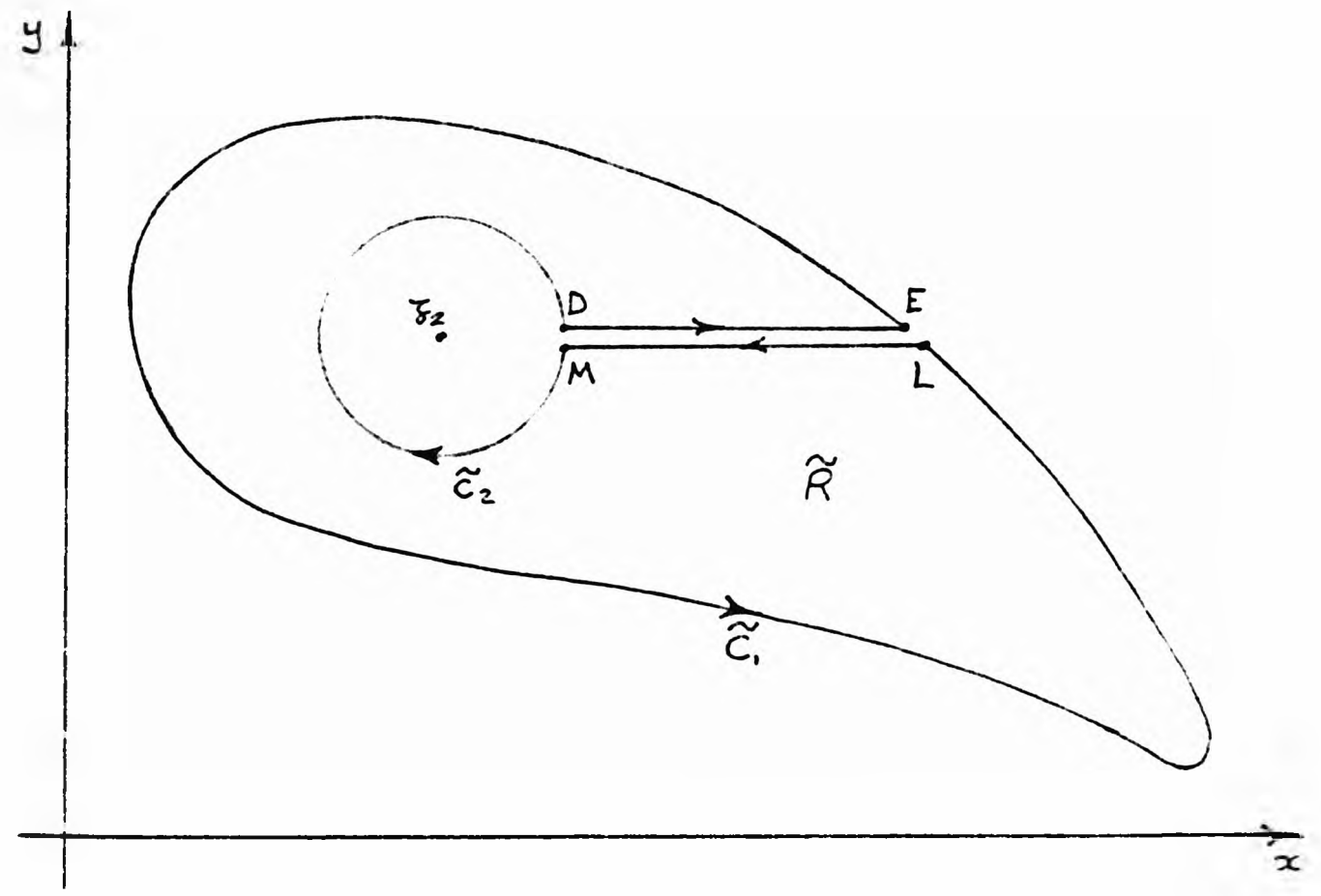

Figure 6-2

On C_1 $\quad \gamma = be^{i\theta}$

On C_2 $\quad \gamma = ae^{i\theta}$

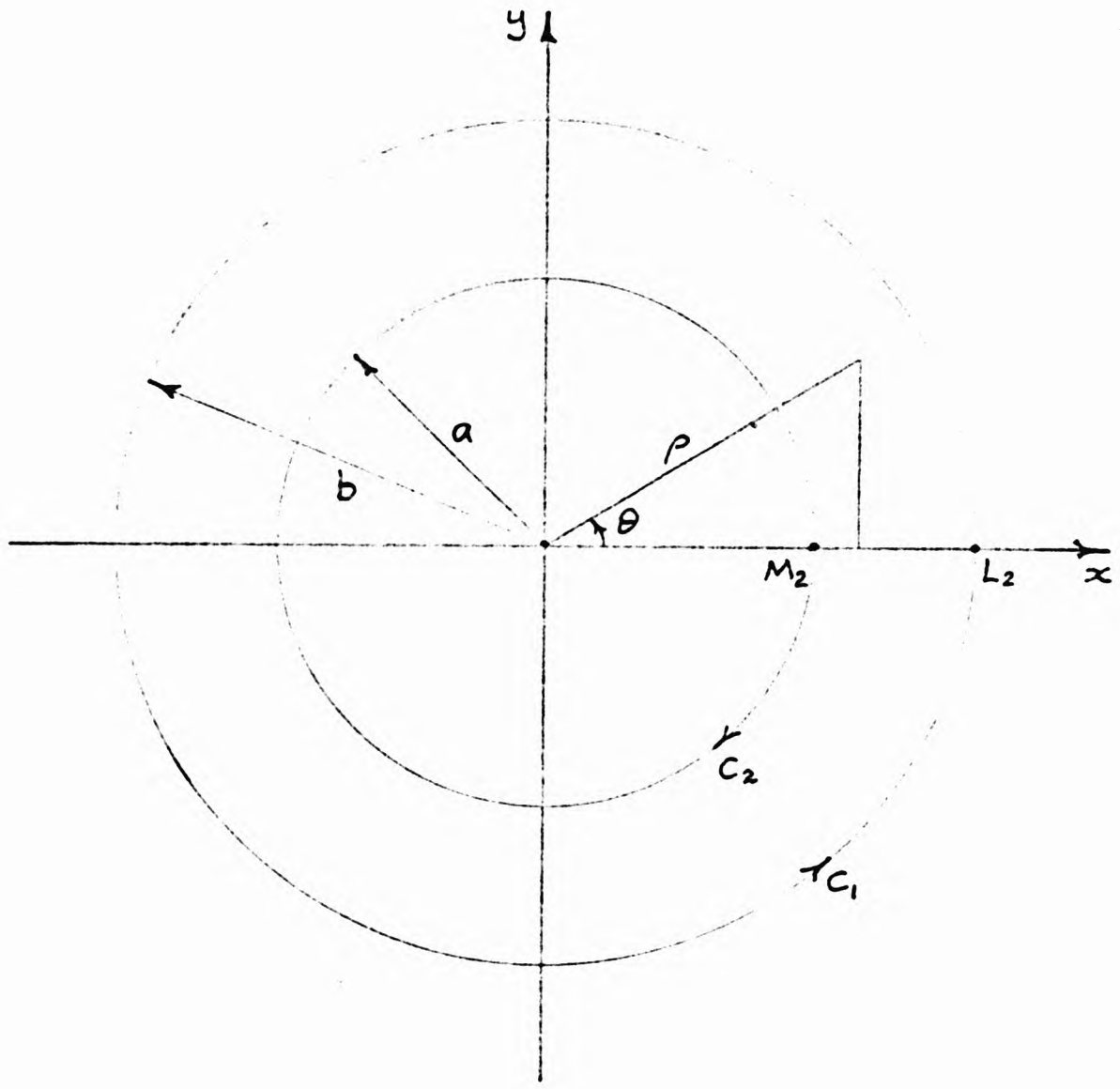

Figure 6-3

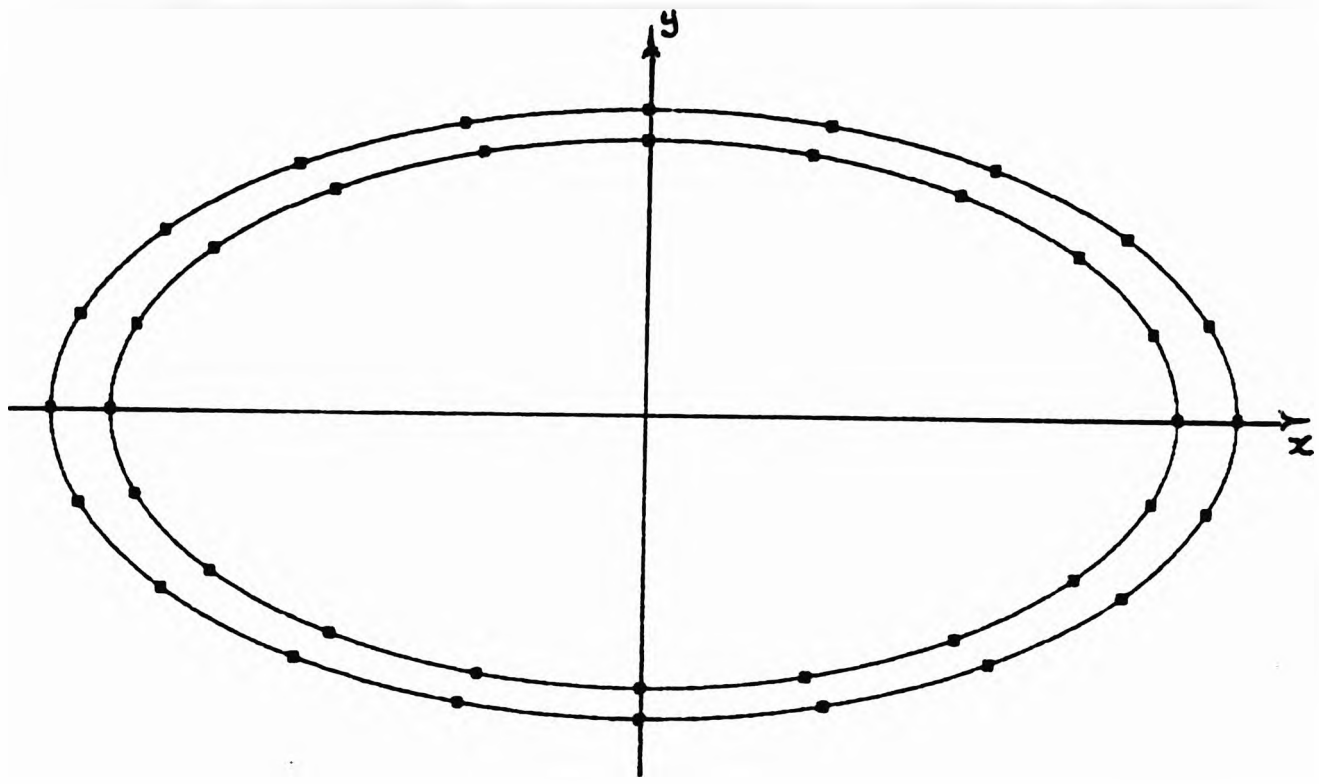

Figure 6-4

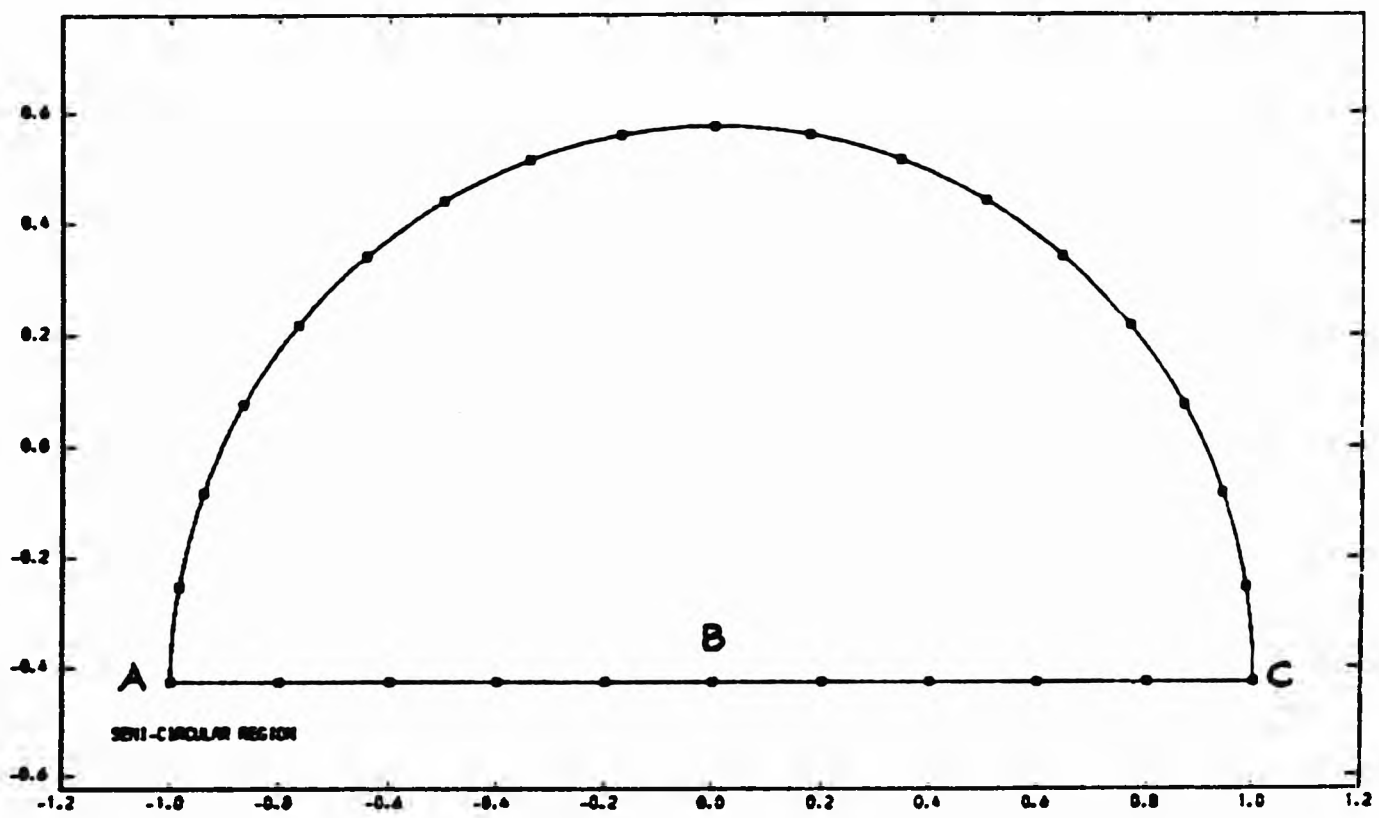

Figure 6-5

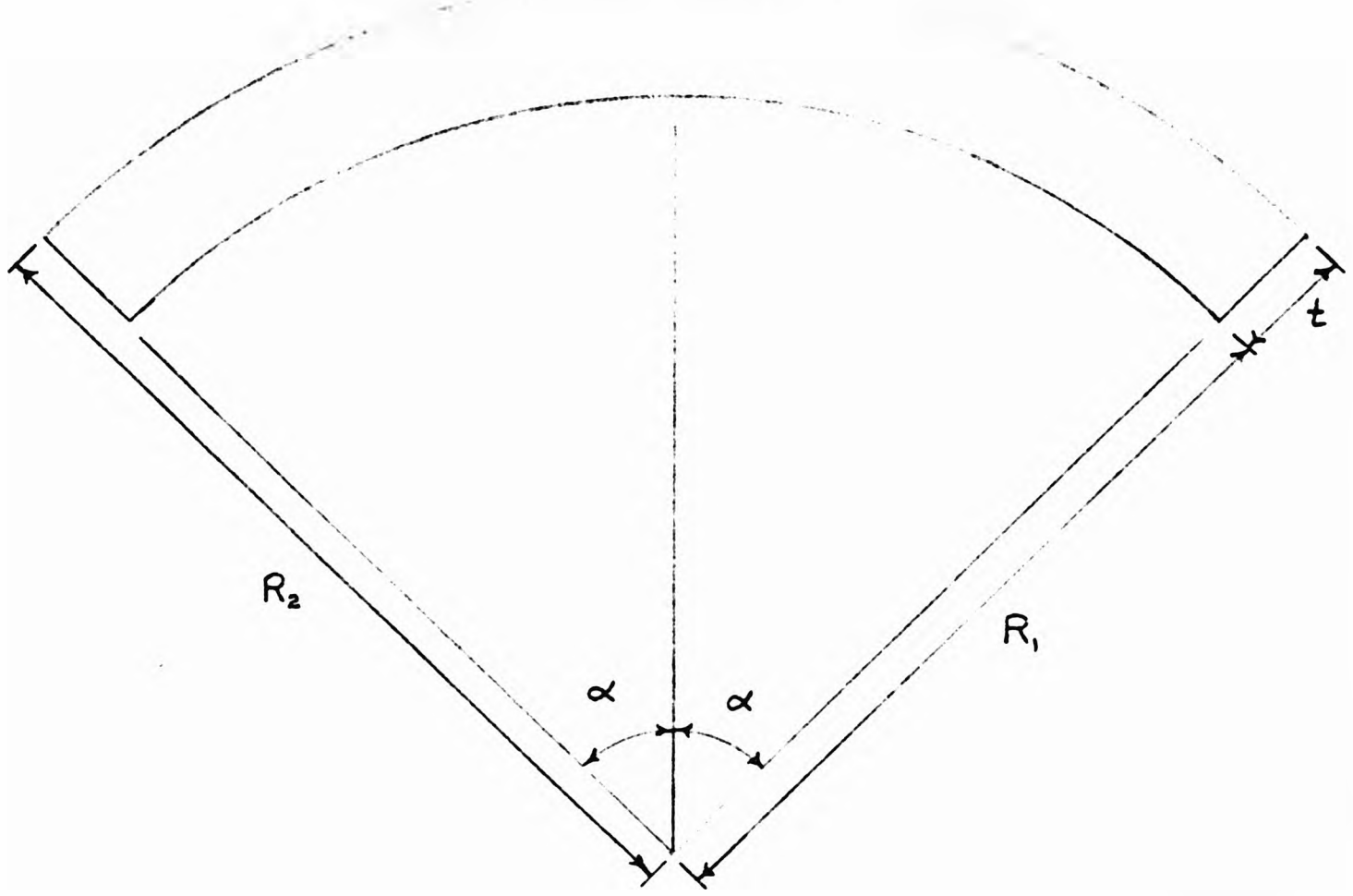

thickness $t = 1$

chord $c = 12$

$\alpha = 45°$

inner radius $R_1 = \frac{1}{2}\left\{\frac{c}{\sin\alpha} - t\right\}$

outer radius $R_2 = R_1 + t$

Figure 6-6

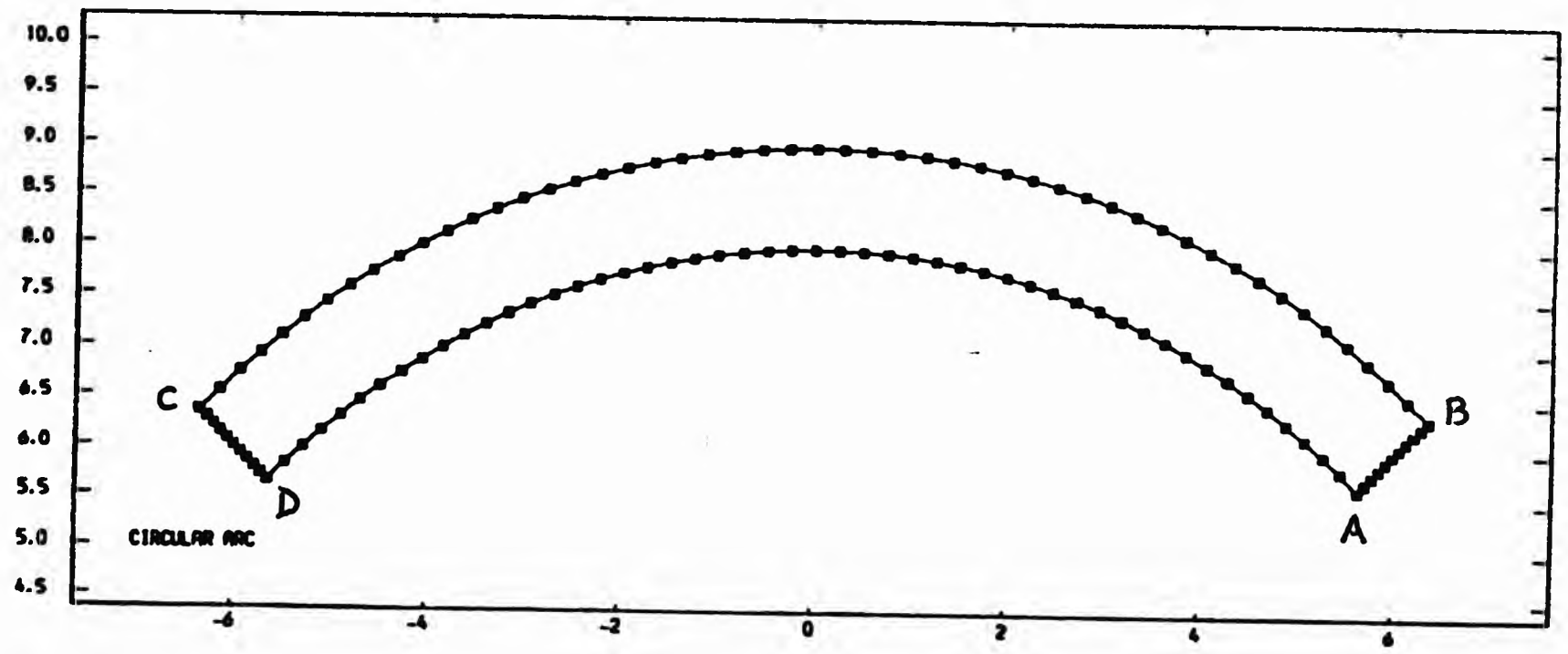

Figure 6-7

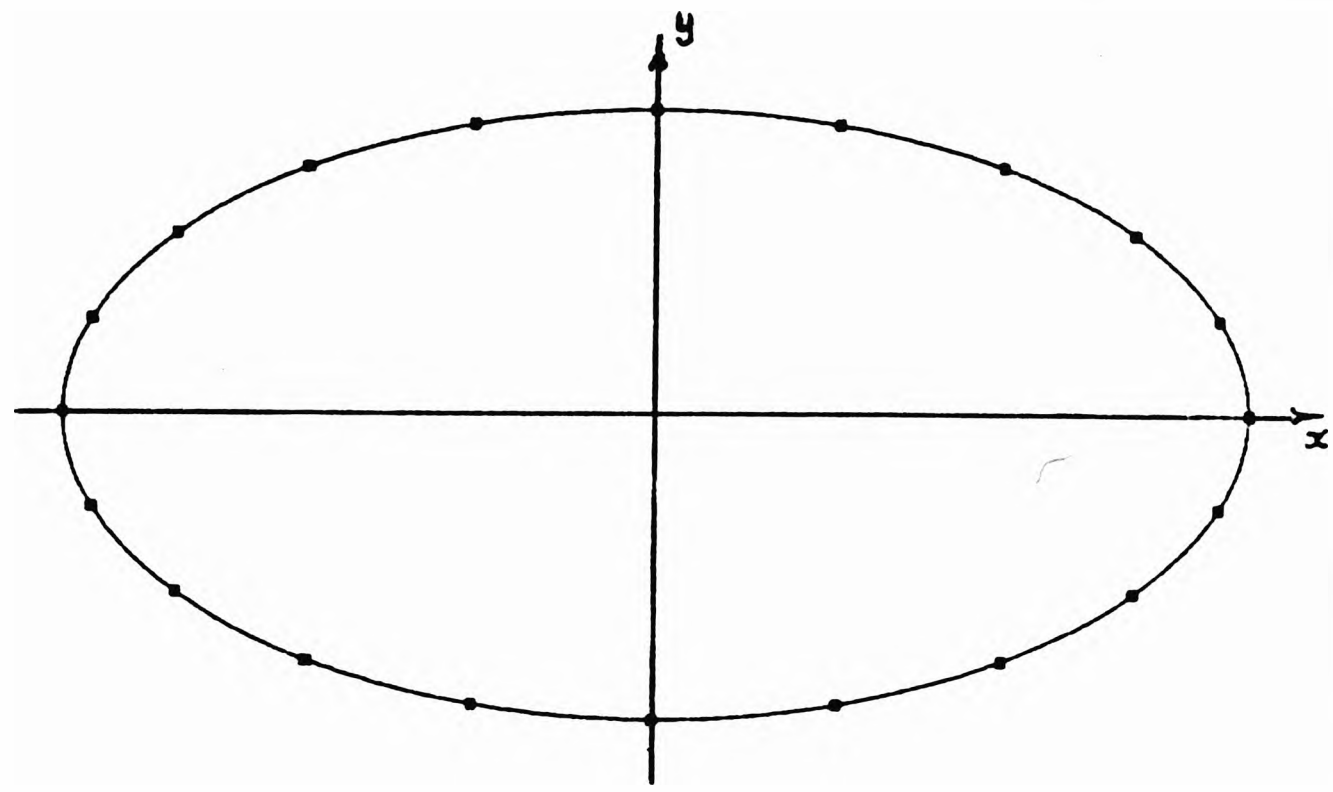

Figure 7-1

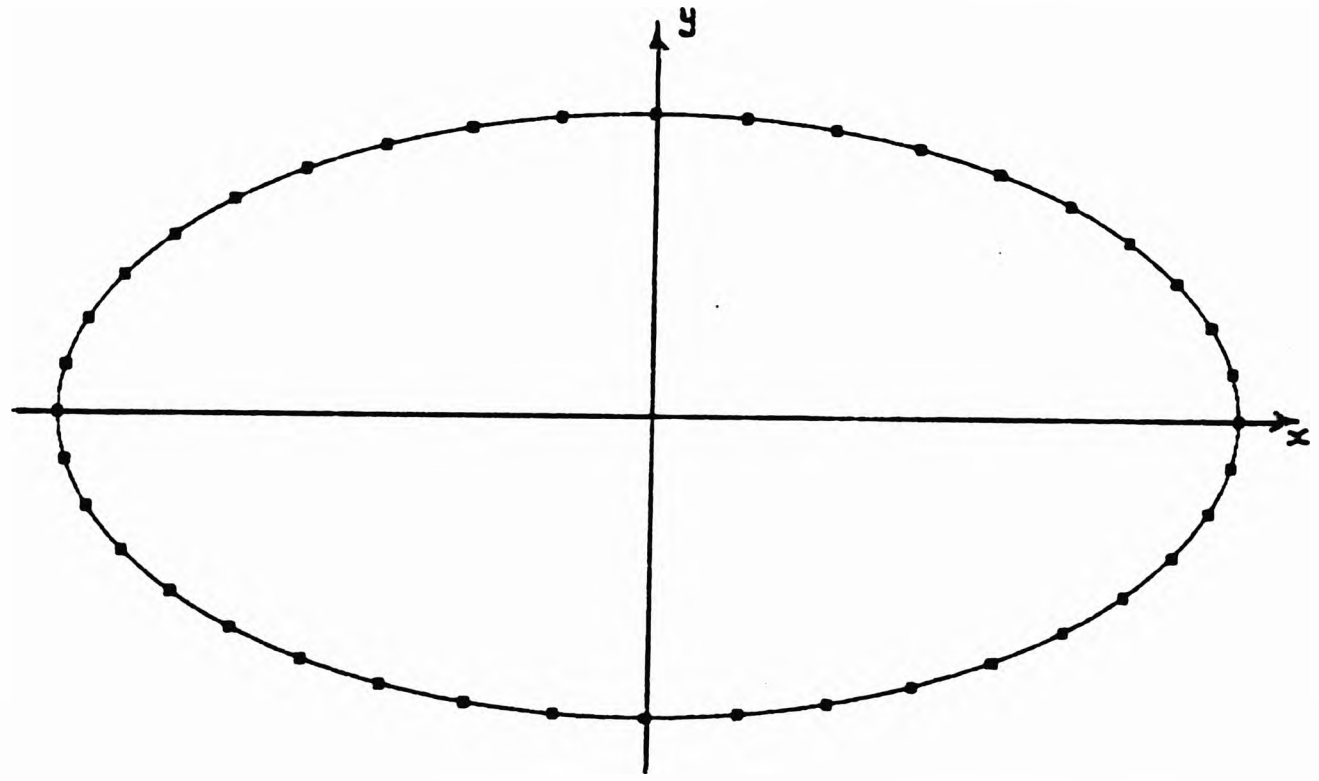

Figure 7-2

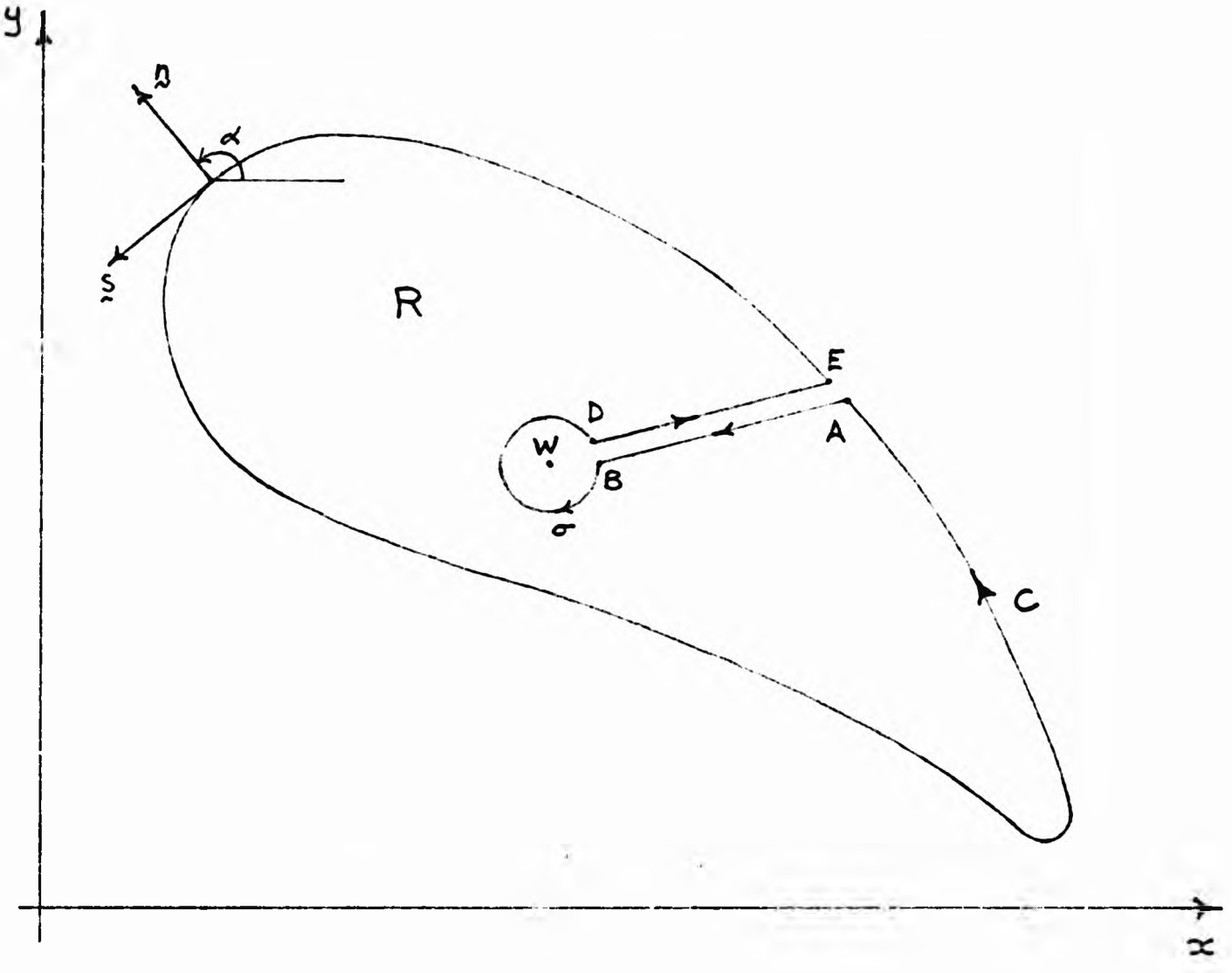

Figure 8-1

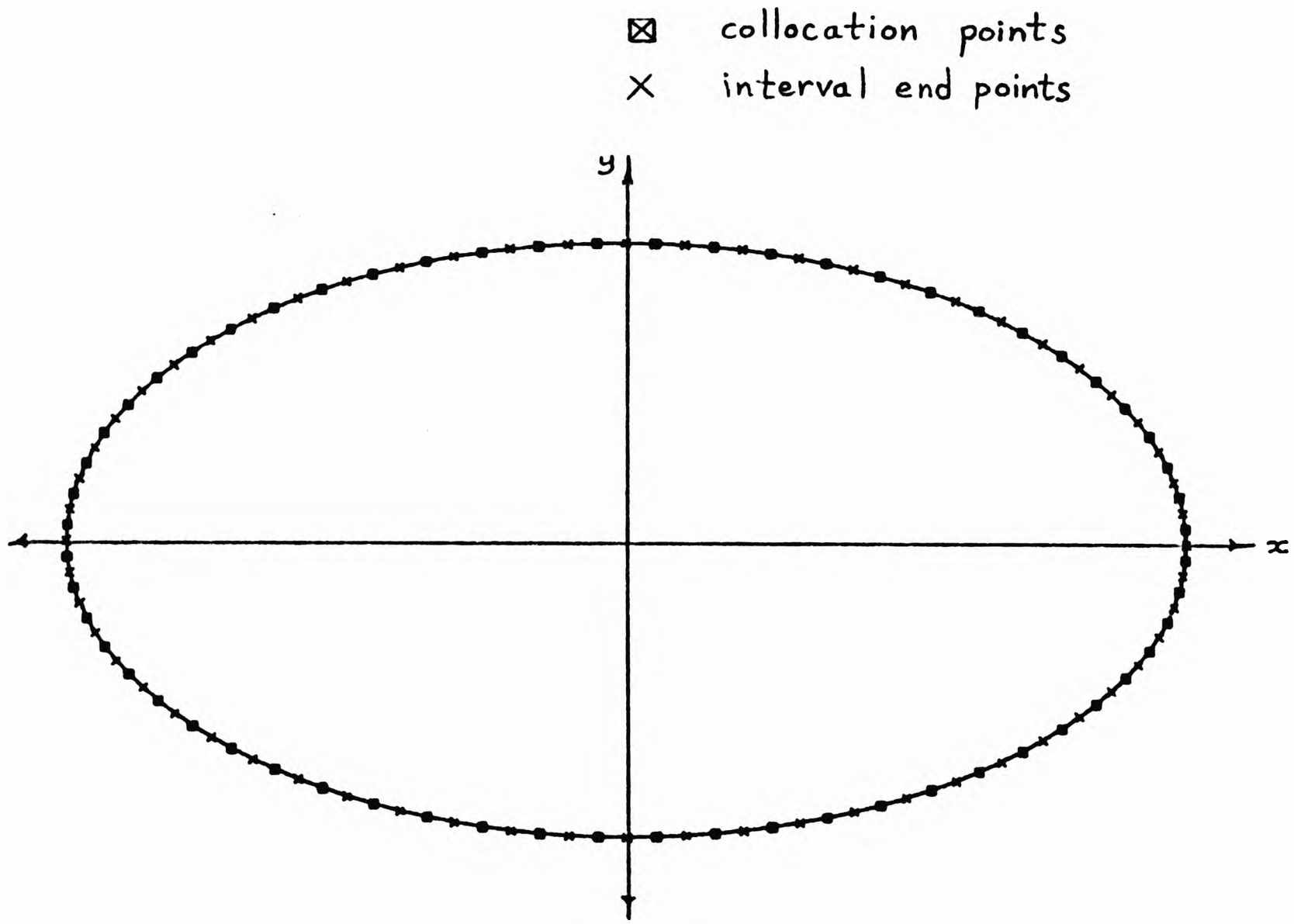

Figure 8-2

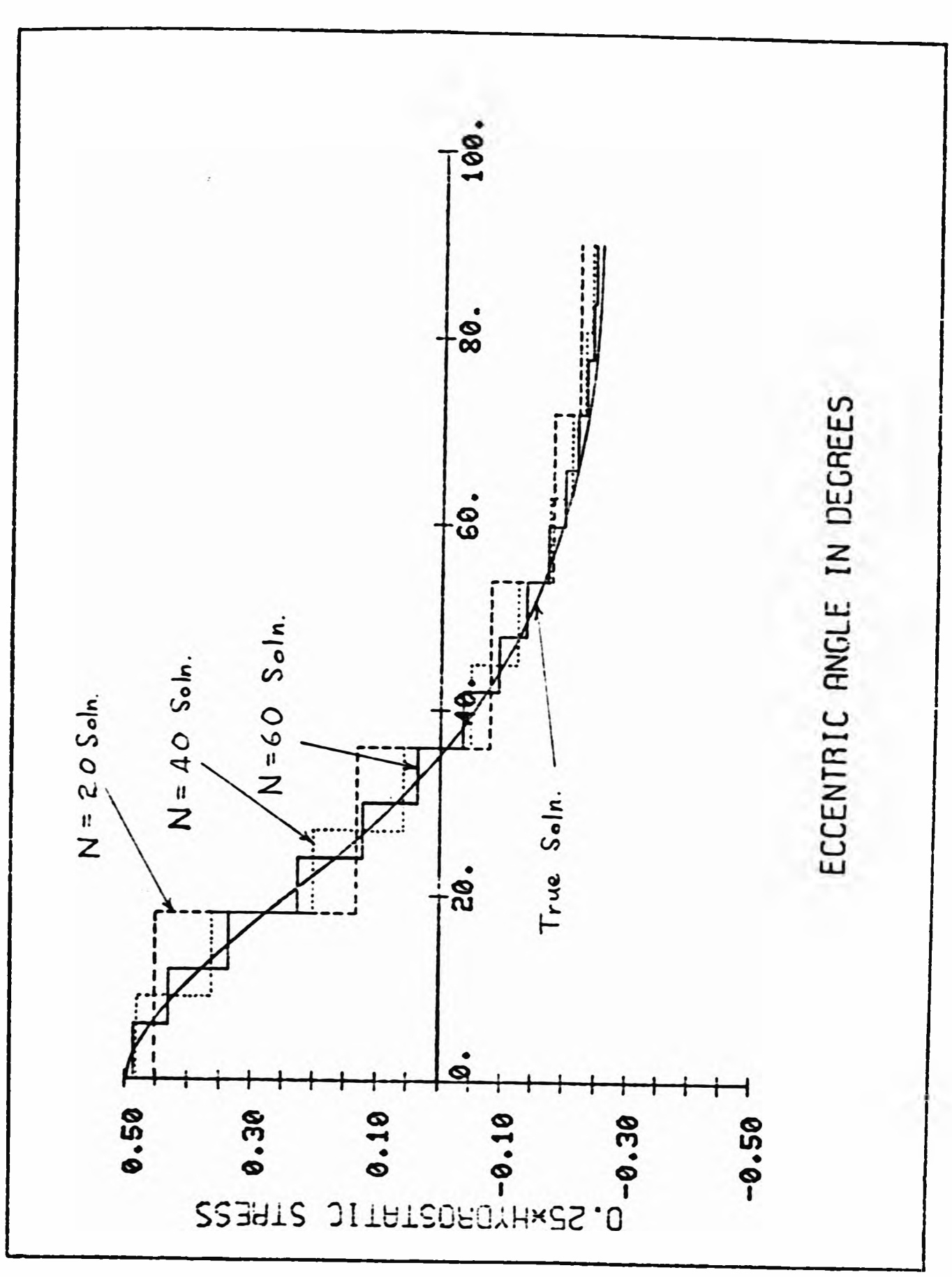
0.25×HYDROSTATIC STRESS
0.50
0.30
0.10
-0.10
-0.30
-0.50
0.
20.
40.
60.
80.
100.
ECCENTRIC ANGLE IN DEGREES
N = 20 Soln.
N = 40 Soln.
N=60 Soln.
True Soln.

Figure 8-3

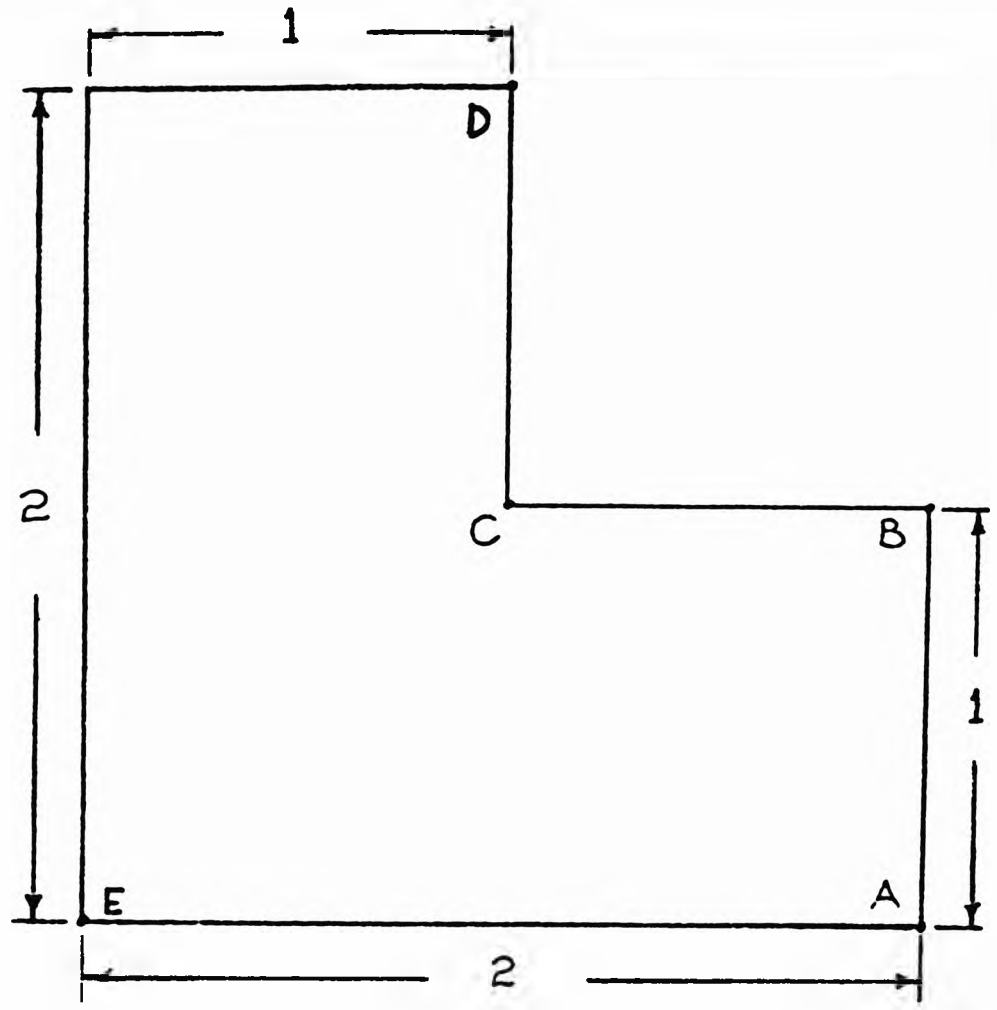

Figure 9-1

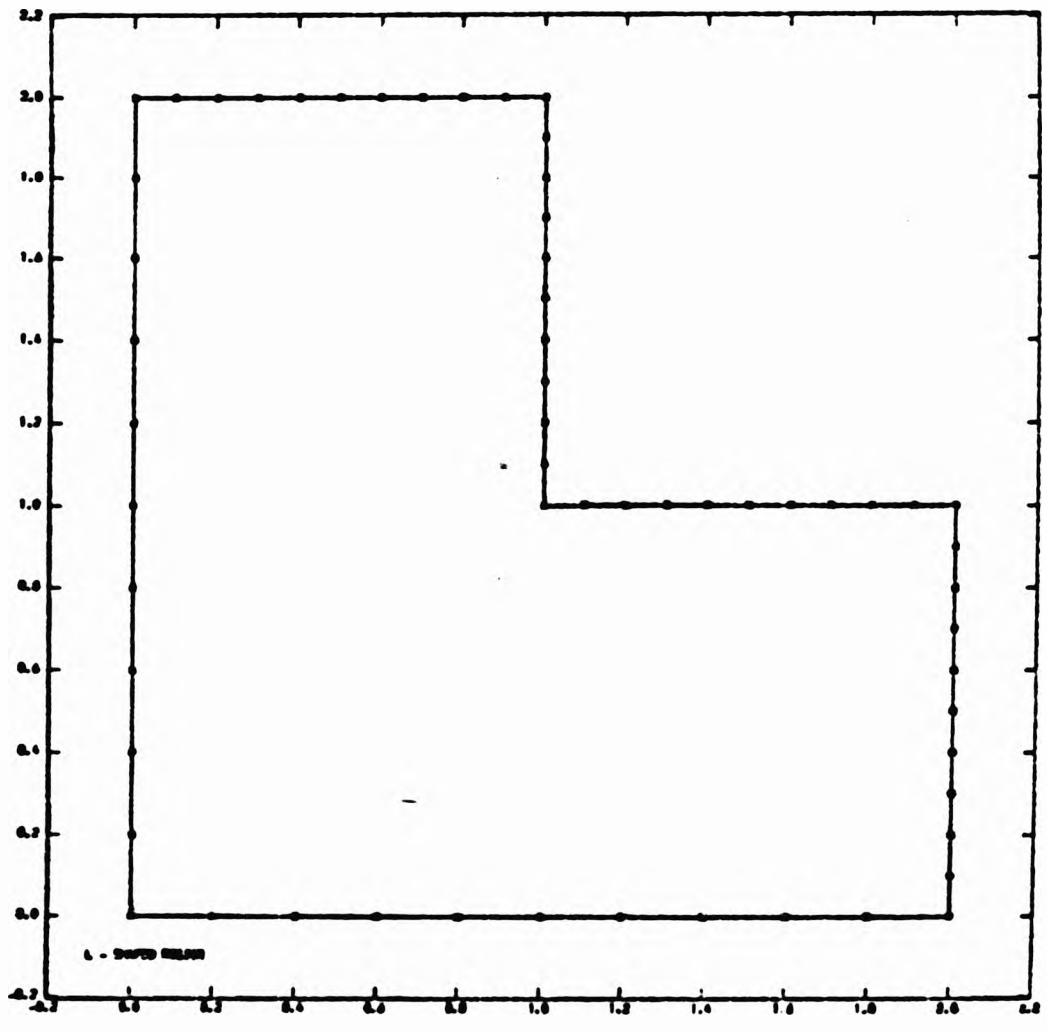

Figure 9-2

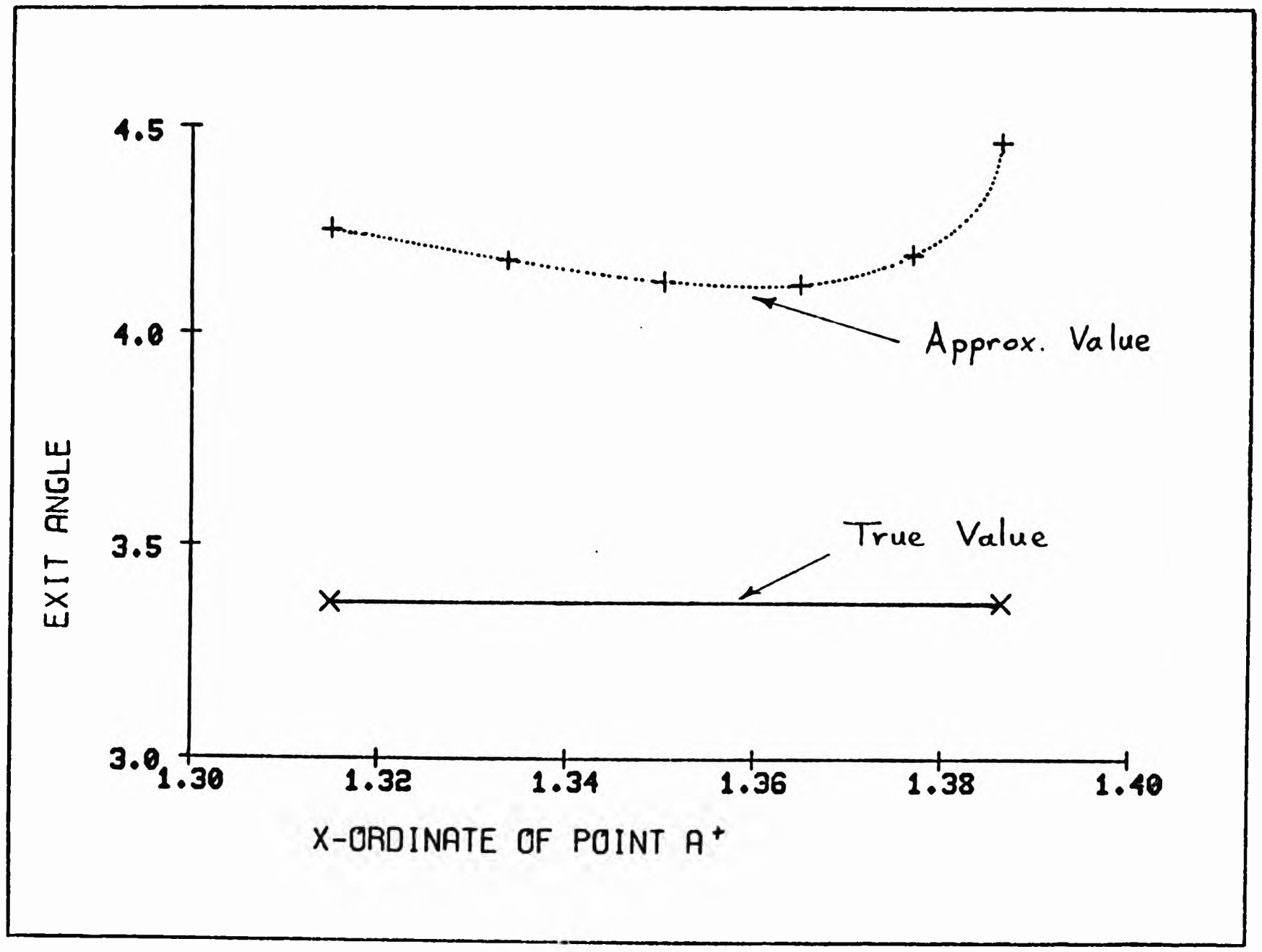
4.5
4.0
3.5
3.0
EXIT ANGLE
Approx. Value
True Value
1.30
1.32
1.34
1.36
1.38
1.40
X-ORDINATE OF POINT A*

Figure 9-3

NOTES

i) Poisson's ratio $\sigma = 0.3$

ii) Writing $\tilde{r} = re^{i\theta}$, the nodes for both boundaries lie on the radial lines $\theta_j = 2\pi(j-1)/N$, $j = 1(1)N$

iii) θ_j is given in degrees rather than radians

iv) Soln.1 is solution by piecewise linear approximation technique of §3.6)
Soln.2 is solution by piecewise quadratic approximation technique of §3.7)

θ_j	Circle: $x^2+y^2 = 1$			N	Circle: $x^2+y^2 = 0.5$		
	Analytic Soln.	Soln.1	Soln.2		Analytic Soln.	Soln.1	Soln.2
0	0.0000	0.0000	0.0000	20	0.0000	0.0000	0.0000
		0.0000	0.0000	40		0.0000	0.0000
		0.0000	0.0000	60		0.0000	0.0000
18	-0.1896	-0.1859	-0.1861	20	-0.4741	-0.4549	-0.4634
		-0.1891	-0.1904	40		-0.4694	-0.4754
		-0.1894	-0.1895	60		-0.4720	-0.4736
36	0.0802	0.0783	0.0655	20	-1.0119	-0.9721	-1.0230
		0.0792	0.0787	40		-1.0021	-1.0144
		0.0797	0.0798	60		-1.0076	-1.0128
54	0.8604	0.8424	0.8695	20	-1.5803	-1.5195	-1.5524
		0.8566	0.8583	40		-1.5652	-1.5837
		0.8582	0.8606	60		-1.5737	-1.5792
72	1.7248	1.6889	1.7010	20	-2.0361	-1.9589	-2.0540
		1.7158	1.7223	40		-2.0169	-2.0401
		1.7208	1.7241	60		-2.0276	-2.0375
90	2.1000	2.0565	2.1112	20	-2.2125	-2.1290	-2.1779
		2.0893	2.0974	40		-2.1917	-2.1267
		2.0953	2.1003	60		-2.2033	-2.2111
Mean		0.0176	0.0386	20	Mean	0.0323	0.0126
Relative		0.0050	0.0047	40	Relative	0.0080	0.0019
Error		0.0024	0.0010	60	Error	0.0035	0.0006

Table 3-1: Flexure of a Hollow Tube - Approximations to $\chi_s(\tilde{r})$

Number of Elements	Strength of Singularity	Relative Error
30	1.0083	0.0083
60	1.0008	0.0008
90	1.0002	0.0002

Table 3-2: Test problem for an L-shaped region

Approximations to singularity strength

Co-ordinates x	Co-ordinates y	number of elements	Approximation to $\psi_3(\tilde{r})$	Analytic Solution	Relative Error
0.0	0.0	30	0.0052	0.0000	
		60	0.0005		
		90	0.0001		
0.2	0.0	30	0.0487	0.0400	0.2175
		60	0.0408		0.0200
		90	0.0402		0.0050
0.4	0.0	30	0.1652	0.1593	0.0370
		60	0.1599		0.0038
		90	0.1595		0.0013
0.6	0.0	30	0.3561	0.3523	0.0108
		60	0.3526		0.0009
		90	0.3524		0.0003
0.8	0.0	30	0.5994	0.5972	0.0037
		60	0.5974		0.0003
		90	0.5972		0.0000
1.0	0.0	30	0.8422	0.8415	0.0008
		60	0.8415		0.0000
		90	0.8415		0.0000
1.2	0.0	30	0.9908	0.9915	0.0007
		60	0.9914		0.0001
		90	0.9914		0.0001
1.4	0.0	30	0.9232	0.9252	0.0022
		60	0.9250		0.0002
		90	0.9251		0.0001
1.6	0.0	30	0.5457	0.5494	0.0067
		60	0.5490		0.0007
		90	0.5492		0.0004
1.8	0.0	30	-0.1041	-0.0982	0.0601
		60	-0.0989		0.0071
		90	-0.0984		0.0020
2.0	0.0	30	-0.7497	-0.7568	0.0094
		60	-0.7561		0.0009
		90	-0.7566		0.0003

On DA $\psi_3(\tilde{r}) = \sin(x^2)$

Table 3-3: Test problem for an L-shaped region
Approximations to $\psi_3(\tilde{r}) - I$

Co-ordinates x	Co-ordinates y	Number of Elements	Approximation to $\psi_s(\tilde{r})$	Analytic Solution	Relative Error
2.0	0.0	30	-0.0019	0.0000	
		60	-0.0002		
		90	0.0000		
2.0	0.1	30	0.2798	0.2716	0.0302
		60	0.2728		0.0044
		90	0.2719		0.0011
2.0	0.2	30	0.6153	0.6069	0.0138
		60	0.6079		0.0016
		90	0.6072		0.0005
2.0	0.3	30	1.0923	1.0853	0.0064
		60	1.0859		0.0006
		90	1.0855		0.0002
2.0	0.4	30	1.8203	1.8194	0.0005
		60	1.8195		0.0001
		90	1.8194		0.0000
2.0	0.5	30	2.9869	2.9761	0.0036
		60	2.9752		0.0003
		90	2.9764		0.0001
2.0	0.6	30	4.7786	4.8012	0.0047
		60	4.7986		0.0005
		90	4.8006		0.0001
2.0	0.7	30	7.6783	7.6423	0.0047
		60	7.6366		0.0007
		90	7.6436		0.0002
2.0	0.8	30	11.8647	11.9550	0.0076
		60	11.9442		0.0009
		90	11.9518		0.0003
2.0	0.9	30	18.3702	18.2641	0.0058
		60	18.2451		0.0010
		90	18.2680		0.0002
2.0	1.0	30	27.0168	27.0168	0.0000
		60	27.0168		0.0000
		90	27.0168		0.0000

On AB $\psi_s(\tilde{r}) = -\sinh(2xy)\cos(x^2-y^2)$

Table 3-4: Test problem for an L-shaped region
Approximations to $\psi_s(\tilde{r})$ – II

N	$q_c^{(N)}$	Relative Error
40	0.8180	0.0184
60	0.8227	0.0127
80	0.8253	0.0096
120	0.8279	0.0065
True Value	0.8333	0

Table 3-5: Flow Past A Joukowski Aerofoil I
Approximations To Speed at Cusp

N	$q_{max}^{(N)}$	Relative Error
40	1.3674	0.0015
60	1.3695	0
80	1.3699	0.0003
120	1.3696	0.0001
True Value	1.3695	0

Table 3-6: Flow Past A Joukowski Aerofoil I
Approximations To Maximum Speed

	Speed at Cusp	Max.Flow Speed	Circulation
True Value	0.8207	2.0988	1.3093
Approximations	0.7927	2.1183	1.3152
Relative Error	0.0339	0.0093	0.0045

Table 3-7: Flow Past A Joukowski Aerofoil II
Various Approximations When N=40

	Speed at Cusp	Max.Flow Speed	Circulation
True Value	0.8207	2.0988	1.3093
Approximations	0.7927	2.1183	1.3152
Relative Error	0.0339	0.0093	0.0045

Table 3-7: Flow Past A Joukowski Aerofoil II
Various Approximations When N=40

m	$(-1)^{m-1}\frac{2^{2m}B_m}{(2m)!}$	m \ K	$(-1)^{m-1}\left\{\frac{2^{2m}B_m}{(2m)!} - \sum_{n=1}^{K-1}\left(\frac{1}{n\pi}\right)^{2m}\right\}$			
			2	3	4	5
1	.333333E+00	1	.130691E+00	.800304E-01	.575146E-01	.448494E-01
2	-.222222E-01	2	-.169026E-02	-.407010E-03	-.153529E-03	-.733259E-04
3	.211640E-02	3	.360792E-04	.357412E-05	.720457E-06	.212566E-06
4	-.211640E-03	4	-.859428E-06	-.360659E-07	-.393958E-08	-.723319E-09
5	.213778E-04	5	.212407E-07	.384688E-09	.230125E-10	.264534E-11
6	.216440E-05	6	-.532500E-09	-.421074E-11	-.139033E-12	-.100560E-13
7	.219259E-06	7	.134284E-10	.466948E-13	.855861E-15	.391058E-16
8	-.222146E-07	8	-.339484E-12	-.521376E-15	-.532625E-17	-.154054E-18
9	.225078E-08	9	.859187E-14	.584303E-17	.33916E-19	.635275E-21
10	-.228052E-09	10	-.217552E-15	-.656153E-19	-.210931E-21	-.330872E-23
11	.231064E-10	11	.550974E-17	.737845E-21	.155096E-23	.206795E-24
12	-.234117E-11	12	-.139553E-18	-.832350E-23	-.387741E-25	-.258494E-25

Table 4-1

number of nodes = 55	true value	approx. value	relative error
max. speed on aerofoil	3.67860	3.58009	0.02678
exit speed	1.00173	1.01691	0.01515
exit angle (degrees)	3.366	10.468	2.10992
inlet angle - exit angle	41.634	34.532	0.17058

TABLE 4-2

number of nodes = 113	true value	approx. value	relative error
max. speed on aerofoil	3.67860	3.66273	0.00431
exit speed	1.00173	1.00432	0.00259
exit angle (degrees)	3.366	5.320	0.58051
inlet angle - exit angle	41.634	39.680	0.04693

TABLE 4-3

Notes

i) Poisson's ratio $\sigma = 0.3$

ii) Writing $z = re^{i\theta}$ the nodes for both boundaries lie on the radial lines $\theta_j = 2\pi(j-1)/N$, $j = 1(1)N$

iii) θ_j is given in degrees rather than radians.

θ_j	Circle: $x^2 + y^2 = 1.0$		N	Circle: $x^2 + y^2 = 0.5$	
	Analytic Soln.	Approx. Soln.		Analytic Soln.	Approx. Soln.
0	-1.1000	-1.0961 -1.0996 -1.0999	20 40 60	-0.9813	-0.9733 -0.9805 -0.9810
18	-1.1370	-1.1316 -1.1366 -1.1368	20 40 60	-0.9446	-0.9359 -0.9439 -0.9444
36	-1.1694	-1.1663 -1.1691 -1.1693	20 40 60	-0.8288	-0.8224 -0.8282 -0.8286
54	-1.0313	-1.0279 -1.0310 -1.0312	20 40 60	-0.6249	-0.6195 -0.6244 -0.6247
72	-0.6194	-0.6182 -0.6193 -0.6194	20 40 60	-0.3382	-0.3357 -0.3379 -0.3381
90	0.0000	0.0000 0.0000 0.0000	20 40 60	0.0000	0.0000 0.0000 0.0000

Mean	0.0027	20	Mean	0.0069
Relative	0.0002	40	Relative	0.0007
Error	0.0001	60	Error	0.0002

Table 5-1: Flexure Of A Hollow Tube - Approximations to $\chi(x,y)$

Outer Boundary: $x^2 + 4y^2 = 1$

20 node case

$\zeta = x + iy$		$\varphi_s(\tilde{\zeta})$	$F(\zeta) = \varphi(\tilde{\zeta}) + i\psi(\tilde{\zeta})$	
x	y		$\varphi(\tilde{\zeta})$	$\psi(\tilde{\zeta})$
1.0000	0.	-.6000	$-.2337 \times 10^{-6}$	.2011
.9511	.1545	-.4280	$-.8817 \times 10^{-1}$	.1653
.8090	.2939	-.1299	-.1427	$.7154 \times 10^{-1}$
.5878	.4045	.1077	-.1427	$-.4435 \times 10^{-1}$
.3090	.4755	.2519	$-.8817 \times 10^{-1}$	-.1381
0.	.5000	.3000	$.3356 \times 10^{-6}$	-.1739

Table 6-1

Inner Boundary: $x^2 + 4y^2 = .81$

20 node case

$\zeta = x+iy$		$\varphi_3(\tilde{\zeta})$	$F(\zeta) = \varphi(\tilde{\zeta}) + i\psi(\tilde{\zeta})$	
x	y		$\varphi(\tilde{\zeta})$	$\psi(\tilde{\zeta})$
.9000	0.	.5400	$-.9015 \times 10^{-6}$	.1441
.8560	.1391	.3852	$-.7142 \times 10^{-1}$	.1151
.7281	.2645	.1169	-.1156	$.3915 \times 10^{-1}$
.5290	.3614	$-.9695 \times 10^{-1}$	-.1156	$.5471 \times 10^{-1}$
.2781	.4280	-.2267	$-.7141 \times 10^{-1}$	-.1306
0.	.4500	-.2700	$.6479 \times 10^{-6}$	-.1597

Table 6-2

Outer Boundary: $x^2 + 4y^2 = 1$

40 node case

$\zeta = x+iy$			$F(\zeta) = \varphi(\tilde{\zeta}) + i\psi(\tilde{\zeta})$	
x	y	$\varphi_3(\tilde{\zeta})$	$\varphi(\tilde{\zeta})$	$\psi(\tilde{\zeta})$
1.0000	0.	-.6000	.1419 x 10^{-5}	.1990
.9877	.7822	-.5508	-.4635 x 10^{-1}	.1898
.9511	.1545	-.4280	-.8817 x 10^{-1}	.1632
.8910	.2270	-.2772	-.1214	.1217
.8090	.2939	-.1299	-.1427	.6942 x 10^{-1}
.7071	.3536	.1206 x 10^{-4}	-.1500	.1148 x 10^{-1}
.5878	.4045	.1077	-.1427	-.4646 x 10^{-1}
.4540	.4455	.1918	-.1214	-.9873 x 10^{-1}
.3090	.4755	.2519	-.8817 x 10^{-1}	-.1402
.1564	.4438	.2880	-.4635 x 10^{-1}	-.1668
0.	.5000	.3000	.2872 x 10^{-6}	-.1760

Table 6-3

Inner Boundary: $x^2 + 4y^2 = .81$

40 node case

$\zeta = x+iy$		$\varphi_s(\tilde{\zeta})$	$F(\zeta) = \varphi(\tilde{\zeta}) + i\psi(\tilde{\zeta})$	
x	y		$\varphi(\tilde{\zeta})$	$\psi(\tilde{\zeta})$
.9000	0.	.5400	$.4416 \times 10^{-6}$	.1420
.8889	$.7040 \times 10^{-1}$	.4957	$-.3755 \times 10^{-1}$	.1345
.8560	.1391	.3852	$-.7142 \times 10^{-1}$	.1130
.8019	.2043	.2495	$-.9830 \times 10^{-1}$	$.7938 \times 10^{-1}$
.7281	.2645	.1169	-.1156	$.3704 \times 10^{-1}$
.6364	.3182	$-.1145 \times 10^{-4}$	-.1215	$-.9894 \times 10^{-2}$
.5290	.3641	$-.9695 \times 10^{-1}$	-.1156	$-.5683 \times 10^{-1}$
.4086	.4010	-.1726	$-.9830 \times 10^{-1}$	$-.9916 \times 10^{-1}$
.2781	.4280	-.2267	$-.7142 \times 10^{-1}$	-.1328
.1408	.4445	-.2592	$-.3755 \times 10^{-1}$	-.1543
0.	.4500	-.2700	$-.1416 \times 10^{-5}$	-.1618

Table 6-4

Nodes per boundary	Approximation to I_s	Approximation to I_w
20	0.108142	0.002757
40	0.108122	0.002760
60	0.107975	0.002760
True Values	I_s = 0.108039	I_w = 0.002760

Table 6-5

Nodes per boundary	Approximation to x_c	Approximation to y_c
20	$-.4331 \times 10^{-5}$	$-.6391 \times 10^{-5}$
40	$-.2109 \times 10^{-4}$	$-.9499 \times 10^{-5}$
60	$.1616 \times 10^{-5}$	$-.2209 \times 10^{-5}$
True Values	x_c = 0.0	y_c = 0.0

Table 6-6

Nodes per boundary	Approximation to I_s	Approximation to x_c	Approximation to y_c
28	.29276	$-.1274 \times 10^{-2}$	.08492
56	.29616	$-.3241 \times 10^{-3}$	.08486
84	.29706	$-.1061 \times 10^{-3}$	.08492
Timoshenko	.298	0.	.08690
Roark	.296	--	--

Table 6-7

Property	Approximation	"Thin-Wall" Result
x_c	$.2302 \times 10^{-3}$	0.
y_c	1.343	1.375
I_s	3.785	4.443
I_w	26.52	26.98

Table 6-8

$\zeta = x+iy$		Exterior Problem	Interior Problem
x	y	$\Phi_s(\tilde{\zeta})$	$\Phi_s(\tilde{\zeta})$
1.000000	.000000	.000000	-.600000
.951057	.154508	-.817337	-.427965
.809017	.293893	-1.235664	-.129925
.587785	.404508	-1.409855	.107703
.309017	.475528	-1.480589	.251893
.000000	.500000	-1.500000	.300000
-.309017	.475528	-1.480589	.251893
-.587785	.404508	-1.409855	.107703
-.809017	.293893	-1.235664	-.129925
-.951057	.154508	-.817337	-.427965
-1.000000	.000000	.000000	-.600000
-.951057	-.154508	.817337	-.427965
-.809017	-.293893	1.235664	-.129925
-.587785	-.404508	1.409855	.107703
-.309017	-.475528	1.480589	.251893
.000000	-.500000	1.500000	.300000
.309017	-.475528	1.480589	.251893
.587785	-.404508	1.409855	.107703
.809017	-.293893	1.235664	-.129925
.951057	-.154508	.817337	-.427965

Table 7-1

COUPLED PROBLEM FOR ISOLATED AEROFOIL
****

NUMBER OF NODES = 20

NODE NUMBER	CO-ORDINATES X	Y	DIRECTION OF NORMAL	DPDN	SUM	DIF	ψ_s	$\frac{\partial \psi}{\partial s}$
1	1.000000	0.000000	0.000000	0.000000	-.598456	-.601566	-.600011	.001555
2	.951057	.154508	33.017398	-.388669	-1.124463	.268532	-.427965	-.696497
3	.809017	.293893	55.464603	-.499836	-1.400208	1.140352	-.129928	-1.270280
4	.587785	.404508	70.035371	-.414346	-1.299659	1.515063	.107702	-1.407361
5	.309017	.475528	80.772355	-.228764	-1.234363	1.738147	.251892	-1.486255
6	0.000000	.500000	90.000000	-.000000	-1.200925	1.800925	.300000	-1.500925
7	-.309017	.475528	99.227645	.228764	-1.234363	1.738148	.251893	-1.486255
8	-.587785	.404508	109.964629	.414346	-1.299659	1.515065	.107703	-1.407362
9	-.809017	.293893	124.535397	.499836	-1.400206	1.140356	-.129925	-1.270281
10	-.951057	.154508	146.982602	.388669	-1.124465	.268534	-.427966	-.696499
11	-1.000000	0.000000	180.000000	-.000000	-.598450	-.601552	-.600001	.001551
12	-.951057	-.154508	-146.982602	-.388669	.271225	-1.127156	-.427966	.699190
13	-.809017	-.293893	-124.535397	-.499836	1.142637	-1.402487	-.129925	1.272562
14	-.587785	-.404508	-109.964629	-.414346	1.516951	-1.301545	.107703	1.409248
15	-.309017	-.475528	-99.227645	-.228764	1.739787	-1.236002	.251893	1.487894
16	0.000000	-.500000	-90.000000	.000000	1.802523	-1.202524	.300000	1.502523
17	.309017	-.475528	-80.772355	.228764	1.739786	-1.236003	.251892	1.487895
18	.587785	-.404508	-70.035371	.414346	1.516952	-1.301546	.107703	1.409249
19	.809017	-.293893	-55.464603	.499836	1.142631	-1.402498	-.129934	1.272565
20	.951057	-.154508	-33.017398	.388669	.271268	-1.127139	-.427936	.699203

SPEED = 1.0000

DIRECTION = 0.0000

CIRCULATION = 0.0000

Table 7-2

COUPLED PROBLEM FOR ISOLATED AEROFOIL
****

NUMBER OF NODES = 40

NODE NUMBER	CO-ORDINATES X	Y	DIRECTION OF NORMAL	DPDN	SUM	DIF	ϕ_3	Φ_S
1	1.000000	0.000000	0.000000	0.000000	-.599997	-.600004	-.600001	.000003
2	.987688	.078217	17.576581	-.223697	-.983637	-.117912	-.550775	-.432862
3	.951057	.154508	33.017398	-.388669	-1.255638	.399706	-.427966	-.827672
4	.891007	.226995	45.540602	-.476965	-1.337026	.782570	-.277228	-1.059798
5	.809017	.293893	55.464603	-.499836	-1.371807	1.111956	-.129925	-1.241881
6	.707107	.353553	63.434949	-.474342	-1.340243	1.340242	-.000000	-1.340242
7	.587785	.404508	70.035371	-.414346	-1.303695	1.519102	.107703	-1.411399
8	.453990	.445503	75.707214	-.329953	-1.261705	1.645266	.191780	-1.453485
9	.309017	.475528	80.772355	-.228764	-1.229195	1.732980	.251893	-1.481087
10	.156434	.493844	85.472070	-.116959	-1.207377	1.783320	.287972	-1.495348
11	0.000000	.500000	90.000000	-.000000	-1.200330	1.800330	.300000	-1.500330
12	-.156434	.493844	94.527930	.116959	-1.207377	1.783320	.287972	-1.495348
13	-.309017	.475528	99.227645	.228764	-1.229195	1.732980	.251893	-1.481087
14	-.453990	.445503	104.292786	.329953	-1.261705	1.645266	.191780	-1.453485
15	-.587785	.404508	109.964629	.414346	-1.303695	1.519102	.107703	-1.411399
16	-.707107	.353553	116.565051	.474342	-1.340243	1.340242	-.000000	-1.340242
17	-.809017	.293893	124.535397	.499836	-1.371807	1.111956	-.129925	-1.241881
18	-.891007	.226995	134.459398	.476965	-1.337026	.782570	-.277228	-1.059798
19	-.951057	.154508	146.982602	.388669	-1.255638	.399706	-.427966	-.827672
20	-.987688	.078217	162.423419	.223697	-.983637	-.117912	-.550775	-.432862
21	-1.000000	0.000000	180.000000	-.000000	-.599997	-.600004	-.600001	.000003
22	-.987688	-.078217	-162.423419	-.223697	-.117906	-.983644	-.550775	.432869
23	-.951057	-.154508	-146.982602	-.388669	.399712	-1.255644	-.427966	.827678
24	-.891007	-.226995	-134.459398	-.476965	.782576	-1.337032	-.277228	1.059804
25	-.809017	-.293893	-124.535397	-.499836	1.111961	-1.371811	-.129925	1.241886
26	-.707107	-.353553	-116.565051	-.474342	1.340246	-1.340247	-.000000	1.340247
27	-.587785	-.404508	-109.964629	-.414346	1.519106	-1.303699	.107703	1.411403
28	-.453990	-.445503	-104.292786	-.329953	1.645269	-1.261709	.191780	1.453489
29	-.309017	-.475528	-99.227645	-.228764	1.732984	-1.229198	.251893	1.481091
30	-.156434	-.493844	-94.527930	-.116959	1.783324	-1.207380	.287972	1.495352
31	0.000000	-.500000	-90.000000	.000000	1.800333	-1.200334	.300000	1.500334
32	.156434	-.493844	-85.472070	.116959	1.783324	-1.207380	.287972	1.495352
33	.309017	-.475528	-80.772355	.228764	1.732984	-1.229198	.251893	1.481091
34	.453990	-.445503	-75.707214	.329953	1.645269	-1.261709	.191780	1.453489
35	.587785	-.404508	-70.035371	.414346	1.519106	-1.303699	.107703	1.411403
36	.707107	-.353553	-63.434949	.474342	1.340246	-1.340247	-.000000	1.340247
37	.809017	-.293893	-55.464603	.499836	1.111961	-1.371811	-.129925	1.241886
38	.891007	-.226995	-45.540602	.476965	.782576	-1.337032	-.277228	1.059804
39	.951057	-.154508	-33.017398	.388669	.399712	-1.255644	-.427966	.827678
40	.987688	-.078217	-17.576581	.223697	-.117906	-.983644	-.550775	.432869

SPEED = 1.0000

DIRECTION = 0.0000

CIRCULATION = 0.0000

Table 7-3

20 node idealisation gives Solution I
40 node idealisation gives Solution II
Error I is relative error of Solution I
Error II is relative error of Solution II

x	y	True Solution	Solution I	Error I	Solution II	Error II
1.000000	.000000	.000000	.001555	-	.000003	-
.951057	.154508	-.817337	-.696497	.147846	-.827672	.012645
.809017	.293893	-1.235664	-1.270280	.028014	-1.241881	.005031
.587785	.404508	-1.409855	-1.407361	.001769	-1.411399	.001095
.309017	.475528	-1.480589	-1.486255	.003827	-1.481087	.000336
.000000	.500000	-1.500000	-1.500925	.000671	-1.500330	.000220

Table 7-4

COUPLED PROBLEM FOR CASCADE AEROFOIL
****

NUMBER OF NODES = 20

NODE NUMBER	CO-ORDINATES X	Y	DIRECTION OF NORMAL	DPDN	SUM	DIF	ϕ_3	ϕ_s
1	1.000000	0.000000	0.000000	0.000000	-.597895	-.602084	-.599990	.002094
2	.951057	.154508	33.017398	-.388669	-.426231	-.429701	-.427966	.001735
3	.809017	.293893	55.464603	-.499836	-.128636	-.131208	-.129922	.001286
4	.587785	.404508	70.035371	-.414346	.108566	.106841	.107704	.000862
5	.309017	.475528	80.772355	-.228764	.252461	.251325	.251893	.000568
6	0.000000	.500000	90.000000	-.000000	.300508	.299493	.300000	.000507
7	-.309017	.475528	99.227645	.228764	.252461	.251325	.251893	.000568
8	-.587785	.404508	109.964629	.414346	.108566	.106840	.107703	.000863
9	-.809017	.293893	124.535397	.499836	-.128638	-.131212	-.129925	.001287
10	-.951057	.154508	146.982602	.388669	-.426228	-.429701	-.427965	.001737
11	-1.000000	0.000000	180.000000	-.000000	-.597903	-.602097	-.600000	.002097
12	-.951057	-.154508	-146.982602	-.388669	-.426228	-.429701	-.427965	.001736
13	-.809017	-.293893	-124.535397	-.499836	-.128638	-.131211	-.129924	.001287
14	-.587785	-.404508	-109.964629	-.414346	.108566	.106841	.107703	.000863
15	-.309017	-.475528	-99.227645	-.228764	.252461	.251325	.251893	.000568
16	0.000000	-.500000	-90.000000	.000000	.300508	.299493	.300001	.000507
17	.309017	-.475528	-80.772355	.228764	.252462	.251326	.251894	.000568
18	.587785	-.404508	-70.035371	.414346	.108565	.106841	.107703	.000862
19	.809017	-.293893	-55.464603	.499836	-.128631	-.131200	-.129915	.001284
20	.951057	-.154508	-33.017398	.388669	-.426277	-.429722	-.427999	.001723

UPSTREAM FLOW SPEED = 0.

UPSTREAM FLOW DIRECTION = 0.

DOWNSTREAM FLOW SPEED = 0.

DOWNSTREAM FLOW DIRECTION = 0.

CIRCULATION = 0.

PITCH = .3000E+01

CHORD = .2000E+01

Table 7-5

COUPLED PROBLEM FOR CASCADE AEROFOIL
****

NUMBER OF NODES = 20

NODE NUMBER	CO-ORDINATES X	Y	DIRECTION OF NORMAL	DPDN	SUM	DIF	ϕ_s	$\frac{\partial \phi}{\partial s}$
1	1.000000	0.000000	0.000000	0.000000	-.597694	-.602270	-.599982	.002288
2	.951057	.154508	33.017398	-.388669	-.426090	-.429842	-.427966	.001876
3	.809017	.293893	55.464603	-.499836	-.128580	-.131261	-.129920	.001341
4	.587785	.404508	70.035371	-.414346	.108532	.106870	.107704	.000834
5	.309017	.475528	80.772355	-.228764	.252369	.251418	.251893	.000476
6	0.000000	.500000	90.000000	-.000000	.300400	.299600	.300000	.000400
7	-.309017	.475528	99.227645	.228764	.252369	.251417	.251893	.000476
8	-.587785	.404508	109.964629	.414346	.108538	.106869	.107703	.000834
9	-.809017	.293893	124.535397	.499836	-.128583	-.131266	-.129924	.001341
10	-.951057	.154508	146.982602	.388669	-.426087	-.429842	-.427964	.001878
11	-1.000000	0.000000	180.000000	-.000000	-.597707	-.602292	-.600000	.002292
12	-.951057	-.154508	-146.982602	-.388669	-.426086	-.429841	-.427964	.001878
13	-.809017	-.293893	-124.535397	-.499836	-.128583	-.131265	-.129924	.001341
14	-.587785	-.404508	-109.964629	-.414346	.108538	.106870	.107704	.000834
15	-.309017	-.475528	-99.227645	-.228764	.252369	.251418	.251894	.000476
16	0.000000	-.500000	-90.000000	.000000	.300401	.299601	.300001	.000400
17	.309017	-.475528	-80.772355	.228764	.252370	.251419	.251895	.000476
18	.587785	-.404508	-70.035371	.414346	.108537	.106869	.107703	.000834
19	.809017	-.293893	-55.464603	.499836	-.128571	-.131246	-.129909	.001338
20	.951057	-.154508	-33.017398	.388669	-.426167	-.429877	-.428022	.001855

UPSTREAM FLOW SPEED = 0.

UPSTREAM FLOW DIRECTION = 0.

DOWNSTREAM FLOW SPEED = 0.

DOWNSTREAM FLOW DIRECTION = 0.

CIRCULATION = 0.

PITCH = .2500E+01

CHORD = .2000E+01

Table 7-6

COUPLED PROBLEM FOR CASCADE AEROFOIL
****

NUMBER OF NODES = 20

NODE NUMBER	CO-ORDINATES X	Y	DIRECTION OF NORMAL	DPDN	SUM	DIF	ϕ_S	$\bar{\phi}_S$
1	1.000000	0.000000	0.000000	0.000000	-.597376	-.602564	-.599970	.002594
2	.951057	.154508	33.017398	-.388669	-.425871	-.430063	-.427967	.002096
3	.809017	.293893	55.464603	-.499836	-.128496	-.131340	-.129918	.001422
4	.587785	.404508	70.035371	-.414346	.108489	.106918	.107704	.000786
5	.309017	.475528	80.772355	-.228764	.252228	.251559	.251893	.000334
6	0.000000	.500000	90.000000	-.000000	.300241	.299759	.300000	.000241
7	-.309017	.475528	99.227645	.228764	.252227	.251559	.251893	.000334
8	-.587785	.404508	109.964629	.414346	.108489	.106919	.107704	.000785
9	-.809017	.293893	124.535397	.499836	-.128501	-.131346	-.129924	.001422
10	-.951057	.154508	146.982602	.388669	-.425864	-.430061	-.427963	.002098
11	-1.000000	0.000000	180.000000	-.000000	-.597398	-.602598	-.599998	.002600
12	-.951057	-.154508	-146.982602	-.388669	-.425864	-.430060	-.427962	.002098
13	-.809017	-.293893	-124.535397	-.499836	-.128500	-.131345	-.129923	.001422
14	-.587785	-.404508	-109.964629	-.414346	.108490	.106920	.107705	.000785
15	-.309017	-.475528	-99.227645	-.228764	.252228	.251561	.251894	.000334
16	0.000000	-.500000	-90.000000	.000000	.300242	.299761	.300001	.000241
17	.309017	-.475528	-80.772355	.228764	.252230	.251561	.251896	.000334
18	.587785	-.404508	-70.035371	.414346	.108487	.106918	.107703	.000785
19	.809017	-.293893	-55.464603	.499836	-.128482	-.131315	-.129899	.001417
20	.951057	-.154508	-33.017398	.388669	-.425997	-.430121	-.428059	.002062

UPSTREAM FLOW SPEED = 0.

UPSTREAM FLOW DIRECTION = 0.

DOWNSTREAM FLOW SPEED = 0.

DOWNSTREAM FLOW DIRECTION = 0.

CIRCULATION = 0.

PITCH = .2000E+01

CHORD = .2000E+01

Table 7-7

COUPLED PROBLEM FOR CASCADE AEROFOIL
****

NUMBER OF NODES = 20

NODE NUMBER	CO-ORDINATES X	Y	DIRECTION OF NORMAL	DPDN	SUM	DIF	ϕ_s^2	$\overline{\phi}_s^2$
1	1.000000	0.000000	0.000000	0.000000	-.596845	-.603052	-.599948	.003103
2	.951057	.154508	33.017398	-.388669	-.425518	-.430423	-.427970	.002452
3	.809017	.293893	55.464603	-.499836	-.128394	-.131437	-.129915	.001522
4	.587785	.404508	70.035371	-.414346	.108371	.107029	.107700	.000671
5	.309017	.475528	80.772355	-.228764	.252018	.251764	.251891	.000127
6	0.000000	.500000	90.000000	-.000000	.300051	.299948	.300000	.000051
7	-.309017	.475528	99.227645	.228764	.252020	.251770	.251895	.000125
8	-.587785	.404508	109.964629	.414346	.108375	.107039	.107707	.000668
9	-.809017	.293893	124.535397	.499836	-.128401	-.131440	-.129920	.001519
10	-.951057	.154508	146.982602	.388669	-.425505	-.430412	-.427958	.002454
11	-1.000000	0.000000	180.000000	-.000000	-.596882	-.603104	-.599993	.003111
12	-.951057	-.154508	-146.982602	-.388669	-.425503	-.430409	-.427956	.002453
13	-.809017	-.293893	-124.535397	-.499836	-.128400	-.131437	-.129918	.001519
14	-.587785	-.404508	-109.964629	-.414346	.108376	.107042	.107709	.000667
15	-.309017	-.475528	-99.227645	-.228764	.252021	.251774	.251897	.000124
16	0.000000	-.500000	-90.000000	.000000	.300051	.299952	.300002	.000050
17	.309017	-.475528	-80.772355	.228764	.252021	.251770	.251896	.000125
18	.587785	-.404508	-70.035371	.414346	.108368	.107032	.107700	.000668
19	.809017	-.293893	-55.464603	.499836	-.128370	-.131393	-.129882	.001511
20	.951057	-.154508	-33.017398	.388669	-.425734	-.430519	-.428126	.002393

UPSTREAM FLOW SPEED = 0.

UPSTREAM FLOW DIRECTION = 0.

DOWNSTREAM FLOW SPEED = 0.

DOWNSTREAM FLOW DIRECTION = 0.

CIRCULATION = 0.

PITCH = .1500E+01

CHORD = .2000E+01

Table 7-8

COUPLED PROBLEM FOR CASCADE AEROFOIL
****

NUMBER OF NODES = 40

NODE NUMBER	CO-ORDINATES X	Y	DIRECTION OF NORMAL	DPDN	SUM	DIF	φ_s	$\bar{\varphi}_s$
1	1.000000	0.000000	0.000000	0.000000	-.599993	-.600008	-.600001	.000007
2	.987688	.078217	17.576581	-.223697	-.550768	-.550781	-.550775	.000007
3	.951057	.154508	33.017398	-.388669	-.427960	-.427971	-.427966	.000006
4	.891007	.226995	45.540602	-.476965	-.277224	-.277233	-.277228	.000004
5	.809017	.293893	55.464603	-.499836	-.129922	-.129928	-.129925	.000003
6	.707107	.353553	63.434949	-.474342	.000002	-.000003	-.000000	.000002
7	.587785	.404508	70.035371	-.414346	.107705	.107702	.107703	.000001
8	.453990	.445503	75.707214	-.329953	.191781	.191780	.191780	.000001
9	.309017	.475528	80.772355	-.228764	.251893	.251892	.251893	.000000
10	.156434	.493844	85.472070	-.116959	.287972	.287972	.287972	.000000
11	0.000000	.500000	90.000000	-.000000	.300000	.300000	.300000	.000000
12	-.156434	.493844	94.527930	.116959	.287972	.287972	.287972	.000000
13	-.309017	.475528	99.227645	.228764	.251893	.251892	.251893	.000000
14	-.453990	.445503	104.292786	.329953	.191781	.191780	.191780	.000001
15	-.587785	.404508	109.964629	.414346	.107705	.107702	.107703	.000001
16	-.707107	.353553	116.565051	.474342	.000002	-.000003	-.000000	.000002
17	-.809017	.293893	124.535397	.499836	-.129922	-.129928	-.129925	.000003
18	-.891007	.226995	134.459398	.476965	-.277224	-.277233	-.277228	.000004
19	-.951057	.154508	146.982602	.388669	-.427960	-.427971	-.427966	.000006
20	-.987688	.078217	162.423419	.223697	-.550768	-.550781	-.550775	.000007
21	-1.000000	0.000000	180.000000	-.000000	-.599993	-.600008	-.600001	.000007
22	-.987688	-.078217	-162.423419	-.223697	-.550768	-.550781	-.550775	.000007
23	-.951057	-.154508	-146.982602	-.388669	-.427960	-.427971	-.427966	.000006
24	-.891007	-.226995	-134.459398	-.476965	-.277224	-.277233	-.277228	.000004
25	-.809017	-.293893	-124.535397	-.499836	-.129922	-.129928	-.129925	.000003
26	-.707107	-.353553	-116.565051	-.474342	.000002	-.000003	-.000000	.000002
27	-.587785	-.404508	-109.964629	-.414346	.107705	.107702	.107703	.000001
28	-.453990	-.445503	-104.292786	-.329953	.191781	.191780	.191780	.000001
29	-.309017	-.475528	-99.227645	-.228764	.251893	.251892	.251893	.000000
30	-.156434	-.493844	-94.527930	-.116959	.287972	.287972	.287972	.000000
31	0.000000	-.500000	-90.000000	.000000	.300000	.300000	.300000	.000000
32	.156434	-.493844	-85.472070	.116959	.287972	.287972	.287972	.000000
33	.309017	-.475528	-80.772355	.228764	.251893	.251892	.251893	.000000
34	.453990	-.445503	-75.707214	.329953	.191781	.191780	.191780	.000001
35	.587785	-.404508	-70.035371	.414346	.107705	.107702	.107703	.000001
36	.707107	-.353553	-63.434949	.474342	.000002	-.000003	-.000000	.000002
37	.809017	-.293893	-55.464603	.499836	-.129922	-.129928	-.129925	.000003
38	.891007	-.226995	-45.540602	.476965	-.277224	-.277233	-.277228	.000004
39	.951057	-.154508	-33.017398	.388669	-.427960	-.427971	-.427966	.000006
40	.987688	-.078217	-17.576581	.223697	-.550768	-.550781	-.550775	.000007

Table 7-9

Number of nodes	Approximation to A_c
60	.5292
120	.5338
180	.5348

Table 9-1

Number of nodes	Approximation to τ on AB	Approximation to τ on EA
60	.7496	1.0230
120	.7529	1.0236
180	.7534	1.0215

Table 9-2

x - ordinate of cusp = 1.39880

True speed of flow at cusp = .9

x-ordinate of points A^+ & A^-	True Speed at A^+	Approx. Speed at A^+	True Speed at A^-	Approx. Speed at A^-
1.38635	.9092	.7978	.8951	.9950
1.37682	.9133	.8466	.8943	.9422
1.36476	.9177	.8630	.8940	.9215
1.35030	.9225	.8694	.8940	.9107
1.33361	.9277	.8722	.8942	.9040
1.31483	.9332	.8735	.8948	.8994

Table 9-3

x-ordinate of cusp = 1.39880

true exit speed = 1.00173

true exit angle = 3.366°

inlet angle - true exit angle = 41.634°

x-ordinates of points A^+ & A^-	Approximate exit speed	Approximate exit angle	Approximation to inlet angle - exit angle
1.38635	1.00303	4.464°	40.536°
1.37683	1.00267	4.187°	40.813°
1.36476	1.00257	4.113°	40.887°
1.35030	1.00258	4.121°	40.879°
1.33361	1.00265	4.172°	40.828°
1.31483	1.00275	4.248°	40.752°

Table 9-4

Speed I is solution based on § A1.2)
Speed II is solution based on § 3.4)
Error I is relative error of Speed I
Error II is relative error of Speed II

co-ordinates		True Speed	Speed I	Error I	Speed II	Error II
x	y					
1.000000	.000000	.000000	.000000	-	.000000	-
.951057	.154508	.817337	.804192	.016083	.733535	.102531
.809017	.293893	1.235664	1.248835	.010659	1.189500	.037360
.587785	.404508	1.409855	1.428070	.012920	1.393850	.011352
.309017	.475528	1.480589	1.497405	.011358	1.474782	.003922
.000000	.500000	1.500000	1.515524	.010349	1.496444	.002371

Table A1-1

D40838 '82

END